وزارة التعليم العالي و البحث العلمي

BADJI MOKHTAR UNIVERSITY - ANNABA
UNIVERSITE BADJI MOKHTAR - ANNABA

جامعة باجي مختار - عنابة

FACULTE DES SCIENCES DE L'INGENIORAT
DEPARTEMENT DE GENIE CIVIL

Année : 2015

THESE

Présentée en vue de l'obtention du diplôme de DOCTORAT ès Sciences

Thème

Contribution to Linear and Nonlinear Static and Dynamic Analysis of Thin Shells by Triangular and Quadrilateral Flat Shell Finite Elements with Drilling Rotational Degree of Freedom

Option : Structures et Matériaux

Par :
Djamel BOUTAGOUGA

Directeur de Thèse : Kamel DJEGHABA Professeur Université de Annaba

Devant le Jury :

Président :	**Mohamed Faouzi HABITA**	Professeur	Université de Annaba
Examinateurs :	**Mohamed GUENFOUD**	Professeur	Université de Guelma
	Lamine BELOUNAR	Professeur	Université de Biskra
	Rachid LASSOUED	Professeur	Université de Constantine
Invité :	**Abdelhacine GOUASMIA**	Docteur	Université de Annaba

الملخـص:

قمنا في هذا العمل بتطوير تحليل ستاتيكي وديناميكي خطي وغير خطي هندسيا للصدفيات الرقيقة باستخدام العناصر المحددة المسطحة ثلاثية ورباعية الأضلع مع درجة حرية دورانية في المستوي. تم الحصول على العناصر الصدفية المسطحة من خلال الجمع بين عناصر صفائح الانحناء "DKT" و "DKQ" في نظرية كيرشوف المتقطعة وعناصر غشائية مع دوران الحفر "drilling rotation". العناصرالغشائية المقدمة هي عنصر رباعي مع دوران الحفر على أساس صياغة التباين المعدلة لـ "Hughes" و "Brezzi" وعنصرثلاثي مع دوران الحفر على أساس صياغة التشوه المحسن EAS.

يتم التحليل الديناميكي العابر باستخدام طريقة نيومارك لتكامل الزمن المباشر، في حين أن التحليل غير الخطي يعتمد على وصف لاغرانج المحدث "updated co-rotational Lagrangian description". لأجل هذا الغرض، طورنا صيغة "co-rotational formulation" في المستوي والتي تأخذ في الحسبان دوران الحفر في المستوي لأجل العناصر الغشائية الثلاثية والرباعية .علاوة على ذلك، تم اعتماد مصفوفة كتلة بسيطة وفعالة في المستوي تأخذ في الحسبان العطالة الدورانية في المستوي، والتي تسمح بالتمثيل الحقيقي لأنماط الاهتزاز في المستوي. وأخيرا، تم ادخال هذه التطويرات على عناصر محددة صدفية مسطحة ثلاثية الأبعاد مع ست درجات حرية. تم أيضا تطوير برنامج تحليل مبني على العناصر المحددة للتحقق من دقة العناصر المقدمة.

تم أولا اختبار العناصر المطورة في تحليل مسائل إجهاد مستو ستاتيكية وديناميكية، من ثم تم اختبارها في مسائل الصدفيات العامة. فعالية هذه العناصر الموضحة من الأمثلة العددية، في التنبؤ للاستجابة الديناميكية غير الخطية للهياكل الصدفية بينما تبقى اقتصادية، تعتبر كافية للتأكد من أن هذه العناصر تقدم أداء جيدا في التحليل الستاتيكي والديناميكي غير الخطي لمسائل الصدفيات العامة.

ABSTRACT

Linear and geometrically nonlinear static and dynamic finite element analysis of thin shells using triangular and quadrilateral flat shell elements with in-plane drilling rotational degree of freedom is presented. The flat shell elements are obtained by combining the "DKT" and "DKQ" Discrete Kirchhoff Theory plate bending elements and membrane elements with drilling rotation. The membrane elements developed are a quadrilateral element with drilling rotation based on the modified HUGHES and BREZZI variational formulation and a triangular element with drilling rotation based on the Enhanced Strain formulation.

The transient dynamic analysis is carried out using Newmark direct time integration method, while the nonlinear analysis adopts the updated co-rotational Lagrangian description. In this purpose, in-plane co-rotational formulation that considers the in-plane drilling rotation is developed and presented for triangular and quadrilateral membrane elements. Furthermore, a simple and effective in-plane mass matrix that takes into account the in-plane rotational inertia, which permit true representation of in-plane vibrational modes is adopted. Finally, these developments are implemented into three dimensional flat shell finite elements with six degrees of freedom. A finite element analysis program is also developed to check the accuracy of the developed elements.

The developed elements are first thoroughly tested for static and dynamic analysis of plane stress problems, then, they are tested for general shell problems. The effectiveness of these elements shown by the selected numerical examples to predict the nonlinear dynamic response of shell structures while remains economic, is adequate to ascertain that these elements would perform well in the case of nonlinear static and dynamic analysis of general shells.

RESUME

Dans ce travail, une analyse linéaire et non-linéaire géométrique statique et dynamique, des coques minces en utilisant des éléments finis de coques à facette plane triangulaires et quadrangulaires avec le degré de liberté de rotation dans le plan dit "drilling rotation" est présenté. Les éléments de coque plane sont obtenus en combinant les éléments de plaque de flexion “DKT” et “DKQ” de la théorie Kirchhoff discrète et des éléments de membrane avec "drilling rotation". Les éléments de membrane développés sont un quadrilatéral avec 'drilling rotation' basé sur la formulation variationnelle modifié de HUGHES et BREZZI et un élément triangulaire avec 'drilling rotation' basé sur la formulation "Enhanced Assumed Strain".

L'analyse dynamique transitoire est accomplie à l'aide de la méthode d'intégration directe de Newmark, tandis que l'analyse non linéaire adopte la description Lagrangienne actualisée co-rotationnelle. Dans ce but, une formulation Co-rotationnelle dans le plan qui considère le degré de liberté rotationnel dans le plan 'drilling rotation' est élaborée et présenté pour les éléments de membrane triangulaires et quadrangulaires. En outre, une matrice de masse simple et efficace qui prend en compte l'inertie de rotation dans le plan, ce qui permet une représentation vrai de modes de vibration dans le plan, est adoptée. Enfin, ces développements sont implémentés dans des éléments finis de coques à facette plane avec six degrés de liberté. Un programme d'analyse par éléments finis est également établit pour vérifier la conformité des éléments développés.

Les éléments développés sont d'abord testés pour l'analyse statique et dynamique des problèmes de contraintes planes, puis, ils sont testés pour des problèmes de coques générales. L'efficacité de ces éléments, représentés par les exemples numériques sélectionnés, pour prédire la réponse dynamique non-linéaire de structures coques tout en restant économique, est adéquat pour assurer que ces éléments seraient de bons précision dans le cas de l'analyse non-linéaire statique et dynamique des coques de formes générales.

TABLE OF CONTENTS

LIST OF FIGURES

INTRODUCTION

Shell structures represent a particular type of structural systems characterized by their geometry, being a three-dimensional solid whose thickness is much smaller than the other two dimensions. These elements are light weight constructions enclosing space using one or more curved surfaces. One basic property with shells, is that they are characterized by the stress resultants in the middle surface presenting in-plane components due to membrane behaviour and normal to the surface components due to bending behaviour. Even with shells of small thickness, heavy loads can be sustained efficiently due to the membrane effect. Therefore, thin shell structures, with their excellent mechanical performance, have been widely used in various fields of structural engineering as: constructions that offer large internal space, cooling towers, mechanics, industrial, automobiles, marine, aerospace …etc. Thus, analysis and design of these structures, with accurate evaluations of the maximum load carried by the structure, are of major importance.

The capability of a design for all engineering structures is being pushed to find more efficient solutions for economic and environmental issues. As it is of crucial interest to increase their performances, shell structures are becoming thinner, lighter, and more flexible, so their deflections may have an important order of magnitude under either static or dynamic loads, which makes their behaviour often characterised as geometrically nonlinear. The importance of studying the dynamic behaviour of shell structures, is so because often such structures are subjected to time varying loadings such as impact, explosion or seismic effects.

The computational mechanics has now reached a level of maturity enabling complex simulations. However, one of the difficulties of nonlinear calculations is the fact that they are based on incremental iterative algorithms. Nevertheless, recent developments in computer technology and in computational mechanics, allow us to formulate computational models capable of delivering accurate results especially by means of the Finite Elements Method.

The objective of this thesis is to formulate an accurate model delivering close approximations of nonlinear and dynamic behaviour of shells. Such a model provides valuable information about the behaviour of shell structures, which enables us to control some important aspects of the design as: the maximum load carried by the structure, the maximum displacement, as well as the equilibrium path in both linear and geometrically nonlinear static and dynamic analysis with large displacements but small strains.

Time-dependent nonlinear problems however, involved high computational cost in the simulations especially when using higher order finite elements. For this reason, flat shell finite

elements theory is highly desirable due to simplicity and numerical efficiency. These elements can be constructed by a simple combination of a plate bending element with a membrane element. However, when conventional flat shell finite elements are used, an ill-conditioned stiffness may arise because there is a missing rotational degree-of-freedom. To avoid this difficulty, the facet-shell formulation must provide a complete description of the nodal translation and rotation fields allowing the definition of six degrees-of-freedom for each node. This problem can be handled by combining a plate bending element with a membrane element which includes the in-plane rotational drilling degrees of freedom. Moreover, the membrane formulation with drilling rotation performs significantly better compared to the formulation without the drilling rotation. This feature, may provide a solution to overcome the in-plane locking of conventional flat shell finite elements, and enhance their performances with both regular and distorted meshes.

The extension of flat shells with drilling rotation to dynamic regime, require a mass matrix formulation that takes into account the in-plane rotational inertia related to the drilling rotational *d.o.f*. Also, to analyse the large deflection nonlinear behaviour of shells, a nonlinear theory that handles efficiently the problem of large rotations is required. The co-rotational formulation has been considered as an effective solution to handle large rotations problem, in which, the main challenge is how to describe the deformed reference plane and how to derive deformational strains from the global displacements and rotations that contain both deformational and rigid-body movements. In this regard, flat shells with drilling rotation need a particular handling of the in-plane rigid body rotations. Furthermore, a geometric stiffness matrix that accounts for the effect of initial stresses has to be included taking into account the effect of the in-plane rotational drilling degree of freedom.

In this work, an efficient handling of the above mentioned issues for triangular and quadrilateral flat shell elements with drilling rotational *d.o.f* are presented. A large displacements and large rotations geometrically nonlinear static and dynamic analysis of flat shells is formulated in the framework of the updated Lagrangian co-rotational formulation, in which, the implicit Newmark direct time integration method is adopted for dynamic analysis.

CHAPTER I

STATE OF THE ART

I- INTRODUCTION

The first general two-dimensional theory of thin shells was developed in 1888 by [LOVE 1888]. Numerous contributions to this subject have been made since then. However, analytical solutions to thin shell structural problems are not applicable to arbitrary shapes, load conditions, and irregular boundary conditions. Nevertheless, these limitations are overcome by the development of the finite elements method. The computational implementation of shell elements has been challenging finite elements researchers to develop elements that were simple and efficient. Numerous theoretical models have been developed and applied. No single theory has proven to be general and comprehensive enough for the entire range of applications. Consequently, the field of finite elements analysis of shell structures has been very widely researched, therefore enormous literature is available regarding creating new and improving existing analysis theories and formulations.

II- HISTORICAL REVIEW

Since the early 1960's, the published literature on modelling of shells and plates in linear and nonlinear analysis and their application to dynamic regime of structures has grown extensively. It is almost impossible to make a review of the developments have been made in computational shell mechanics. In this section, we attempt to summarize the important developments achieved by the finite element community in the area of shell finite elements. It would be impossible to cover all such publications, therefore some selected segments of the literature are presented. We gave just an overview of the major approaches that have been used to develop shell finite elements, focussing on the shortcomings and difficulties that have faced the development of early shell finite elements. Early developments concerning triangular and quadrilateral thin plate bending elements as well as membrane elements are also presented. A special attention is focussed on membrane elements with rotational degree of freedom as well as flat shell elements with drilling rotation. We concluded by presenting the developments that have been made for flat shell elements with drilling rotation in dynamic and nonlinear analysis.

II-1. Thin Shell Finite Elements for Linear Analysis

Before the early applications of shell finite elements, one should mention the direct application of three-dimensional solids to model a shell problem as a three-dimensional one using the so-called Iso-parametric elements by [ERGATOUDIS et al 1966, 1968]. This procedure, which is essentially used in arch dam problems, is primarily reserved for the relatively thick shells. With the advent of the high speed digital computers, and the subsequent development of the finite element method, full three-dimensional treatment of any structure is a rather simple matter. The advantage of this approach, besides taking into account thickness changes throughout deformation and using 3*D* material laws, is that there are no theoretical limitations and, no assumptions other than those used in elasticity are needed. However, constraints of economy and efficiency prohibit the use of three-dimensional analysis except when it is absolutely necessary.

Solid elements are preferred in nonlinear structural mechanics in a wide range of applications due their low computational cost. However, in bending problems, the low-order solid element exhibits a low-precision results due to stiffening effects known as locking. Moreover the use of several nodes towards thickness of the shell using solid three-dimensional elements, leads to a large number of degrees of freedom along the thickness. As the shell becomes thinner, it becomes ill-conditioned since the thickness is too small relative to other dimensions.

The so-called "solid-like" or solid-shell elements is an alternative approach aims to overcome these disadvantages of the standard solid elements. The solid-shell is a solid element that has incorporated features from shell elements. So, besides having the same *d.o.f* of solid element, and integration over a 3*D* domain, these elements use the assumption of "normal to the mid-surface remains straight" and other shell elements features in order to remove transverse shear locking. Hence, Solid-like shell elements can be applied not only for moderately thick but also for thin shell structures.

Many efforts has been oriented toward ameliorating the performances of solid-like shell elements. [WILSON et al 1973-a] proposed an Iso-parametric 8-node hexahedric with nodal translational *d.o.f*. However, this element was very sensible to locking problems especially when bending is dominant. In the same work, they presented the incompatible modes method and used it to ameliorate the hexahedric element's behaviour. Later, [TAYLOR et al 1976] presented a modified versions of the 8-node hexahedric, in which the element pass the path test.

To overcome the over stiffness, and locking problems, Solid-shell elements usually adopt the Enhanced Assumed Strain technique by [DVORKIN & BATHE 1984] for the in-plane shear strains and normal strains, while adopt the Assumed Natural Strain technique by [SIMO & RIFAI 1990] for the transverse shear and normal strains. Also, reduced and selective integrations technics with stabilisation of hourglass modes are also widely used in solid-shell elements.

The solid-shell elements are attractive ones. Currently, there is a trend to use solid-shell elements to treat plates and shells as a 3*D* continuum. A class of solid-like shell elements using the above mentioned technics has been investigated by many researchers: [WANG & BELYTSCHKO 1987; BELYTSCHKO & BINDEMAN 1993; FREISCHLÄGER & SCHWEIZERHOF 1996; ZHU & CESCOTTO 1996; KLINKEL & WAGNER 1997; CHO et al 1998; HAUPTMANN & SCHWEIZERHOF 1998; MIEHE 1998; KLINKEL et al 1999; DOLL et al 2000; PUSO 2000; REESE et al 2000; SZE & YAO 2000; WALL et al 2000; HAUPTMANN et al 2000, 2001; HARNAU & SCHWEIZERHOF 2002; SZE et al 2002; VU-QUOC & TAN 2003-a, 2003-b; CHEN & WU 2004; KIM et al 2005; TAN & VU-QUOC 2005; KLINKEL et al 2006; REESE 2007; CARDOSO et al 2007; KIM & BATHE 2008; LI et al 2011-a, 2011-b; RAH et al 2011; HAJLAOUI & JARRAYA 2012; COCCHETTI et al 2013; EDEM & GOSLING 2013; KWON 2013; NACEUR et al 2013; RAH et al 2013-a, 2013-b; AHMED & SLUYS 2014].

The specific geometric properties of shells have been exploited to create numerous bi-dimensional models, which, in general, have provided significant simplifications compared to the 3-D continuum mechanics solution approach. In fact, any two-dimensional theory of shells, approximates the real three dimensional problem. Hence, researchers have been seeking better

approximations for the exact three-dimensional elasticity solutions for shells. Intensive works have been conducted towards the development of simple and efficient shell finite elements of quadrilateral and triangular shapes through three major approaches:

- The bi-dimensional curved shell elements derived from classical shell theory;
- The degenerated shell elements derived from three-dimensional solid elements;
- The flat shell elements, obtained by the combination of the membrane and bending behaviours of flat elements.

Each element type has its deficiencies and its benefits, and it is still difficult to identify which approach is the most advantageous, especially, when incremental iterative nonlinear analysis is involved. Several comparisons studies between shell elements of deferent theories, and other classifications and reviews can be found in many references: [BATHE & HO 1981; IDELSOHN 1981; MEEK & TAN 1986-a; YANG et al 1990; BUECHTER & RAMM 1992; HO 1992; CHROSCIELEWSKI et al 1997; YANG et al 2000].

Among these approaches, flat shell elements, are regarded to be the most attractive as they can be built by combining existing plate and membrane elements. They have been used extensively because of the simplicity in their formulation, the effectiveness in performing computation, and the flexibility in applications to both deep and shallow shells and folded plate structures. However the use of "higher order" shell elements still present a necessity for a large class of engineering applications. By the sixties, flat shells, manly constructed by triangular elements, were the first shell elements available for computational mechanics of shell structures. They were followed by higher-order curved shell elements and degenerated shell elements. Due to mathematical complexities of curved classical shell theory, curved elements have not been widely adopted. Furthermore, they usually use higher order displacement's derivatives, resulting in a large number of *d.o.f* per node. The Iso-parametric degenerated shell elements, particularly dominated research activities in the following decades despite their numerical difficulties referred to as shear and membrane locking.

II-1.1. Bi-Dimensional Curved Elements Derived From Classical Shell Theories

These types of elements which are divided into singly and doubly curved shell elements, are very efficient in modelling structures with curved geometry. However, because of the complexities involved, the development of acceptable curved shell element was obstructed by many difficulties, such as:

- The choice of an appropriate shell theory.
- Description of the shell element geometry.
- Satisfaction of continuity and compatibility requirements.
- Correct representation of the rigid body modes.

Before the advent of the patch test by [IRONS 1966; IRONS & RAZZAQUE 1972], satisfaction of completeness in the form of continuity, compatibility, and correct representation of rigid body and constant curvature modes, was identified as fundamental for convergence to the analytical solution. Many elements were developed which had some of these difficulties, and were used with different degrees of success.

Earlier development of two dimensional linear theories of thin shells include important contributions of [SANDERS 1959; FLUGGE 1960] in which, the initial curvature effect is taken into consideration, and the deformation is based on the Love-Kirchhoff assumption.

The singly curved elements were first developed in the axisymmetric form for the analysis of shells of revolution. [GRAFTON & STROME 1963] developed a method based on the direct stiffness method for the structural analysis of shells of revolution, composed of materials with orthotropic properties. In the following years, various improvements have been done by various researchers: [POPOV et al 1964; PERCY et al 1965; DONG 1966; NAVARATNA 1966; FULTON et al 1966; BEITCH 1966; CANTIN & CLOUGH 1968].

[CONNOR & BREBBIA 1967] developed a rectangular cylindrical shallow shell element with 20 *d.o.f*. They used a polynomial expression to express the radial displacement by 12 terms, and a linear expression for the membrane displacements. For this element, the rigid body modes are not included nor is the compatibility satisfied. [BOGNER et al 1967] developed a 4-node cylindrical shell element with 12 *d.o.f* per node based on "Novozhilov" shell theory. They used 16 term polynomial for all three displacement components. Rigid body modes are not included in this element. Compatibility requirements are however satisfied. [CANTIN & CLOUGH 1968] developed a curved cylindrical shell element including rigid body motion. They added the six rigid body modes explicitly by introducing the appropriate trigonometrical terms into the displacement functions. [POPOV & SHARIFI 1971] described an axisymmetric curved finite element for shells of revolution by using cubic polynomials in terms of local Cartesian coordinates.

[SABIR & LOCK 1972; ASHWELL & SABIR 1972] used a strain based formulation, in which certain terms were omitted from the displacement function of [CANTIN & CLOUGH 1968] to derive a nonconforming strain-based rectangular cylindrical element. The element has 12 *d.o.f*, and it

includes correct representation of rigid body displacements, and satisfies the constant strain condition. Many other quadrilateral and triangular, singly and doubly curved shell elements, based on the same approach was developed by Sabir and co-workers: [SABIR & CHARCHAFCHI 1982; SABIR 1983; SABIR & RAMADANHI 1985; SABIR 1987; MOUSA & SABIR 1994].

[FONDER & CLOUGH 1973] explicitly added four missing rigid body modes in a cylindrical shell element with 24 *d.o.f*, and they found significant improvement over the performances of the same element without this addition. [GALLAGHER 1975] presented a 24 *d.o.f* conforming element using the complete bi-cubic hermit interpolation functions.

Early doubly curved axisymmetric shell elements was constructed by [JONES & STROME 1966; STRICKLAND & LODEN 1968]. They used curved meridional elements rather than conical segments. They do not however, assure the continuity of displacements, along the sides of elements and do not represent the rigid-body motion correctly.

[UTKU 1967; GREENE et al 1968; STRICKLAND & LODEN 1968; ARGYRIS & SCHARPF 1968-a, 1968-b] presented curved finite elements based on two-dimensional shell theory. [UTKU 1967] achieved a relatively simple algebraic representation for curved triangular elements by using linear variations for the three displacement and two angular displacement components. However, the element experienced considerable strain under rigid body rotation. [STRICKLAND & LODEN 1968] developed a triangular element based on shallow shell theory, in which, the normal displacement was incompatible, and it was deficient in the representation of rigid body modes. [ARGYRIS & SCHARPF 1968-a, 1968-b] proposed a higher order polynomial for all three displacement fields. [YANG 1973] developed a high order 48 *d.o.f* shallow shell finite element with two principal radii of curvature and a twist radius.

The Discrete Kirchhoff Theory, was successfully used to develop a number of singly and doubly curved shear-locking-free shell elements. Among the first ones, was a rectangular cylindrical element presented by [WEMPNER et al 1968]. [DHATT 1969] presented a number of DKT based triangular curved shallow shell elements. [MURTHY & GALLAGHER 1983] presented a three-node triangular cylindrical shell element based on the *DKT* assumptions using 27 *d.o.f*, with displacement components based on the triangular natural area coordinates.

Another developed family of shell elements, which imposes certain constraints on the shear stress to satisfy the discrete Kirchhoff assumption is the Semi-Loof shell elements by [IRONS 1974; IRONS & RAZZAQUE 1976]. These elements are general curved triangles and quadrilaterals, with three degrees of freedom (u, v, and w) at each corner and mid-side node, and with normal and

parallel rotations at the so-called "Loof" nodes along each side. These thin shell elements have proved to be very efficient for engineering shell applications, however, it is difficult to implement in a finite element program. Therefore, it is not much used.

Most of the presented quadrilateral elements were limited to regular shapes. [BATHE & DVORKIN 1986] presented the tensor mathematics that has been used in the formulation of skewed curved quadrilateral shell elements.

[DUPUIS & GOEL 1996] presented a curved triangular finite shell element based on the Koiter-Sanders model, in which the shell surface is described in a curvilinear coordinate system. The element correctly represents rigid-body motions and assures convergence in energy.

Applications of curved shell elements to large displacement analysis of shells have been reported by many authors, see for instance: [HARBORD 1973; SABIR & LOCK 1973; THOMAS & GALLAGHER 1975; GALLAGHER 1976; WOOD & ZIENKIEWICZ 1977; HORRIGMOE 1978; JAVAHERIAN et al 1980; CHROSCIELEWSKI et al 1992; KEULEN et al 1993; BUCHTER et al 1994; KEULEN & BOOIJ 1996; CAMPELLO et al 2003; PIMENTA et al 2004; LI et al 2008]. However, excellent accuracy of curved elements is obtained at the cost of a time-consuming element. This fact leads to expansive nonlinear analysis.

II-1-2. Shells Degenerated From Three-Dimensional Solid Elements

The appearance of the Iso-parametric finite element by [ERGATOUDIS et al 1966, 1968], has motivated many attempts to improve the basic accuracy of this three dimensional element in order to make it possible to be used for shell analysis. The motivation for development of a shell element, which would be based on three-dimensional continuum mechanics, is mainly due the computational difficulties associated with a full three-dimensional model for a thin shell or plate structure. Complex mathematical expressions and assumptions of shell theories, particularly for nonlinear shells, could be avoided using the Iso-parametric elements.

Since the pioneering work modifying a three-dimensional Iso-parametric element to ordinary bi-dimensional shell element by [AHMAD 1969; AHMAD et al 1970], the analysis of shell elements by the so-called degenerated solid approach or "degenerated shell elements" has been widespread. It is mainly because of their relative efficiency, and versatility of treating variable thickness and composite laminated structures beside their extensibility to nonlinear analysis.

In this theory, a three-dimensional solid element is degenerated (reduced) to a shell element having only mid-surface nodal variables. The procedure of creating degenerated shell elements,

consists to eliminate nodes by enforcing different constraints on the behaviour of the element, see [BATHE 1982] for more details:

1. The line connects bottom node with top node called "fibre", remain straight and inextensible;
2. The elongation of fibers is governed by conservation of mass and/or the constitutive equation;
3. Plane stress state;
4. The elastic modulus in normal direction is assumed to be zero.

Degenerated shell elements are capable of representing the coupled effects between membrane and bending actions. Moreover, the measure of the transverse shear deformation, is permitted since the mid-surface normal are not necessarily to be kept normal during deformation. Therefore, degenerated shell elements give good results for thick shells. Unfortunately, fully integrated stiffness matrix overestimates the stiffness of the shell as its thickness decreases "the shear-locking problem". In the case of moderately thick and thin shells, the results were found to be departed considerably from analytical solutions, and the elements were found to be too stiff with a very slow rate of convergence. The results was worsened as the shell become thinner, see [ZIENKIEWICZ et al 1971; PARISCH 1979]. The reduced integration technique by Too and Irons applied by [ZIENKIEWICZ et al 1971] and [PAWSEY & CLOUGH 1971] gave remarkably improved results for moderate to thin shells. Nevertheless, below a certain thinness the element behaviour was unreliable. [HUGHES et al 1978] introduced the selective reduced integration technique, in which, a reduced order of integration is used for membrane and shear energy terms to underestimate their effects in thin situations, see also: [BELYTSCHKO et al 1984-a; STANLEY et al 1986; BELYTSCHKO et al 1989]. The Assumed Strain method has also been used successfully to resolve the problem of locking phenomenon in degenerated shell elements, so they can be applied to thin, thick, and laminated composite shells. [MACNEAL 1982] used an assumed-strain field related to nodal displacements by line integration along straight line segments between pairs of nodal points, resulting with a high accuracy shell element for both thick and thin shell problems.

Several researchers had modified and extended the original degenerated shell element to improve its behaviour for both thick and thin shells and overcome drawbacks associated with earlier degenerated shell elements: [ONÃTE et al 1978; STOLARSKI & BELYTSCHKO 1983; BUCALEM & BATHE 1993]. The addition of nonconforming displacement modes method by [WILSON et al 1971], substitute shear strain fields by [DVORKIN & BATHE 1984; HUANG & HINTON 1986-a], and stress projection technic [BELYTSCHKO et al 1985] have been used successfully to overcome shear locking problem. Thus, degenerated elements originated as a tool for analysing thick shells, have been successfully applied to thin shell situations as well.

Applications of degenerated shell elements to large displacement analysis have been reported by [WOOD 1973; KRAKELAND 1977; PARISCH 1978]. Further development for nonlinear analysis using total or updated Lagrangian formulations have been made by [BATHE & BOLOURCHI 1980; HUGHES & LIU 1981; PARISCH 1981; SURANA 1983; DVORKIN & BATHE 1984; OLIVER & ONÃTE 1984; MILFORD & SCHNOBRICH 1986; HUANG & HINTON 1986-b]. Also, the co-rotational formulation was used by: [HUGHES & LIU 1981; BELYTSCHKO et al 1984-b; STANLEY et al 1986; JIANG et al 1994; JIANG & CHERNUKA 1994; VALENTE et al 2003].

II-1.3. Flat shell Elements

Because of the difficulties involved by the tow former approaches, they have several formulation complexities. Consequently, they are generally expensive in computation and, therefore, their application to non-linear problems, in particular, can be limited.

Modelling shell structures with series of flat elements, which is simpler and easier to implement, became more popular. In this approach the shell's surface is approximated by an assemblage of flat elements constructed by combining the uncoupled membrane and plate bending behaviours. The major limitations of flat elements is the discontinuity in geometry, caused by these elements in representing a curved surface due the flatness of the elements. Moreover, the absence of coupling between membrane and bending within the element, and the lack of inter-element compatibility, represent the crucial shortcomings of these elements.

Several studies are available concerning convergence and error estimation of approximation of shell problems by flat shell elements, see for instance: [KIKUCHI 1984; TAYLOR & SIMO 1985; BERNADOU et al 1988; BERNADOU & TROUVE 1989; BERNADOU et al 1989; DESTUYNDER & SALAÜN 1998]. Many authors suggested that, the flat shells approach is more cost effective, and very attractive for the analysis of shell structures than higher order shells because of the simplicity of development. Also, higher order elements take three times more solution effort than lower order elements. Another drawback of higher order elements is the use of high order numerical integration schemes to avoid spurious zero energy modes. Moreover flat shells approach does not present membrane locking at the individual element level. Coupling between membrane and bending strains occur only on the inter-element boundary, which makes this approach very proper to study membrane locking. Some of the major attractive features of this modelling as cited by [COOK 1974-a; ZIENKIEWICZ 1971-a] are:

- Simplicity of formulation;
- Capability of modelling rigid body motion without including strains;

- The use of these elements would still less expensive than using elements based on three dimensional continuum mechanics.

More importantly, good results were obtained when sufficiently fine meshes were used. This is one of the reasons for the continued use of flat elements in shell analysis.

Since the 60's, studies have been conducted using flat shell elements comprising any triangular/quadrilateral membrane element and a triangular/quadrilateral plate bending element. Various authors [ZIENKIEWICZ 1971-a; HORRIGMOE 1977; BERNADOU et al 1989, 1994; HO 1992] have studied the advantages and disadvantages of the various types of these elements.

They were [GREENE et al 1961; ARGYRIS 1965-a; MELOSH 1965] who first suggested the concept of using a built up element by combining membrane and plate bending elements to develop 'faceted form' flat elements to model arbitrary shaped shell structures. Early efforts in the analysis of shells by flat shell elements were of triangular shaped elements, see: [UTKU & MELOSH 1967; CLOUGH & JOHNSON 1968; HERRMANN & CAMPBELL 1968; ZIENKIEWICZ et al 1968; ARGYRIS et al 1977-a, 1980]. These elements, used the CST membrane element to model the membrane action since the CST element could be easily matched with the available three-noded plate bending elements. Most of theme, were with 5 *d.o.f* (two in-plane translations, transverse displacement and two slopes). [ARGYRIS et al 1977-a] used the mixed second-order derivative of the lateral displacement as nodal parameters, together with the usual 5 *d.o.f* to get and 18 *d.o.f* triangular element. Note that, early elements did not work well in some problems because of poor response and locking of membrane elements.

Triangular shaped elements, have been the most used shell elements, for the simple reason that the subdivision of an arbitrary shell geometry into flat elements, can be well-approximated with triangles. However, the cardinal problem at the time was the lack of efficient plate elements capable of performing sufficiently. Hence, the success of such analysis, was delayed until formulations of plate bending elements became well grounded. When good plate elements were developed. It was a simple matter to extend their use to shell type structures.

Among earlier successful developments, we could mention, the triangular elements by: [DHATT 1970; BATOZ & DHATT 1972; CHU & SCHNOBRICH 1972; DAWE 1972]. Among them, the Triangular element presented by [DAWE 1972] might be the simplest flat shell element. It is obtained by superposing the "constant moment" triangular bending element by [MORLEY 1971] and the constant strain triangle "CST" by [TURNER et al 1956]. It involves a total of only twelve *d.o.f* "three translations at each corner node and one rotation at the mid-side", which correspond

to linear and quadratic interpolating polynomials for the in-plane and transverse displacements. [BATOZ & DHATT 1972] used the discrete Kirchhoff assumption to present the formulation of a triangular shell element with 15 *d.o.f*, and a quadrilateral shell element with 20 *d.o.f*, by combining four triangular elements with mid-side nodes. Actually, only shells with regular curved surfaces can be well-modelled using rectangular or quadrilateral flat shell elements.

[DHATT 1970; BATOZ et al 1976] presented triangular flat shell elements, based on the *DKT* bending element and a quadratic strain triangular membrane element. These elements performed better than those used the CST membrane element.

[MACNEAL 1978] presented a four-node Iso-parametric quadrilateral shell element with reduced integration of shear strain for the standard membrane element. To deal with the deficiency in the bending strain energy, he used and additional residual bending flexibility in the transverse shear terms of the plate element. He also discussed the enforcement of curvature compatibility and coupling between bending and stretching.

[BATOZ et al 1980; BATOZ & BENTAHAR 1982] developed the famous successful DKT triangular and the DKQ quadrilateral plate bending elements, which have been applied for shell analysis successfully. There is a rich literature regarding shell elements that are built from a flat membrane element and the DKT plate bending element: [GARNET & PIFKO 1983; BATHE & DVORKIN 1983-a; CARPENTER et al 1986; FAFARD et al 1989; CHEN 1992; ERTAS et al 1992; SAMANTA & MUKHOPADHYAY 1999; KIM & KIM 2002].

[DHATT et al 1986] presented a six node triangular shell element based on a discrete Kirchhoff plate element called DKTP and the LST membrane element. [SYDENSTRICKER & LANDAU 2000] used some discrete triangular plate elements to form flat shells in order to study the behaviour of triangular discrete plate and shell elements, also, membrane and shear locking are studied.

[STOLARSKI et al 1984; CARPENTER et al 1986] formulated flat shell elements with a membrane bending coupling device. [CARPENTER et al 1986] formulated four flat triangular shell elements based on the Merguerre shallow shell theory. The four elements combines the DKT plate element, with different membrane stiffness: the CST membrane element, the membrane element by [OLSON & BEARDEN 1979], and two versions of their own formulation.

[BATHE & HO 1981] showed the use of the DKT element in combination with the CST membrane element for the analysis of general shell structures. They studied shell problems using higher order shell elements versus the use of lower order flat shells. They introduced a fictitious stiffness for the in-plan rotational degrees of freedom.

A family of flat shell elements based on the semi-Loof shell elements by [IRONS 1974; IRONS & RAZZAQUE 1976] was developed. These elements have normal and parallel rotations at the so-called "Loof" nodes along each side. [MEEK & TAN 1986-a] developed a triangular flat element with "Loof" nodes comprising the LST membrane element and a plate bending element that has six nodes with three degrees of freedom (u, v, and w), and six Loof nodes with one rotation, along the edge. Also, [POULSEN & DAMKILDE 1996] presented a flat triangular shell element with Loof nods by a combination of a plate element of their own formulation and the LST membrane element.

Argyris and co-workers developed a series of triangular shear-deformable flat shell elements based on the patch test: the "TRUMP element" by [ARGYRIS et al 1977-a], "TRUNC element" by [ARGYRIS et al 1977-b; ARGYRIS et al 1986], "LACOT element" by [ARGYRIS & TENEK 1994] and the "TRIC element" by [ARGYRIS et al 1997; 1998, 1999], for the analysis of thin and moderately thick isotropic and composite plate and shell structures. Its formulation is based on the natural mode finite element method by [ARGYRIS et al 1979], a method that separates the pure deformational modes from the rigid body movements of the element.

[IDELSOHN 1981] studied and summarized the different thin shell theories. He presented a comparison of the deep shell theory against flat shell and shallow shell theories. The shallow shell theory is a very simple and effective way to build thin curved shell elements. "Donelle" shallow shell theory is expressed in curvilinear coordinates, while "Marguerre" shallow shell theory is expressed in Cartesian coordinates. In the shallow shell theory of Marguerre [MARGUERRE 1950], a curved surface is considered as a deformed configuration of a flat shell element. In this theory a point on the curved surface is represented by projection on the reference plane. Consequently resulting shell element is constructed by superposing membrane, bending, and coupling matrices as flat shell element. This theory takes into account bending coupling between membrane and bending strains via the coupling matrix, see also: [DEBONGNIE 1979; JETTEUR & FREY 1986; EL-KHALDI 1987, DJEGHABA 1990].

[MORLEY & MOULD 1987] studied the effect of the bending part of flat shells using a triangular flat shell element, in which, the plate bending element by [MORLEY 1971] has the three displacement *d.o.f* at the vertices, and the rotational degrees-of-freedom at mid-side. [KNIGHT 1997] compared the results of various flat shell elements including the DKT element, with inherent coupling between three modes of deformation: bending, extension and twist.

[BATOZ et al 1998-b; BATOZ et al 2000] presented a new quadrilateral discrete Kirchhoff flat shell element with 16 degrees of freedom (three displacements *u*, *v*, *w* at each corner, and a rotation at each mid-side node). The purpose of their work is to present a quadrilateral shell element with

relative balance of precision between the membrane and bending energies by combination of the rational quadrilateral membrane element by [ZHONG & ZENG 1996] and a quadrilateral discrete Kirchhoff plate bending element by [BATOZ et al 1998-a].

[SABOURIN & BRUNET 1995; ONÃTE & ZARATE 2000; GUO et al 2002] proposed a new family of rotation-free triangular plate/shell elements with translational *d.o.f* only, based on Kirchhoff thin plate theory. [CRISFIELD & TAN 2001] proposed a triangular and a quadrilateral shell elements with only out-of-plane bending rotation *d.o.f* at mid-side of element.

When the plate elements are based on the Kirchhoff theory, there is the problem of consistency between the displacements of the two adjacent non-coplanar elements, because the membrane field is often linearly interpolated while the bending field is cubic. If the Reissner-Mindlin plate theory is used, the continuity of displacements between adjacent flat shell elements no longer exists, because only C^0 continuity is required. In which, displacements and rotations are described independently and functions of the same order are used. Many flat shell elements with Reissner-Mindlin plate elements was presented: [MACNEAL 1978; NUKULCHAI 1979; BELYTSCHKO et al 1992; ONÃTE 1994; TENEK & HAGIWARA 1994; GROENWOLD & STANDER 1995; SYDENSTRICKER & LANDAU 1996].

Flat shell elements have been extended to solve nonlinear large displacement shell problems by: [ARGYRIS & DUNNE 1975; HORRIGMOE 1976, 1977; ARGYRIS et al 1977-a; HORRIGMOE & BERGAN 1978]. This subject has been developed by many authors: [CHEN 1979; MEEK & TAN 1986-b; RANKIN & BROGAN 1986; SCHOOP 1986-a, 1986-b; HSIAO 1987; TALBOT & DHATT 1987; FAFARD et al 1989; SCHOOP 1989; PERIC & OWEN 1991; PENG & CRISFIELD 1992; BOUT 1993; LIU & TO 1995; TO & LIU 1995; MEEK & RISTIC 1997; TO & WANG 1998-a; PROVIDAS & KATTIS 1999; SAMANTA & MUKHOPADHYAY 1999]. The wide range of numerical examples studied in these references indicate that flat finite elements may be very useful in the analysis of nonlinear shell problems.

Up to now, flat shell elements are used extensively in engineering practice. Many flat shell triangular elements have been presented for static, nonlinear, and dynamic analysis, such as: [HAMMERAND & KAPANIA 2000; GUO et al 2002; BATTINI & PACOSTE 2004; IZZUDDIN 2005; FELIPPA & HAUGEN 2005; BATTINI & PACOSTE 2006; LOMBOY et al 2009; AREIAS et al 2011; WU 2013; NGUYEN-VAN et al 2014; WANG & SUN 2014].

II-2. Flat Shell Elements in Non-Linear Updated Lagrangian Co-rotational Formulation

The simplicity and low cost of flat shell elements, make them suitable for nonlinear analysis of thin shell structures. Hence, it has been of considerable interest to investigate the geometric nonlinear behaviour of flat shell finite elements undergoing large displacements and large rotations. Large displacement geometrically nonlinear analysis formulations of flat shell finite elements were developed by [ARGYRIS & DUNNE 1975; ARGYRIS et al 1977-a; HORRIGMOE 1976, 1977]. Usually, geometrically nonlinear analysis implies large rotations. Since the nodal rotations are not vectorial quantities, an extension to the analysis of large rotations is not straightforward. Several large rotation formulations based on the total Lagrangian formulation have been presented, in which the large rotations of the shell director are described by using the large rotation matrix or by using nonlinear trigonometric functions [SURANA 1983; SIMO & FOX 1989; PARISCH 1991; IBRAHIMBEGOVIC 1994; BRANK et al 1995].

Nevertheless, if the rigid-body motion can be eliminated from the total displacements of the element, the deformational part of the element will always be small relative to the local element axis. This will then allow the use of the small displacement theory and thus circumvent the large rotation problem. Thus, the updated Lagrangian formulation has been predominantly used in the non-linear flat shell formulations available in the existing literature.

[ARGYRIS et al 1977-a] developed a three-node flat triangular shell element for nonlinear elastic stability. He presented a formulation denoted as the "natural mode technique", it is based on decomposing the displacements into rigid body and straining modes. [HORRIGMOE & BERGAN 1978] presented a large displacement analysis formulation of free-form shell structures using triangular and quadrilateral flat shell elements, based on the updated Lagrangian description with co-rotational coordinate system. Large rotations were handled by distinguishing between rigid body rotations and deformational rotations.

There exist a large literature concerning the geometrically nonlinear analysis of flat shells where a co-rotational reference configuration is used to eliminate large body translations and rotations. The majority of published works was dealing with triangular elements, in which, the membrane behaviour was represented by the CST or LST membrane elements. Thus, the resulting shell element has three displacements and two out of plane rotational degrees-of-freedoms at corner nodes, therefore only five degrees of freedom are needed at each node.

[CHEN 1979] presented a flat shell element by combination of the CST element and the plate element by [MORLEY 1971]. The shell element was extended for updated Lagrangian formulation

with a local coordinate system which rotates with the element. [BATHE & HO 1981] used a flat triangular shell by combining the CST and the DKT elements to present the updated Lagrangian description of shells using a co-rotational formulation to remove the rigid body rotations. [BELYTSCHKO et al 1984-b] presented a finite element formulation for the nonlinear large deflection and materially nonlinear response of impulsively loaded shells using a four-node quadrilateral element with single-point quadrature and a simple hourglass control. The geometric nonlinearities are treated by using a co-rotational description wherein a coordinate system that rotates with the material is embedded at the integration point.

[RANKIN & BROGAN 1986] presented a co-rotational procedure which is independent of the finite element employed. Their formulation is adequate for quadrilateral and triangular shell elements. They implemented their formulation for shells using two types of flat quadrilateral plate elements.

[HSIAO 1987] presented a flat triangular shell element comprising the CST and the DKT elements for geometrically nonlinear analysis of general shell structures by flat triangular shell elements. The Nonlinear formulation is based on the updated Lagrangian description. In order to remove the restriction of small rotation between two successive increments, he used a coordinate system that rotates and translates with the element's movement to eliminate rigid body motions.

[FAFARD et al 1989] presented two updated Lagrangian formulations for a six-node triangular flat shell element. The element results from combining the LST element and the 6-node plate element by [DHATT et al 1986]. In the first formulation, all nonlinearities are considered in the computation of stresses and the tangent stiffness matrix. However, in the second formulation, a linearized incremental formulation is calculated using co-rotational formulation.

The co-rotational framework for triangular shell elements has also been presented by [NOOR-OMID & RANKIN 1991], who presented the flat triangle shell element by [ARGYRIS et al 1979] for geometrically nonlinear analysis by removing the rigid body displacements from the total displacements. [PENG & CRISFIELD 1992] used a flat triangular element, which is a combination of the CST membrane element and the plate element by [HERRMANN 1967]. They used a co-rotational updated Lagrangian formulations for the geometric nonlinear analysis.

[MEEK & RISTIC 1997] presented the flat shell triangle with "Loof" nodes "DKL+LST" by [MEEK & TAN 1986-b] for geometrically nonlinear analysis using the updated Lagrangian co-rotational formulation. The element under consideration has six nodes with three degrees of freedom (*u*, *v*, and *w*) and six "Loof" nodes with one rotation, along the edge.

[PACOSTE 1998; ERIKSSON & PACOSTE 2002] introduced a different parameterisation of the finite global rotations based on the incremental rotation and rotation vectors.

In [YANG et al 1999] the rigid body rule for an initially stressed body undergoing rigid body rotations is applied to derive an approximate geometric stiffness matrix for a three-node triangular flat shell element.

[BATTINI & PACOSTE 2004] presented an investigation concerning the essentiality of choosing a co-rotational local frame invariant to the node ordering for triangular shell elements. A detailed description of co-rotational formulation was presented by [FELIPPA & HAUGEN 2005].

Specific issues concerning the choices of the local frame and the linear elements has been addressed in [BATTINI & PACOSTE 2006]. They investigated three-node triangular shell elements comprising one of the three following elements: the DKT plate element, the TRIC plate element by [ARGYRIS et al 1997], or the AQR Kirchhoff element by [MILITELLO & FELIPPA 1991], which is based on the assumed natural deviatoric strain (ANDES) formulation. The membrane element was one of the following: the CST element, Allman's triangle by [ALLMAN 1988-a], or the element by [FELIPPA 2003]. [BATTINI 2007] proposed the introduction of three modifications in the co-rotational framework for triangular shell elements. The first one is a simplified definition of the local rotations. The second one is a reduction of the number of local degrees of freedom from 18 to 15. The third and principal one concerns the parameterisation of the global finite rotations.

[WANG & SUN 2014] presented a 4-node "quadrilateral area coordinate method based" quadrilateral flat shell element for geometrically nonlinear analyses of thin and moderately thick laminated shell structures using the co-rotational formulation.

[IZZUDDIN 2005] presented a 4-node co-rotational quadrilateral flat shell element with hierarchic freedoms, where the two bisectors of the element diagonals and their cross-product were employed to define the co-rotational framework.

[LOMBOY et al 2009] presented a four-node shell element based on the quasi-conforming technique for geometric and material nonlinearity. The formulation was presented using an updated Lagrangian stress resultant co-rotational approach.

The wide range of numerical examples studied in the above mentioned works, indicate that flat shell finite elements when extended to geometrically nonlinear large displacements and rotations analysis using the updated Lagrangian co-rotational formulation, can be a very useful approach in the analysis of nonlinear shell problems.

II-3. Thin Plate Bending Elements

There has been considerable interest in the development of plate bending elements ever since their use became popular for representing the bending behaviour of shell elements. The first successful applications of the finite elements method to plate bending problems were published in 1960 by [ADINI & CLOUGH 1960; MELOSH 1961]. They were obtained using rectangular elements, none of which satisfied the requirements of compatibility and completeness. Until 1965 only rectangular elements gave satisfactory results. The major source of difficulties in plates is due to continuity requirements, where attaining normal rotations inter-element compatibility posed serious problems.

II-3.1. Triangular plate bending elements

Triangular plate bending elements are popular for discretizing irregular plates. They are most efficient for discretizing arbitrary shell geometries, so they have been attracting lots of interest. In the early sixties, [CLOUGH & TOCHER 1965] used the out of plane displacement and rotations to create a triangular element which satisfied the displacement compatibility conditions by dividing the main triangle into three sub-triangles. This procedure involved the use of three ten-term polynomials within each triangular region. The resulting plate element produced excellent results and was named the HCT element, after Hsieh, Clough and Tocher.

Area coordinates are used instead of Cartesian coordinates by [BAZELEY et al 1966; CHU & SCHNOBRICH 1970] to develop the first successful non-conforming elements. [BAZELEY et al 1966] element's has nine *d.o.f* with cubic displacement functions in terms of the nodal displacement and rotations. They found that this non-conforming element does not pass the patch test and does not converge toward the exact solution for some mesh configurations.

The constant bending moment triangle was reported by [HERRMANN 1967] based on the Reissner mixed-variational principle, and by [HELLAN 1967] in a similar work resulting in a positive non-definite stiffness matrix. [MORLEY 1971] presented a non-conforming but convergent constant bending moment triangle based on the Kirchhoff plate theory, with a quadratic displacement functions, using an equivalent displacement-based formulation. Thus, some authors tried to achieve full inter-element compatibility by using higher order polynomials. Conforming triangular plate element with 21 *d.o.f* "normal displacement, and its first and second derivatives at each vertex, and angular displacement at each mid-side point" was independently developed by several authors [ARGYRIS et al 1968; BOSSHARD 1968; BELL 1969].

The first application of mixed formulation was actually to the plate bending problem by [HERRMANN 1967] to derive a "mixed model" triangular element, involving simultaneous assumptions on displacements and stresses. Its formulation is based on Reisner's variational principle, which includes both the moments and the displacements as primary variables. [VISSER 1969] showed some improvements in the solution over the [HERRMANN 1967] element by adopting higher order polynomials.

[BERGAN 1980-a; BERGAN & NYGARD 1981] followed a non-traditional line of approach based on the so called "individual element test" to derive triangular plate bending elements based on the so called "free formulation".

The so-called discrete Kirchhoff technique (DKT) was successfully used to construct shear-locking-free plate bending finite elements by many authors: [DHATT 1970; FRIED 1973; FRIED & YANG 1973; FRIED 1974; BATOZ et al 1980; BATOZ 1982; GARNET & PIFKO 1983]. A successful (DKT) three-nodded triangular plate bending element with nine *d.o.f* (two rotations and a perpendicular displacement per node) which could be utilized for shell analysis, was developed in 1980 by [BATOZ et al 1980]. They developed three plate elements: the "DKT" element, based on the Discrete Kirchhoff Theory, the "HSM" element based on the Hybrid Stress Method, and the "SRI" element that includes transverse shear deformation based on Selective Reduced Integration scheme. The HSM element is based on the hybrid stress method. It has a linear distribution of bending moment in the interior, a cubic displacement variation along the edges, and a linear normal slope variation along the edges. The DKT element's formulation includes shear deformations based on the Mindlin theory. They considered transverse shear strain to be present in the element in the initial development and then removed the transverse shear strain terms by applying discrete Kirchhoff constraints in a discrete manner on the corner and mid-side nodes. The numerical behaviour of DKT elements was also studied and discussed, by [BATOZ 1982; BATOZ & LARDEUR 1989; BATOZ et al 2001]. The Kirchhoff assumptions are also introduced at the centroid of the element in addition to corner and mid-side nodes by [JEYACHANDRABOSE et al 1985] to get an efficient triangular plate element. [MEEK & TAN 1985] presented a six-node discrete Kirchhoff triangular plate bending element with "Loof nodes", in which, the transverse displacement is expressed in terms of the corner and mid-side nodal displacements, and "Loof" nodal rotations. The rotations of the shell normal about the local Cartesian coordinates, are interpolated in terms of the values at the "Loof" nodes. Then, they are eliminated in terms of the rotations of the shell normal about the edges at the "Loof" nodes by imposing Kirchhoff assumptions at discrete points.

[TESSLER & HUGHES 1985] presented a three-nodded non-conforming shear deformable element based on the Reissner-Mindlin theory in which the transverse displacements are expressed in terms of the standard quadratic basis in area coordinates. The use of a suitable shear correction factor results in an element that is applicable for both thick and thin plates.

[DHATT et al 1986] presented a six node discrete Kirchhoff element called DKTP with one order higher interpolations of the transverse displacement and normal rotations, than those used in the DKT element. However, this element present no remarkable improvement than the DKT element. [FELIPPA & BERGAN 1987] presented a successful triangular plate bending element based on the free formulation. They modified the cubic terms of the nine-term polynomial in area coordinates given by [BAZELEY et al 1966]. A simple successful modification of the element by [BAZELEY et al 1966] was introduced by [SPECHT 1988], in which, fourth order terms are used in place of the originally used cubic terms.

II-3-2. Quadrilateral plate bending elements

Quadrilateral plate bending elements are popular in analysing regular plates and regular shaped shell structures. They are usually used owing to their better performance with respect to convergence rates than that of triangular elements.

Early attempts to solve plate bending problems using finite elements method, was made by [ADINI & CLOUGH 1960] using a rectangular C^0 continuity non-conforming element. The rectangular element has 12 degrees of freedom and uses a complete third order polynomial aligned with the rectangle sides, plus two additional x^3y and xy^3 terms. The element satisfies completeness, but normal slope continuity is only maintained at corner nodes. This pioneering work, showed the difficulties in constructing C^1 conforming thin plate elements.

A rectangular plate element constructed with beam-like edge functions was proposed by [MELOSH 1961; ZIENKIEWICZ & CHEUNG 1964] using 12 term polynomials to represent compatible normal displacement. Again C^0 continuity was achieved but not C^1 except at corners.

Among the first successful conforming fully compatible plate elements, was the rectangular element having 16 *d.o.f* "four for each node" by [BOGNER et al 1965] through complete third order bi-cubic Hermitian interpolation functions. Numerical results indicate that in addition to exhibiting monotonic convergence, a good approximation of the displacement behaviour was achieved. A higher order conforming rectangular plate bending element with “Loof” nodes was presented and discussed by [GOPALACHARYULU 1973; IRONS 1973].

First arbitrary quadrilateral plate bending elements involved combining two or four triangular plate bending elements, and eliminating internal *d.o.f* by static condensation. [CLOUGH & FELIPPA 1968] presented a quadrilateral element built up from four triangles. They derived a compatible quadrilateral element having four corner nodes, only with three *d.o.f* each. [DE-VEUBEKE 1968] derived a compatible arbitrary quadrilateral finite element with 16 *d.o.f*. The quadrilateral is formed by a macro-assembly of four triangles by the two diagonals, condensing out the interior degrees of freedom and assuming a complete cubic polynomial displacement field within each triangle. The two diagonals are selected as a skew Cartesian coordinate system to develop the finite element fields.

[MACNEAL 1978] developed a four-node quadrilateral shell element using Iso-parametric shape functions. This element gives very good results for plate bending.

[ROBINSON & HAGGENMACHER 1979] developed a quadrilateral plate bending element based on stress parameters rather than displacement fields. This element gives very good results for plate bending. [BERGAN et al 1982; BERGAN & NYGARD 1984; BERGAN & WANG 1984] used the "individual element test" approach to derive rectangular and general quadrilateral plate bending elements with 12 *d.o.f* based on the so called "free formulation". [BATOZ & BEN-TAHAR 1982] developed a four node quadrilateral element based on the Discrete Kirchhoff theory. A quadratic approximations of the rotations are used to establish a new quadrilateral 8-*d.o.f* discrete Kirchhoff plate bending element by [BATOZ et al 1998-a], in which, the shear strain energy is neglected and the Kirchhoff hypothesis are introduced in a discrete manner on the corner and mid-side nodes.

The numerical behaviour of the Discrete Kirchhoff Theory elements of various shapes was studied and discussed by [BATOZ & BEN-TAHAR 1982; BATOZ & LARDEUR 1989; BATOZ et al 2001]. Other successful quadrilateral C^0 elements have been developed by [HUGHES et al 1977; PUGH et al 1978; CRISFIELD 1983-a; DVORKIN & BATHE 1984; PRATHAP 1984; BOOT & MOORE 1984].

II-4. Membrane elements

Membrane elements usually require only two degrees of freedom at each node, in which the state of strain is uniquely described in terms of the *u* and *v* in-plane translations at each node. This type of elements is simple to derive and has been widely used. Several formulations of triangular and quadrilateral membrane elements have been developed since the early stages of the finite element method. With the introduction of Iso-parametric elements, membrane elements received special attention and they were extensively used in the analysis of plane problems. The simplest form of plane membrane elements is the tree-noded constant-strain triangle "*CST*" that was first introduced by [TURNER et al 1956], and the four-noded bilinear quadrilateral element. [TAIG 1961] presented the first Iso-parametric version of the bilinear quadrilateral element. Unfortunately, these tow simple elements, were discovered to suffer from serious drawbacks of locking under a variety of situations. The "*CST*" does not perform well under bending load due to the presence of spurious shear strain, and it has a slow convergence rate. The four-noded quadrilateral also suffer from locking of elements of trapezoidal shape subjected to in-plane bending [PRATHAP 1985; MACNEAL 1987]. These difficulties, become much more severe with distorted mesh, see [LEE & BATHE 1993], or when studying incompressible or nearly incompressible materials.

Higher order elements were developed involving the mid-side nodes, the most famous is the six-node "*LST*" triangular element developed by [DE-VEUBEKE 1965]. A quadrilateral eight-node element was also developed. However, this class of elements is more computationally expensive compared to those with only corner nodes.

The problem of locking and other shortcomings of low order membrane elements with corner nodes, particularly parasitic shear in quadrilateral elements, has been the topic of many investigations using several approaches. Among the first works to formulate good finite elements for elasticity problems was by [WILSON et al 1973-a] to improve the performance of [TAIG & KERR 1964] quadrilateral element by introducing incompatible displacement modes. Subsequently, several contributions has been introduced by using different concepts:

- Reduced integration [ZIENKIEWICZ et al 1971; MALKUS & HUGHES 1978; FLANAGAN & BELYTSCHKO 1981; MURTHY 1994];
- Incompatible modes [WILSON et al 1973-a; TAYLOR et al 1976];
- Strain based approach [SABIR & SALHI 1986; SABIR & SFENDJI 1995; BELARBI & MAALAM 2005];

- Mixed/assumed stress methods [PIAN 1964; HERRMANN 1965; PIAN & SUMIHARA 1984; BELYTSCHKO et al 1984-a, 1985; YEO & LEE 1997];
- Assumed strain method [MACNEAL 1982; SIMO & HUGHES 1986; SIMO & RIFAI 1990; STOLARSKI & CHEN 1995-a; PILTNER & TAYLOR 1995];
- Hybrid finite elements [COOK & AL-ABDULLA 1969; COOK 1974-b, 1975; CHEN & CHEUNG 1987; JIN et al 1990; JIROUSEK & VENKATESH 1992; YEO & LEE 1997];
- Hu-Washizu principle and stabilization matrix [BELYTSCHKO & BACHRACH 1985];
- Energy orthogonal functions "FF" [BERGAN 1980-a; BERGAN & NYGÅRD 1984];
- Drilling degree of freedom [ALLMAN 1984; BERGAN & FELIPPA 1985].

We can also mention other contribution made by several researchers with different approaches, such as the individual element test [BERGAN & HANSSEN 1976], the quasi-conforming element [CHEN & TANG 1981; TANG et al 1984], the assumed natural strain [PARK & STANLEY 1986], the approach by [ZHONG & ZENG 1996], and the quadrilateral area coordinate method by [LONG et al 1999-a, 1999-b].

Note that, the enrichment of membrane elements using all above mentioned methods, and extension for nonlinear analysis, have been an active research area till now days, see for instance: [PILTNER & TAYLOR 1999; SZE & GHALI 2000; DOHRMANN et al 2000; XIAO-MING et al 2004; PILTNER & TAYLOR 2005; DU & CEN 2008; FELIPPA 2006; CAYLAK & MAHNKEN 2011; MOSTAFA et al 2013; YANG et al 2014].

The drilling *d.o.f* approach, improves the performances of membrane elements, through increasing the order of displacement polynomials by using nodal in-plane rotations as additional degrees of freedom. This will also provide a desirable membrane component that provides the sixth *d.o.f* in a flat shell element. This approach, leads to a class of finite elements that performs better than those above mentioned elements without increasing the number of element nodes.

The idea of including in-plane normal-rotation degree of freedom at corner nodes of membrane elements is an old one. However, early attempts [BERGAN 1967; TOCHER & HARTZ 1967; HOLAND & BERGAN 1968; DUNGAR & SEVERN 1969; MACLEOD 1969; LYONS 1970; ROBINSON 1980; MOHR 1982; BERGAN & NYGÅRD 1984] were unsuccessful. Successful progress in this direction was first made by [ALLMAN 1984], who introduced the concept of the vertex rotation, and [BERGAN & FELIPPA 1985] using the so-called free formulation, also by [COOK 1986] who gave a geometrical interpolation of mid-side transverse displacement of quadratic elements in relation to vertex rotations.

[ALLMAN 1984], in a pioneering work, introduced the in-plane rotational *d.o.f* in the constant strain triangle (CST) by choosing the normal and tangential displacement components defined in terms of triangular area co-ordinates to be quadratic and linear functions respectively. This simple formulation radically improved the in-plane behaviour of this element. However, the element suffer from a zero energy mode. This shortcoming is removed in a later work [ALLMAN 1988-a] using a cubic polynomial displacement field. [BERGAN & FELIPPA 1985] in an independent work introduced the in-plane rotational *d.o.f* in the constant strain triangle using the free formulation of [BERGAN & NYGÅRD 1984].

[CARPENTER et al 1985] presented a triangular element with nodal in-plane rotations introduced by the use of a cubic constraint functions along each side of the triangle. The stiffness matrix was evaluated using a reduced integration scheme. This under integrated element gave better results compared to the fully integrated element, but the reduced order integration resulted in spurious zero energy modes. The three "spurious modes" of [CARPENTER et al 1985] element's were eliminated later by [FISH & BELYTSCHKO 1992] using a stabilization scheme.

Incorporating the in-plane rotation as an additional degree of freedom has also extended to quadrilateral membrane elements. [COOK 1986; ALLMAN 1988-b] independently presented quadrilateral elements with drilling *d.o.f* derived from the Allman's triangle. Since then, many similar methods have been proposed for triangular and quadrilateral elements: [COOK 1987; MACNEAL & HARDER 1988; JAAMEI 1988; FREY 1989; MACNEAL 1989; COOK 1990, 1991; ALLMAN 1993].

The concept proposed by Allman represents, even today, the theoretical support for the development of several triangular and quadrangular finite elements. This type of elements, however, suffers from two major drawbacks. The first one is the rank deficiency, this problem could be controlled by applying a stabilization mechanism based on the inclusion of an additional energy penalty stiffness matrix obtained by introducing a relation between the finite element global rotation and the nodal rotations, see: [MACNEAL & HARDER 1988; COOK 1993, 1994]. The second shortcoming, is the use of the vertex rotation, which does not represent the true in-plane rotation.

The work on membrane elements with drilling rotation has been pursued seeking for two objectives: having elements with true drilling rotation, or having looking free with high convergence rate elements even with vertex rotation.

In an attempt to interpolate the true drilling rotation, [SABIR 1985] using strain based approach, derived rectangular and triangular non-conforming elements incorporating the in-plane rotation

calculated through continuum mechanics. Recently [BELARBI & BOUREZANE 2005; HAMADI & BELARBI 2006; REBIAI & BELOUNAR 20013, 2014] used the same method in their works. However, numerical resets show that only rectangular elements provide good results.

The problem of true drilling rotation has also treated by Ibrahimbegovic and co-workers [IBRAHIMBEGOVIC et al 1990; IBRAHIMBEGOVIC & WILSON 1991-a] presenting a class of membrane elements with drilling *d.o.f* based on a variational formulation initially suggested by [HUGHES & BREZZI 1989; HUGHES et al 1989], in which, The kinematic variables of displacement and rotation are separated by introducing both symmetric field for displacement and skew-symmetric field for drilling rotation. This approach employs an independent rotation field and Allman-type shape functions to achieve quadrilateral membrane elements incorporating drilling rotation, with a high order of accuracy. The relation between drilling *d.o.f* and translational displacement is established through a penalty function term, which will modify drilling *d.o.f* to close true rotation, see also [SIMO et al 1992-a; IURA & ATLURI 1992; CAZZANI & ATLURI 1993; IBRAHIMBEGOVIC 1993]. On the same basis, a class of finite elements with drilling *d.o.f* is developed using the incompatible modes method [IBRAHIMBEGOVIC 1990; WILSON & IBRAHIMBEGOVIC 1990; IBRAHIMBEGOVIC & FREY 1992, 1993]. Also, Following the works by Hughes and by Allman, triangular three node elements has derived by [FISH & BELYTSCHKO 1992; CHINOSI et al 1997].

Using the context of the assumed natural deviatoric strain (ANDES), [FELIPPA 2003] studied the formulation of triangular membrane elements with the drilling degrees of freedom, using the earlier work on the extended free formulation (EFF) by [ALVIN et al 1992; MILITELLO & FELIPPA 1991; FELIPPA & MILITELLO 1992; FELIPPA & ALEXANDER 1992]. These elements require extra-free parameters to be chosen to optimize the element performances.

Due the absence of an explicit methodology of incorporating the true drilling rotation, almost, all existing membrane elements with in-plane rotational *d.o.f* are formulated using the vertex rotation. Even though they does not represent the true drilling rotational *d.o.f*, elements with vertex rotation are widely used to avoid shear locking, and due their high convergences rate. Thus, triangular and quadrilateral membrane element with corner rotational *d.o.f* has been formulated in a widely varying manners, for linear analysis.

[YUQIU & YIN 1994-a] presented two generalized conforming triangular membrane elements with rigid vertex rotations, and in [YUQIU & YIN 1994-b] they suggested a new definition of vertex rigid rotation and developed corresponding two new generalized conforming quadrilateral membrane elements. The elements' formulation is based on displacement superposition, in which, the in-

plane displacements are decomposed into a regular low-order components, and a higher-order incomplete polynomials components due the nodal in-plane rotations.

An effective way to eliminate locking and develop high-performance finite elements, is the Mixed, Hellinger-Reissner functional, and assumed stress method. This class of elements generally shows a good behaviour in terms of displacements and stresses and found to be less sensitivity to mesh distortion. [PIAN & SUMIHARA 1984] presented a quadrilateral element with four nodes and five stress parameters. [COOK 1987] presented a plane triangular element with rotational *d.o.f*, formulated using the assumed-stress hybrid method based on independent descriptions of stresses by three hybrid constant stress sub-elements, and the drilling *d.o.f* are incorporated in the interpolation of displacements defined on the boundary. [SZE et al 1992] proposed a mixed quadrilateral element with drilling *d.o.f* using orthogonal stress modes and by using Allman's interpolation scheme. [CAZZANI & ATLURI 1993] presented a family of new four-noded membrane elements with drilling degrees of freedom using unsymmetric assumed stresses derived from a mixed variational principle originally formulated for finite strain analysis.

[TO & LIU 1994] presented three variations of triangular plane stress elements that are built on the basis of Allman Triangle, while effort has been directed to include the drilling *d.o.f* and couple them with in-plane displacements based on the Hellinger-Reissner hybrid strain formulation. [CANNAROZZI & CANNAROZZI 1995] proposed the use of self-equilibrated stress fields based on Airy solutions in Cartesian coordinates. He derived a mixed four-node element with nine stress parameters, and compatible displacements interpolation. Other Mixed/Hybrid membrane elements using the Allman-type shape functions have also presented with different degrees of success [YUNUS 1988; YUNUS et al 1989; AMINPOUR 1992-a, 1992-b; SZE & GHALI 1993; DI & RAMM 1994; RENGARAJAN et al 1995; GEYER & GROENWOLD 2002; BILOTTA & CASCIARO 2002; GROENWOLD et al 2004].

[GROENWOLD & STANDER 1995] presented the development of "five point quadrature" quadrilateral shell element, through the introduction of a 'soft' higher-order deformation mode. [ZHU & ZACHARIA 1996] presented the development of "one point quadrature" quadrilateral shell element with drilling degrees of freedom.

Hu-Washizu variational principle and Enhanced Strain method are used resulting with good class of elements. [PIMPINELLI 2004] studied a four-node quadrilateral membrane with drilling degrees of freedom, in which the enhanced strain and enhanced rotation fields are included. [PILTNER & TAYLOR 2000] used three sets of enhanced strain functions for the improvement of the three-node Allman's triangle.

Many other works on drilling degree of freedom have been presented, for a summary, see references: [CARPENTER et al 1985; LEE & YOO 1988; HARRIS & BARTHOLOMEW 1989; LIN et al 1990; PIANCASTELLI 1992; YEH & CHEN 1993; SUN et al 1997; LI & ZHAN 2000; XUE-ZHANG et al 2002; ZHANXIN & ZHONGQI 2002; YANG & ZHANG 2002].

In more recent works, presented in the last decade: [LONG et al 2006] presented a numerical investigation into the effect of penalty parameters in elements with drilling degrees of freedom and penalized equilibrium. They investigated the penalty parameter relates the in-plane translations to drilling rotations, and the penalty parameter results due to enforcement of stress equilibrium in assumed stress elements with drilling rotations. [WISNIEWSKI & TURSKA 2006] presented the formulation of a four-node quadrilateral element based on Allman shape functions via the Enhanced Assumed Displacement Gradient (EADG) method. [TIAN & YAGAWA 2007] presented triangular elements, in which, the Allman's rotations are presented in the partition of unity form. [CHOO et al 2006, CHOI et al 2006] introduced drilling *d.o.f* to the hybrid Trefftz quadrilateral and triangular plane elements by using Allman's quadratic displacement.

[CHEN et al 2004; PRATHAP & SENTHILKUMAR 2008] presented quadrilateral elements based on area coordinates in order to reduce the sensitivity to mesh distortion. See also [RAJENDRAN 2010]. [KUGLER et al 2010] presented a new quadrilateral membrane element with drilling rotation. They derived a variational principle employing an independent rotational field similar to that obtained by Hughes and Brezzi. [HUANG et al 2010] presented a modified version of the original Allman triangle in an attempt to involve the true drilling rotation instead of vertex rotation. [CEN et al 2011] derived a 4-node hybrid stress-function (HS-F) membrane element with drilling d.o.f. stress fields are derived from the first seven fundamental analytical solutions of Airy stress function, and the assumed displacements along element boundaries employ compatible mode of Allman functions.

[MOREIRA & RODRIGUES 2011] presented a quadrilateral membrane finite element with nodal drilling rotations based on a displacement field formulation, using a conforming interpolation operator, and contains an independent rotational field that is enhanced through the application of an incompatible interpolation operator.

[MADEO et al 2012] Presented a mixed quadrilateral four node membrane finite element based on Allman interpolation, in which, displacement and stress interpolations are defined by 12 kinematical *d.o.f* and 9 stress parameters. [PAJAND & KARKON 2013] Derived a four-node hybrid stress membrane element with drilling degrees of freedom based on hybrid variational principle and analytical solution. The stress fields of the element are found from analytical solution of bi-harmonic compatibility equation.

II-5. Flat Shell Elements with drilling rotational degree of freedom

In the formulation of a flat shell element, the relative balance of precision between the membrane and bending energies is an advantage. This is not the case with flat shell elements with conventional membrane elements, where the bending part is relatively better than the membrane one. [KNOWLES et al 1976] observed that in general, adequate performance can be obtained when either membrane predominant or bending predominant. However, when the membrane and bending stiffness are strongly coupled, the performance is extremely poor.

Conventional shell elements have three translational and two rotational degrees of freedom at a node. This results in many difficulties of model construction and numerical ill-conditioning when it is used to represent a three-dimensional geometry, because there is a missing rotation degree-of-freedom. Moreover, due to the absence of in-plane drilling rotations, an artificial stiffness needs to be added in order to ensure numerical stability in shell analysis. Hence for, the flat-shell formulation must provide a complete description of the nodal translation and rotation fields, which necessitate the introduction of an additional degree of freedom in the two dimensional plane element, allowing the definition of the six spatial degrees-of-freedom for each node of the finite element. That additional degree of freedom can be presented by the in-plane rotation or "drilling rotation" of the plane membrane element.

For a flat shell element, the inclusion of drilling degrees of freedom is much simpler than the case of curved shell elements. Thus, earlier developments of membrane elements with in-plane rotational *d.o.f* were followed by several contributions to introduce them to be a part of both triangular and quadrilateral flat shell elements [OLSON & BEARDEN 1979; BATHE & HO 1981; BERGAN & NYGARD 1986; BERNADOU & TROUVÉ 1989; CARPENTER et al 1985, 1986; ALLMAN 1988-c; ALLMAN 1991; COOK 1993, 1994].

[BATHE & HO 1981] presented a flat shell element based on the DKT plate element in combination with the CST element for linear and nonlinear analysis of general shell structures. They used a fictitious rotational stiffness in order to remove the singularity of the assembled stiffness matrix. [CARPENTER et al 1985] developed an 18 *d.o.f* triangular flat shell element formulated using the DKT bending element and a new membrane stress formulation with nodal in-plane rotations, introduced by the use of a cubic constraint function along each side of the triangle with one point integration method. This under integrated element gave better results compared to the fully integrated element, but the reduced order integration resulted in spurious zero energy modes. [TAYLOR & SIMO 1985] applied the same basic approach as presented in [CARPENTER et al 1985] to develop a DKQ based quadrilateral element. However, for many shell geometries, the flat

quadrilateral element does not give accurate results. [BERGAN & NYGARD 1986] developed a triangular flat thin shell element with in-plane rotational d.o.f based on the free-formulation theory.

[JETTEUR 1986; JETTEUR 1987; JAAMEI 1988; JAAMEI et al 1988; FREY 1989] developed and studied some quadrilateral flat shell elements based on Marguerre's shallow shell theory. The bending behaviour was the DKQ discrete Kirchhoff element, and the membrane behaviour was a biquadratic incomplete quadrilateral Allman-type element with in-plane rotational *d.o.f.*

[ORAL & BARUT 1991] combined the membrane element by [ALLMAN 1988-a] and the plate bending element by [TESSLER & HUGHES 1985], to produce a three-node flat shell element.

[CHEN 1992] presented a numerical assessment of the triangular membrane element with cubic interpolation functions of [ALLMAN 1988-a] by examining the performance of the element when combined with a triangular plate bending element in a general shell analyses. He also compared its performances with a shell element comprising the CST element by combining them with the DKT element. He also compared the performance of the reduced order (4 integration points) and the fully integrated (6 integration points) elements. He presented several benchmark problems to demonstrate that the shell element with Allman's triangle was more efficient.

[ERTAS et al 1992] presented a triangular flat shell element for the static analysis of anisotropic shells. The element is a combination of the DKT and a membrane similar to the Allman triangle. Membrane-bending coupling is brought about as a result of anisotropic material properties.

[FISH & BELYTSCHKO 1992] presented the stabilized, one-point integrated triangular element with drilling rotation by [CARPENTER et al 1985] for linear and buckling analysis. They found that in some cases, the under integrated element gave better results than the fully integrated element even for coarse meshes, but the element was too soft for finer meshes.

[AMINPOUR 1992-a, 1992-b] presented the formulation of some 4-node assumed-stress hybrid 4-node shell elements with drilling degrees of freedom. [ALLMAN 1988-c, 1994; COOK 1993] presented triangular flat shell finite elements for the analysis of general thin shells with in-plane rotational *d.o.f.* In addition, they discusses rather comprehensively the ability of flat elements to represent curved shells.

[TO & LIU 1994] Presented and studied series of three-node flat triangular shell elements with in-plane rotations. The elements are based on the Hellinger-Reissner hybrid strain formulation. Each of these elements is considered as a combination of a degenerated triangular bending element. The plane stress elements are built on the basis of Allman Triangle using the Hellinger-Reissner hybrid strain formulation. Comparing the performance of the three Allman-based elements and the three

CST-based elements, Allman-based elements play a crucial role in achieving satisfactory accuracy and convergence of shell elements. Later [TO & WANG 1998-b] developed the Hybrid strain-based element by [TO & LIU 1994] for laminated plates and shells.

[CHINOSI 1994; CHINOSI et al 1997] discussed the combination of membrane element with drilling rotation with plate bending element resulting in a shell elements with six degrees of freedom each node. They also constructed and tested a new shell element with drilling *d.o.f.*

[ZHU & ZACHARIA 1996] discussed the development of "one point quadrature" quadrilateral shell element with drilling degrees of freedom. They presented a four-node element based on the degenerated continuum approach. All locking phenomena (such as transverse shear, in-plane shear and membrane locking) are controlled by an assumed strain method. Also, a physical stabilization approach for control of spurious zero-energy modes is proposed.

[ZHANG et al 1998] developed a generalized conforming three-node flat shell element with drilling *d.o.f*. [YANG et al 1999] presented a triangular flat shell element, which is a combination of [COOK 1991] triangular membrane element and [BATOZ et al 1980] triangular plate element.

These works show that the introduction of drilling rotational *d.o.f* in flat shell elements have lessened the difficulty of ridge-like intersections. However, the presence of the drilling *d.o.f* may also cause undesirable locking phenomena in the shell analysis, see [COOK 1993].

Several works on flat triangular shell elements with drilling rotations, which use Allman-type displacement field, has shown over-stiffness when dealing with problems where the pure bending is the main deformation mode due membrane locking. [COOK 1993; PROVIDAS & KATTIS 2000] states that flat shell finite elements with drilling rotation connectors when used as components in flat shell elements exhibits membrane locking in certain deformation modes, especially in linear stress situation. [PROVIDAS & KATTIS 2000] presented and compared tow flat shell finite elements. The First element is a combination of the CST which includes artificial rotational stiffness with a three-node bending element by [ALLMAN 1970]. The second one is the incompatible cubic triangle of Allman with rotational *d.o.f* by [ALLMAN 1988-a] which is also combined with the same bending element. They stated that the artificial rotational *d.o.f* is found to be very effective when the artificial rotational stiffness multiplier is a small value (10^{-8}).

[ALLMAN & MORLEY 2000] presented a three-noded flat triangle comprising a plate bending element with constant approximation of the bending moment and the CST membrane element. [SYDENSTRICKER & LANDAU 2000] used some discrete triangular plate elements to form flat shells with and without drilling rotation. They studied both membrane and shear locking in flat

shells with drilling rotation. [TESSLER 2000; TESSLER & MOHR 2000] studied interdependent interpolations for membrane and bending kinematics of three-node triangular element with drilling rotation for a higher-order plate theory. [ZENGJIE & WANJI 2003] proposed flat shell elements that were formed through assembling refined triangular discrete Mindlin plate elements [WANJI & CHEUNG 2001] and the CST with a fictitious stiffness for the first element, or the Allman's triangle for the second element. They studied the singularity of the stiffness matrix and membrane locking for the presented elements.

Also, 4-node flat shell elements with drilling rotation which use the Allman-type displacement show a tendency toward membrane locking especially when coarse meshes are used despite their general good performance [COOK 1994; GROENWOLD & STANDER 1995; CHOI et al 1999].

[COOK 1994] presented a four-node quadrilateral shell element with 24 *d.o.f* including the drilling degrees of freedom with a device for membrane-bending coupling. The author stated that numerical results are good but the element is not the best available four-node shell element.

Many technics have been proposed to alleviate membrane drilling rotation locking. [CHOI & LEE 2003] Studied the membrane locking of flat shells with drilling rotation and presented an efficient scheme to remove the membrane locking of four-node quadrilateral flat shell elements by adding of hierarchical non-conforming modes to the displacement fields of membrane component of the flat shell element. A series of flat shell elements are established by combination of non-conforming membrane and plate-bending elements which show no signs of membrane locking even though the coarse meshes are used. [CHEN & CEN 2003] proposed a triangular flat shell element based on a thin-thick plate bending element with semi-Loof constraint and a generalised conforming membrane element with rotational *d.o.f*. One point quadrature with stabilisation is used for both elements to avoid membrane locking. Also, [GEYER & GROENWOLD 2003] used a modified reduced integration to overcome undesirable locking actions in flat shell finite elements based on assumed stress membrane finite elements with drilling degrees of freedom.

[KIM et al 2003] presented two Quasi-conforming four-node stress-resultant shell elements based on the assumed strain method. The rotational degree of freedom about the shell normal is included using the quasi-conforming formulation. [ZHANG & KIM 2005-a] presented a refined non-conforming triangular shell element comprising a conforming triangle membrane element with drilling degrees of freedom in Cartesian coordinates by [YANG & ZHANG 2002] and the refined non-conforming triangular plate-bending element by [CHEUNG & CHEN 1995], in which Kirchhoff kinematic assumption was adopted. Membrane locking is avoided in the proposed element due to the application of stabilization scheme. They employed a coupled displacement constraint method

proposed by [CHEN & CHEUNG 1999] to ensure convergence and improve accuracy of the present element for thin shell analysis.

[NGUYEN-VAN et al 2009] presented a novel smoothed quadrilateral flat element with drilling rotations for composite plate/shell structures. The element is developed by incorporating a strain smoothing technique into a flat shell element comprising the membrane element by [IBRAHIMBEGOVIC et al 1990] and a four-node Mindlin–Reissner type plate element.

[LONG et al 2009] Investigated the effects of selected membrane, plate and flat shell finite element formulations on optimal topologies. Two membrane components are considered. The first is a standard four-node bilinear quadrilateral, and the other is a four-node element with in-plane rotations. The plate elements include the discrete Kirchhoff quadrilateral (DKQ) element and two Mindlin–Reissner-based elements, one employing selective reduced integration (SRI), and the other an assumed natural strain (ANS) formulation. They found that optimal topologies computed with elements with drilling degrees of freedom performs better. [MOREIRA & RODRIGUES 2011] presented a non-conforming quadrilateral flat shell finite element with drilling *d.o.f.* The element is a combination of a new nonconforming membrane element with rotational *d.o.f* and the plate finite element *Q4γ* based on the assumed natural strain by [BATOZ & DHATT 1990].

[ZHANG et al 2011] developed a flat shell element through combining the (ANDES) element with optimal parameters by [FELIPPA 2003] and the plate element by [WANJI & CHEUNG 2001], they showed that the element worked well in both thin and thick shell problems.

[WANG & HU 2012] proposed two quasi-conforming triangular flat shell elements using Timoshenko's beam function. One element was attached with fictitious stiffness, while an Allman-type drilling rotation was attached to the second element. The results shows that the drilling rotation locking phenomenon occurred on the second element, but not on the first one.

[SHIN & LEE 2014] proposed a three-node triangular flat shell element based on the assumed natural deviatoric strain (ANDES) formulation by [FELIPPA & MILITELLO 1992] for membrane, and the discrete Kirchhoff-Mindlin triangle plate element by [KATILI 1993-a] for bending. The (ANDES) template must determine the included free parameters. The numerical results demonstrate that the optimal parameters proposed by Felippa, provide a behaviour that is too stiff for a flat shell element. The strain smoothing technique was used for the basic stiffness of the (ANDES) element in order to further enhance the membrane behaviour. The drilling rotation locking problem is primarily caused by the higher order stiffness of the membrane element, in order to avoid this, the free parameter value that scales the higher order stiffness was modified.

II-5.1. Flat Shells with Drilling Rotation for Nonlinear Analysis

Many flat shell finite elements with drilling rotation have been applied to non-linear analysis of shells. Usually non-linear numerical tests are computed for general shell structures, but values of drilling rotations are not reported.

[BERGAN & NYGARD 1986] developed and presented a triangular flat thin shell element with in-plane rotational *d.o.f* based on the free-formulation theory for linear and geometrically nonlinear analysis. [JETTEUR & FREY 1986; JETTEUR 1987; JAAMEI et al 1987, 1989] developed and studied four-node flat shells with six *d.o.f* based on the DKQ plate element in Marguerre's shallow shells theory for geometrically nonlinear analysis. The nonlinear kinematics are dealt with through the total co-rotational Lagrangian formulation. Rotations are assumed to be small. Only examples of curved shell geometries are studied.

[LEE & YOO 1988] developed a new triangular membrane element with in-plane rotational *d.o.f* and combined it with a plate bending element to formulate a shell element. Large displacement analysis based on the updated Lagrangian formulation is presented.

[SIMO et al 1989; FOX & SIMO 1992] presented a drilling rotation formulation for stress resultant geometrically exact shell model. [ORAL & BARUT 1991] combined the membrane element by [ALLMAN 1988-a] and the plate bending element by [TESSLER & HUGHES 1985] and applied this element for geometrically nonlinear large deflection and instability analysis of shells.

[FISH & BELYTSCHKO 1992] presented the stabilized, one-point integrated triangular element with drilling rotation by [CARPENTER et al 1985] for buckling analysis. They also employed a one-point integration scheme to compute the geometric stiffness matrix in an attempt to soften the element. [GRUTTMANN et al 1992] presented a nonlinear 4-noded quadrilateral shell element with drilling degrees of freedom. The membrane element formulation was based on the introduction of a mixed functional with independent in-plane rotation field and skew-symmetric part of membrane forces. They presented only one in-plane example consists of in-plane bending of a beam under tip loading for large displacement analysis.

[IBRAHIMBEGOVIC 1993; IBRAHIMBEGOVIC & FREY 1993] extended The Hughes-Brezzi mixed variational formulation, for plane geometrically non-linear elements with in-plane drilling rotation. [IBRAHIMBEGOVIC 1993] Used the mixed finite element method to construct a four-node membrane element with drilling rotations for geometrically nonlinear elasticity. He presented in-plane bending of a cantilever under end moment for nonlinear analysis. The nonlinear behaviour of the presented element was a bit stiff even with a fine mesh.

[IBRAHIMBEGOVIC 1994; IBRAHIMBEGOVIC & FREY 1994, 1995] presented a consistent theoretical framework for a stress resultant geometrically nonlinear shell theory with drilling *d.o.f*. They constructed a quadrilateral membrane element with drilling rotations with incompatible modes for geometrically nonlinear analysis. They presented in-plane bending of a roll-up of a cantilever with free-end moment, and a cantilever under free-end force.

[MADENCI & BARUT 1994] presented an updated Lagrangian formulation for geometrically nonlinear analysis using a flat triangular shell element. The element is a combination of the triangular membrane element with drilling rotation by [BERGAN & FELIPPA 1985] and the plate element by [FELIPPA & BERGAN 1987] which are based on the free-formulation.

[RENGARAJAN et al 1995] developed an assumed-stress hybrid shell element with drilling *d.o.f* for buckling and free vibration analyses. [ZHU & ZACHARIA 1996] presented the development of a new quadrilateral shell element with drilling degrees of freedom using one point quadrature, and used this element for the analysis of nonlinear geometrical and material problems. Since they used a rate formulation for non-linear continuum mechanics, the rate forms of variational formulation are linear. Therefore, Hughes-Brezzi variational principle based on linear formulation can be directly extended to the non-linear element within the context of rate formulation. The presented element was a four-node quadrilateral based on the degenerated continuum approach. They presented a cantilever beam subjected to an end moment modelled using (2 x 24) in-plane elements mesh for nonlinear analysis.

Geometrically nonlinear analysis of composite plates and shells based on an updated Lagrangian co-rotational formulation using triangular flat shell element is presented by [KAPANIA & MOHAN 1996] comprising membrane triangle with drilling *d.o.f*, and the DKT plate bending element. Also [MOHAN & KAPANIA 1997, 1998] presented flat triangular shell finite element for geometrically nonlinear analysis of composite and laminated shells using the updated Lagrangian formulation.

[PACOSTE 1998] formulated and studied three flat triangular shell elements. The elements have three nodes combining either the CST element, or Allman's triangle by [ALLMAN 1988-a] membrane elements, with the plate bending element by [ARGYRIS & TENEK 1993]. The co-rotational approach was used to describe the motion of the structure. In the formulation of the membrane stiffness of the membrane element by [ALLMAN 1988-a], reduced integration was used to alleviate the effects of membrane locking. The result was an improvement in the accuracy, for membrane dominated problems compared to the elements combines the CST element. No details handling the drilling rotation were presented. The load-displacement curves for a cantilever beam subjected to an in-plane end force was presented.

[YANG et al 1999] presented a flat triangular shell element for non-linear analysis. It is a combination of [COOK 1991] triangular membrane element and [BATOZ et al 1980] triangular plate bending element. A three-node generalized conforming flat shell element with drilling degrees of freedom was developed by [ZHANG et al 1998] for geometrically nonlinear analysis.

[SAMANTA & MUKHOPADHYAY 1999] conducted geometric nonlinear static analysis of shallow and deep stiffened shells on the basis of a combination of Allman's plane stress triangle and Discrete Kirchhoff triangle (DKT) plate bending element. The nonlinear formulation is based on the total Lagrangian description. The nonlinear membrane stiffness was taken into account. [CHEN & CEN 2003] proposed a triangular flat shell element based on a plate element with "semi-Loof" constraint and a generalised conforming membrane element with rotational *d.o.f*. One point quadrature with stabilisation is used for both elements to avoid membrane locking. The updated Lagrangian formulation is used for the geometrically nonlinear analysis of plates and shells.

[PARK & OH 2004] presented a new four-node quadrilateral shell element with drilling rotation to improve accuracy and efficiency of springback simulation base on the rate form equations.

[LEE & WOOH 2004] studied the analysis of folded structures and box beams by using drilling degree of freedom. The obtained results show good agreement with the semi analytical solutions.

[ZHANG & KIM 2005-a] presented a refined non-conforming triangular shell element for linear and geometrically nonlinear analysis of plates and shells. The element is a combination of a conforming triangular membrane element with drilling degrees of freedom in Cartesian coordinates by [YANG & ZHANG 2002] and the refined non-conforming triangular plate-bending element by [CHEUNG & CHEN 1995]. The geometrically nonlinear analysis was based on the updated Lagrangian formulation. The presented examples was for plates and shell geometries only.

[WISNIEWSKI & TURSKA 2006] presented a quadrilateral membrane element based on (EADG) with Allman shape functions for finite drilling rotations. They presented two in-plane nonlinear examples with fine mesh.

[BATTINI & PACOSTE 2006] Investigated three-node triangular shell elements, in which, the membrane element is one of the following: the CST element, Allman's triangle by [ALLMAN 1988-a], or the membrane element with rotational *d.o.f* by [FELIPPA 2003].

[KHOSRAVI et al 2007] developed a triangular flat shell finite element for the geometrically nonlinear analysis of thin shell structures using the co-rotational approach. The flat shell element is developed by combining the DKT plate bending element by [BATOZ et al 1980] and the optimal membrane triangle by [FELIPPA 2003]. Later, [KHOSRAVI et al 2008] developed a triangular flat

shell finite element for the geometrically nonlinear analysis of laminated composite structures using the co-rotational approach. The flat shell element is developed by combining the discrete Kirchhoff-Mindlin plate bending element by [KATILI 1993-a] and the optimal membrane triangle by [FELIPPA 2003]. The membrane-bending coupling effect of composite laminates is incorporated in the formulation. The in-plane geometric stiffness was evaluated using the LST membrane element shape functions. However in-plane co-rotational formulation was not presented. Also no in-plane examples were reported.

[KANG et al 2009] presented a new four-node quadrilateral and three-node triangular flat shell elements based on Kirchhoff assumptions and generalized conforming theory for linear and geometrically nonlinear analysis using update Lagrangian formulation. However, the study was not interested on the in-plane behaviour (no in-plane examples were presented).

[ALMEIDA & AWRUCH 2011] presented a facet triangular shell element obtained by combining the membrane element by [FELIPPA 2003] and a simple plate element developed by [ZHANG & KIM 2005-b] to nonlinear transient dynamic analysis of laminated composite structures based on the co-rotational formulation.

[YANG & XIA 2012-a] presented a triangular flat thin shell element with three nodes and 18 *d.o.f*, constructed by combination of the optimal membrane element by [FELIPPA 2003] and the DKT plate element. The element was extended to the geometric nonlinear analysis of thin shells with large rotation and small strain. [ZAGARI et al 2013] presented a geometrically nonlinear finite element analysis of folded-plate and shell structures based on the co-rotational approach. The shell element used is the flat shell quadrilateral element with four nodes and 6 *d.o.f* per node proposed by [MADEO et al 2012], which is a mixed element, based on the Reissner–Mindlin plate theory, with an Allman-like quadratic interpolation for displacements and an equilibrated isostatic interpolation for the stress resultants.

[BARBERO et al 2014] presented a quadrilateral shell element for static linear and buckling analysis of folded laminated composite structures. The shell element was comprising the quadrilateral by [ALLMAN 1988-b] and a hybrid mixed formulation plate bending element.

In the above mentioned works that presents flat shells with drilling rotation for geometrically nonlinear analysis, the formulation of nonlinear behaviour is made by the same manner of conventional flat shells, in which the in-plane displacements are considered as infinitesimal. So their derivatives are small, and hence their quadratic variations can be neglected. Thus, only the second degree terms in the deflection were retained. The contribution of the geometrical or "initial

stress" matrix related to the in-plane displacement field is excluded. So, the in-plane stiffness matrix is often taken to be just equal to its linear matrix. This treatment could has no effect on the accuracy of the finite element solution, as reported by many authors, but will affect the convergence rate of the equilibrium-iteration scheme. Moreover, the in-plane nonlinear formulation was not presented. As a consequence, only examples handling plates and shell geometries are presented for nonlinear analysis, and the nonlinear behaviour of membrane elements with drilling rotation was not reported. Only few works reported the in-plane nonlinear behaviour. In these works, the nonlinear formulations are either based on the total Lagrangian formulation or use the rate-form equations.

II-5.2. Flat Shells with Drilling Rotation for Dynamic Analysis

Many works on dynamic of general shells by flat shell elements has been presented: [CLOUGH & WILSON 1971; BELYTSCHKO et al 1984-b; SIMO et al 1992-b; SIMO & TARNOW 1994; KUHL & RAMM 1996; SANSOUR et al 1997; BRANK et al 1998; TO & WANG 1998-a; ZHONG & CRISFIELD 1998; KUHL & RAMM 1999; MOHAMMADI et al 1999; BOTTASSO et al 2002; ONÃTE et al 2002; KHARE et al 2004; PARK et al 2006; YANG & XIA 2012-b; WU 2013]. However, due the absence of in-plane rotational *d.o.f*, the in-plane rotational vibrational modes was neglected.

There is only few shell elements with drilling rotation that are presented for dynamic analysis: [TO & WANG 1998-a; KIM et al 2003; ALMEIDA & AWRUCH 2011; NGUYEN-VAN et al 2011]. However, in these elements formulations, no masses corresponding to the in-plane rotational degrees of freedom of membrane elements was associated to the shell element's mass matrix, despite that this shells incorporate the drilling rotational *d.o.f* in the stiffness matrix formulation. It is recommended that the mass matrix does not include any coupling to corner rotations in order to avoid excitation of spurious modes. Thus, in these elements, no change was made to the mass matrix of the flat shell element.

[HUGHES et al 1995] addressed the issue of zero masses corresponding to the rotational degree of freedom of membrane elements with drilling rotation, and they presented techniques for defining consistent and lumped rotational mass matrices. The studied element was a quadrilateral element based on the variational principle in which displacements and rotations are interpolated independently. They used α method for time integration linear dynamic analysis and they presented a plane/stress cantilever beam with a parabolically varying shear applied at the free end. They found that the adding of drilling stiffness will increase frequencies. A lumped mass matrix corresponding to rotational *d.o.f* is designed in order to compensate for this effect.

[ALLMAN 1996] derived bending and membrane consistent mass matrices for a triangular flat facet finite element for the analysis of general thin shells. He included the effect of the rotatory inertia associated with the drilling rotation degree of freedom in the membrane mass matrix. He presented a kind of complicated form of the mass matrix using the higher order displacement interpolation presented by [Allman 1988-a]. Natural frequencies and normal modes are calculated for folded plates only. No in-plane examples were presented.

[KAPANIA & MOHAN 1996] tested the triangular flat shell element presented by [ERTAS et al 1992] for static, thermal, and free vibration analysis of laminated plates and shells. The shell element is a combination of the (DKT) plate bending element and Allman triangle derived from the Linear Strain Triangular (LST) element. The mass matrix corresponding to the degrees of freedom of the membrane element is obtained by applying the transformation given by Cook (1986) to the 12x12 mass matrix of the LST element. The frequencies of free vibration are obtained by solving the eigenvalue problem. Several numerical examples are solved for plates and shell geometries. However, no in-plane examples were reported.

[KARAKÖSE & ASKES 2010] Investigated the linear dynamic performance of the generalized conforming four-noded quadrilateral membrane element with rotational *d.o.f* by [YUQIU & YIN 1994-b]. Dynamic analysis was conducted using Newmark's method. One example representing a cantilever beam that is subjected to a tip vertical point load is presented. However no reference solution is used in order to verify the results of the presented numerical example.

[NGUYEN-VAN et al 2011] presented buckling and free vibration analysis of composite plate/shell structures via a smoothed quadrilateral flat element with drilling rotations [NGUYEN-VAN et al 2009]. The element is developed by incorporating a strain smoothing technique into a flat shell approach. No in plane mass matrix formulation and no geometric stiffness details are presented. Numerical tests was on plate and shell geometries.

[NETO et al 2012] presented a triangular element with drilling rotation for static and dynamic analysis of light-weight laminated composite structures. The authors adopted the in-plane mass matrix presented by [ALLMAN 1996]. Again, no in-plane examples were presented.

III- OBJECTIVES AND SCOOPS

It is clear from the above review of previous works in the subject of linear and nonlinear static and dynamic analysis of shells, that a reliable general theory is not yet available. On one hand, higher order finite shell elements provide better representation of the shell surface, and the bending-membrane coupling is embedded within each element, so they provide better performances. Unfortunately, they exhibit serious problems and complexities of formulation. The major difficulty of curved elements relies in the choice of displacement functions and the representation of the rigid body displacement, their extension to nonlinear analysis is not straightforward. Degenerated shell elements, in their original formulation, failed to converge to the thin shells solution. Considerable improvements was achieved by means of the reduced/selective integration and many other techniques that result with a time-consuming element. Both, classical curved, and degenerated shell finite elements, use high number of *d.o.f* and therefore they are computationally very expensive, which makes them less attractive especially for nonlinear and dynamic analysis.

On the other hand, flat shell elements, besides their computational cost efficiency, they has the advantage of being simple to apply for linear and nonlinear analysis. This approach has proved to be an attractive alternative for engineering purposes. The extremely simple and efficient formulation make them very well suited for dynamic and nonlinear applications, in particular when used in the framework of the updated Lagrangian formulation. However, due to the geometric approximation of the curved surface and the absence of the flexural-stretching coupling within the elements, flat shells may exhibit poor behaviour, especially for problems involving large membrane stresses. Nevertheless, these shortcomings, does not induce a major problem as many such elements have been proved to be successful and convergent to both shallow and deep shell solution. The geometric error and incompatibility, diminish with increasing mesh fineness leading to achieve a good approximation even for deep shells.

A great number of 3-nodded and 4-nodded flat shell elements formulations with good performances have been presented to date. However, there is still room for improvement in stability, robustness and accuracy. The major shortcoming of conventional flat shell elements, is that the rotation about the normal to the shell middle surface is usually neglected. This introduces a problem of stiffness matrix singularity when adjacent elements are coplanar. The common solution that implies the introduction of a rotational fictitious stiffness, disturbs the shell performances, because an artificial stiffness of the rotation about the normal of one shell restricts bending in the other shell. The error introduced in this case can’t be diminished by mesh

refinement. Moreover, standard Iso-parametric interpolations of low order membrane elements result in rather stiff finite elements, both for linear and geometrically nonlinear analysis.

To avoid these difficulties, the facet-shell formulation must provide a complete description of the nodal translation and rotation fields, allowing the definition of the six spatial degrees-of-freedom for each node of the finite element by using some special interpolation schemes. However, despite the growing interest on this formulation, there is still a lack in accurate and effective solutions, especially in nonlinear and dynamic analysis. Publications that describe geometrical nonlinearity of the in-plane behaviour of membrane element with rotational *d.o.f* are few, and often they are based on the total Lagrangian formulation or on the rate form. Also, these elements, at the author knowledge, have not been extended to nonlinear dynamic analysis.

Thus, an appropriate extension of triangular and quadrilateral flat shell elements with drilling rotation to nonlinear dynamic analysis is required. A simple and effective possibility to construct a geometrically nonlinear shell finite element with six degrees of freedom per node, is to extend the original ideas of [ALLMAN 1984], which has proven to be efficient in linear analysis, to be applicable for nonlinear and dynamic analysis. The classical formulation of the Allman-type displacement field is valid only for small in-plane rotations, because only the lateral component of the mid-side higher order displacement is linked with nodal rotations. Hence, the extension to large displacement and large rotation, but small strain, nonlinear analysis, can be accomplished by means of the co-rotational updated Lagrangian formulation. The co-rotational formulation assumes that the linear formulation is set in a local rotating frame, decoupling the rigid part of the motion form the elastic response, which allows an easy application of linear finite elements to geometrically nonlinear analysis. Nevertheless, the construction of accurate recovery of rotational fields is absolutely necessary in this case.

In view of the foregoing, the developments presented in this work have been motivated by the lack of general locking-free flat shell finite element that is robust and reliable in both bending and membrane dominated situations, and give accurate and reliable numerical results, not only for linear analysis, but also for geometrically nonlinear static and dynamic analysis.

The objective of this study is to present and investigate the capability of flat shell finite elements with drilling rotational degree of freedom, to represent geometric nonlinearity with effective handling of large in-plane displacements and rotations, and to simulate the in-plane rotational dynamic response.

In view of the aforementioned shortcomings:

- A new triangular membrane element with rotational *d.o.f* is developed based on the Enhanced Assumed Strain formulation. The developed element is drilling-rotation-locking free. This development was motivated by the poor behaviour and locking of existing triangular membrane elements with rotational *d.o.f*.
- A co-rotational formulation with some new aspects, for triangular and quadrilateral plate elements and membrane elements with drilling rotation is developed.
- The geometric stiffness matrix of flat shell elements is enlarged to take into account the second order terms of the in-plane displacement field due the in-plane drilling rotational degree of freedom.
- The in-plane mass matrix is enlarged to take into account, three degree of freedom including the rotational one. This development will overcome the problem of zero mass associated to the in-plane rotational *d.o.f* of flat shell finite elements.

When these new developments concerning membrane elements with rotational *d.o.f* are incorporated in triangular and quadrilateral flat shell elements for nonlinear dynamic analysis, they will provide more accuracy and stability and give true physical signification to the dynamic response of shell structures. However, we should mention that this study is limited to elastic, isotropic, and homogenous materials.

IV- THESIS OVERVIEW

This thesis consists of six chapters. After having an overview of the subject and the state of the art of shell finite elements in *chapter I,* shell theories and models from thin to thick first order and higher order plate/shell are presented in *chapter II*. *Chapter III* presents an overview of the construction of flat shell finite elements with drilling rotation. An important established triangular membrane finite elements with drilling rotation is presented in this chapter.

In *chapter IV* transient dynamic analysis of flat shell elements using Newmark method is presented. *Chapter V* presents the extension of triangular and quadrilateral flat shell elements with drilling rotation, to large displacement and large rotation geometrically nonlinear static and dynamic analysis, using the updated Lagrangian co-rotational formulation.

Chapter VI presents the path following technics, which are used to truck the equilibrium path and trace the load-displacement curve of geometrically nonlinear problems.

The *chapter VII* conclude the thesis with the application and tests of the contributions have been made in this work by the treatment of selected benchmarks and test cases, each one illustrates a different aspects of shell modelling.

CHAPTER II

SHELL THEORIES AND MODELS

I- INTRODUCTION

A shell is defined as a solid material enclosed between two curved surfaces. The specific geometry of this oriented structures promote the use of particular kinematic instead of general kinematic of solid bodies. Shell theory is concerned with reducing the three dimensional stress problem of elasticity to two dimensions for that particular class of structures. For this purpose, governing equations are reduced, via imposing some hypothesis on the displacement field, to a set of bi-dimensional equations related to a reference surface commonly situated at mid-thickness so-called the mid-surface.

Thus, three-dimensional theory is employed as the point of departure, and subsequently, certain simplifying assumptions are introduced to reduce the three-dimensional problem to be applicable for bi-dimensional shells. This objective may be realized if the deformations of any point in the shell can be uniquely described in terms of the displacements of the middle surface.

The reduction of the three dimensional problem requires the use of some kinematic assumptions, when employed together with the standard variational procedure lead to the two dimensional shell equations, which provide the basis for the finite element discretization.

In this chapter we will form kinematic and mechanic relations of Discrete Kirchhoff thin flat shell elements. These ones are established related to the mid-plane’s displacement and rotations. Strain-displacement, stress-strain, and internal forces relations are presented for plate bending elements and also for membrane elements.

II- GEOMETRY OF A SHELL

A shell is a three-dimensional body enclosed between two curved surfaces, for which one of its dimensions (thickness) is much smaller than any other of its dimensions (lengths) is.

The surface which bisects the thickness is known as the middle surface. By specifying the form of the middle surface, and the thickness at each point the shell is geometrically defined.

Let us consider a fixed orthogonal Cartesian system (O, x_1, x_2, x_3).

Let $\Omega \in R^3$ be a three-dimensional domain bounded by two surfaces $S^+ \in R^2$, $S^- \in R^2$ and the lateral surface $S^\times \in R^2$, so that $\partial\Omega = S^\pm \cup S^\times$.

The surfaces S^+ and S^- are called the upper and lower surfaces. They are symmetrically situated with respect to the reference mid-surface $S^0 \in R^2$. S^0 is called the mid-surface of the shell, and ℓ_0 defines its boundary line.

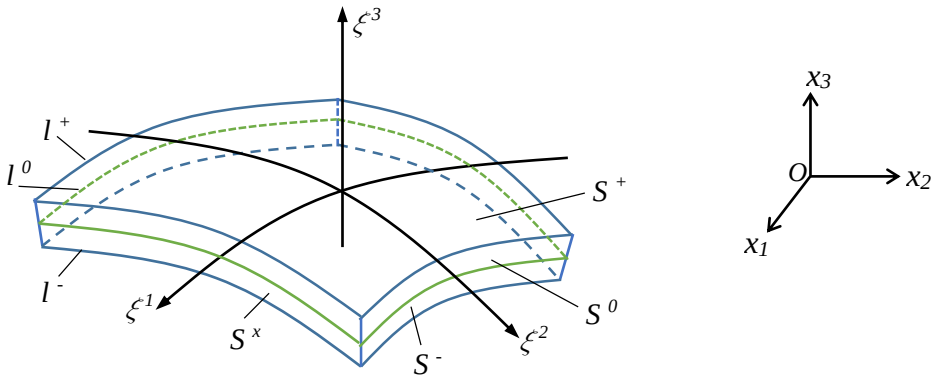

***Fig. II.1.* Geometry of a shell**

Any point in the shell can be located by its global orthogonal Cartesian coordinates. Besides, a curvilinear set of coordinates (ξ^1, ξ^2, ξ^3), called shell coordinates, can be established to locate points within the shell. Let ξ^1, ξ^2, and ξ^3 refer to the curvilinear coordinates on the shell mid-surface S^0, where ξ^1 and ξ^2 are tangent to the middle surface, and ξ^3 normal to it, *Fig. II.1*. Furthermore, it is assumed that the thickness h does not change and the coordinate line ξ^3 remains rectilinear and normal to S^0. Thus, the undeformed configuration of the shell is defined by:

$$\Omega = \left\{ \xi^m \mid \xi^\alpha \in S^0, \left|\xi^3\right| \le \frac{h}{2} \right\} \qquad \textit{[II-1]}$$

The boundary of Ω, denoted by S, consists of the upper and lower surfaces:

$$S^\pm = \left\{ \xi^m \mid \xi^\alpha \in S^0, \xi^3 = \pm\frac{h}{2} \right\} \qquad \textit{[II-2]}$$

and, the lateral surface:

$$S^{\times} = \left\{ \xi^m \mid \xi^\alpha \in l^0, \left|\xi^3\right| < \frac{h}{2} \right\} \qquad \textit{[II-3]}$$

i.e., $\partial\Omega \rightarrow S = S^{\pm} \cup S^{\times}$.

The boundary curves of the top and bottom surfaces $S^{\pm}$ are defined by:

$$l^{\pm} = \left\{ \xi^m \mid \xi^\alpha \in l^0, \xi^3 = \pm\frac{h}{2} \right\} \qquad \textit{[II-4]}$$

There are two different classes of shells: thick shells and thin shells. If the thickness of the shell is small compared to its minimum radius of curvature of the middle surface, the shell is considered thin, otherwise it is thick. For engineering applications, a value of $\frac{R}{h} = 20$ is usually considered as the lower limit for thin shell theory [VENTSEL & KRAUTHAMMER 2001]. In reality, the boundary between thin and thick shells depends also upon the boundary conditions, smoothness of variation of external loads, and other geometrical parameters of shells.

III- SHELL THEORIES

The analysis of shell structures often involves two distinct theories: The First one, is when it is subjected to uniform pressures, shells can usually resist the loads by membrane (in-plane stress). It is the most desirable situation in which a shell is subjected to a uniform load causing tensile stresses, because the material can be used to its full strength. Concentrated loads on the other hand, introduce local bending stresses, which are much more likely to cause failure of the shell.
Subsequently, the earliest effort toward the analysis of shells was based on the assumption of membrane behaviour of shells, where the bending resistance of the shell is neglected. This theory is found in the works of [BELTRAMI 1881; LAME & CLAPEYRON 1833].

These theories were simple, and in certain cases “of geometry and loading” gave a completely correct results. However, one needs a general theory to account for the bending of the shell, also for changes in thickness, boundary conditions, arbitrary geometry, and concentrated loadings. These effects cannot be approximated by means of the membrane theory only.

Several theories have been proposed and each one has its application areas and limitations. In general, there are two groups of basic assumptions on which the shell theories are based. The often used classical shell model is the Koiter-model [KOITER 1960-a] which is based on the Kirchhoff-Love hypothesis [KIRCHHOFF 1850; LOVE 1888]. This model implies restrictions on the

deformation of the normal to the shell mid-surface, which represents assumptions for theories of thin shells such as theories of Koiter [KOITER 1960-b], Love [LOVE 1944], and Novozhilov [NOVOZHILOV 1959]. The development of these theories was motivated by the successful development of plate theory by [KIRCHHOFF 1876]. This theory was based on the assumption that a normal to the undeformed mid-surface remains unstretched and normal to the deformed mid-surface. They are also limited by the assumption of the thickness of the shell mast be small when compared to the minimum radius of curvature of the middle surface.

Using these assumptions, [ARON 1874] made the first attempt to develop a general theory of thin shells from the general equations of elasticity. This was followed by the successful development of such a theory in 1888 by [LOVE 1888], known as Love's first approximation. However, the strain-displacement relations of Love's first approximation do not give zero strains under rigid body rotations. The work of [KOITER 1960-a] was very significant in establishing the nature of Love's first approximation. Several variants of this theories were developed by [FLUGGE 1934; VLASOV 1944; SANDERS 1959; NOVOZHILOV 1961], but the differences in these formulations seem to be rather insignificant.

[KOITER 1960-a] established that, Love's expression for strain energy for a thin shell as the sum of stretching and bending energies, is indeed a consistent first approximation, and the relative error in this approximation does not exceed the proportion between thickness and the minimum radius of curvature of the shell.

All previous assumptions applied in thin shells are commonly named KIRCHHOFF-LOVE theory. These theories, however, neglect the transverse shear deformation effects, so they differ significantly from the elasticity solution with the increase of plate thickness.

The other group of assumptions relates to the theories of moderately thick shells. It’s based on the lowest-order well-known Naghdi-model [NAGHDI 1963]. It contains the necessary assumptions of moderately thick plate’s theory including the effect of transverse shear deformation. This theory assumes that the displacement components are linear functions of the thickness coordinate, except the constant transverse deflection. In this group, the shear deformable theory due to [REISSNER 1945] or [MINDLIN 1951] is the most commonly used among several formulations. REISSNER-MINDLIN theory provides a useful and economical alternative approach to expensive three-dimensional stress analysis without significant loss of accuracy.

IV- SHELL MODELS

Since the early works in 19th century on thin plates, especially the first order models of Kirchhoff-Love and Reissner-Mindlin, many theories have been developed from kinematic field or even from stress field, in which certain simplifying assumptions are introduced to reduce the three dimensional problem to be applicable for bi-dimensional shells. The resulting shell theory as well as the finite element formulation depend on the nature of the assumed kinematic constraints. Basically, three groups can be distinguished:

1. Kirchhoff-Love type models;
2. Mindlin-Reissner type models;
3. Higher order models.

The choice, which type of theory one intends to use, depends on several factors; among them are: The simplicity factor, the smoothness and continuity factor, the accuracy factor, and the cost factor. We interest, in what follows, of the main models derived from the kinematic field, limiting our discussion here to the small displacements theory.

IV-1. Kirchhoff-Love Models

Kirchhoff-Love models are based on a linear distribution of displacements in the thickness [REISSNER & STAVSKY 1961; YANG et al 1966]. The assumption made is that of Kirchhoff-Love [KIRCHHOFF 1850] in which:

- Through the thickness, shell fibers remain straight and inextensible during the deformation;
- Deformations due to transverse shear are neglected;
- The normal keep straight and perpendicular to the mid-surface after having deformed;
- Normal strains and stresses in the out-of plane direction are also considered negligible.

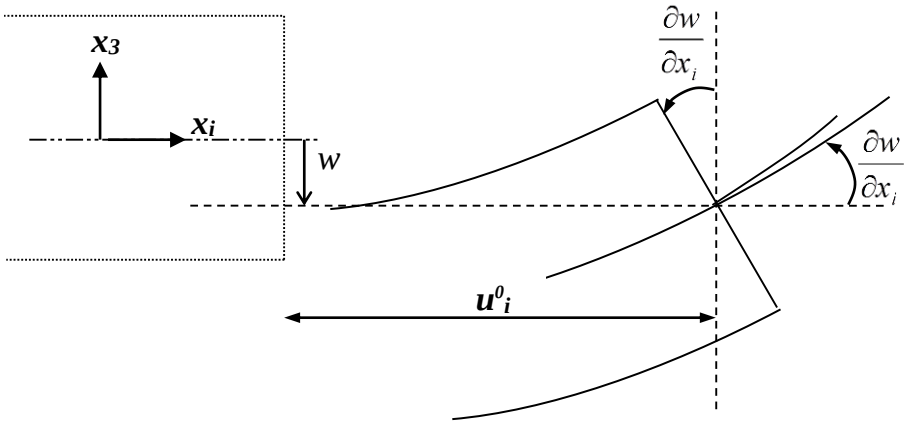

Fig. II.2. **Kirchhoff-Love theory kinematic**

The displacement field of Kirchhoff- Love is then written as:

$$u_i(x_1, x_2, x_3 = z) = u_i^0(x_1, x_2) - z \cdot \frac{\partial w(x_1, x_2)}{\partial xi} \quad i = 1,2 \qquad \textit{[II-5]}$$

$$u_3(x_1, x_2, x_3 = z) = w(x_1, x_2) \qquad \textit{[II-6]}$$

With:

u_i^0 : the mid-surface's in-plane displacement (membrane displacement) in the direction x_i;

u_i : the in-plane displacement in the direction x_i;

w : the out of plane displacement due to bending (deflection of the plate),

$\frac{\partial w}{\partial x_i}$: the out of plane rotation due to bending (slope) when transvers shear is neglected.

IV-2. Reissner-Mindlin Models

In order to consider the effect of transverse shear, kinematic hypothesis of Mindlin is adopted [MINDLIN 1951], in which, assumptions on the vanishing of the transverse shear strain and on the preservation of the normal was abandoned. Due to the transverse shear effect, normal remains straight but not perpendicular to the mid-surface after having deformed *Fig. II.3*.

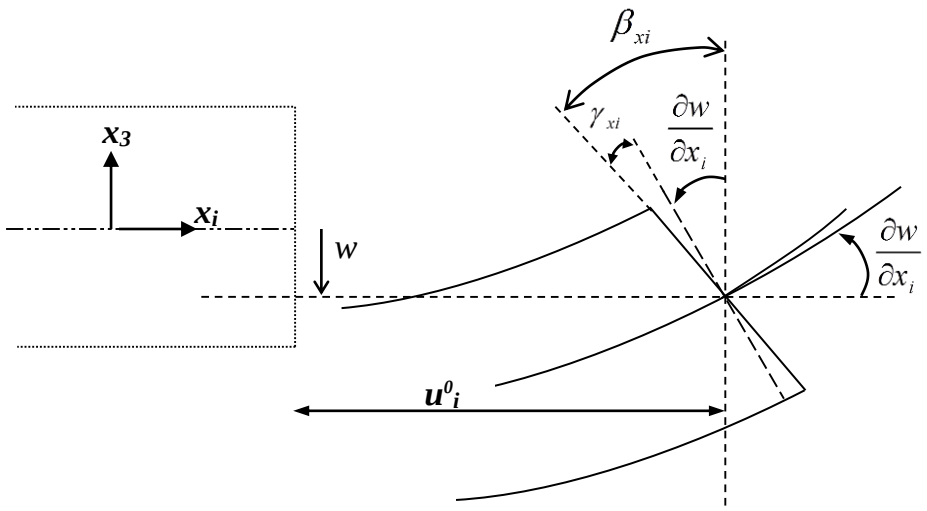

Fig. II.3. **Reissner-Mindlin theory kinematic**

The displacement field of Reissner-Mindlin is written as:

$$u_i(x_1, x_2, x_3 = z) = u_i^0(x_1, x_2) + z \cdot \beta_{xi}(x_1, x_2) \quad i = 1,2 \qquad \textit{[II-7]}$$

$$u_3(x_1, x_2, x_3 = z) = w(x_1, x_2) \qquad \textit{[II-8]}$$

With: $\beta_{xi} = (\frac{\partial w}{\partial x_i} + \gamma_{xi})$ is the rotation of the normal to the mid-surface around x_i axe, and γ_{xi} is the transverse shear strain.

Basing on this choice of displacement field shape, the transverse deformations and shear stress are constant along *z* (the thickness). This poor description of shear strain and stress requires introducing coefficients to better take into account the effects of transverse shear in the energy expression: [WHITNEY 1973]. In addition, in laminated shells/plates, shear stresses are uniform in each layer and discontinuous between the layers and, the study of thick composites remains uncertain by such cinematic approach.

Actually, the basic assumptions employed in the Mindlin-Reissner shell theory exclude the transverse normal deformation and thus they are restricted to small strain problems. From the computational point of view the main advantage compared with the Kirchhoff-Love type shell theory is the fact that only *C°* inter element continuity is required, which simplifies considerably the construction of finite elements.

IV-3. Higher Order Models

Higher-order approximation theories were appeared in order to overcome the limitations of first-order shell/plate theories. Several authors have proposed and used higher order theories: [LIBERSCU 1967; WHITNEY 1973; NELSON & LORCH 1974; LO & CHRISTENSEN 1977-a, 1977-b; REDDY 1984; TOURATIER 1991; IDLBI et al 1997; KANT & SWAMINATHAN 2002; SWAMINATHAN & RAGOUNADIN 2004]. These higher-order models are more accurate than the first order models. They are based on a non-linear distribution through the thickness trying to represent the warping of transversal section in the deformed configuration, *Fig. II.4*.

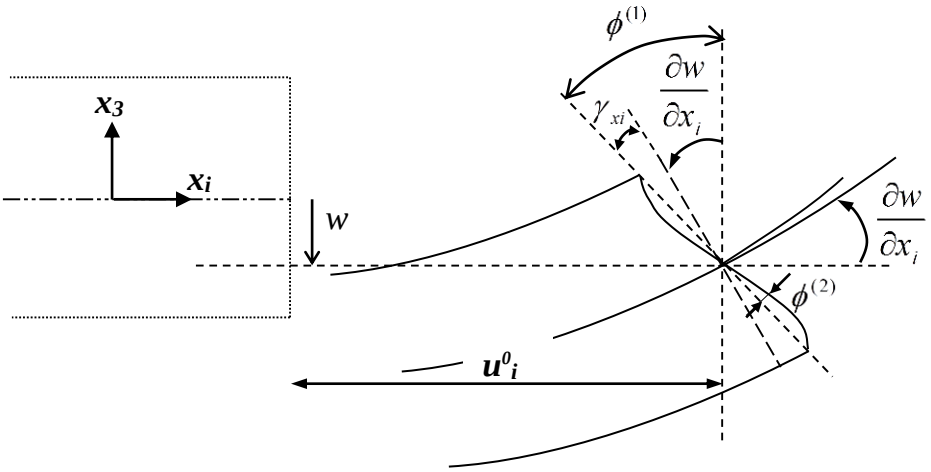

Fig. II.4. **Higher-order theory kinematic**

Most of the existing higher order models employ Taylor series development of the displacement fields that are written as:

$$u_i(x_1,x_2,x_3) = u_i^0(x_1,x_2) + z\cdot\phi_i^{0(1)}(x_1,x_2) + z^2\cdot\phi_i^{0(2)}(x_1,x_2) + z^3\cdot\phi_i^{0(3)}(x_1,x_2) + ... \qquad [II\text{-}9]$$

With: $i \in \{1,2,3\}$.

Using this expression, accuracy is increased with the order of development, i.e. the number of independent variables of displacement that exceeds that of former models (three in the Love-Kirchhoff model and five for Reissner-Mindlin model).

In the particular case of the first-order theories of Reissner-Mindlin we get:

$\phi_i^{0(j)} = 0,\ and\ \phi_3^{0(1)} = 0$.

[HILDEBRAND et al 1949] were the first to introduce these refinements with: $\phi_i^{0(4)} = \phi_i^{0(3)} = 0$. [NELSON & LORCH 1974] use the same development by introducing correction coefficients. [LO & CHRISTENSEN 1977-b] proposed a model that takes into account the effect of normal deformation: $\phi_i^{0(4)} = 0, and\ \phi_3^{0(3)} = 0$.

In several works, in order to reduce the number of parameters of displacement, various simplifications are used. Often the conditions of nullity of transverse shear stresses at the upper and lower surfaces of the plate is imposed.

[TOURATIER 1991; IDLBI et al 1997] proposes the "sine" model that is different from other higher order models since it does not use polynomial function for displacement fields. A sinusoidal trigonometric function is introduced to model the distribution of shear stress through the thickness. The function of the transverse shear is written as below:

$$f(z) = \frac{h}{\pi}\sin\left(\frac{\pi\cdot z}{h}\right) = \frac{h}{\pi}\sum_{n=0}^{\infty}\frac{(-1)^n}{(2n+1)!}\left(\frac{\pi\cdot z}{h}\right)^{(2n+1)} = z\left(1-\frac{\pi^2}{3!}\frac{z^2}{h^2}+\frac{\pi^4}{5!}\frac{z^4}{h^4}-\frac{\pi^6}{7!}\frac{z^6}{h^6}+...\right) \qquad [II\text{-}10]$$

Depending on the chosen truncation, one obtains the Love-Kirchhoff theory, Reissner-Mindlin theory or higher-order model. The transverse shear stresses determined by the "sine" take a "cosine" shape model in the thickness of the plate. The accuracy of this model compared to the exact solution is better than the theory of [REDDY 1984].

Recently, [AFAQ et al 2003] proposed an exponential model with a richer cinematic. The function of transverse shear is of the following form:

$$f(z) = ze^{-2\left(\frac{z}{h}\right)^2} \qquad [II\text{-}11]$$

While that the "sine" function [TOURATIER 1991] allows only impairs powers development, the choice of the exponential function is used in a development of pairs and impairs power of the variable *z* (thickness).

V- PLATE BENDING IN KIRCHHOFF THEORY

In the Kirchhoff-Love theory, the displacement field of the reference surface is the only independent kinematical variable. It is a thin shell theory, in which transverse shear is neglected. This theory requires continuity of the normal slope across the inter-element boundaries (C^1 continuity). The requirement to ensure the C^1 inter-element continuity leads to a high order interpolation polynomials.

Kirchhoff-Love theory is based on the following three hypotheses:

• *straight-normals assumption*: any normal to the mid-plane of an undeformed plate will remain rectilinear, will keep its length, and will remain orthogonal to the mid-surface that the mid-plane becomes after the plate is deformed;

• *no-pressure assumption*: all surfaces which are parallel to the mid-surface do not interact in their normal direction, which led to consider, $\sigma_{zz} = 0$;

• *no-shear assumption*: the shear stresses τ_{xz} and τ_{yz}, are neglected in the expression of energy in comparison to the work of σ_{xx}, σ_{yy}, and τ_{xy}. Thus, strains and stresses related to "z" axis are considered null: $\varepsilon_{zz} = 0$, $\gamma_{xz} = 0$, $\gamma_{yz} = 0$, $\tau_{xz} = 0$, and $\tau_{yz} = 0$.

V-1. Discrete Kirchhoff Assumptions

The aforementioned limitations and difficulties led to the development of the discrete Kirchhoff theory (DKT), for which the requirement of C^1 continuity is relaxed, but additional techniques are used to incorporate the Kirchhoff assumptions at a discrete number of points. Within this approach the formulation starts with the Mindlin-Reissner plate or shell theory. Subsequently, Kirchhoff hypothesis are enforced at some discrete points (usually, corner nodes, or mid-side nodes).

However, relaxation of the Kirchhoff assumptions is not without problems. It has been found that the convergence rate is slow for some finite elements of this class. The slow rate of convergence is due to the fact that the transverse shear energy, which is a very small part of the total strain energy, contributes more than its fair share to the total strain energy of the element. This led to an over stiffening in the plate/shell element.

Let us consider the plate element of *Fig. II.5*. The displacement of any material point "*P*" following (x_i) axis is: $u_i = z \cdot \tan(\beta_i)$. In small displacement we can write: $\tan(\beta_i) = \beta_i$, so:

$$u_i = z \cdot \beta_i \qquad \textit{[II-12]}$$

- In the thin plate Kirchhoff model, the transverse shear strains are negligible, so:

$$\begin{cases} \gamma_{xz} = \dfrac{\partial w}{\partial x} + \beta_x = 0 \\ \gamma_{yz} = \dfrac{\partial w}{\partial y} + \beta_y = 0 \end{cases} \qquad \textit{[II-13]}$$

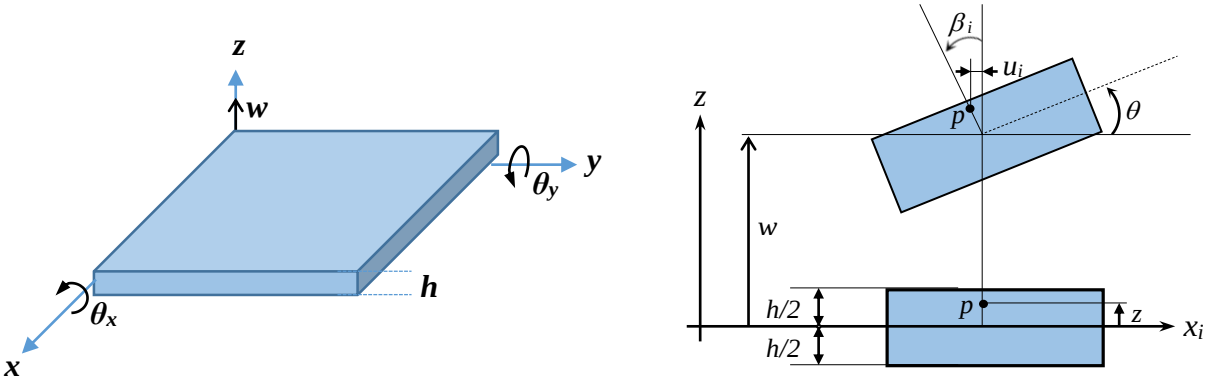

***Fig. II.5.* Thin plate kinematic in Kirchhoff theory**

This relates the mid-plane deflection with out-of-plane rotations as:

$$\begin{cases} \beta_x = \theta_y \\ \beta_y = -\theta_x \end{cases} \qquad \textit{[II-14]}$$

$$\begin{cases} \theta_x = \dfrac{\partial w}{\partial y} \\ \theta_y = -\dfrac{\partial w}{\partial x} \end{cases} \qquad \textit{[II-15]}$$

Using *Eq. [II-12]*, *Eq. [II-14]* and *Eq. [II-15]*, the displacement field is expressed using the deflection *w* only:

$$\begin{cases} w = w(x, y, z) \\ u = -z\dfrac{\partial w}{\partial x} \\ v = -z\dfrac{\partial w}{\partial y} \end{cases} \qquad \textit{[II-16]}$$

- Curvatures $\kappa = \begin{bmatrix} \kappa_{xx} & \kappa_{yy} & \kappa_{xy} \end{bmatrix}^T$ at the plate mid-plane point are defined as:

$$\kappa_{xx} = -\frac{\partial \theta_y}{\partial x};\ \kappa_{yy} = \frac{\partial \theta_x}{\partial y};\ \kappa_{xy} = \frac{\partial \theta_x}{\partial x} - \frac{\partial \theta_y}{\partial y} \qquad \textit{[II-17]}$$

Using *Eq. [II-12]*, the vector of curvatures for Kirchhoff plate model is:

$$\{\kappa\}^T = \left\langle \frac{\partial^2 w}{\partial x^2} \quad \frac{\partial^2 w}{\partial y^2} \quad 2\frac{\partial^2 w}{\partial x \partial y} \right\rangle \qquad \textit{[II-18]}$$

- Transverse strain quantities γ_{xz} , γ_{yz} are neglected. Strain-displacement relation becomes:

$$\begin{cases} \varepsilon_x = -z\dfrac{\partial^2 w}{\partial x^2} \\ \varepsilon_y = -z\dfrac{\partial^2 w}{\partial y^2} \\ \gamma_{xy} = -2 \cdot z\dfrac{\partial^2 w}{\partial x \partial y} \end{cases} \qquad \textit{[II-19]}$$

This leads to the following expressions for nonzero in-plane strains $\varepsilon = \begin{bmatrix} \varepsilon_{xx} & \nu_{yy} & \varepsilon_{xy} \end{bmatrix}^T$:

$$\varepsilon_{xx} = -z \cdot \kappa_{xx};\ \varepsilon_{yy} = -z \cdot \kappa_{yy};\ 2\varepsilon_{xy} = -z \cdot \kappa_{xy} \qquad \textit{[II-20]}$$

- Assuming the plate is made of isotropic elastic material characterized by elastic modulus *E* and Poisson's ratio *v*, the elastic behaviour is described well by the plane stress Hook's law:

$$\begin{Bmatrix} \sigma_x \\ \sigma_y \\ \tau_{xy} \end{Bmatrix} = \frac{E}{1-\upsilon^2} \begin{bmatrix} 1 & \upsilon & 0 \\ \upsilon & 1 & 0 \\ 0 & 0 & \dfrac{1-\upsilon}{2} \end{bmatrix} \qquad \textit{[II-21]}$$

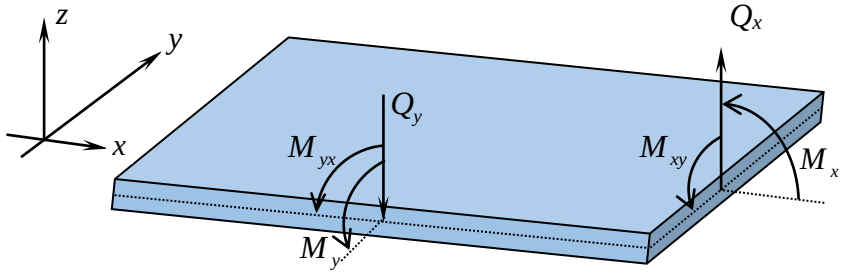

Fig. II.6. **Thin plate stress resultant**

- In order to form a bi-dimensional theory, we must integrate stress through thickness to get stress resultant internal forces. Integration through the plate thickness leads to the plate bending moments $M = \begin{bmatrix} M_{xx} & M_{yy} & M_{xy} \end{bmatrix}^T$ with the dimension of moment per unit length defined as:

$$\begin{Bmatrix} M_x \\ M_y \\ M_{xy} \end{Bmatrix} = D \begin{bmatrix} 1 & \upsilon & 0 \\ \upsilon & 1 & 0 \\ 0 & 0 & \dfrac{1-\upsilon}{2} \end{bmatrix} \begin{Bmatrix} \dfrac{\partial^2 w}{\partial x^2} \\ \dfrac{\partial^2 w}{\partial y^2} \\ 2\dfrac{\partial^2 w}{\partial x \partial y} \end{Bmatrix} \qquad \textit{[II-22]}$$

With: $D = \dfrac{E \cdot h^3}{12(1-\upsilon^2)}$

Also, we gets the following shear forces:

$$\begin{cases} Q_x = -D \dfrac{\partial}{\partial x}\left(\dfrac{\partial^2 w}{\partial x^2} + \dfrac{\partial^2 w}{\partial y^2} \right) \\ Q_y = -D \dfrac{\partial}{\partial y}\left(\dfrac{\partial^2 w}{\partial x^2} + \dfrac{\partial^2 w}{\partial y^2} \right) \end{cases} \qquad \textit{[II-23]}$$

- Total potential energy is:

$$U = \frac{1}{2}\int_v \{\sigma\}^T \{\varepsilon\} \cdot dv \qquad \textit{[II-24]}$$

$$U = \frac{1}{2}\int_v z\left(\sigma_x \frac{\partial^2 w}{\partial x^2} + \sigma_y \frac{\partial^2 w}{\partial y^2} + 2\tau_{xy} \frac{\partial^2 w}{\partial x \partial y} \right) \cdot dv \qquad \textit{[II-25]}$$

$$U = \frac{1}{2}\int_A \{\kappa\}^T [D_b] \{\kappa\} \cdot dA \qquad \textit{[II-26]}$$

VI- PLANE-STRESS MEMBRANE THEORY

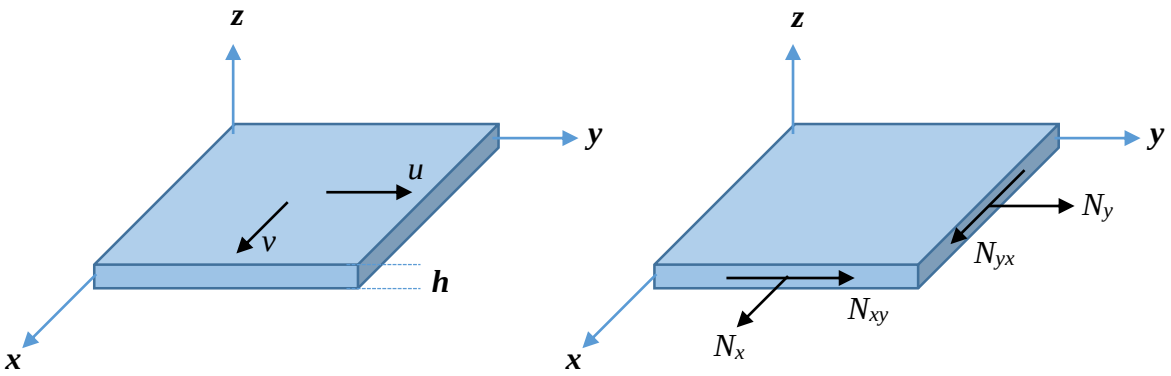

Fig. II.7. **Plane stress: *a*- Kinematic; *b*- Stress resultant**

- Strain-displacement relations are: $\varepsilon_x = \frac{\partial u_0}{\partial x}$, $\varepsilon_y = \frac{\partial v_0}{\partial y}$, $\gamma_{xy} = \frac{\partial u_0}{\partial y} + \frac{\partial v_0}{\partial x}$.
- For this element, loads are in-plane forces affecting in the mid-plane. For a plane stress problem, integration through the plate thickness leads to the strain resultant in-plane forces $N = \left[N_{xx} \quad N_{yy} \quad N_{xy}\right]^T$ with dimension of force per unit length.

Normal forces: N_x, N_y are:
$$\begin{cases} N_x = \int_{-\frac{h}{2}}^{\frac{h}{2}} \sigma_x dz \\ N_y = \int_{-\frac{h}{2}}^{\frac{h}{2}} \sigma_y dz \end{cases} \qquad [II\text{-}27]$$

Tangential forces: N_{xy}, N_{yx} are:
$$\begin{cases} N_{xy} = \int_{-\frac{h}{2}}^{\frac{h}{2}} \tau_{xy} dz \\ N_{yx} = \int_{-\frac{h}{2}}^{\frac{h}{2}} \tau_{yx} dz \end{cases} \qquad [II\text{-}28]$$

Plane stress constitutive equation:

$$\begin{Bmatrix} \sigma_x \\ \sigma_y \\ \tau_{xy} \end{Bmatrix} = \frac{E}{1-\nu^2} \begin{bmatrix} 1 & \nu & 0 \\ \nu & 1 & 0 \\ 0 & 0 & \frac{1}{2}(1-\nu) \end{bmatrix} \begin{Bmatrix} \varepsilon_x \\ \varepsilon_y \\ \gamma_{xy} \end{Bmatrix} \qquad [II\text{-}29]$$

Total potential energy is:

$$U = \frac{1}{2}\int_v \{\sigma\}^T \{\varepsilon\} \cdot dv \qquad [II\text{-}30]$$

$$U = \frac{1}{2}\int_v \{\varepsilon\}^T [D_m] \{\varepsilon\} \cdot dv \qquad [II\text{-}31]$$

CHAPTER III

FLAT SHELL FINITE ELEMENTS

I- INTRODUCTION

In the early stages of finite elements analysis, plane stress elements were the first developed finite elements. Then, several efficient plate elements were developed. It was a simple matter then, to extend their use to the discretization of shell structures, according to which, a shell finite element is obtained from the superposition of membrane and bending behaviours. Generally good results are obtained with sufficiently fine meshes. Beside their simplicity in use, these are the reasons for the continued use of flat elements in shell analysis even when good curved shell elements were developed. Nevertheless, this approach has its drawbacks, and limitations beside their advantages.

Flat shell elements still attract much attention in the literature, and the research to represent the shell behaviour by flat elements and to overcome the associated difficulties continues to attract much attention. In this section, the formulations of the various shell finite elements used in the numerical experiments, are briefly outlined. Detailed formulation is presented only for the new AES triangular plane stress element with rotational degree of freedom developed in this work.

II- APPROXIMATION OF SHELLS WITH FLAT ELEMENTS

The simplest and the most used approximation of the finite element method to the analysis of shells involved the replacement of the curved shape of shell structures by a juxtaposition (assemblage) of flat triangular or quadrilateral elements, obtained by superposition of membrane and flexural behaviour. By superposing the independent membrane element (plane stress element) and plate bending element together with the appropriate spatial transformation, the desired shell element will be developed. Among the major attractive features of this modelling approach of shells, see [COOK 1974-a; YANG et al 1990] are:

1. They are simple to formulate;
2. It is easy to mix with other types of elements;
3. They are capable of modelling rigid body motions without inducing strains;
4. They exclude at the element level the coupling of membrane and bending behaviour so they avoid membrane locking;
5. Input data describing the geometry is much easier;
6. Convergence is assured and good results are obtained with refine meshes;
7. The requirement of using a relatively large number of elements provides the advantage of a convenient incorporation of complex loading and boundary conditions.

Nevertheless, the use of flat finite elements to solve shell problems has several drawbacks, see [ORAL & BARUT 1991; CHEN 1992; ALLMAN 1994]:

1. The geometry of a curved shell surface is replaced by a faceted, folded structure. Nevertheless, the error introduced by this approximation tends to decrease with mesh refinement;
2. The restriction to triangular shapes when general shells are to be treated;
3. The coupling of bending and membrane behaviours at the element level which is present in curved structures, is absent in flat shells;
4. Compatibility is lost when flat elements are used to represent curved structures;
5. They give rise to the presence of "discontinuous" bending moments, which do not appear in continuously-curved shells;
6. They lead to ill-conditioned or even singular stiffness matrices, whenever elements are coplanar or nearly so.

That last one deficiency, arise from the fact that conventional plane stress elements make use only of the nodal translational degrees of freedom (2 d.o.f), while the in-plane rotation about the normal to the shell middle surface is usually neglected. The superposition of such element with a plate element having (3 d.o.f), produces a shell element with only (5 d.o.f) at each node. The sixth *d.o.f* which represents in plane rotation θ_z about the normal axis at corner node, is not necessary for the elementary formulation. Therefore, it is not taken as a nodal parameter. Consequently, rigidity corresponding to this *d.o.f* is null at the local stiffness matrix.

$$[k]=\left|\begin{array}{ccc}[k_m] & [0] & 0\\ [0] & [k_b] & 0\\ 0 & 0 & 0\end{array}\right|$$

Add a small stiffness

The elementary stiffness matrix for a flat shell element is first assembled by superposing the membrane stiffness and bending stiffness at each node in the local coordinate system, then it will be transformed from the local to the global coordinate system where the shell element have to deal with six *d.o.f* at each corner node. However, the rigidity corresponding to the sixth *d.o.f* is null at the shell stiffness matrix level. That means that the sixth row and column of the elementary stiffness matrix contain only zeros. Remember that there was no stiffness associated with the local in-plane rotational degrees of freedom. Therefore, the global stiffness matrix will be rank deficient if all elements are coplanar.

As a consequence, a difficulty arises if all the elements meeting at a node are co-planar, because that formulation does not produce equations associated with this rotational parameter. In this case the global stiffness matrix contains rows and columns contain only zeros, and hence, numerical problems due to singularity of the stiffness matrix arise at the numerical level.

Many solutions have been used to avoid this problem [CLOUGH & WILSON 1971; ZIENKIEWICZ 1977; GOTSIS 1994]. They were based on various artificial means such as a fictitious beam along the edges of an element or a fictitious springs; we can mention among these methods:

- Eliminate the null term rows and columns from the stiffness matrix associated with the drilling rotation *d.o.f* to obtain a non-singular stiffness matrix. However, this method has many limitations, See [CLOUGH & WILSON 1971; LEE & LEE 2001] for further details;
- The addition of fictitious in-plane beams along the edges of the element;
- The addition of a fictitious torsional-spring elements normal to the shell surface. That solution implies the insertion of a fictitious small torsional rigidity, it's an arbitrary stiffness associated with the sixth degree of freedom at each one of the corner nodes [ZIENKIEWICZ et al 1965]. This technic is the simplest, the most cost-effective and the most common method;
- Or, interpolate the sixth degree of freedom in order to build a shell element which handles with six *d.o.f* at corner nodes. This in-plane rotational degree of freedom associated with the shell normal rotation is commonly referred to as drilling degree-of-freedom. This method is relatively recent and coming to be more adopted.

Till now days, the most common method is to associate to the sixth *d.o.f* a fictitious torsional rigidity at each node [ZIENKIEWICZ 1977]. It is placed at its position within the elementary stiffness matrix to avoid system singularity. However, the additional stiffness, does not improve the in-plane bending behaviour but rather makes it even stiffer. Moreover, such artificial solution introduces a problem at shell intersections because, neglecting the rotation about the normal and the use of an artificial stiffness of one shell restricts bending in the other shell. The error introduced in this case does not vanish by mesh refinement. As a result, this approach can lead to critical errors [JETTEUR 1986; GOTSIS 1994] in linear analysis especially for warped geometry [ZHU & ZACHARIA 1996]. These deficiencies become particularly severe (numerical instabilities and divergence) in nonlinear and post-buckling analysis. Furthermore, solution could converge, and these errors become more severe in dynamic analysis either linear or non-linear as we will show in the numerical simulation chapter in this work.

II-1. Fictitious Stiffness

Among those technics cited above, a method which is commonly used to account for the in-plane rotation is simply by add a small fictitious stiffness to each drilling *d.o.f.* [ZIENKIEWICZ et al 1965; ZIENKIEWICZ 1977; BATHE & HO 1981] proposed to use a fictitious stiffness in the direction of this degree of freedom i.e. associate a fictitious small stiffness at the sixth *d.o.f* of each node. It is

a constant inserted at appropriate places within the elementary stiffness matrix to avoid system singularity when all the elements meeting at one node are co-planar.

This fictitious stiffness may be injected at the principal diagonals alone (6x6), (12x12) and (18x18) …etc., or at off-diagonal of the element stiffness matrix too (6x12), (6x18) …etc., see: [ZIENKIEWICZ 1977; COOK 1993; GOTSIS 1994; BELYTSCHKO & LEVIATHAN 1994].

Based on the assumption that a nodal rotation θ_{zj} about the *z* local axis of any element's node is responsible only for the development of resisting couples M_{zi}, The sum of resisting couples is always taken to be zero to ensure static equilibrium, where:

$$\sum_{i=1}^{n} M_{zi} = 0 \qquad \textit{[III-1]}$$

Where *n* represents the number of nodes of one element.

The fictitious rotation is defined in the way that it does not perturb the local equilibrium of the finite element. This could be achieved by adding the following term in the potential energy of each element:

$$\bar{\pi}_e = \pi_e + \int_A \alpha \cdot E \cdot h^k \cdot (\theta_z - \bar{\theta}_z)^2 \, dA \qquad \textit{[III-2]}$$

With, α is an undetermined fictitious elastic parameter, *E* is the elasticity modulus, *A* is the air, and $\bar{\theta}_z$ is the mean rotation of each element.

[ZIENKIEWICZ & TAYLOR 2000] have observed that if *n=3*, which mean that the additive fictitious stiffness is related to h^3, numerical results are less sensitive to the choice of the value of the parameter "α". He suggested the following overall form approximation of the moment-rotation relationship for triangular elements:

$$\begin{Bmatrix} M_{z1} \\ M_{z2} \\ M_{z3} \end{Bmatrix} = \frac{\alpha \cdot E \cdot h^k \cdot A}{36} \begin{bmatrix} 1 & -0.5 & -0.5 \\ -0.5 & 1 & -0.5 \\ -0.5 & -0.5 & 1 \end{bmatrix} \begin{Bmatrix} \theta_{z1} \\ \theta_{z2} \\ \theta_{z3} \end{Bmatrix} \qquad \textit{[III-3]}$$

Some authors used the following relationship:

$$\begin{Bmatrix} M_{z1} \\ M_{z2} \\ M_{z3} \end{Bmatrix} = \frac{\alpha \cdot E \cdot h^3}{12(1-\mu^2)} \begin{bmatrix} 1 & -0.5 & -0.5 \\ -0.5 & 1 & -0.5 \\ -0.5 & -0.5 & 1 \end{bmatrix} \begin{Bmatrix} \theta_{z1} \\ \theta_{z2} \\ \theta_{z3} \end{Bmatrix} \qquad \textit{[III-4]}$$

[COOK 1993] Introduces an elastic restraining term between the three drilling rotations and the mean drilling rotation value of a triangular element, as:

$$\bar{\theta}_z = \theta_z^i - \frac{1}{3}\left(\theta_z^1 + \theta_z^2 + \theta_z^3\right) = \frac{1}{3}\langle d_i \rangle \left\{\theta_z^1 \;\; \theta_z^2 \;\; \theta_z^3\right\} \qquad \textit{[III-5]}$$

Where $\langle d_i \rangle$ are: $\langle d_1 \rangle = \langle 2 \quad -1 \quad -1 \rangle$, $\langle d_2 \rangle = \langle -1 \quad 2 \quad -1 \rangle$, and $\langle d_3 \rangle = \langle -1 \quad -1 \quad 2 \rangle$

The fictitious stiffness matrix can be written as:

$$[k] = \frac{1}{3}\alpha\, E\, A h \left(\langle d_1 \rangle \{d_1\} + \langle d_2 \rangle \{d_2\} + \langle d_3 \rangle \{d_3\}\right) = \alpha\, E\, A h \begin{bmatrix} 2 & -1 & -1 \\ -1 & 2 & -1 \\ -1 & -1 & 2 \end{bmatrix} \qquad \textit{[III-6]}$$

According to [COOK et al 2002] the additional stiffness provides each drilling *d.o.f* with a fictitious stiffness, but offers no resistance to the mode $\theta_z^1 = \theta_z^2 = \theta_z^3 = \theta_z^i$, or any other rigid mode.

We should note that, this technic led to an additional fictitious in-plane shear deformation as a consequence of the addition of a fictitious in-plane rotation. Nevertheless, this does not influence the resultant stress. In addition, the sum of all additional terms is null. Then, rigid rotations condition is always guaranteed.

[NUKULCHAI 1979; PROVIDAS & KATTIS 2000] presented another variant of fictitious stiffness, using an additional constraint to link the nodal rotations to the average in-plane rotation of the mid-surface.

[CHANG et al 2003] proposed a practical approach to account for the sixth *d.o.f* for flat shell elements, in which, the in-plane rotation θ_z is incorporated into the shell element formulation based on the mixed variational principle, see also [WANG & SUN 2014].

The "drilling rotation locking" effect provided by the fictitious in-plane rotational stiffness values over the bending stiffness terms, could be alleviated by assuming a cubic exponent for the thickness parameter as in [ZIENKIEWICZ & TAYLOR 2000]. Moreover, some experimentation is usually necessary in order to select a suitable value of the scaling parameter "α", but for precision, usually extra small values of "α" are recommended in order to reduce the effect of the additional fictitious stiffness, [ZIENKIEWICZ et al 1965]. Usually a value between 10^{-3} and 10^{-6} is recommended.

Even if the use of artificial stiffness can solve the problem of stiffness matrix singularity; it doesn't represent the real in plane behaviour because of the fact that a fictitious stiffness has been added. Furthermore, some research works on the effect of varying the scaling parameter "α" determined that a displacement error of about *10%* in linear analysis is caused by introducing "α" value as large as 1.0, see [JETTEUR 1986; GOTSIS 1994], in addition to errors determined in natural

frequencies analysis, see [SESHU & RAMAMURTI 1989]. In conclusion, satisfactory results are obtained as "α" is the smallest admissible value, in order to produce only small perturbations of the strain energy of the shell, [BERNADOU & TROUVE 1989]. This is not always possible especially in nonlinear analysis. A high level of risk exists when using this method which includes remarkably errors and instabilities in both geometrically and materially nonlinear analysis.

II-2. The Sixth Degree-of-Freedom

In order to avoid the use of artificial solution to the sixth *d.o.f* problem, which does not give satisfactory results, an alternative method requires extending the number of in-plane nodal parameters from two to three. This approach, aims to interpolate the in plane rotations of corner nodes about the normal axis called "*drilling rotation*" or "*in-plane drilling rotational d.o.f*". The superposition of such an element with a plate element having (3 d.o.f) per node produces a flat shell element having (6 d.o.f) each node [CHINOSI 1994], as presented in *Fig. III.1*.

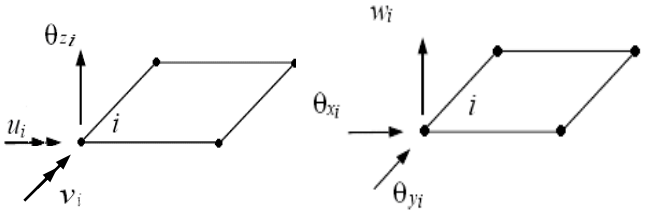

Fig. III.1. **Four-node shell element with *"Drilling Rotation"***

This *d.o.f* is particularly advantageous for analysis of shells with the aim of extending the range of applicability of shell elements. Moreover, in many finite element formulations, the absence of the rotation about the shell normal as a degree of freedom can lead to serious errors and spurious modes. Hence, as the technic of fictitious stiffness can lead to incorrect results, much works has been directed toward including the in-plane rotation as an effective *d.o.f* [ALLMAN 1984; BERGAN & FELIPA 1985; COOK 1986; ALLMAN 1988-*a*, 1988-*b*; HUGHES & BREZZI 1989; IBRAHIMBEGOVIC et al 1990; COOK 1991; IURA & ATLURI 1992].

The main objectives behind including normal in-plane rotational degrees of freedom at corner nodes of plane-stress finite elements are:

- To improve the in-plane behaviour of plane strain/stress elements because a higher order membrane element could be formulated. This improvement can also improve the shell element performances;
- To overcome stiffness matrix singularity and avoid using artificial solutions;

- To impose nodal kinematic compatibility at branching points and provide reliable modelling of connections between plates, shells, beams and Stiffeners, using a complete set of degrees-of-freedom.

A significant progress in including the in-plane rotational degrees of freedom began with the independent works by [ALLMAN 1984] who used a non-conventional interpolation, and by [BERGAN & FELIPA 1985] using the free formulation. Extensive attempts to develop plane stress finite elements with drilling rotation have shown that the sixth *d.o.f* can be formulated and built into the element in a widely varying manner. Basically, two cases can be distinguished:

- The drilling rotation;
- The vertex rotation.

II-3. Drilling Rotation

According to continuum mechanics, in two-dimensional linear elasticity, the true physical drilling rotation is interpreted as:

$$\varphi = \frac{1}{2}\left(\frac{\partial v}{\partial x} - \frac{\partial u}{\partial y}\right) \qquad \textit{[III-7]}$$

Where u, v are the in-plane components of displacement through the in-plane coordinates x, y respectively. This definition is invariant and it is independent of coordinate system.

In-plane drilling degree of freedom may be physically interpreted as the rotation of the vertex bisecting the angle between adjacent edges of an element. A schematic of the angle bisector and its associated partial derivatives is shown in *Fig. III.2*.

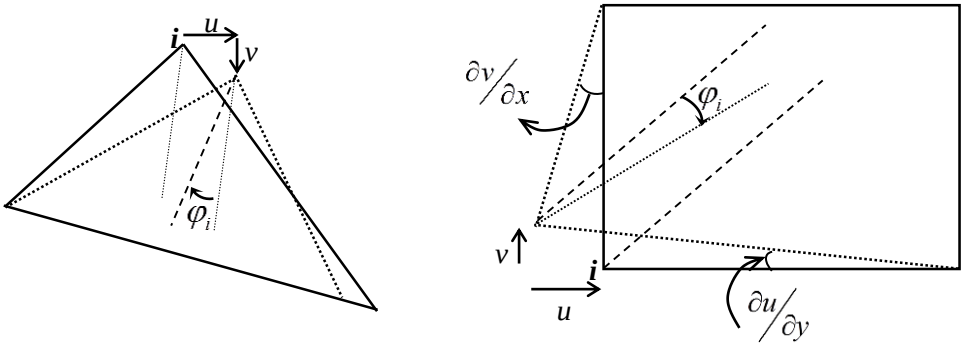

Fig. III.2. **Drilling rotation interpretation**

The idea of including the *drilling rotation* as a nodal parameter in the formulation of membrane finite elements go back to 1960s however, no successful application could be made despite the advantage in using the drilling rotation for shell analysis. This was due the absence of understanding how to relate φ with the in-plane displacement.

The present trend is to relate the in-plane rotational degrees of freedom to the average in-plane rotation of the shell reference surface as a constraint by the penalty function method based on the Hughes's variational formulation, which could lead to a close definition of drilling rotation [HUGHES & BREZZI 1989; FOX & SIMO 1992]. However, strong enforcement of such a constraint can lead to strong in-plane locking.

II-4. Vertex Rotational Degree of Freedom

First progress in this direction was made by Allman in 1984, who introduced the concept of the "vertex rotation" [ALLMAN 1984]. Allman have included the "vertex rotations" into the "Constant Strain Triangular" element to improve its performances. In this approach, for each element's side, the tangential displacement is taken to be linear, whereas, the normal displacement is quadratic.

The vertex rotations "rotation of element's side" is geometrically interpolated in relation to the in-plane transverse displacement of the mid-side between two nodes (*i*) and (*j*) of a quadratic element as presented in *Fig. III.3*.

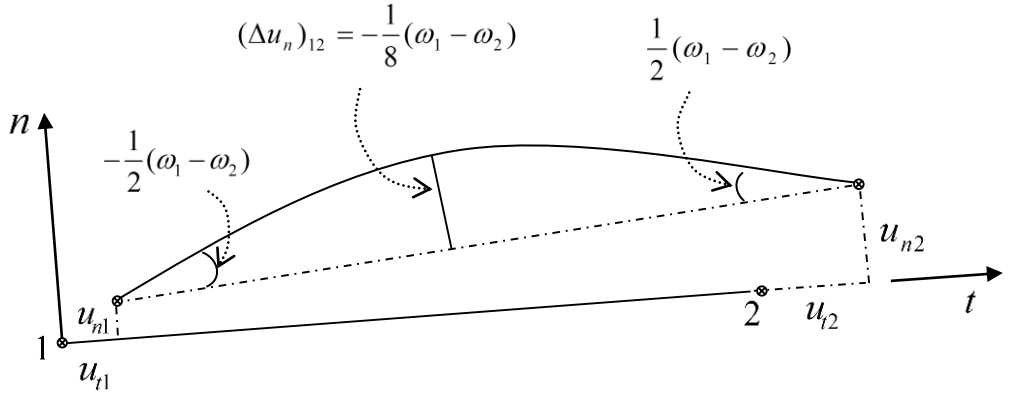

Fig. III.3. **Higher order in-plane displacement interpolation**

For any given side of length ***l***, in the local system (*s*, *n*), the side-tangent displacement u_t is interpolated linearly, as:

$$u_t = \left(1 - \frac{s}{l}\right) u_{t1} + \frac{s}{l} u_{t2} \qquad \textit{[III-8]}$$

The side-normal displacement u_n is interpolated as a quadratic function, as:

$$u_n = \left(1-\frac{s}{l}\right)u_{n1} + \frac{s}{l}u_{n2} + 4\frac{s}{l}\left(1-\frac{s}{l}\right)\Delta u_{n12} \qquad \textit{[III-9]}$$

Vertex rotations are then defined by:

$$u_{n,s}(s = L_{12}) - u_{n,s}(s = 0) = \omega_1 - \omega_2 \qquad \textit{[III-10]}$$

Where: $\boldsymbol{\omega_1}$ and $\boldsymbol{\omega_2}$ are the vertex rotations at nodes (*1*) and (*2*) respectively.

Thus, vertex rotations are related to the derivatives of the displacements computed at the nodes of the element. Nevertheless, it is obvious that this rotation $\boldsymbol{\omega}$ is different from the true drilling rotation φ.

u_n is interpolated in function of vertex rotations ω_2 and ω_1 as:

$$u_n = \left(1-\frac{s}{l}\right)u_{n1} + \frac{s}{l}u_{n2} - \frac{s}{2}\left(1-\frac{s}{l}\right)(\omega_1 - \omega_2) \qquad \textit{[III-11]}$$

This interpolation assure inter elements continuity, and improve in-plane behaviour. However, such a *d.o.f* is not the true in-plane drilling rotation. In shell elements case, when element is involved to deal with plates and other structural elements, vertex rotation *d.o.f* could not assure displacement compatibility as shown in *Fig. III.4*.

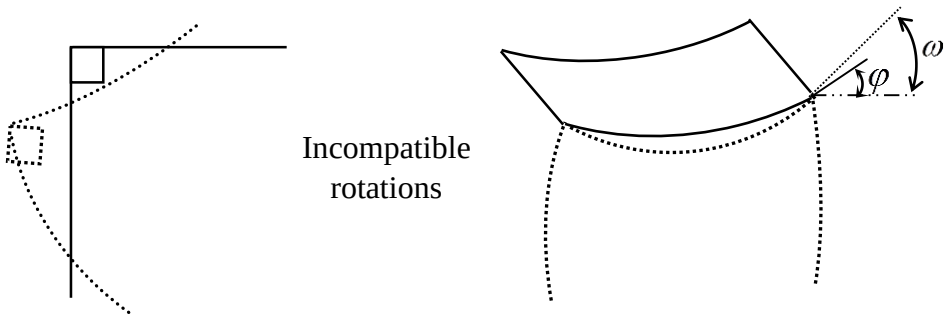

Fig. III.4. **Incompatible rotations**

It became clear that the vertex rotation does not represent the true drilling rotation. Therefore, special care must be taken when using elements based on this concept. Nevertheless, vertex rotation *d.o.f* is still widely used, just in order to improve the convergence rate of plane stress/strain and shell elements.

II-5. Drilling Rotation Locking of Flat Shell Finite Elements

By adding the drilling rotational *d.o.f* to the shell element, we can enhance the shell element's behaviour and compatibility, and we can avoid connectivity and singularity problems that occur in conventional shell elements. However, the presence of the drilling rotational *d.o.f* may cause undesirable locking when flat shell elements are used for modelling curved shells. This observation was reported by [COOK 1993].

Let us consider a curved shell structure represented by flat shell elements E_1, $E_2 \ldots E_n$. As represented by *Fig. III.5*, the out-of-plane nodal rotation θ_b due bending of element E_3, when decomposed in the local system of element E_2, it has a rotational component about the normal axis of element E_2 (i.e., $\theta_b \times sin(\alpha)$) to be added to the membrane rotation θ_m of element E_2. Thus, a bending rotation of element E_3 is in part resisted by membrane stiffness of element E_2. When the shell becomes thinner, the bending stiffness, which is proportional to (h^3), decreases more rapidly than the membrane stiffness, which is proportional to (h). Thus, in the thin shell limit, the large membrane stiffness of element E_2 would tend to lock the bending rotational *d.o.f* of element E_3 and vis-versa. Thus, the drilling rotation locking becomes more pronounced in thin shells.

This effect, was also designated as membrane locking by many authors: [CARPENTER et al 1985; MACNEAL & HARDER 1988; FISH & BELYTSCHKO 1992; ZHU & ZACHARIA 1996; CHOI & LEE 2003]. Nevertheless, drilling rotation locking vanishes as elements become coplanar.

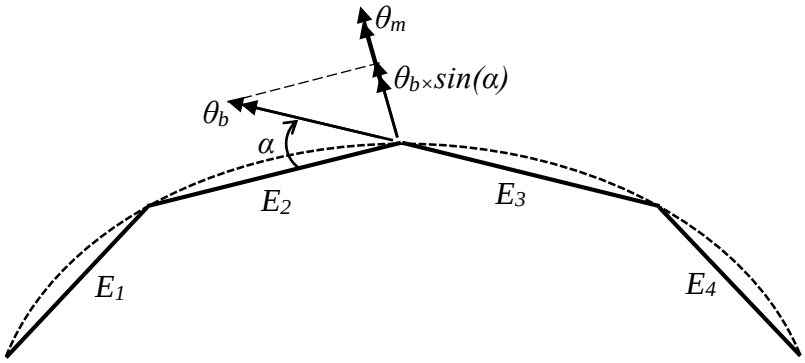

Fig. III.5. **Inter-element bending-membrane coupling**

In order to alleviate the drilling rotation locking, [COOK 1993] multiplied the stabilization matrix by a factor that is related to the 'amount of non-coplaneness'. The reduced integration was also used to alleviate the drilling rotation locking, which was considered as membrane locking problem, see: [CARPENTER et al 1985; FISH & BELYTSCHKO 1992]. Many other works on the problems related to the drilling rotation locking of flat shell elements have presented by: [CARPENTER et al 1985; FISH & BELYTSCHKO 1992; COOK 1994; GROENWOLD & STANDER 1995;

SYDENSTRICKER & LANDAU 2000; CHOI & LEE 2003; KUGLER et al 2011]. However, the solution for complete removal of membrane locking of flat shell elements has not yet been found.

This locking effect is common for flat shell elements that incorporates drilling rotation interpolation or those with fictitious rotational stiffness. Also, this locking tend to vanish when the adjacent finite elements tend to be coplanar. So it could be alleviated, simply by increasing the finite element mesh, as the mesh is refined, flat elements tend to be coplanar, and the inter-element bending-membrane coupling tend to vanish.

As common locking phenomenon does not vanish by refining mesh, the author believe that the "the drilling rotation locking" is due locking of some membrane elements under in-plane bending or other situations when membrane is dominated. Therefore, even if most of the deformation energy results from bending deformation, the over stiffness of membrane component from the adjacent elements will prevail over the bending stiffness leading to incorrect results. For example, the Triangular element with rotational *d.o.f* by [ALLMAN 1984] exhibits membrane locking. As can be seen from the numerical tests presented in *Chapter VI*, Allman's triangle lock and cannot achieve the true solution of a hinged arch even with refined mesh. In this example Allman's triangle converges toward a stiffer solution. So, the author believe that the best cure of this problem is by using locking free membrane elements. For this purpose, a locking removal technic mast be used.

The EAS method has proven to be an efficient solution to overcome all kinds of locking problems. So it is adopted in this work to develop a new locking free triangular membrane element with rotational *d.o.f*. Formulation and details are presented in § *III-1.2.*

III- LINEAR FLAT SHELL FINITE ELEMENTS

In this section, the linear formulations of the various shell finite elements used in the numerical experiments during this work are outlined.

Each shell finite element, with associated elemental displacements and rotations, can be decomposed as:

$$[k]\{q\} = \begin{bmatrix} [k_m] & [0] \\ [0] & [k_b] \end{bmatrix} \begin{Bmatrix} q_m \\ q_b \end{Bmatrix} \qquad \textit{[III-12]}$$

Where $[k_m]$ and $[k_b]$ are: the membrane and plate stiffness matrices respectively.

$[k]$: represents the stiffness matrix in a locally defined coordinate system, with related local nodal displacements and rotations vector $\{q\}$. There will be no coupling stiffness between membrane and plate actions at the element level.

The associated local nodal displacements $\{q\}$ are decomposed into terms associated with membrane displacements $\{q_m\}$, and terms associated with the bending plate displacements $\{q_b\}$.

Specifically, $\{q_m\}=[u \quad v \quad \varphi]^T$, when the in-plane rotational drilling *d.o.f* is considered, else $\{q_m\}=[u \quad v]^T$; where ***u***, *and* ***v*** represent the in-plane nodal translations, and ***φ*** denotes the in-plane nodal rotation at each node. The bending plate out of plane nodal displacement and rotations are denoted by: $\{q_b\}=[w \quad \theta_x \quad \theta_y]^T$.

The thin plate bending elements used in this study are the famous *DKT* triangle, and the *DKQ* quadrilateral Discrete-Kirchhoff Theory elements.

The membrane elements used in this study for the formulation of triangular and quadrilateral flat shell elements are:

- The constant strain triangle (CST);
- Allman triangle with rotational *d.o.f* by [ALLMAN 1984];
- The standard bilinear four nodes quadrilateral element;
- The mixed quadrilateral element with rotational *d.o.f* by [IBRAHIMBIGIVICH et al 1990];

These elements are Iso-parametric elements formulated in the natural coordinate system. [IRONS 1966], introduced the concept of Iso-parametric elements in stiffness methods, that maps the element geometry in terms of natural coordinates regardless of the orientation of an element in the global coordinate system. However, the relationship between the two systems must be used in the element formulation [COOK 1974-a].

- Finally, we contributed in this work by the development of a new triangular element with rotational *d.o.f* based on the Enhanced Assumed Strain method. This element is based on the Allman triangle formulation using area coordinates. This contribution was motivated by the poor behaviour of the existing library of triangular elements even with drilling rotational degree of freedom.

III-1. Membrane Elements

These elements are used for analysing structures subjected to in-plane forces. Assuming that the structure is in the *x-y* plane, the displacement field can be expressed using two *d.o.f* each node (*u* and *v* which are, the translation according to *x* direction and, *y* direction respectively). The stresses of interest are the in-plane normal stresses σ_{xx}, σ_{yy}, and the in-plane shear stress τ_{xy}. Membrane elements are mainly used to model the membrane action in shells.

III-1.1. Conventional Membrane Elements

In the classical "standard" formulations, membrane elements usually has only the translational nodal values of displacement components ***u*** and ***v*** as *d.o.f* at each corner node.

The formulation of these elements is very simple, and it is directly inspired from the bi-dimensional continuum mechanics. However, the performance is very poor.

1- CST: 6 degrees of freedom

Constant strain triangle [TURNER et al 1956]: This is the simplest of all plane-stress/strain elements. The *CST* element is so-named because the strains within the element are independent of the coordinates and hence are constant over the element. It has 6 degrees of freedom (the nodal translational values ***u*** and ***v*** at each of the three corner nodes). Each displacement component is interpolated between the nodal values. The implementation uses standard Iso-parametric procedures, and numerical integration is carried out by Hamer scheme (3 integration points).

The element is conforming (displacement continuity is preserved along all sides) and satisfies all requirements for convergence. However, good accuracy, requires fine mesh.

The *CST*'s formulation, neglects the in-plane rotational field φ, and possesses only two degrees of freedom per node: $\{q_m\} = [u \quad v]^T$, where *u*, *v* represent the in-plane nodal displacements.

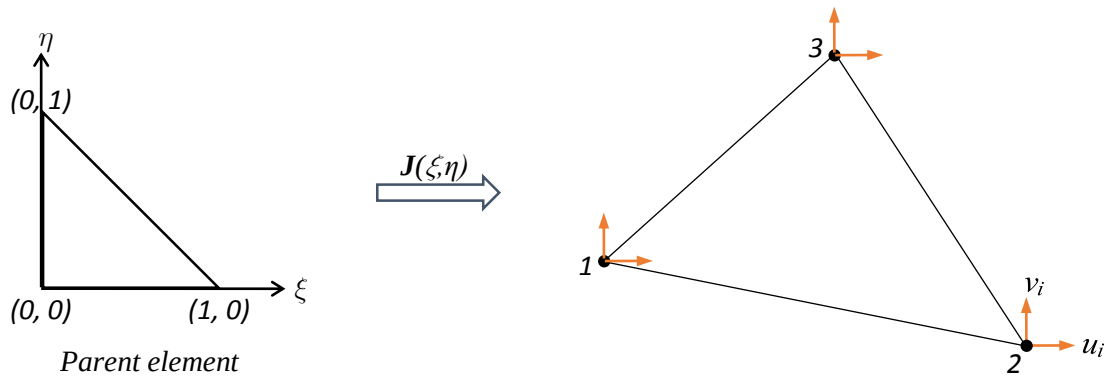

***Fig. III.6. CST* triangular element**

The element's shape functions are expressed in terms of the local coordinates (ξ, η). Cartesian coordinates can be expressed in terms of the shape functions and nodal coordinates by:

$$\begin{Bmatrix} x(\xi,\eta) \\ y(\xi,\eta) \end{Bmatrix} = N_i(\xi,\eta) \begin{Bmatrix} x_i \\ y_i \end{Bmatrix} \qquad [III\text{-}13]$$

For the triangular element, the Iso-parametric shape functions are:

$N_1(\xi,\eta) = 1-\xi-\eta$; $N_2(\xi,\eta) = \xi$; $N_3(\xi,\eta) = \eta$.

The nodal internal forces are:

$$\begin{bmatrix} f_x^i & f_y^i \end{bmatrix} = \int_A \begin{bmatrix} N_{i,x} & N_{i,y} \end{bmatrix} \begin{bmatrix} \sigma_{xx} & \sigma_{xy} \\ \sigma_{xy} & \sigma_{yy} \end{bmatrix} \cdot h \cdot J \cdot d\xi \cdot d\eta \qquad [III\text{-}14]$$

2- Q4: 8 degrees of freedom

This is the standard quadrilateral element with bilinear displacement field. It has 8 *d.o.f*, which are the nodal values of translational components ***u*** and ***v*** at each of the four corner nodes. Each displacement component is interpolated between the nodal values. The implementation uses the standard Iso-parametric procedure. Numerical integration is carried out by gauss quadrature (*2x2* integration points). [TAIG 1961; ERGATOUDIS et al 1968] developed the shape functions used to formulate the element stiffness matrix for the four nodes Iso-parametric quadrilateral element.

The element is conforming (displacement continuity is preserved along all sides) and satisfies all requirements for convergence. Good accuracy however, requires a fine mesh.

This element formulation neglects the in-plane rotational field φ, and possesses only two degrees of freedom per node: $\{q_m\} = \begin{bmatrix} u & v \end{bmatrix}^T$, where *u*, *v* represent the in-plane nodal displacements.

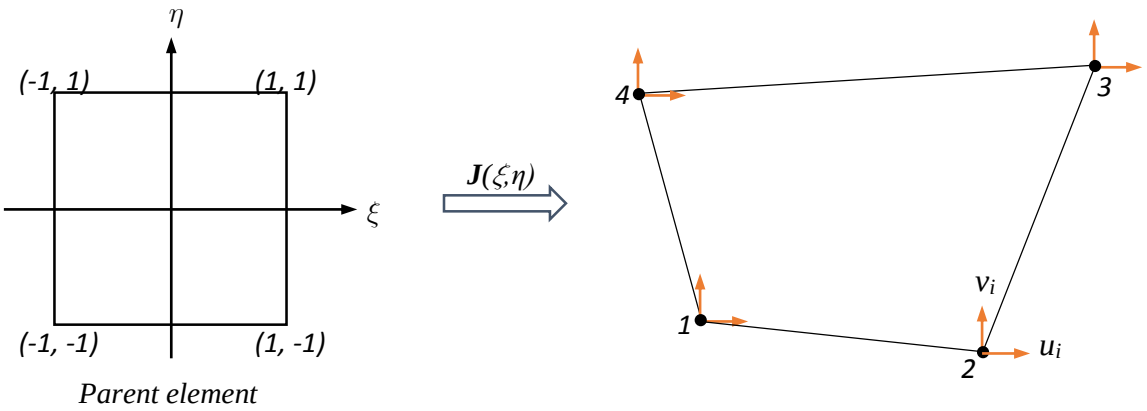

***Fig. III.7. Q4* quadrilateral element**

The element's shape functions are expressed in terms of the local coordinates (ξ, η). Cartesian coordinates can be expressed in terms of the shape functions and nodal coordinates by:

$$\begin{Bmatrix} x(\xi,\eta) \\ y(\xi,\eta) \end{Bmatrix} = N_i(\xi,\eta) \begin{Bmatrix} x_i \\ y_i \end{Bmatrix} \qquad \textit{[III-15]}$$

For the quadrilateral element, the Iso-parametric shape functions are:

$$N_i(\xi,\eta) = \frac{1}{4}(1+\xi_i\xi)(1+\eta_i\eta) \qquad \textit{[III-16]}$$

III-1.2. Membrane Elements with Drilling Rotation

In this formulation, plane stress elements are having (3 d.o.f) at each node. An Allman type displacement field which incorporates the in-plane rotation is used [COOK 1986]. The main feature of this formulation is that the in plane displacement field become quadratic due to the in plane rotations effect, *Fig. III.8*. Furthermore, for quadrilateral elements, Hughes's simplified variational formulation by [HUGHES & BREZZI 1989; IBRAHIMBEGOVIĆ et al 1990] is used to enforce the vertex rotation to be close to the true drilling rotation.

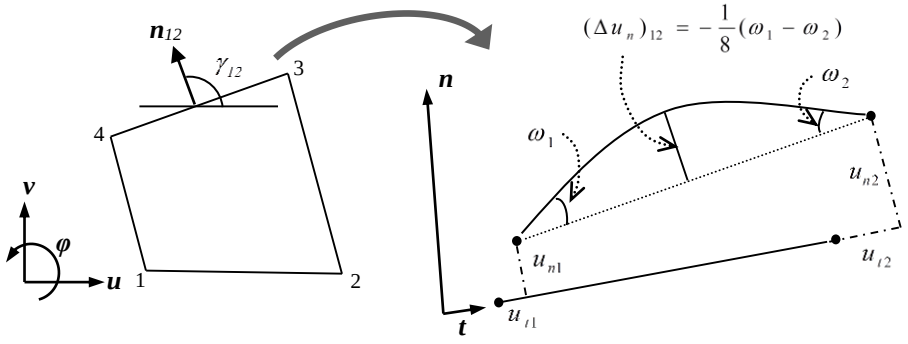

Fig. III.8. **In-plane displacement due corner nodes rotations**

ω: represent the vertex in plane rotation (rotation of the element's side), which is clearly different from the true real drilling degree of freedom: $\varphi = \frac{1}{2}\left(\frac{\partial v}{\partial x} - \frac{\partial u}{\partial y}\right)$.

Then, the quadratic Allman-type interpolation of the in-plane displacement is written:

$$\{U\} = \begin{Bmatrix} u \\ v \end{Bmatrix} = \sum N_i(\xi,\eta) \begin{Bmatrix} u_i \\ v_i \end{Bmatrix} + \sum NS_k(\xi,\eta) \frac{l_{ij}}{8}(\phi_j - \phi_i) \begin{Bmatrix} C_{ij} \\ S_{ij} \end{Bmatrix} \qquad \textit{[III-17]}$$

Where, N_i are the Triangular/quadrilateral shape functions of linear interpolation, and NS_k are the Triangular/quadrilateral quadratic serendipity shape functions.

$$\begin{cases} C_{ij} = \cos\gamma_{ij} = y_{ij}/l_{ij} \\ S_{ij} = \sin\gamma_{ij} = -x_{ij}/l_{ij} \end{cases} \qquad \textit{[III-18]}$$

1- Allman Triangular Element

The 3-nodded membrane element with in-plane rotational *d.o.f* presented in *Fig. III.9*. is derived by combining the standard *CST* and a higher order in-plane displacements using Allman-type interpolation functions [ALLMAN 1984]. Only a brief review is presented here.

[ALLMAN 1984] presented the first successful triangular membrane element with in-plane rotational degrees of freedom. The formulation of this element, popularly known as the Allman triangle is simple, but it suffers from zero energy mode (singularity) which occurs when all the nodal rotations are identical. Practically, this singularity is automatically removed by the application of kinematic boundary conditions. [ALLMAN 1988-*a*] removed that rank deficiency in a revised version of the element.

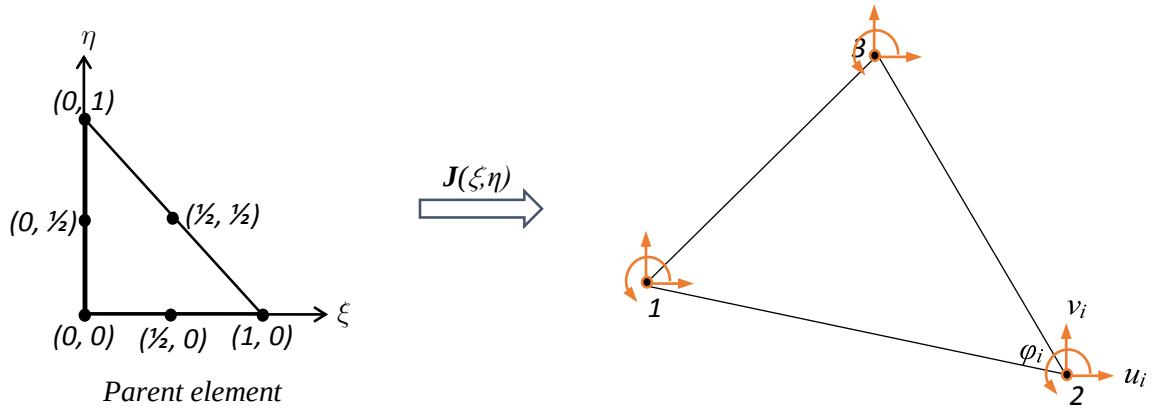

***Fig. III.9.* Triangular element with drilling rotations**

[COOK 1986] showed that Allman's triangle can be derived from the *LST* element using a simple transformation which relates the mid-side displacements in terms of the corner displacements and rotations. Allman type displacement field interpolation for a three-node triangle is:

$$\{U\}=\begin{Bmatrix}u\\v\end{Bmatrix}=\sum_{i=1}^{3}N_i(\xi,\eta)\begin{Bmatrix}u_i\\v_i\end{Bmatrix}+\sum_{k=4}^{6}NL_k(\xi,\eta)\frac{(\phi_j-\phi_i)}{8}\begin{Bmatrix}X_{ij}\\Y_{ij}\end{Bmatrix} \qquad \textit{[III-19]}$$

With: $\{U_i\}=\begin{Bmatrix}u_i\\v_i\end{Bmatrix}$ is the nodal displacements vector.

$$N_1(\xi,\eta)=1-\xi-\eta\,;\; N_2(\xi,\eta)=\xi\,;\; N_3(\xi,\eta)=\eta \qquad \textit{[III-20]}$$

NL: represent the shape functions of a 6-node triangle:

$$\begin{cases}NL_4(\xi,\eta)=4\xi(1-\xi-\eta)\\NL_5(\xi,\eta)=4\xi\eta\\NL_6(\xi,\eta)=4\eta(1-\xi-\eta)\end{cases} \qquad \textit{[III-21]}$$

Strain vector is:

$$\varepsilon = sym(\nabla u) = \left[\frac{\partial u}{\partial x} \quad \frac{\partial v}{\partial y} \quad \frac{\partial u}{\partial y} + \frac{\partial v}{\partial x} \right]^T \qquad \textit{[III-22]}$$

Which is written in matrix notation as:

$$\varepsilon = \sum_{i=1}^{3} \left([B_i]\{U_i\} + \{G_i\}\phi_i \right) \qquad \textit{[III-23]}$$

Whit: ϕ_i are the nodal in-plane rotations.

The strain matrix $[\bar{\bar{B}}]$ is written as:

$$[\bar{\bar{B_i}}] = \left\{ [B_i] \ , \ \{G_i\} \right\} \qquad \textit{[III-24]}$$

$$[B_i] = \begin{bmatrix} \partial N_i / \partial x & 0 \\ 0 & \partial N_i / \partial y \\ \partial N_i / \partial y & \partial N_i / \partial x \end{bmatrix} \qquad \textit{[III-25]}$$

$$\{G_i\} = \frac{1}{8} \begin{Bmatrix} l_{ji} C_{ji} \left(\partial NL_l / \partial x \right) - l_{ik} C_{ik} \left(\partial NL_m / \partial x \right) \\ l_{ji} S_{ji} \left(\partial NL_l / \partial y \right) - l_{ik} S_{ik} \left(\partial NL_m / \partial y \right) \\ l_{ji} C_{ji} \left(\partial NL_l / \partial y \right) - l_{ik} C_{ik} \left(\partial NL_m / \partial y \right) + l_{ji} S_{ji} \left(\partial NL_l / \partial x \right) - l_{ik} S_{ik} \left(\partial NL_m / \partial x \right) \end{Bmatrix} \qquad \textit{[III-26]}$$

We get the stiffness matrix as:

$$[K] = \int_{\Omega} [\bar{\bar{B}}]^T [D] [\bar{\bar{B}}] d\Omega \qquad \textit{[III-27]}$$

$[\bar{\bar{B}}]$ is written as:

$$[\bar{\bar{B_i}}] = \left\{ [B_i] \ , \ \{G_i\} \right\} \qquad \textit{[III-28]}$$

With: $[K] \cdot \{q\} = \{f\}$, and $\{q\}^T = \langle u_1, v_1, \varphi_1; \ldots\ldots\ldots ; u_3, v_3, \varphi_3 \rangle$.

Numerical integration is carried out by 3 integration points.

2- Quadrilateral Element with Drilling Rotation [IBRAHIMBEGOVIĆ et al 1990]

The 4-noddee membrane element with drilling rotational *d.o.f* presented in *Fig. III.10*. is derived by combining the standard bilinear quadrilateral and a higher order in-plane displacements using Allman-type interpolation functions. This element uses an independent standard bilinear rotational interpolation, then they are related to the in-plane displacements employing the variational formulation presented by [HUGHES & BREZZI 1989].

Details of the formulation can be found in [IBRAHIMBEGOVIĆ et al 1990]. Only a brief review is presented here.

Allman type displacement field interpolation for a four-node quadrilateral is:

$$\{U\}=\begin{Bmatrix}u\\v\end{Bmatrix}=\sum_{i=1}^{4}N_i(\xi,\eta)\begin{Bmatrix}u_i\\v_i\end{Bmatrix}+\sum_{k=4}^{8}NS_k(\xi,\eta)\frac{(\phi_j-\phi_i)}{8}\begin{Bmatrix}X_{ij}\\Y_{ij}\end{Bmatrix} \qquad [III\text{-}29]$$

The independent in plane rotation is taken to be:

$$\phi=\sum_{i=1}^{4}N_i(\xi,\eta)\cdot\varphi_i \qquad [III\text{-}30]$$

With: $N_i(\xi,\eta)=\frac{1}{4}(1+\xi_i\xi)(1+\eta_i\eta)$

NS: represent Serendipity shape functions for the 8-node quadrilateral element:

$$\begin{cases}NS_k(\xi,\eta)=\frac{1}{2}(1-\xi^2)(1+\eta_k\eta) & for\ k=5,7\\ NS_k(\xi,\eta)=\frac{1}{2}(1+\xi_k\xi)(1-\eta^2) & for\ k=6,8\end{cases} \qquad [III\text{-}31]$$

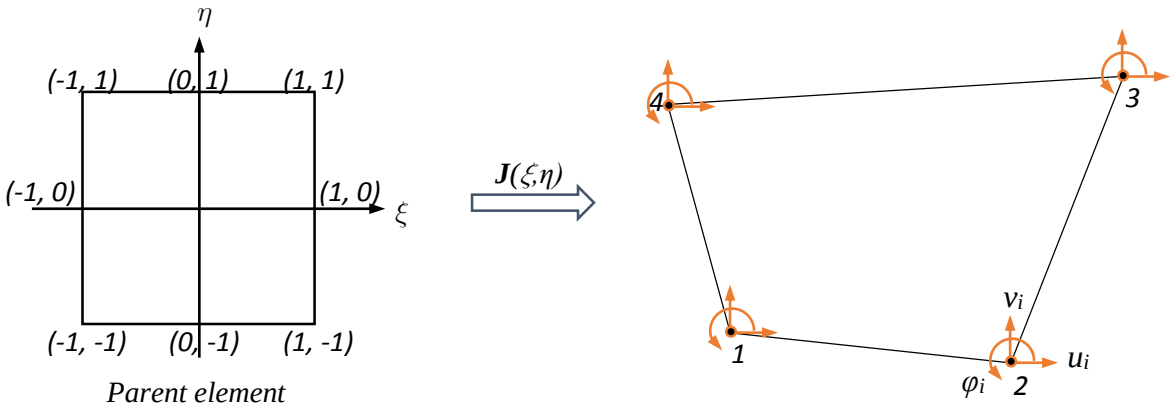

***Fig. III.10.* Quadrilateral element with drilling rotations**

Following the same steps above we get:

$$\varepsilon = sym(\nabla u) = \sum_{i=1}^{4}\left([B_i]\{U_i\} + \{G_i\}\varphi_i\right) \qquad \textit{[III-32]}$$

$$[B_i] = \begin{bmatrix} \partial N_i/\partial x & 0 \\ 0 & \partial N_i/\partial y \\ \partial N_i/\partial y & \partial N_i/\partial x \end{bmatrix} \qquad \textit{[III-33]}$$

$$\{G_i\} = \frac{1}{8}\begin{Bmatrix} l_{ji}C_{ji}\left(\partial NS_l/\partial x\right) - l_{ik}C_{ik}\left(\partial NS_m/\partial x\right) \\ l_{ji}S_{ji}\left(\partial NS_l/\partial y\right) - l_{ik}S_{ik}\left(\partial NS_m/\partial y\right) \\ l_{ji}C_{ji}\left(\partial NS_l/\partial y\right) - l_{ik}C_{ik}\left(\partial NS_m/\partial y\right) + l_{ji}S_{ji}\left(\partial NS_l/\partial x\right) - l_{ik}S_{ik}\left(\partial NS_m/\partial x\right) \end{Bmatrix} \qquad \textit{[III-34]}$$

The stiffness matrix is calculated using:

$$[K] = \int_{\Omega} \overline{[B]}^{T}\,[D]\,\overline{[B]}\,d\Omega \qquad \textit{[III-35]}$$

With: $\overline{[B_i]} = \{\,[B_i]\,,\ \{G_i\}\,\}$, $[k]\cdot\{q\} = \{f\}$, and $\{q\}^T = \langle u_1, v_1, \varphi_1; \ldots\ldots; u_4, v_4, \varphi_4 \rangle$.

The Variational Formulation:

Considering the problem of determining the equilibrium state of an elastic solid body, the solution consists of determining the unknown variables (u, φ, S), in which, u is the displacement field, ϕ is the rotation field, and S represents the stress field. The equilibrium state is described by:

The equilibrium equation: $div(\sigma) + f = 0$;

The stress symmetry condition: $skew(\sigma) = 0$;

The In-plane rotation-displacement relation: $\varphi = skew(\nabla u)$;

The constitutive relation: $sym(\sigma) = C \cdot sym(\nabla u)$;

With: $\sigma = sym(\sigma) + skew(\sigma)$.

$sym(\sigma) = \frac{1}{2}\left(\sigma + \sigma^T\right)$, the symmetric part of stress tensor σ.

$skew(\sigma) = \frac{1}{2}\left(\sigma - \sigma^T\right)$, the anti-symmetric part of stress tensor σ.

In order to simplify the problem and make it applicable [HUGHES & BREZZI 1989] established a modified variant of Reissner's variational formulation in a weak form. It is written in the following form:

$$\frac{1}{2}\int_{\Omega} sym\ (\nabla \delta u)\cdot C\cdot sym\ (\nabla u)\cdot d\Omega + \qquad \textit{[III-36]}$$

$$+\rho\int_{\Omega}\left(a\text{ntisym}(\nabla \delta u)-\delta\phi\right)\cdot\left(a\text{ntisym}(\nabla u)-\phi\right)d\Omega=\int_{\Omega}\delta u\cdot f\ \cdot d\Omega$$

With: $\varepsilon = sym\,(\nabla u)$.

In this variational formulation, a penalty term is introduced, which is the second term of the left side of *Eq. [III-36]*.

Hence, According to this formulation, the stiffness matrix is penalised by a penalty matrix [*P*].

Finally, we get the stiffness matrix in its final form as:

$$\left[K^{m}\right]=[K]+[P] \qquad \textit{[III-37]}$$

The penalty stiffness matrix [*P*] relates the in-plane rotation field and the in-plane displacement field, it is calculated as follows:

$$skew(\nabla u)-\phi=\sum_{i=1}^{4}\left(\langle b_i\rangle\{u_i\}+g_i\varphi_i\right) \qquad \textit{[III-38]}$$

In which:

$$\langle b_i\rangle=\left\{-\frac{1}{2}\frac{\partial N_i}{\partial y},\ \frac{1}{2}\frac{\partial N_i}{\partial x}\right\} \qquad \textit{[III-39]}$$

$$g_i=-\frac{1}{16}\left(l_{ji}C_{ji}\left(\partial NS_l/\partial y\right)-l_{ik}C_{ik}\left(\partial NS_m/\partial y\right)+l_{ji}S_{ji}\left(\partial NS_l/\partial x\right)-l_{ik}S_{ik}\left(\partial NS_m/\partial x\right)\right)-N_i \qquad \textit{[III-40]}$$

Then, we get:

$$\langle \bar{\bar{b}}_i\rangle=\left\{\ \langle b_i\rangle\ ,\ g_i\ \right\} \qquad \textit{[III-41]}$$

$$[P]=\rho\int_{\Omega}\langle \bar{\bar{b}}\rangle^{T}\ \langle b\rangle\cdot d\Omega \qquad \textit{[III-42]}$$

For isotropic materials, the penalization parameter ρ is taken to be the shear modulus, $\rho = G$.

It is noticed that in-plane behaviour dose not exhibit sensibility to the value of ρ while $\rho \le G$, [LIU et al 2000; LONG et al 2006]. However, when this in-plane element is used within a flat shell element, many researchers propose the value: $10^{-3} \le \frac{\rho}{G} \le 10^{-2}$, see [GEYER & GROENWOLD 2003; WISNIEWSKI & TURSKA 2006].

We have used: $\rho = 0.05G$, as suggested by [PIMPINELLI 2004].

The finite element implementation uses standard Iso-parametric procedure, and numerical integration is carried out by gauss quadrature scheme.

This membrane element is free from parasitic shear locking and also from trapezoidal locking due to mesh distortion. It performs satisfactory in pure bending situations, so it is selected as the membrane part of the quadrilateral flat shell element with drilling rotation.

3- The New EAS Triangle with Rotational Degree of Freedom

The enhanced assumed strain (EAS) formulation, is widely used in many element formulation to prevent over-stiffness of finite elements response. The main idea behind this formulations that is based mainly on [SIMO & RIFAI 1990; SIMO & ARMERO 1992; ANDELFINGER & RAMM 1993] works, is the enhancement of the variational principle into a 3–field functional well known as Hu–Washizu variational formulation, which can be written as:

$$\Pi = \int_v \left(\frac{1}{2} \varepsilon^T C \varepsilon - u^T \bar{f} \right) dv - \int_S u^T \bar{T} dS - \int_v \sigma^T \varepsilon^h dv \qquad \textit{[III-43]}$$

By introducing the enhanced strains $\boldsymbol{\varepsilon}^h$ in addition to the original strains we get:

$$\varepsilon = [B] u + \varepsilon^h \qquad \textit{[III-44]}$$

In this formulation, the enhanced strains is written as:

$$\varepsilon^h = [B]^h \lambda \qquad \textit{[III-45]}$$

Where α denotes the additional degrees of freedom. This additional strain may not cause any energy within the element formulation:

$$\int_{v^e} \sigma^T \cdot \varepsilon^h dv^e = 0 \qquad \textit{[III-46]}$$

In the Allman's displacement field interpolation of *Eq. [III-19]*, the lateral displacement along each side is taken to be quadratic due corner node rotations. However, tangential displacement remain linear, while in the *LST* higher order element interpolation, both lateral and tangential

displacements are quadratic. So, our methodology consists of adding the missing quadratic tangential components along each side in Allman's interpolation comparing to the *LST* triangle interpolation by using additional incompatible displacements.

Let us assume that α_k will be the tangential mid-side displacement of a side *(ij)* as presented in *Fig. III.11-c*. Thus, the enhanced displacement due mid-side tangential displacement *d.o.f* α_k could be written as:

$$\{U^h\} = \begin{Bmatrix} u^h \\ v^h \end{Bmatrix} = \sum_{k=4}^{6} NL_k(\xi,\eta)\cdot\alpha_k \cdot \begin{Bmatrix} \cos(\Gamma_{ij}) \\ \sin(\Gamma_{ij}) \end{Bmatrix} \qquad \textit{[III-47-a]}$$

Using $\gamma_{ij} - \Gamma_{ij} = \dfrac{\pi}{2}$ yields:

$$\{U^h\} = \begin{Bmatrix} u^h \\ v^h \end{Bmatrix} = \sum_{k=4}^{6} NL_k(\xi,\eta)\cdot\alpha_k \cdot \begin{Bmatrix} S_{ij} \\ -C_{ij} \end{Bmatrix} \qquad \textit{[III-47-b]}$$

The total displacement field is taken to be $u = u^c + u^h$, thus:

$$\{U\} = \begin{Bmatrix} u \\ v \end{Bmatrix} = \sum_{i=1}^{3} N_i(\xi,\eta)\begin{Bmatrix} u_i \\ v_i \end{Bmatrix} + \sum_{k=4}^{6} NL_k(\xi,\eta)\frac{(\phi_j - \phi_i)}{8}\begin{Bmatrix} y_{ij} \\ -x_{ij} \end{Bmatrix} + \sum_{k=4}^{6} NL_k(\xi,\eta)\cdot\alpha_k \cdot \begin{Bmatrix} S_{ij} \\ -C_{ij} \end{Bmatrix} \qquad \textit{[III-48]}$$

Where u^c represents the original compatible Allman's-type displacement.

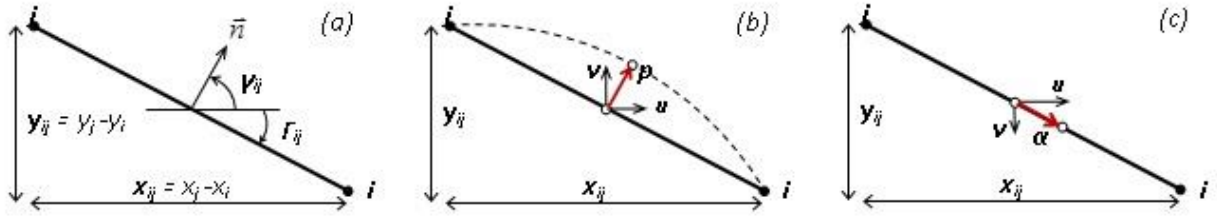

Fig. III.11. **Higher order in-plane lateral and tangential displacements**

The three parameters α_1, α_2 and α_3 associated with the incompatible enhanced strain terms can be eliminated by static condensation so that the nine degrees of freedom are left for the enhanced element, see [SIMO & RIFAI 1990].

The obtained numerical results of the present elements are found to be identical to that of the EAS triangular element by [PILTNER & TAYLOR 2000] called TE4 with three parameters λ_2, λ_3, and λ_4, in which, the enhanced displacement is written in area coordinates as:

$$\begin{Bmatrix} u^h \\ v^h \end{Bmatrix} = \begin{Bmatrix} \lambda_2 x_{21} L_1 L_2 + \lambda_3 x_{32} L_2 L_3 + \lambda_4 x_{13} L_3 L_1 \\ \lambda_2 y_{21} L_1 L_2 + \lambda_3 y_{32} L_2 L_3 + \lambda_4 y_{13} L_3 L_1 \end{Bmatrix} \qquad \textit{[III-49-a]}$$

This enhanced displacement could be written in natural coordinates as:

$$\begin{Bmatrix} u^h \\ v^h \end{Bmatrix} = \sum_{k=4}^{6} NL_k(\xi,\eta) \cdot \lambda_i l_{ij} \cdot \begin{Bmatrix} -S_{ij} \\ C_{ij} \end{Bmatrix} \qquad \textit{[III-49-b]}$$

The difference between the present element and the TE4 element is obvious. However, as the parameters λ_i are independent, the terms $\lambda_i \cdot l_{ij} \cdot \begin{Bmatrix} -S_{ij} \\ C_{ij} \end{Bmatrix}$ used for the TE4 element formulation could be equivalent to the terms $\alpha_i \cdot \begin{Bmatrix} S_{ij} \\ -C_{ij} \end{Bmatrix}$ used in our formulation if we set $\alpha_i = -\lambda_i l_{ij}$.

[PILTNER & TAYLOR 2000] introduced another incompatible mode in order to avoid the spurious zero energy mode as:

$$\begin{Bmatrix} u^h \\ v^h \end{Bmatrix} = \lambda_1 \begin{Bmatrix} y_{12} L_1 L_2 + y_{23} L_2 L_3 + y_{31} L_3 L_1 \\ -x_{12} L_1 L_2 - x_{23} L_2 L_3 - x_{31} L_3 L_1 \end{Bmatrix} \qquad \textit{[III-49-c]}$$

We get the same mode by considering additional incompatible displacements that represent lateral mid-side displacements using the same approach used with tangential mid-side displacement as:

$$\{U^h\} = \begin{Bmatrix} u^h \\ v^h \end{Bmatrix} = \sum_{k=4}^{6} NL_k(\xi,\eta) \cdot \frac{\alpha_i}{8} \cdot \begin{Bmatrix} y_{ij} \\ -x_{ij} \end{Bmatrix} \qquad \textit{[III-50]}$$

However, this displacement does not meet the requirement of that a set of incompatible modes should be independent of the compatible strain field. This problem can be avoided by using one incompatible parameter for the three modes as:

$$\{U^h\} = \begin{Bmatrix} u^h \\ v^h \end{Bmatrix} = \alpha_4 \sum_{k=4}^{6} \frac{1}{8} NL_k(\xi,\eta) \cdot \begin{Bmatrix} y_{ij} \\ -x_{ij} \end{Bmatrix} \qquad \textit{[III-51]}$$

Thus, the total enhanced displacement u^h is written as

$$\{U^h\} = \begin{Bmatrix} u^h \\ v^h \end{Bmatrix} = \sum_{k=4}^{6} NL_k(\xi,\eta) \cdot \alpha_i \cdot \begin{Bmatrix} S_{ij} \\ -C_{ij} \end{Bmatrix} + \alpha_4 \left(\sum_{k=4}^{6} \frac{1}{8} NL_k(\xi,\eta) \begin{Bmatrix} y_{ij} \\ -x_{ij} \end{Bmatrix} \right) \qquad \textit{[III-52]}$$

In fact the addition of the first three incompatible displacements overcome the problem of spurious zero energy mode related to Allman's interpolation. However, the element still be

insensitive to the nodal rotation average, which can be avoided, as suggested by [MACNEAL & HARDER 1989].

The obtained element is equivalent to the TE4 element by [PILTNER & TAYLOR 2000]. It represents a rational approach of the TE4 EAS triangular element formulation.

Finally, we get the following enhanced strain matrix $\left[B^e\right]$:

$$\left[B^e\right]=\begin{bmatrix} B_{11} & B_{12} & B_{13} & B_{14} \\ B_{21} & B_{22} & B_{23} & B_{24} \\ B_{31} & B_{32} & B_{33} & B_{34} \end{bmatrix} \qquad \textit{[III-53]}$$

With: $B_{11}=S_{12}\dfrac{\partial NL_4}{\partial x}$, $B_{12}=S_{23}\dfrac{\partial NL_5}{\partial x}$, $B_{13}=S_{31}\dfrac{\partial NL_6}{\partial x}$, $B_{14}=\dfrac{1}{8}\dfrac{\partial(NL_4y_{12}+NL_5y_{23}+NL_6y_{31})}{\partial x}$

$$B_{21}=-C_{12}\frac{\partial N_4}{\partial y},\ B_{22}=-C_{23}\frac{\partial N_5}{\partial y},\ B_{23}=-C_{31}\frac{\partial N_6}{\partial y},\ B_{24}=-\frac{1}{8}\frac{\partial(NL_4x_{12}+NL_5x_{23}+NL_6x_{31})}{\partial y}$$

$$B_{31}=-C_{12}\frac{\partial N_4}{\partial x}+S_{12}\frac{\partial N_4}{\partial y},\ B_{32}=-C_{23}\frac{\partial N_5}{\partial x}+S_{23}\frac{\partial N_5}{\partial y},\ B_{13}=-C_{31}\frac{\partial N_6}{\partial x}+S_{31}\frac{\partial N_6}{\partial y},$$

$$B_{34}=-\frac{1}{8}\frac{\partial(NL_4x_{12}+NL_5x_{23}+NL_6x_{31})}{\partial x}+\frac{1}{8}\frac{\partial(NL_4y_{12}+NL_5y_{23}+NL_6y_{31})}{\partial y}$$

$$\frac{\partial N_k}{\partial x}=j_{11}\frac{\partial N_k}{\partial \xi}+j_{12}\frac{\partial N_k}{\partial \eta}$$

$$\frac{\partial N_k}{\partial x}=j_{21}\frac{\partial N_k}{\partial \xi}+j_{22}\frac{\partial N_k}{\partial \eta}$$

The enhanced strain must be replaced here by $\left[\overline{B}^h\right]=\left[B^h\right]-\dfrac{1}{A}\iint_A\left[B^h\right]dA$ in order to make the resulting strains orthogonal to constant stress terms, as suggested in [IBRAHIMBEGOVIC & WILSON 1991]. Thus, $\dfrac{\partial N_k}{\partial \xi}$ and $\dfrac{\partial N_k}{\partial \eta}$ are replaced by the following:

$$\frac{\partial \overline{N}_1}{\partial \xi}=\frac{\partial N_1}{\partial \xi},\ \frac{\partial \overline{N}_2}{\partial \xi}=\frac{\partial N_2}{\partial \xi}-\frac{4}{3},\ \frac{\partial \overline{N}_3}{\partial \xi}=\frac{\partial N_3}{\partial \xi}+\frac{4}{3}$$

$$\frac{\partial \overline{N}_1}{\partial \eta}=\frac{\partial N_1}{\partial \eta}+\frac{4}{3},\ \frac{\partial \overline{N}_2}{\partial \eta}=\frac{\partial N_2}{\partial \eta}-\frac{4}{3},\ \frac{\partial \overline{N}_3}{\partial \eta}=\frac{\partial N_3}{\partial \eta}$$

III-2. Plate Bending Elements

Among various thin plate bending elements, discrete Kirchhoff elements appear most attractive. They are widely accepted due to their efficiency and simplicity. One of the reasons for their popularity, is also the fact that they involves a direct interpolation of the transverse displacement w and the rotations θ_x and θ_y as the nodal degrees of freedom.

Due to the independent interpolations, the continuity requirement is only C^0. The interpolations are constructed such that the Kirchhoff constrain is satisfied only in discrete points, in which, normal rotations are approximated within the element, and independent description is used for transverse displacement on the element boundary. This concept was applied early by [WEMPNER et al 1968; STRICKLIN et al 1969; DHATT 1970]. More developments and applications with DKT elements have been established: [BATOZ et al 1980; BATOZ 1982; JEYACHANDRABOSE et al 1985; JEYACHANDRABOSE & KIRKHOPE 1986; BATOZ & LARDEUR 1989; KATILI 1993-a].

The concept of the discrete Kirchhoff constraint has also been applied successfully to quadrilateral elements by [BATOZ & BEN-TAHAR 1982; JEYACHANDRABOSE et al 1987; KATILI 1993-b]. The triangular "DKT" and quadrilateral "DKQ" elements has been considered as the most efficient elements among the class of thin plate bending elements with 3-dof at corner nodes.

1- DKT: 9 degrees of freedom

The Discrete Kirchhoff Triangular plate bending element, is one of the most popular thin plate triangular elements. It is a triangular thin plate element having (3 d.o.f) at each node.

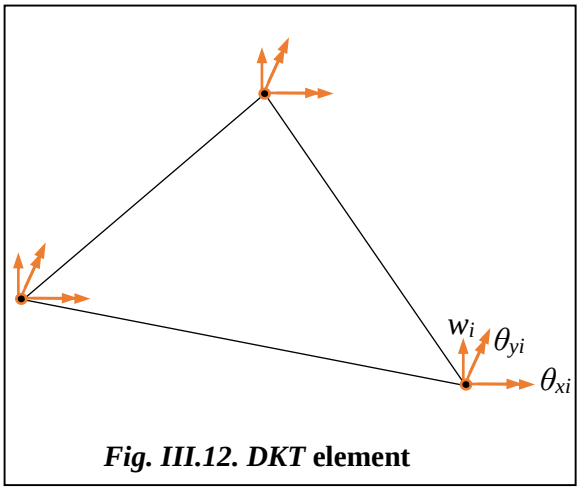

***Fig. III.12. DKT* element**

Since transverse shear deformation is not permitted, results are available for deflection, rotations, moments and transverse forces, but no transverse shear stress. The formulation of the *DKT* element is well known [BATOZ et al 1980], and will therefore not be presented in details here. The stiffness matrix of the *DKT* element is defined in the standard manner for displacement models. This simple plate bending element satisfies all convergence criteria, and it is very effective and reliable for thin plate bending analysis, besides, it has a good behaviour with respect to element distortions.

2- DKQ: 12 degrees of freedom

The Discrete Kirchhoff Quadrilateral plate element formulated by [BATOZ & BEN-TAHAR 1982], is a quadrilateral thin plate element having (3 d.o.f) at each node. It is commonly used in the analysis of thin plate problems. Since transverse shear deformation is not permitted, results are available for deflection, rotations, moments and transverse forces, but no transverse shear stress. The formulation of the *DKQ* element is well known, and will therefore not be presented in detail here. The stiffness matrix of the *DKQ* element is defined in the standard manner for displacement models. As for the DKT element, the DKQ satisfies all convergence criteria, and it is very effective and reliable for thin plate bending analysis, besides, it has a good behaviour with respect to element distortions.

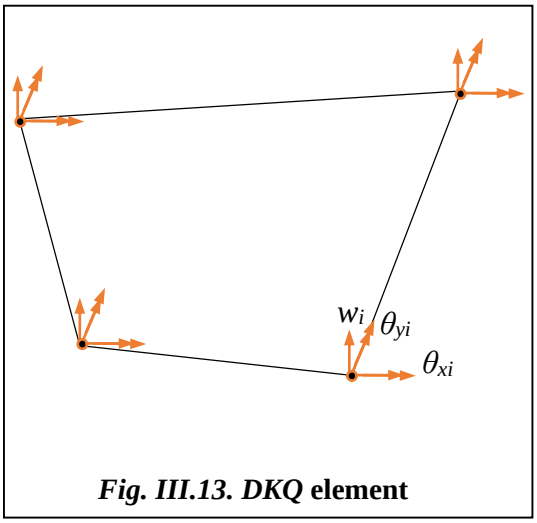

***Fig. III.13. DKQ* element**

III-3. Construction of Flat Shell Elements

The membrane and plate bending elements formulations presented in the above sections can be combined to form quadrilateral and triangular shell elements. By considering all nodes of a flat shell element are placed at mid-plane, the stiffness matrix can be formed by combining the membrane stiffness and the plate stiffness obtained independently as follows:

$$[k_{shell}] = \begin{vmatrix} [k_m] & 0 \\ 0 & [k_b] \end{vmatrix} \qquad [III\text{-}54]$$

By combining the DKT and the DKQ plate bending elements with plane membrane elements, various thin shell elements can be constructed. In the framework of this investigation, we have constructed four flat shell finite elements that will be tested for linear and geometrically non-linear static and dynamic analysis.

III-3.1. Triangular Flat Shell Elements

Triangular elements are preferred for modelling arbitrary shaped geometry and hence are used quite extensively for the analysis of planar and curved spatial structures due the fact that they could reproduce any geometry batter then quadrilateral elements.

1) The first triangular flat shell element implemented in order to be tested for dynamic non-linear analysis is denoted "*Trian*". It is a combination of the *DKT* triangular plate bending element by

[BATOZ et al 1980], and the *CST* triangular standard plane-stress element. The solution of fictitious stiffness is adopted to avoid stiffness matrix singularity. The following approximation of the moment-rotation relationship is adopted:

$$\begin{Bmatrix} M_{z1} \\ M_{z2} \\ M_{z3} \end{Bmatrix} = \alpha \cdot E \cdot t^3 \cdot A \cdot \begin{bmatrix} 1 & -0.5 & -0.5 \\ -0.5 & 1 & -0.5 \\ -0.5 & -0.5 & 1 \end{bmatrix} \begin{Bmatrix} \theta_{z1} \\ \theta_{z2} \\ \theta_{z3} \end{Bmatrix} \qquad [III\text{-}55]$$

The obtained Flat shell element cinematic is shown in *Fig. III.14*.

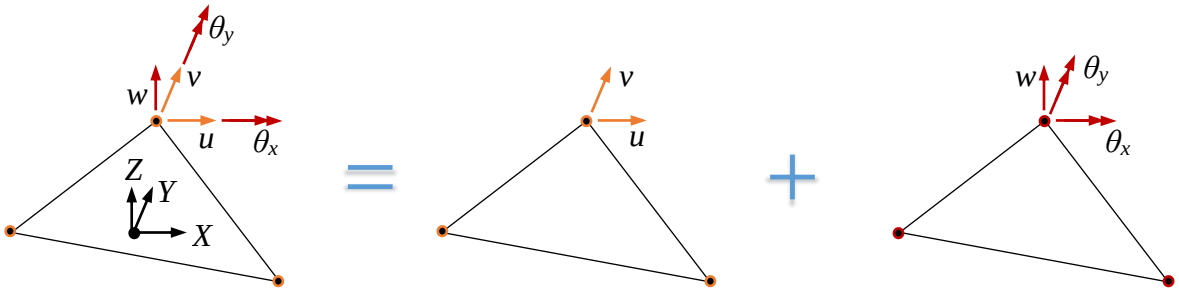

Fig. III.14. 3*-Node triangular flat shell element with five *d.o.f

2) The second triangular flat shell element denoted "*Tdrill*", is a combination of the *DKT* triangular plate bending element by [BATOZ et al 1980], and the new *EAS* triangular plane-stress element with drilling rotational *d.o.f* presented in § *III-1.2.3*. In this case the rotational θ_z degree of freedom is included in the plane-stress theory formulation as a parameter in the in-plane displacement field interpolation. The obtained flat shell element cinematic is shown in *Fig. III.15*.

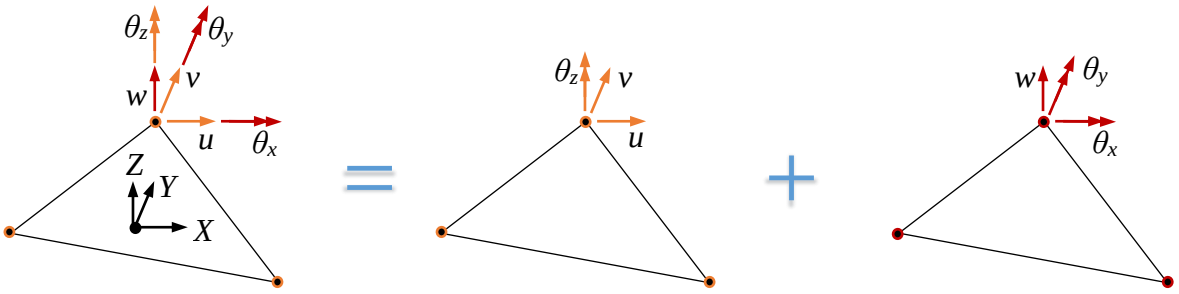

Fig. III.15. 3*-Node triangular flat shell element with six *d.o.f

III-3.2. Quadrilateral Flat Shell Elements

Quadrilateral elements are more convenient when regular mesh is possible than triangular elements since they are of higher order. Nevertheless, they have some limitations with irregular mesh and warped geometries. In these cases triangular elements are preferred.

1) The first quadrilateral shell denoted "*Quad*" is a four node quadrilateral flat shell element results from the combination of the *DKQ* quadrilateral plate bending element by [BATOZ & BEN-TAHAR 1982], and the standard bilinear quadrilateral plane-stress element. The solution of fictitious stiffness is adopted to avoid stiffness matrix singularity. The following approximation of the moment-rotation relationship is adopted:

$$\begin{Bmatrix} M_{z1} \\ M_{z2} \\ M_{z3} \\ M_{z4} \end{Bmatrix} = \alpha \cdot E \cdot t^3 \cdot A \cdot \begin{bmatrix} 1 & -1/3 & -1/3 & -1/3 \\ -1/3 & 1 & -1/3 & -1/3 \\ -1/3 & -1/3 & 1 & -1/3 \\ -1/3 & -1/3 & -1/3 & 1 \end{bmatrix} \begin{Bmatrix} \theta_{z1} \\ \theta_{z2} \\ \theta_{z3} \\ \theta_{z4} \end{Bmatrix} \qquad [III\text{-}56]$$

The obtained flat shell element cinematic is shown in *Fig. III.16*.

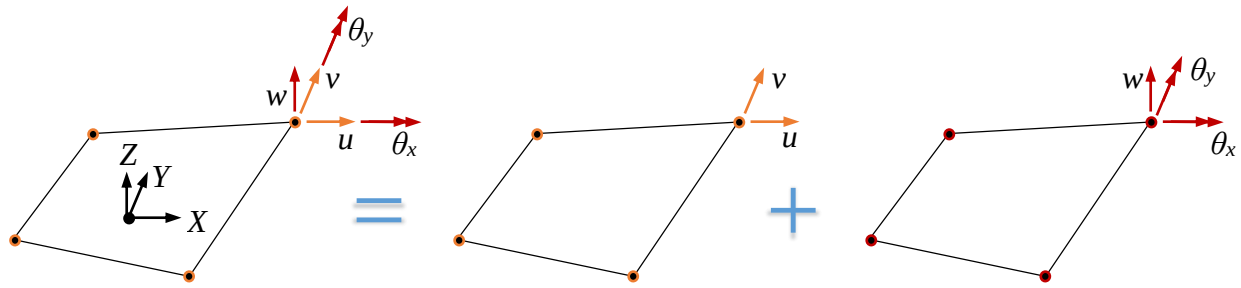

Fig. III.16. 4*-Node quadrilateral flat shell element with five *d.o.f

2) The second quadrilateral shell element denoted "*Qdrill*" is a four-node quadrilateral flat shell element. It is a combination of the *DKQ* quadrilateral plate bending element by [BATOZ & BEN-TAHAR 1982], and the mixed quadrilateral plane-stress element with drilling rotation by [IBRAHIMBEGOVIC et al 1990]. In this case the rotational θ_z *d.o.f* is considered in the displacement field interpolation. The obtained flat shell element cinematic is represented in *Fig. III.17*.

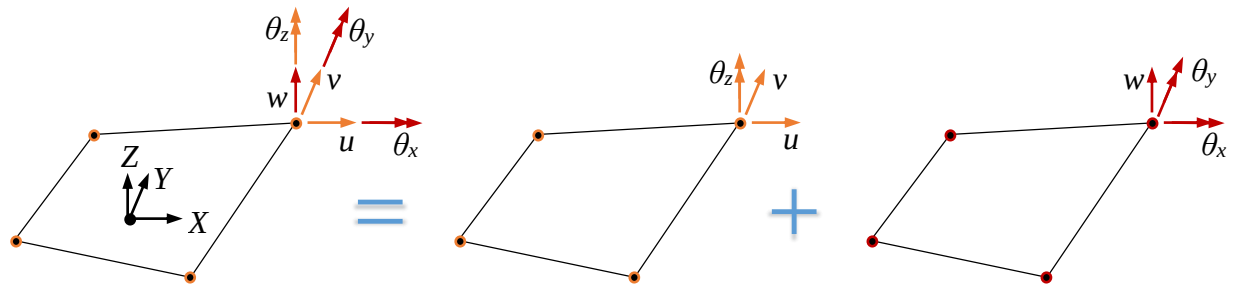

Fig. III.17. 4*-Node quadrilateral flat shell element with six *d.o.f

CHAPTER IV

DYNAMIC ANALYSIS

I- INTRODUCTION

Dynamic analysis is the most general case that can be studied as it takes into account all the forces acting on it. Dynamic loads can be caused due to impact, explosions and earthquakes, which are of considerable importance in the safety studies.

When the external loads and displacements are applied very slowly, the inertia forces can be neglected and a static analysis which is a simplified approach of the problem can be justified. However, if a body is in motion, the inertia forces, from Newton's second law, are equal to the mass times the acceleration, then at any instant of time *(t)*, Newton's law of motion implies that the sum of all forces must be equal to the inertial force. Therefore, the governing equations lead to a dynamical problem.

In numerical integration of dynamic problems the equations of motion are first discretised in space. This procedure is called semi-discretisation and yields a set of ordinary differential equations in time. Furthermore, the development of an implicit time-step algorithm, considering finite rotations as degrees of freedom is a challenging task due to the more complicated nature of such a problem.

II- DYNAMIC EQUILIBRIUM

In dynamic analysis, it is assumed that a known equilibrium configuration exists at time *(t)* and the solution at time *(t+Δt)* has to be determined.

The force equilibrium of a single-degree-of-freedom as a function of time can be expressed by the following relationship:

$$F_I(t) + F_D(t) + F_E(t) = p(t) \qquad \textit{[IV-1]}$$

In which, the time dependent variables:

$\boldsymbol{F_I}(t)$ is the inertia forces at time (*t);*

$\boldsymbol{F_D}(t)$ is the viscous damping forces at time (*t);*

$\boldsymbol{F_E}(t)$ is the internal forces at time (*t);*

$\boldsymbol{p}(t)$ is the externally applied loads at time (*t).*

Eq. [IV-1] is valid for both linear and nonlinear systems if equilibrium is formulated with respect to the deformed geometry of the structure.

In the case of a system with multi degrees of freedom, acting forces on the system with several degrees of freedom are the inertia forces, the elastic forces, the damping forces and externally applied loads. Once these forces have been identified and calculated, the formulation of the equations of motion reduces to a problem of writing of the equilibrium equations.

In order to obtain the finite element formulation of the equilibrium, the behaviour of the structure is assumed to be elastic linear. Hence, the equation of equilibrium governing the dynamic response of a structure at time *(t+Δt)* is approximated to the following set of second-order, linear, differential equations, written on matrix form as:

$$M\ddot{u}(t) + C\dot{u}(t) + Ku(t) = P(t) \qquad \textit{[IV-2]}$$

In which: The time-dependent vectors: $u(t)$, $\dot{u}(t)$, $\ddot{u}(t)$ and $P(t)$ are respectively the nodal displacements, velocities, accelerations and the applied load vector.

M : Overall structural mass matrix

C : Structural damping matrix

K : Structural stiffness matrix

As dynamic analysis is a direct extension of static analysis, the elastic stiffness matrices are the same for both dynamic and static analysis. The addition of inertia forces and energy dissipation forces will satisfy dynamic equilibrium.

There are many different mathematical methods that can be used to obtain the solution of *Eq. [IV-2]*. However, the majority of both linear and nonlinear systems can be solved with numerical methods.

III- METHODS OF INTEGRATION

Eq. [IV-2] represents a system of linear differential equations of second order. The standard procedures for the solution of differential equations can be very expensive. Therefore, there exist several different methods of integration to solve the dynamic equilibrium problem. Each method has advantages and disadvantages that depend on the type of structure and loading. To provide a general background, the different numerical solution methods are summarized below:

III-1. Mode Superposition Analysis

The most common and effective approach for dynamic analysis of linear structural systems is the mode superposition method. This method transforms the equilibrium equations into a more effective form, in which, the equations of motion are projected onto the modal basis hence they integrated. The objective of the transformation is to obtain new system matrices, which have a smaller bandwidth than the original system matrices. Thus, after a set of orthogonal vectors have been evaluated, this method reduces the large set of global equilibrium equations to a relatively small number of uncoupled second order differential equations.

Modal superposition has the advantage of significantly reducing the number of equations limiting the response of the structure to the first Eigen-modes. It has been shown that seismic motions excite only the lower frequencies of the structure. Hence, neglecting the higher frequencies and mode shapes of the system normally does not introduce errors. However, this method is not well suited to complex excitations shock type.

In view of the high computational cost of direct integration methods, the application of mode superposition method to material and geometrical nonlinear analysis become an active research area [NICKELL 1976; BATHE & GRACEWSKI 1981; CHANG & MOHRAZ 1990; VILLAVERDE & HANNA 1992; KHUDADA & GESCHWINDNER 1997; VALIPOUR 2011]. It is based on the incremental approach, and can be classified in two groups:

The first group, can provide a history of the changes in the modal properties of the system. It consists of updating the eigenvalues and eigenvectors as well as the transformation to modal coordinates at every time step [NICKELL 1976; MORRIS 1977; IDELSOHN & CARDONA 1985; MOHRAZ et al 1991]. Whereas in the second group, recalculation of the eigenvalue/eigenvectors is not required, because, the nonlinear terms appear in the right-hand side of the equations of motion as "pseudo-forces", therefore the eigenvalues/eigenvectors of the linear system are used during the entire nonlinear analysis [BATHE & GRACEWSKI 1981; GESCHWINDNER 1981].

III-2. Response Spectra Analysis

The basic mode superposition method, which is restricted to linearly elastic analysis, has two major disadvantages. First, the method produces a large amount of output information that can require an enormous amount of computational effort. The second one, is that the analysis must be repeated for several different earthquake motions to ensure that all the significant modes are excited.

There are significant computational advantages in using the response spectra method of seismic analysis for prediction of displacements and forces in structural systems. The method involves the calculation of only the maximum values of the displacements and forces in each mode using smooth design spectra that are the average of several earthquake motions. (combination methods; CQC, SRSS and CQC3)

III-3. Direct Time Integration Analysis

Direct time integration is a more general method for dynamic analysis, which treats the entire frequency content of the load imposed on the structure. It nevertheless remains very time consuming calculation. It is an incremental method performs a step by step integration of the equations of motion *Eq. [IV-2]*. This involves, after the solution is defined at time zero, the attempt to satisfy dynamic equilibrium at discrete points in time. Most methods use equal time intervals $(t+\Delta t)$, $(t+2\Delta t)\ldots$, $(t+n\Delta t)$. There are a large number of different incremental solution methods. In general, they involve a solution of the complete set of equilibrium equations at each time increment.

For very large structural systems, a combination of mode superposition and incremental methods has been found to be very efficient.

IV- TRANSIENT DYNAMIC ANALYSIS

The procedure used in this work to solve the above transitory system is the step-by-step direct integration method, in which, we solve dynamic system of equations using numerical direct time integration to obtain direct transient response since the solution and the excitation are time varying. In this family of methods, it is assumed to satisfy *Eq. [IV-2]* only at discrete time intervals. Accordingly, dynamic equations are discretized in time and the problem is solved step-by-step by using numerical integration algorithm. It is apparent that all solution techniques employed in static analysis can also be used effectively in direct integration.

IV-1. Direct Time Integration Methods

In these methods, the term "direct" means that, no transformation of the equations into a different form is carried out prior to the numerical integration. There exist a large number of numerical integration methods where they differ by the manner used to express the relationship between displacement, velocity and acceleration: [HOUBOLT 1950; NEWMARK 1959; WILSON et al 1973-b; HILBER et al 1977; HILBER & HUGHES 1978; WOOD et al 1980; ZIENKIEWICZ et al 1980; BAZZI & ANDERHEGGEN 1982; SENJANOVIC 1984].

Structural nonlinear dynamic analysis using direct time integration methods could be a time-demanding task. Therefore, researchers continue trying to enhance the accuracy, efficiency and stability of finite element formulations and solution schemes, see: [BATHE & WILSON 1973, BELYTSCHKO 1976; FELIPPA & PARK 1979; KLEIN & TRUJILLO 1983; WILSON 1985; BERT & STRICKLIN 1988; HOFF & PAHL 1988; KUAN-JUNG & WILSON 1988; DOKAINISH & SUBBARAJ 1989; SUBBARAJ & DOKAINISH 1989; JINTAI & GREGORY 1994; FAN et al 1997; XIAOQIN et al 1995; MENGFU & AU 2006; LEONTYEV 2010].

Basically, all methods can fundamentally be classified as either explicit or implicit integration methods. Generally, implicit algorithms are most effective for structural dynamic problems (low frequency modes), while explicit algorithms are very efficient for wave propagation problems (high frequency modes).

The method is implicit if the solution at time ($t+\Delta t$) requires to satisfy the differential equation of equilibrium at time (t) and the method requires the solution of a set of simultaneous equations at each time step. Implicit integration methods directly solve for the displacements at each time step. For these reasons implicit methods require greater time per step as compared with explicit methods. They could be conditionally or unconditionally stable, and thus allow the use of larger time step, which is restricted only by the accuracy requirements. Typical most used implicit

methods include: Newmark method [NEWMARK 1959], Houbolt method [HOUBOLT 1950], and θ-Wilson method [WILSON et al 1973-b].

Explicit methods are basically based on first finding accelerations at each time step, and hence proceed to the computation of displacements, these methods use the differential equation of equilibrium at time (t) to predict the solution at time ($t+\Delta t$). Very small time step is required in order to obtain a stable solution. Therefore, all explicit methods are conditionally stable. Typical most used explicit methods include: central differences method, Runge-Kutta method [RUNGE 1895; KUTTA 1901], and the Newmark method with ($\beta=0, \gamma=1/2$), see § *IV-2*.

In order to circumvent the limitations of implicit and explicit methods, mixed methods have been developed in which features of both methods are attributed. [BELYTSCHKO & MULLEN 1976] have presented a formulation in which the elements are partitioned into: implicit, explicit and interface groups of elements; and the nodes are partitioned into: implicit and explicit nodes. [HUGHES & LIU 1978-a, 1978-b; HUGHES et al 1979] introduced the implicit-explicit concept, in which the elements are partitioned into implicit group and explicit group.

The choice of which integration method to use in a practical analysis is governed by the cost of solution, which in turn is determined by the number of time steps required in the integration.

Generally, when a single-step scheme is used for the direct time integration, the variation of the acceleration in each time step is assumed to be either constant or linear. This approximation yields a discontinuous distribution for the acceleration in time.

Furthermore, there exist a large number of multi-step (higher-order) methods which assume that the acceleration is a smooth function, and a large number of single step methods which assume that the acceleration is not smooth function (because of some phenomenon in real structures like: buckling of elements, nonlinear hysteresis behaviour of material, and contacts between parts of structure). In this work, we adopted the single step Newmark method, which is the most widely used family of implicit methods for solving discrete equations of motion that represent dynamic analysis of structural problems.

Note that, it has been shown in many works that the Newmark method, fails to produce stable and accurate solutions in severe nonlinear problems, especially when nonlinear problems must be integrated for a long time: [CRISFIELD & SHI 1994; SIMO & TARNOW 1994]. This problem motivated the development of many algorithms, based on the idea of conserving or decaying the system energy: [CHUNG & HULBERT 1993; KUHL & RAMM 1996; KUHL & CRISFIELD 1999; IBRAHIMBEGOVIC & MAMOURI 2002; BATHE & BAIG 2005].

IV-2. Newmark Method

[NEWMARK 1959] presented a family of single-step integration methods for the solution of structural dynamic problems for both blast and seismic loadings. Since then, Newmark's method has been modified and improved by many other researchers.

This method is the most widely used implicit method of direct time integration for solving semi-discrete equations of motion, it has been applied to the dynamic analysis of many practical engineering structures.

Let us assume that a known solution of dynamic equilibrium equations exists at time *(t).*The solution of this linear dynamic equilibrium equations at time *(t+Δt)* is to be calculated, in this subject, *Eq. [IV-2]* is considered at time (*t+Δt)*, as:

$$M\ddot{u}_{t+\Delta t} + C\dot{u}_{t+\Delta t} + Ku_{t+\Delta t} = F_{t+\Delta t} \qquad \textit{[IV-3]}$$

Where $u_{t+\Delta t}$, $\dot{u}_{t+\Delta t}$, and $\ddot{u}_{t+\Delta t}$ are respectively, the $u(t+\Delta t)$, $\dot{u}(t+\Delta t)$, and $\ddot{u}(t+\Delta t)$ approximations at time (*t+Δt)*.

Two variants exists: The first one calculates the acceleration $\ddot{u}_{n+1}$ first, while the other one calculates the displacement u_{n+1} first.

In Newmark acceleration method, to begin the iterative process, we must first calculate $\ddot{u}_0$, where: $M\ddot{u}_0 = F_0 - C\dot{u}_0 - Ku_0$.

Hence, the direct use of Taylor's series provides a rigorous approach to obtain the following two additional equations:

$$\begin{cases} u_{t+\Delta t} = u_t + \Delta t \cdot \dot{u}_t + \dfrac{\Delta t^2}{2} \cdot \ddot{u}_t + \dfrac{\Delta t^3}{6} \cdot \dddot{u}_t + ... \\ \dot{u}_{t+\Delta t} = \dot{u}_t + \Delta t \cdot \ddot{u}_t + \dfrac{\Delta t^2}{2} \cdot \dddot{u}_t + ... \end{cases} \qquad \textit{[IV-4]}$$

Newmark, truncated these equations and expressed them in the following form:

$$\begin{cases} u_{t+\Delta t} = u_t + \Delta t \cdot \dot{u}_t + \dfrac{\Delta t^2}{2} \cdot \ddot{u}_t + \beta \cdot \Delta t^3 \cdot \dddot{u} \\ \dot{u}_{t+\Delta t} = \dot{u}_t + \Delta t \cdot \ddot{u}_t + \gamma \cdot \Delta t^2 \cdot \dddot{u} \end{cases} \qquad \textit{[IV-5]}$$

Assuming the acceleration to be linear within the time step, the term $\dddot{u}$ could be written in the following form:

$$\dddot{u} = \frac{(\ddot{u}_{t+\Delta t} - \ddot{u}_t)}{\Delta t} \qquad \textit{[IV-6]}$$

The substitution of *Eq. [IV-6]* into *Eq. [IV-5]* produces Newmark's equations in standard form:

$$\begin{cases} u_{t+\Delta t} = u_t + \Delta t \cdot \dot{u}_t + \left(\frac{1}{2} - \beta\right)\Delta t^2 \cdot \ddot{u}_t + \beta \cdot \Delta t^2 \cdot \ddot{u}_{t+\Delta t} \\ \dot{u}_{t+\Delta t} = \dot{u}_t + (1-\gamma)\Delta t \cdot \ddot{u}_t + \gamma \cdot \Delta t^2 \cdot \ddot{u}_{t+\Delta t} \end{cases} \qquad \textit{[IV-7]}$$

Newmark used *Eq. [IV-7]* and *Eq. [IV-3]* iteratively, for each time step, for each displacement *d.o.f* of the structural system. Later, Wilson formulated Newmark's method in matrix notation, added stiffness and mass proportional damping, and eliminated the need for iteration by introducing the direct solution of equations at each time step. This requires that *Eq. [IV-7]* be rewritten in the following form:

$$\begin{cases} \ddot{u}_{t+\Delta t} = b_1(u_{t+\Delta t} - u_t) + b_2\dot{u}_t + b_3\ddot{u}_t \\ \dot{u}_{t+\Delta t} = b_4(u_{t+\Delta t} - u_t) + b_5\dot{u}_t + b_6\ddot{u}_t \end{cases} \qquad \textit{[IV-8]}$$

The substitution of *Eq. [IV-8]* into *Eq. [IV-3]* allows the dynamic equilibrium of the system at time *(t+Δt)* to be written in terms of the unknown node displacements $u_{t+\Delta t}$ as:

$$(b_1 M + b_4 C + K)u_{t+\Delta t} = F_{t+\Delta t} + M(b_1 u_t - b_2\dot{u}_t - b_3\ddot{u}_t) + C(b_4 u_t - b_5\dot{u}_t - b_6\ddot{u}_t) \qquad \textit{[IV-9]}$$

Where the constants b_1 to b_6 are defined as:

$$b_1 = \frac{1}{\beta\Delta t^2} \quad b_2 = \frac{-1}{\beta\Delta t} \quad b_3 = (1 - \frac{1}{2\beta}) \quad b_4 = \gamma \cdot \Delta t \cdot b_1 \quad b_5 = 1 + \gamma \cdot \Delta t \cdot b_2 \quad b_6 = \Delta t(1 + \gamma b_3 - \gamma)\,.$$

β and γ are parameters that control the stability and accuracy of the algorithm. Newmark, had originally proposed an unconditionally stable scheme with constant acceleration over the time step, in this case: $\gamma = 1/2$ and $\beta = 1/4$.

Note that the constants b_i need to be calculated only once for both linear and nonlinear analysis.

The matrix $\overline{K} = K + b_1 M + b_4 C$ is usually considered as the effective stiffness matrix. It is formed and triangularized only once for linear analysis, where *M*, *C* and *K* are time invariant masse, damping and stiffness matrices.

In the other side, the effective load vector is taken to be:

$$\overline{F}_{t+\Delta t} = F_{t+\Delta t} + M(b_1 u_t - b_2\dot{u}_t - b_3\ddot{u}_t) + C(b_4 u_t - b_5\dot{u}_t - b_6\ddot{u}_t) \qquad \textit{[IV-10]}$$

Common forms of the Newmark's method are: Newmark average acceleration: $\beta=1/4,\ \gamma=1/2$; Newmark linear acceleration: $\beta=1/6,\ \gamma=1/2$; Newmark central difference (explicit): $\beta=0,\ \gamma=1/2$.

The average acceleration form appears to be the most popular one and it is used exclusively in this investigation.

Damping matrix is taken as a linear combination of the stiffness and mass matrices as Rayleigh suggested, see: [BATHE 1982]:

$$C = a \cdot M + b \cdot K \qquad \textit{[IV-11]}$$

Where ***a*** and ***b*** are Rayleigh's constants. They are determined experimentally.

The recurrence scheme of Newmark method is presented in appendix *A*.

IV-3. Mass matrix

The extension of a finite element from static analysis to dynamic analysis implies the construction of mass matrix. To consider the effect of rotary inertia, the formulation and use of the consistent mass matrix is required. In order to make possible for plane stress elements with drilling rotation to represent true in-plane dynamic behaviour, we formulated simple in-plane consistent mass matrices for triangular and quadrilateral membrane elements with drilling rotation, taking into account the in-plane rotational inertia. Therefore, in-plane frequencies are no more neglected and they represent true modes, and we will see that membrane elements with drilling rotational degrees of freedom can give very good representation of in-plane frequencies.

The developments presented here are based on the Allman-type displacement field. We aim in this work to present a unified formulation for both triangular and quadrilateral elements with in-plane rotational *d.o.f.* So, mass matrices developed in this work could be used for all elements with in-plane rotational *d.o.f* that are based on Allman-type displacement field.

Generally, the elementary consistent mass matrix is derived from the kinetic energy expression using the virtual work principle. It is given by:

$$[M] = \int_v [S]^T [P][S] \cdot dv \qquad \textit{[IV-12]}$$

Where, [*P*] is the inertia matrix, and [*S*] is the shape function matrix that can be the same shape function adopted for the displacement field interpolation.

The mass matrix derived from the above equation, is called the *consistent mass matrix,* and it is symmetric positive-definite and non-diagonal.

When fictitious stiffness is used to overcome singularity of static linear stiffness matrix, the in-plane rotational inertia is also a fictitious mass associated to the in-plane rotational degree of freedom, and it's injected in the mass matrix to avoid numerical instability in non-linear analysis (as we'll see later). In this case, it is apparent that frequencies associated with the in-plane normal rotations are wrong and have no physical significance.

In this work, we made a step toward mitigating this problem by proposing a unified form of in-plane mass matrix for triangular and quadrilateral membrane elements with in-plane rotational *d.o.f*, in order to make it possible for the shell finite element to represent true in-plane dynamic behaviour.

The mass matrixes used in this work for membrane elements with rotational *d.o.f*, is derived from the *Eq. [IV-12]* by adopting Allman-type interpolation for the in-plane displacement field. Thus, these masse matrices adopted herein for "*Qdrill*" and *"Tdrill"* elements, are natural and have no fictitious mass associated to the in-plane rotational degrees of freedom. Therefore, in-plane frequencies are no more neglected and they represent true modes. As we will see in chapter *VII*. The shell element with drilling rotational degrees of freedom gives very good representation of the in plane frequencies.

Let us denote the mass density of the material by $\boldsymbol{\rho}$, and elementary mass matrix by M^e.

For a Lagrangian mesh, the mass matrix is time independent. So it needs to be evaluated only at the beginning of either linear or non-linear dynamic analysis in the resting configuration.

If the shape functions are expressed in terms of parent element coordinates, then:

$$M^e = \int_v \rho \cdot S^T S \cdot dv = h \cdot \int_A \rho \cdot S^T S \cdot dA = h \cdot \int_\Delta \rho \cdot S^T S \cdot J d\Delta \qquad \textit{[IV-13]}$$

Since $\boldsymbol{J}$ *and* $\boldsymbol{\rho}$ are time dependent, masse matrix M^e appears to be time dependent too.

To show that the mass matrix is in fact time independent, let us consider the total mass in the indeformed configuration, which is: $m_0 = \rho_0 \cdot v_0$.

In the undeformed configuration, from mass conservation, we get: $m_{(t)} = m_0 = C^{st}$.

Since shape functions are time independent, M^e must be time independent. The mass matrix in *Eq. [IV-13]* can be called *total Lagrangian* since it is evaluated in the reference (undeformed) configuration.

During assembly, elementary mass matrices are assembled to form a global mass matrix in exactly the same manner as the stiffness matrix.

IV-3-1. Conventional Membrane Elements

1- CST mass matrix

For the in-plane mass matrix, we must consider both displacements *u* and *v* along *x* and *y* directions, since motion along both axes generates the inertia forces.

With constant thickness *h* and mass density ρ, using the interpolation functions and the virtual work principle, the mass matrix can be written as follows:

$$M^e = \int_v \rho \cdot S^T S \cdot dv = \rho \cdot h \cdot \int_A S^T S \cdot dA \qquad \textit{[IV-14]}$$

$[M_{CST}]$: Masse matrix of the CST element is calculated by substituting the following $[S]$matrix in the *Eq. [IV-14]*, with:

$$[S] = \begin{bmatrix} \overline{N}_1 & \overline{N}_2 \end{bmatrix} \qquad \textit{[IV-15]}$$

$$\left[\overline{N}_1\right] = \langle N_1 \quad 0 \quad N_2 \quad 0 \quad N_3 \quad 0 \rangle^T \qquad \textit{[IV-16]}$$

$$\left[\overline{N}_2\right] = \langle 0 \quad N_1 \quad 0 \quad N_2 \quad 0 \quad N_3 \rangle^T \qquad \textit{[IV-17]}$$

Where:

$N_1 = 1 - \xi - \eta,\ N_2 = \xi,\ N_3 = \eta$

Putting this in matrix form gives:

$$M^e = \rho \cdot h \cdot \int \begin{bmatrix} N_1^2 & 0 & N_1N_2 & 0 & N_1N_3 & 0 \\ & N_1^2 & 0 & N_1N_2 & 0 & N_1N_3 \\ & & N_2^2 & 0 & N_2N_3 & 0 \\ & & & N_2^2 & 0 & N_2N_3 \\ & Sym & & & N_3^2 & 0 \\ & & & & & N_3^2 \end{bmatrix} J \cdot d\xi \cdot d\eta$$

With: $dv = h \cdot J \cdot d\xi \cdot d\eta$

$N_i = N_i(\xi, \eta)$

The mass matrix for an iso-parametric element may be computed by numerical integrations. So, for two-dimensional Triangular element the mass matrix is given by:

$$M^e = \rho \cdot h \cdot \iint N^T N \cdot J \cdot d\xi \cdot d\eta = \rho \cdot h \cdot \sum_{i=1}^{3} N^T N.J.w_i \qquad \textit{[IV-18]}$$

The order of quadrature used for standard integration will be sufficient for accurately compute the mass matrix.

The element's Jacobian determinant for the initial configuration of the triangular element is given by $J = 2A$, where A is the area of the considered element. Carrying out matrix multiplication and integrating over the triangle, the consistent mass matrix is:

$$M^e = \frac{\rho \cdot A \cdot h}{12}\begin{bmatrix} 2 & 0 & 1 & 0 & 1 & 0 \\ 0 & 2 & 0 & 1 & 0 & 1 \\ 1 & 0 & 2 & 0 & 1 & 0 \\ 0 & 1 & 0 & 2 & 0 & 1 \\ 1 & 0 & 1 & 0 & 2 & 0 \\ 0 & 1 & 0 & 1 & 0 & 2 \end{bmatrix}$$

2- Bi-linear quadrilateral Q4 mass matrix

The mass matrix of the standard Iso-parametric bi-linear quadrilateral element can be written as follows:

$$M_{SBQ} = \rho \cdot h \cdot \iint S^T S \cdot J \cdot d\xi \cdot d\eta \qquad \textit{[IV-19]}$$

The shape functions matrix $[S] = [\bar{N}_1 \quad \bar{N}_2]$, is constructed using:

$$[\bar{N}_1] = \langle N_1 \quad 0 \quad N_2 \quad 0 \quad N_3 \quad 0 \quad N_4 \quad 0 \rangle^T \qquad \textit{[IV-20]}$$

$$[\bar{N}_1] = \langle 0 \quad N_1 \quad 0 \quad N_2 \quad 0 \quad N_3 \quad 0 \quad N_4 \rangle^T \qquad \textit{[IV-21]}$$

Where:

$$N_i = \frac{1}{4}(1-\xi_i \xi)(1-\eta_i \eta)$$

By substituting $[S]$matrix in the *Eq. [IV-19]*, the mass matrix is evaluated by numerical integration.

By considering: $N_i = N_i(\xi, \eta)$

$J(\xi, \eta)$: is the determinant of the Jacobian of the transformation of the parent element to the initial configuration.

h: is the thickness of the undeformed element.

Putting this in matrix form gives:

$$M^e = \rho \cdot h \cdot \int_{-1}^{1}\int_{-1}^{1} \begin{bmatrix} N_1^2 & 0 & N_1N_2 & 0 & N_1N_3 & 0 & N_1N_4 & 0 \\ 0 & N_1^2 & 0 & N_1N_2 & 0 & N_1N_3 & 0 & N_1N_4 \\ & & N_2^2 & 0 & N_2N_3 & 0 & N_2N_4 & 0 \\ & & & N_2^2 & 0 & N_2N_3 & 0 & N_2N_4 \\ & & & & N_3^2 & 0 & N_3N_4 & 0 \\ & & Sym & & & N_3^2 & 0 & N_3N_4 \\ & & & & & & N_4^2 & 0 \\ & & & & & & & N_4^2 \end{bmatrix} J \cdot d\xi \cdot d\eta$$

IV-3-2. Elements with Drilling Rotation

As we have seen in the construction of the conventional membrane elements mass matrices, only translations *u* and *v* are involved. So, in-plane rotational inertia about the *z* axis is omitted. Since in-plane rotational motion around *z* axis generates inertia forces, mass matrix must takes into account for the in-plane rotational inertia effect.

In this purpose the in-plane mass matrix is enlarged to take account inertias corresponding to the three in-plane degrees of freedom including the rotational one.

Thus, we defined herein two mass matrices derived from *Eq. [IV-12]* as follow:

$[M_{Td}]$: The mass matrix for the triangular element with drilling *d.o.f.*

$\lfloor M_{Qd} \rfloor$: The mass matrix for the quadrilateral element with drilling *d.o.f.*

Consistent mass matrices used in this work for "*Qdrill*" and *"Tdrill"* elements with drilling rotations, are derived from the *Eq. [IV-12]* using quadratic interpolation of translations (*u*, and *v*) which involves the rotational degree of freedom φ in the formulation, resulting with a mass matrix that contains in-plane rotational inertia using the following form of shape functions in *Eq. [IV-12]*:

$$[S] = \begin{bmatrix} \overline{N}_1 & \overline{N}_2 \end{bmatrix} \qquad \textit{[IV-22]}$$

With:

$$\begin{Bmatrix} u \\ v \end{Bmatrix} = \begin{bmatrix} \overline{N}_1 \\ \overline{N}_2 \end{bmatrix} \{q\} \qquad \textit{[IV-23]}$$

Shape functions $\overline{N}_1$, and $\overline{N}_2$ for the triangular and quadrilateral geometries are presented in what follows:

1- Triangle with drilling rotation

Expressing the in-plane displacement field that is used to calculate initial mass matrix, we limited to the original Allman-type displacement field terms even if the element used a complimentary terms to describe the displacement field. In fact, these neglected additional terms have no considerable effect.

$[M_{Td}]$: is calculated by using:

$$[M_{Td}] = \rho \cdot h \cdot \iint S^T S \cdot J \cdot d\xi \cdot d\eta \qquad \textit{[IV-24]}$$

Where: $[S]$ is a matrix that takes into account the three in-plane *d.o.f* including the rotational one.

$$\{q\}^T = \langle u_1 \; v_1 \; \omega_1 \; u_2 \; v_2 \; \omega_2 \; u_3 \; v_3 \; \omega_3 \rangle \qquad \textit{[IV-25]}$$

Using natural coordinates, Allman-type displacement field is written as:

$$\begin{Bmatrix} u \\ v \end{Bmatrix} = \sum_{i=1}^{n} N_i(\xi,\eta) \begin{Bmatrix} u_i \\ v_i \end{Bmatrix} + \sum_{k=n+1}^{2n} NL_k(\xi,\eta)(\varphi_j - \varphi_i) \begin{Bmatrix} y_{ji} \\ -x_{ji} \end{Bmatrix} \qquad \textit{[IV-26]}$$

For a triangular element, it could be written as:

$$\begin{cases} u = \sum_{i=1}^{3} N_i(\xi,\eta)\{u_i\} + \omega_1\left(NL_6 y_{13} - NL_4 y_{21}\right) + \omega_2\left(NL_4 y_{21} - NL_5 y_{32}\right) + \omega_3\left(NL_5 y_{32} - NL_6 y_{13}\right) \\ v = \sum_{i=1}^{3} N_i(\xi,\eta)\{v_i\} + \omega_1\left(-NL_6 x_{31} + NL_4 x_{21}\right) + \omega_2\left(-NL_4 x_{21} + NL_5 x_{32}\right) + \omega_3\left(-NL_5 x_{32} + NL_6 x_{13}\right) \end{cases} \qquad \textit{[IV-27]}$$

Where: NL_k are shape functions for the LST element.

Using *Eq. [IV-22]*, we write:

$$\begin{aligned} [\overline{N}_1] &= \langle N_1 \quad 0 \quad Py_1 \quad N_2 \quad 0 \quad Py_2 \quad N_3 \quad 0 \quad Py_3 \rangle^T \\ [\overline{N}_2] &= \langle 0 \quad N_1 \quad Px_1 \quad 0 \quad N_2 \quad Px_2 \quad 0 \quad N_3 \quad Px_3 \rangle^T \end{aligned} \qquad \textit{[IV-28]}$$

With:

$$\begin{array}{l|l} Py_1 = \left(NL_6 y_{13} - NL_4 y_{21}\right) & Px_1 = \left(NL_4 x_{21} - NL_6 x_{13}\right) \\ Py_2 = \left(NL_4 y_{21} - NL_5 y_{32}\right) & Px_2 = \left(NL_5 x_{32} - NL_4 x_{21}\right) \\ Py_3 = \left(NL_5 y_{32} - NL_6 y_{13}\right) & Px_3 = \left(NL_6 x_{13} - NL_5 x_{32}\right) \end{array}$$

Where: $N_1 = 1 - \xi - \eta$, $N_2 = \xi$, $N_3 = \eta$.

$NL_4 = 4\xi(1 - \xi - \eta)$

$NL_5 = 4\xi\eta$

$$NL_6 = 4\eta(1-\xi-\eta)$$

2- Quadrilateral with drilling rotation

$\lfloor M_{Qd} \rfloor$: is calculated by similar way using *Eq. [IV-22]* with:

$$\{q\}^T = \langle u_1\ v_1\ \omega_1\ u_2\ v_2\ \omega_2\ u_3\ v_3\ \omega_3\ u_4\ v_4\ \omega_4 \rangle \qquad \textit{[IV-29]}$$

For a quadrilateral element with drilling rotation, in-plane displacement field is:

$$\begin{cases} u = \sum_{i=1}^{4} N_i(\xi,\eta)\{u_i\} + \omega_1(NS_8 y_{14} - NS_5 y_{21}) + \omega_2(NS_5 y_{21} - NS_6 y_{32}) + \\ + \omega_3(NS_6 y_{32} - NS_7 y_{43}) + \omega_4(NS_7 y_{43} - NS_8 y_{13}) \\ v = \sum_{i=1}^{4} N_i(\xi,\eta)\{v_i\} + \omega_1(-NS_8 x_{14} + NS_5 x_{21}) + \omega_2(-NS_5 x_{21} + NS_6 x_{32}) + \\ + \omega_3(-NS_6 x_{32} + NS_7 x_{43}) + \omega_4(-NS_7 x_{43} + NS_8 x_{14}) \end{cases} \qquad \textit{[IV-30]}$$

Where: NS_k are the shape functions for serendipity element.

Using *Eq. [IV-22]*, *u* and *v* are expressed using the following shape functions:

$$\begin{aligned} [\overline{N}_1] &= \langle N_1 \quad 0 \quad Py_1 \quad N_2 \quad 0 \quad Py_2 \quad N_3 \quad 0 \quad Py_3 \quad N_4 \quad 0 \quad Py_4 \rangle^T \\ [\overline{N}_2] &= \langle 0 \quad N_1 \quad Px_1 \quad 0 \quad N_2 \quad Px_2 \quad 0 \quad N_3 \quad Px_3 \quad 0 \quad N_4 \quad Px_4 \rangle^T \end{aligned} \qquad \textit{[IV-31]}$$

$$\begin{array}{l|l} Py_1 = (NS_8 y_{14} - NS_5 y_{21}) & Px_1 = (NS_5 x_{21} - NS_8 x_{14}) \\ Py_2 = (NS_5 y_{21} - NS_6 y_{32}) & Px_2 = (NS_6 x_{32} - NS_5 x_{21}) \\ Py_3 = (NS_6 y_{32} - NS_7 y_{43}) & Px_3 = (NS_7 x_{43} - NS_6 x_{32}) \\ Py_4 = (NS_7 y_{43} - NS_8 y_{14}) & Px_4 = (NS_8 x_{14} - NS_7 x_{43}) \end{array}$$

Where: $N_i = \frac{1}{4}(1-\xi_i\xi)(1-\eta_i\eta)$.

$$\begin{array}{l|l} NS_5(\xi,\eta) = \frac{1}{2}(1-\xi^2)(1-\eta) & NS_7(\xi,\eta) = \frac{1}{2}(1-\xi^2)(1+\eta) \\ NS_6(\xi,\eta) = \frac{1}{2}(1+\xi)(1-\eta^2) & NS_8(\xi,\eta) = \frac{1}{2}(1-\xi)(1-\eta^2) \end{array}$$

CHAPTER V

GEOMETRICALLY NONLINEAR STATIC AND DYNAMIC ANALYSIS

I- INTRODUCTION

In linear analysis, we assume that displacements are infinitesimally small and materials are linearly elastic. However, in many engineering problems, the structural behaviour can be nonlinear. Materials behave nonlinearly if stress level exceeds some limit value. Moreover, displacements may be so large that they can change the structure's shape, which can significantly change the stiffness and orientation of the structure. Besides, boundary conditions may change during loading. Consequently, structure behaves nonlinearly if one or more of this phenomena revealed. Thus, Structural nonlinearities can be in general classified in three categories:

1. Geometrical nonlinearities: Due the effect of large displacements and large rotations on the overall geometric configuration of the structure. In this case, the strain-displacement relation becomes nonlinear.

2. Material nonlinearities: Material behaviour is nonlinear i.e. it depends on current deformation state and possibly past history of the deformation. In this case, constitutive equation relates stresses and strains becomes nonlinear. Several factors can cause the material behaviour to be nonlinear as: the dependency of the material rheology on the load history (nonlinear elastic, elasto-plastic, viscoelastic, visco-plastic…), load duration (creep), and temperature (thermo-plasticity).

3. Boundary nonlinearities: in this case, all or some boundary conditions are displacement dependent. The most frequent boundary nonlinearities are encountered in contact problems, fluid structure interaction, forming process… etc.

Structures that exhibit nonlinear behaviour are of special importance, and require special treatment. For instance, the initial state of stress commonly known as "residual stresses" (from heat treatment, welding, cold forming …etc.) is important and requires special handling. Also, the structural behaviour is remarkably non-proportional to the applied load and hence, the principle of superposition cannot be applied. Therefore, the sequence of application of loads (loading history) may be important. This is a reason for dividing loads into small increments in nonlinear FE analysis. As a consequence, nonlinear analysis is generally carried out using a method of incremental resolution. It is based upon the progressive increase of the applied forces, to obtain in an incremental way, the nonlinear response of the structure satisfying the equilibrium equations in successive discrete time increments. During each time step between time (t) and ($t+\Delta t$), the configuration $C_{(t+\Delta t)}$ to be calculated, is obtained starting from the configuration $C_{(t)}$ considered as known. Often, the analysis introduces a reference configuration, which is a particular known state of the structure at a time (t_0). This known configuration is used as reference when describing the

geometrical transformations undergone by the structure as it moves between two successive configurations.

Note that, for static nonlinear analysis, the "time" variable represents a pseudo time, which denotes the intensity of the applied loads at certain step. Whereas, for nonlinear dynamic analysis and nonlinear static analysis with time-dependent material properties (e.g., creep), "time" represents the real time associated with the loads application.

Geometrical nonlinearity is considered in this chapter. Large displacements and large rotations are taken into account but not large strains. The Updated Lagrangian Co-rotational Description of motion is adopted, in which, large displacements and large rotations are decomposed into large rigid and relatively small translations and rotations.

Tangent stiffness matrices of the triangular and quadrilateral flat shell elements presented in *Chapter III*, are developed in the framework of the updated Lagrangian co-rotational formulation. The co-rotational formulation for triangular and quadrilateral plate bending elements is presented. Also, the co-rotational formulation for membrane elements with drilling rotation is developed and presented for both triangular and quadrilateral elements, in which, the finite rotations of the co-rotational reference frame, including the drilling degrees of freedom, are simply determined from the finite displacement vectors of the nodes of the element in the global reference frame.

II- GEOMETRICAL NONLINEARITIES

In small displacement analysis, the change in geometry and spatial orientation of structures, are assumed small enough that the change in its stiffness can be ignored. However, in large displacement analysis, the displacement induced deformations, could be a major source of nonlinearities. Structures undergoing large displacements due to load-induced deformations, can have significant changes in their overall configuration (geometry and/or orientation), which can cause the structure to respond nonlinearly in a stiffening and/or a softening manner.

In finite element analysis, the overall stiffness of a structure depends on the stiffness contribution of each of its finite elements. During large displacements, the nodal coordinates will change causing the elements to deform and to change their spatial orientations. Subsequently, the element stiffness contribution in the overall stiffness will also change. Thus, large displacement analysis can be classified as:

a- Finite Strain Analysis:

In this formulation, as the structure deflects, the localized deformations are large such that the local element stiffness will change as a result of the element shape change. The deformation of rubber-like materials is a typical analysis in which finite strains are experienced.

b- Large Deflection Analysis:

In this formulation, the change in the spatial orientation of elements can be finite but the induced strains must remain small. The overall stiffness of the structure will change as a result of the change of the global stiffness contribution of its elements due to the change in their spatial orientation.

III- DISCRIPTION OF MOVEMENT

The representation of kinematic and mechanical variables of material point is called description. That one is completely defined by the knowledge of the initial and the final state of the material point. There are generally two main conventional approaches used to describe the movement in the context of deformable continuum mechanics. They are Eulerian description (representation related to a geometric point) or Lagrangian description (representation related to a material point).

The differences between Lagrangian and Eulerian descriptions are most clearly seen in terms of the behaviour of the nodes. If the mesh is Lagrangian, the nodes are coincident with material points. If the mesh is Eulerian, the nodes are coincident (fixed) with spatial points. This is illustrated in *Fig. V.1*.

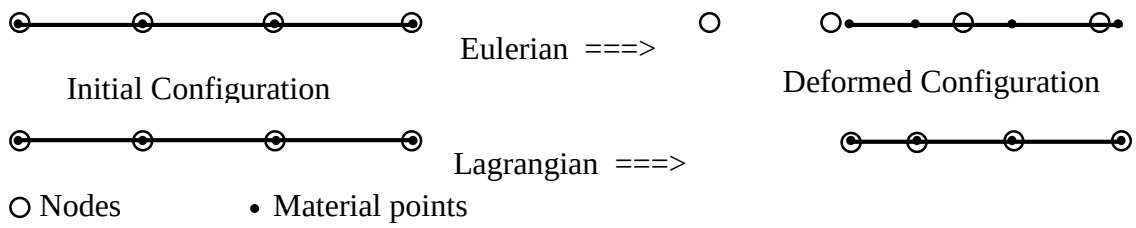

Fig. V.1. **Eulerian and Lagrangian descriptions of movement**

At any given time (*t*), let us consider the continuum domain noted $C_{(t)}$, in which a particle was initially at position $\vec{x}_0$ is now at the position $\vec{x}_t$.

Lagrangian description is then, to identify each particle configuration by its position in the reference configuration. Any physical quantity can then be expressed as a function of the particle to which it is attached and time. We can therefore define a vector function which describes the spatial correspondence between the initial and current configurations as: $\vec{x} = \vec{\tau}(\vec{x}_0, t)$. Therefore, it is clear that nodal trajectories are coincident with material point trajectories, and no material passes between elements, *Fig. V.2*.

For solid mechanics problems, the Lagrangian description is often preferred, since this description is used to follow the motion of the same particle over time.

As opposed to the Lagrangian description, the Eulerian description does not attempt to identify particles over time in relation to an initial configuration, but is instead to define at every moment and at every point of coordinates $\vec{x}$ of the current configuration, the velocity $\vec{v}(\vec{x}, t)$ of the particle located at point of coordinates $\vec{x}$. This means, taking at every moment, the current configuration as reference configuration. It should also take into account the conservation of material, which is, the case in fluid mechanics and aero-acoustics, for which the Eulerian description is often more appropriate. In Eulerian meshes, the material point at a given quadrature point changes with time, which complicates the treatment of materials in which the stress is history-dependent.

Also, in Eulerian meshes, the element dimensions are constant in time, and they are unchanged by the deformation of the material, so no degradation in accuracy occurs because of material deformation. Note that there are some particular class of problems whose choice is not clear (fluid structure interaction, forming process ...), in these cases, the combination of both descriptions is more advantageous.

IV- LAGRANGIAN DESCRIPTION

In Lagrangian description, the nodes and elements move with the material. Boundaries and interfaces remain coincident with element edges, so that their treatment is simplified. Element quadrature points remain coincident with material points, so constitutive equations are always evaluated at the same material points, which is advantageous for history dependent materials. For these reasons, Lagrangian meshes are widely used for solid mechanics. However, in Lagrangian description, element lengths change with time, mesh can become severely distorted, and magnitude of deformation that can be simulated with a Lagrangian mesh is limited.

In Lagrangian description, we do not focus on the description of the motion during deformation, but only the final state of the body when the solid has reached its equilibrium configuration. Lagrangian description is the most common formulation used for describing the passage between two adjacent configurations. It consists to express the principle of virtual work between a reference configuration $C_{(r)}$ (which is not necessarily coincident with the initial configuration $C_{(0)}$), and the current configuration $C_{(t)}$.

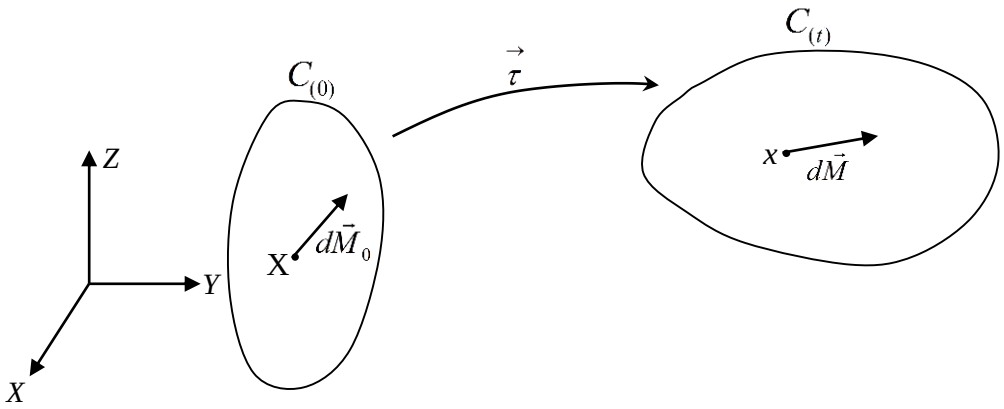

Fig. V.2. **Linear elastic body in movement**

IV-1. Different Configurations of a Solid Body in Movement

Let us consider an elastic solid body at time (t), occupying the volume $\boldsymbol{V}$ and bounded by a boundary $\boldsymbol{S}$. The state in which the solid is at this moment, defines what is called the current configuration of the solid. This configuration is denoted $\boldsymbol{C_{(t)}}$, and characterized by a combination of mechanic and kinematic variables, such as the geometrical positions of material particles, constraints, strain, and stress. Generally, a known configuration implies that all kinematic and mechanical quantities characterizing the configuration are known.

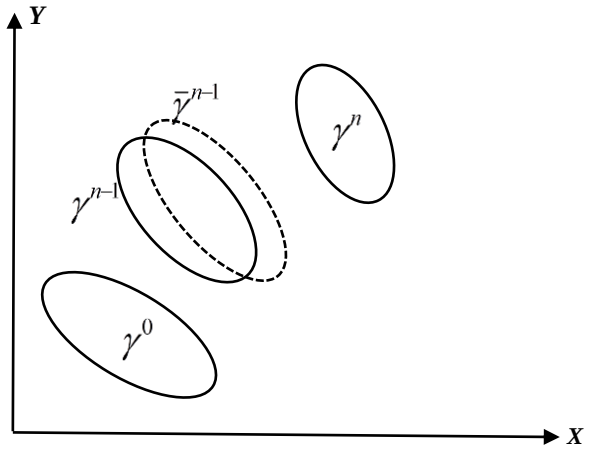

Fig. V.3. **Different configurations of a solid body in movement**

Let us now, consider the deformed process of the solid body and divide the loading path into a number of equilibrium states: γ^0, γ^1,... γ^{n-1}, γ^n …. *Fig. V.3.*

Conventionally, three typical positions (configurations) that a solid body can occupies during its movement are used to describe the deformation of the solid body under applied loadings: the initial configuration γ^0, the last known configuration γ^{n-1}, and the current configuration γ^n.

Where: γ^0 is the initial undeformed configuration of the solid body, it is the resting state of the body. It corresponds to time (t_0). The coordinates of a material point in this configuration will be noted ${}^0x_i$;

γ^{n-1}: is an intermediate state (intermediate configuration);

γ^n: is the current configuration to be calculated, unknown a priori. The coordinates of the same material point in this configuration will be noted ${}^t x_i$;

We could define also a fourth position denoted $\bar{\gamma}^{n-1}$, which is a configuration very close to γ^{n-1} obtained after a rigid body movement of γ^0.

The problem under discussion is the definition of the kinematic and mechanical quantities in the γ^n state.

In order to avoid any confusion between different quantities, additional superscript and subscript are used for variables notation ${}^{t2}_{t1}V$ as follows:

t_1: is the date of the reference position; t_2: the date at which the variable is considered.

Accordingly, the displacement of a material point is defined as follows:

$$\begin{cases} {}^{t}_{0}u_i = {}^{t}x_i - {}^{0}x_i \\ {}^{t+\Delta t}_{0}u_i = {}^{t+\Delta t}x_i - {}^{0}x_i \end{cases} \qquad [V\text{-}1]$$

The displacement increment between γ^{n-1} and γ^{n} is written as:

$$\delta_t u = {}^{t+\Delta t}u_i - {}^{t}u_i \qquad [V\text{-}2]$$

When describing the motion of the body, we need a configuration to which various kinematic and mechanical quantities are referred; this is called the *reference configuration*. The importance of the reference configuration arise from the fact that motion is defined with respect to this configuration. Obviously, the initial configuration is used as the reference configuration. However, other intermediate configurations can be used as the reference configuration.

There are two common formulations for the description of structural behaviour, [BATHE 1982; WASHIZU 1982]. A description (or formulation) of the solid body movement is called:

- Total Lagrangian Description (*TLD*): If the initial undeformed configuration is taken as a reference configuration;
- Updated Lagrangian Description (*ULD*): If the current (deformed) configuration is taken as a reference configuration;
- Co-rotational Lagrangian Description (*CLD*): If the reference configuration is replaced by a very close undeformed configuration. This co-rotational undeformed configuration is much easier to handle because it is known and not distorted.

The formulations that are used in this chapter for the nonlinear analysis, are detailed in many references, for more details, see: [BATHE et al 1975; ZIENKIEWICZ 1977; BATHE & BOLOURCHI 1980; BATHE 1982; DJEGHABA 1990; CHIN et al 1994; BONET & WOOD 1997; FELIPPA 2007].

IV-1.1. the Total Lagrangian Description

The "*TLD*" uses the initial undeformed configuration as a reference. In this formulation, all quantities (displacements, strains, stresses and integrals) that describe the response of the structure are expressed with respect to the initial undeformed configuration. So, to obtain the exact nonlinear solution, the nonlinear Green-Lagrange strain tensor must be complete (no terms neglected). The Green-Lagrange second order terms are very complicated and imply second derivatives of all the components of the displacement vector.

IV-1.2. the Updated Lagrangian Description

The "*ULD*" uses a deformed configuration as a reference. Taking advantage of the fact that γ^{n-1} is known and that we want to obtain a subsequent configuration γ^{n} not too far from γ^{n-1}. Hence, in this formulation, an intermediate configuration γ^{n-1} is used as a reference configuration to obtain the current configuration. The response of the structure is described with respect to its previous configuration supposed to be known, and this is continually updated as the calculation proceeds. Therefore, we can consider approximate nonlinear strain displacement relations instead of the complicated exact ones.

IV-1.3. the Co-rotational Lagrangian Description

[WEMPNER 1969; BELYTSCHKO & HSIEH 1973, 1974; BATHE et al 1975] established the co-rotational approach, which enables to simplify the "*TLD*" and the "*ULD*" using a co-rotational reference system of axes which translates and rotates with the finite element. In this formulation, the motion of an element is decomposed into rigid body motion and a relatively small displacement, so that the geometrical nonlinearities are attributed to the finite rigid body rotations, while the relative small deformational displacements are associates with the constitutive equations of the element. In this formulation, the configuration $\bar{\gamma}^{n-1}$ is used as a reference configuration.

IV-1.4. Element -Based Lagrangian Formulation

A new variant of the Lagrangian description was established by [NUKULCHAI & WONG 1988] and referred to as the "Element-Based Lagrangian Formulation", see also [LEE & NUKULCHAI 1998; HAN et al 2008]. In this formulation all of the equations governing a deformed body, can be expressed in the natural system in terms of the natural coordinates. So it appears simpler than those of the two traditional Lagrangian descriptions.

IV-2. Strain and Stress Measures

Unlike linear continuum mechanics, in nonlinear mechanics, the method of measuring strain and stress becomes a more complex problem. Many measures of strain and stress can be defined [BATHE 1982; CHEVALIER 1996; FOREST et al 2006]. A stress definition must be energetically conjugate to the strain adopted, i.e. the integral of the product of the stress and the strain for a volume would correctly represent the deformation energy in the same volume. In geometrically nonlinear analysis, (Green-Lagrange and Cauchy strain tensors) with their conjugate stress (2^{nd} Piola-Kirchhoff and Cauchy stress tensors) must be introduced. We will consider the following measures of strain and stress, which are the most widely used in the finite elements method:

IV-2.1. Strain Measures

Let us consider the deformed process of an elastic solid body occupied the configuration $C_{(0)}$ at time (t_0) and occupying the configuration $C_{(t)}$ at time (t) *Fig. V.4*.

The problem under discussion is the definition of the stress tensor in the configuration $C_{(t)}$.

In a Cartesian coordinates system, a material point '*M'* has the coordinates "*X"* at time (t_0), and the coordinates "*x"* at time (t).

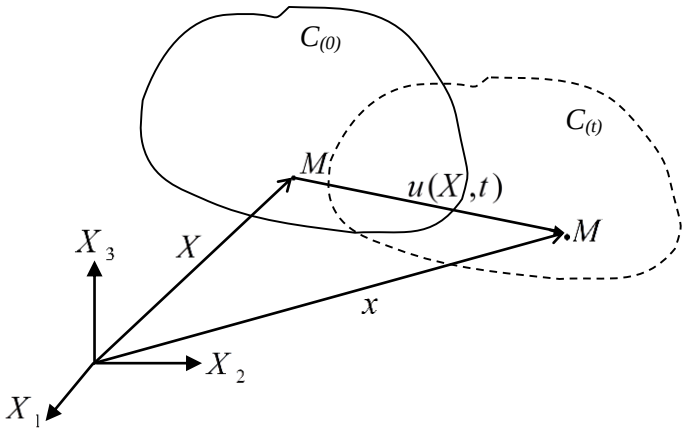

Fig. V.4. **Elastic solid body deformation process**

The movement of a material point could be described as:

$$x = u(X,t) + X \qquad [V\text{-}3]$$

With *u(X, t)*: is the displacement vector.

Let us consider an infinitesimal vector $\overrightarrow{dX}$ around the point '*M'*. During movement the vector $\overrightarrow{dX}$ transforms via $\vec{F}$ to the vector $\overrightarrow{dx}$ around the point '*M'*. The deformation is completely defined by knowing the deformation gradient vector $\vec{F}$ defined as:

$$\vec{F} = \frac{\overrightarrow{\partial x}}{\overrightarrow{\partial X}} \qquad [V\text{-}4]$$

The deformation gradient, contains all information about the local deformation in the solid, and can be used to form many strain quantities offered by the continuum mechanics (Biot strain, Almansi strain, Green-Lagrange strain, Hill strain, Hencky strain) which are used for large displacement problems. However, any reasonable representation of strains must be able to represent rigid body motion without producing any strain. If a strain measure fails to meet this requirement (as the engineering strain), it will reveal the development of non-zero strains and

stresses in an undeformed body due to rigid body translations and rotations. Three strain measures are considered here:

1- Cauchy strain (ε): Linear strain tensor

When the displacement gradient is small, we may linearize the strain to obtain Cauchy strain tensor. Cauchy strain is calculated with respect to the original undeformed configuration, so it is an Eulerian tensor. It is written using the first spatial derivatives of the displacement vector $\vec{U}$ as:

$$\varepsilon = sym(\nabla \vec{U}) = \frac{1}{2}\left(\nabla \vec{U} + \nabla \vec{U}^{T}\right) \qquad [V\text{-}5]$$

With ∇ represents the Hamilton operator. In a Cartesian coordinate system:

$$\nabla = \frac{\partial}{\partial x}\vec{i} + \frac{\partial}{\partial y}\vec{j} + \frac{\partial}{\partial z}\vec{k} \qquad [V\text{-}6]$$

So, ε could be written as:

$$\varepsilon_{ij} = \frac{1}{2}\left(\frac{\partial u_i}{\partial x_j} + \frac{\partial u_j}{\partial x_i}\right) \qquad [V\text{-}7]$$

Cauchy strain tensor is a symmetric tensor, also called the symmetric part of the deformation gradient.

2- Green-Lagrange strain (e): Quadratic Lagrangian strain tensor

Green-Lagrange strain, contains derivatives of the displacements with respect to the original configuration $C_{(0)}$. Their values therefore represent strains in material directions. The Green's strain tensor is exact and present a nonlinear measure of shape changes.

This definition results from studying the variation of the square quantity of the distance between two adjacent points before and after deformation, i.e. ($(d\vec{x})^2 - (d\vec{X})^2$).

Let us consider the following vectorial product:

$$d\vec{x}^{T} \cdot d\vec{x} - d\vec{X}^{T} \cdot d\vec{X} = (\underline{\underline{F}} \cdot d\vec{x})^{T} \cdot \underline{\underline{F}} \cdot d\vec{x} - d\vec{X}^{T} \cdot d\vec{X} \qquad [V\text{-}8]$$

Green-Lagrange strain tensor $\underline{\underline{e}}$ is defined as follows:

$$d\vec{x}^{T} \cdot d\vec{x} - d\vec{X}^{T} \cdot d\vec{X} = 2 \cdot d\vec{X}^{T} \cdot \underline{\underline{e}} \cdot d\vec{X} \qquad [V\text{-}9]$$

It can be seen that $\underline{\underline{e}}$ is defined at the initial configuration $C_{(0)}$, it is written as:

$$\underline{\underline{e}}(X,t)=\frac{1}{2}\left(\underline{\underline{F}}(X,t)^T\,\underline{\underline{F}}(X,t)-\underline{\underline{I}}\right) \qquad [V\text{-}10]$$

Green-Lagrange is expressed in a Cartesian coordinate system as:

$$e_{ij}(X,t)=\frac{1}{2}\left(\frac{\partial x_k(X,t)}{\partial X_i}\cdot\frac{\partial x_k(X,t)}{\partial X_j}-\delta_{ij}\right) \qquad [V\text{-}11]$$

With $\delta_{ij}=\dfrac{\partial X_i}{\partial X_j}$: is Kronnecker delta quantity defined as: $\begin{cases}\delta_{ij}=1 & if\ i=j\\ \delta_{ij}=0 & if\ i\neq j\end{cases}$

By substituting *Eq. [V-3]* in *Eq. [V-11]*, Green-Lagrange strain is written related to the displacement as:

$${}^t_0e_{ij}=\frac{1}{2}\left({}^t_0u_{i,j}+{}^t_0u_{j,i}+\sum_1^3({}^t_0u_{k,i}\cdot{}^t_0u_{k,j})\right) \qquad [V\text{-}12]$$

Green-Lagrange strain tensor could also be expressed as:

$$\begin{cases}\underline{\underline{e}}(\vec{U},\vec{U})=\dfrac{1}{2}\left(\nabla\vec{U}+\nabla^T\vec{U}\right)+\dfrac{1}{2}\left(\nabla^T\vec{U}\cdot\nabla\vec{U}\right)\\ \underline{\underline{e}}(\vec{U},\vec{U})=\underline{\underline{\varepsilon_l}}(\vec{U})+\underline{\underline{\varepsilon_q}}(\vec{U},\vec{U})\end{cases} \qquad [V\text{-}13]$$

3- Euler-Almansi strain (E): Quadratic Eulerian strain tensor

When expressing strain at the current configuration $C_{(t)}$:

$$d\vec{x}^T\cdot d\vec{x}-d\vec{X}^T\cdot d\vec{X}=d\vec{x}^T\cdot d\vec{x}-(F^{-1}\cdot d\vec{x})^T(F^{-1}\cdot d\vec{x}) \qquad [V\text{-}14]$$

Euler-Almansi strain tensor $\underline{\underline{E}}$ is defined as follows:

$$d\vec{x}^T\cdot d\vec{x}-d\vec{X}^T\cdot d\vec{X}=2\cdot d\vec{x}^T\cdot\underline{\underline{E}}\cdot d\vec{x} \qquad [V\text{-}15]$$

$$\underline{\underline{E}}=\frac{1}{2}\left(\underline{\underline{I}}-\underline{\underline{F}}^T\,\underline{\underline{F}}\right) \qquad [V\text{-}16]$$

Euler-Almansi strain tensor is Eulerian, because it is relative to the current configuration.

IV-2.2. Stress Measures

We will consider three measures of stress:

1. The Cauchy stress tensor ***T***;

2. The First Piola-Kirchhoff stress tensor $\boldsymbol{\sigma}$;

3. The second Piola-Kirchhoff stress tensor ***S***.

1- Cauchy stress (T)

Cauchy stress, also known as the *true stress* is the most fundamental and commonly used stress quantity. Cauchy stress tensor, which is an Eulerian stress tensor, is defined by resolving an internal force at the configuration $C_{(t)}$ in the directions of the stationary reference system. Both, the force components and the normal to the area have fixed directions in space. The forces are calculated per unit area at the configuration $C_{(t)}$.

Cauchy stress tensor $\underline{\underline{T}}$ is defined as:

$$d\vec{f} = \underline{\underline{T}} \cdot \vec{n} \cdot ds \qquad [V\text{-}17]$$

Stress vector $\vec{P}(M,\vec{n})$ of normal $\vec{n}$, is related to Cauchy stress tensor $\underline{\underline{T}}$ by the following relation:

$$\vec{P}(M,\vec{n}) = \underline{\underline{T}} \cdot \vec{n} \qquad [V\text{-}18]$$

In a Cartesian coordinates system: $P_i = T_{ij} \cdot n_j$.

2- First Piola-Kirchhoff stress (σ)

It is a multi-axial generalization of the engineering stress (nominal stress). This stress is defined as the force in the current configuration acting on the original area, i.e. it is defined by resolving an internal force at the configuration $C_{(t)}$ in the directions of the stationary reference system. However, the forces are calculated per unit area at the initial configuration $C_{(0)}$.

First Piola-Kirchhoff stress is an unsymmetric tensor, and is for that reason less attractive to work with. The transpose of the first Piola-Kirchhoff stress is called the nominal stress. The definition of the nominal stress "***P***" is similar to that of the Cauchy stress, except that it is expressed in terms of the area and normal of the underformed reference surface. When expressing $d\vec{f}$ on the initial configuration $C_{(0)}$, first Piola-Kirchhoff stress tensor $\underline{\underline{\sigma}}$ is defined as:

$$d\vec{f} = \underline{\underline{\sigma}} \cdot \vec{n}_0 \cdot ds_0 \qquad [V\text{-}19]$$

With: $\underline{\underline{\sigma}} = \det \underline{\underline{F}} \cdot \underline{\underline{T}} \cdot \underline{\underline{F}}^{-T}$

3- Second Piola-Kirchhoff stress (S)

The second Piola-Kirchhoff stress tensor is defined along the material directions (Lagrangian). It is defined by resolving an internal force along the material directions, and by calculating the force per unit area at the configuration $C_{(t)}$.

Cauchy stress tensor and second Piola-Kirchhoff stress tensor are symmetric. We get second Piola-Kirchhoff stress tensor $\underline{\underline{S}}$ by transporting $d\vec{f}$ in the initial configuration $C_{(0)}$ with:

$$d\vec{f}_0 = \underline{\underline{F}}^{-1} \cdot d\vec{f} \qquad [V\text{-}20]$$

$$d\vec{f}_0 = \underline{\underline{S}} \cdot \vec{n}_0 \cdot d\vec{s}_0 \qquad [V\text{-}21]$$

Where: $\underline{\underline{S}} = \det \underline{\underline{F}} \times \underline{\underline{F}}^{-1} \times \underline{\underline{\underline{\sigma}}} \times \underline{\underline{F}}^{-T}$

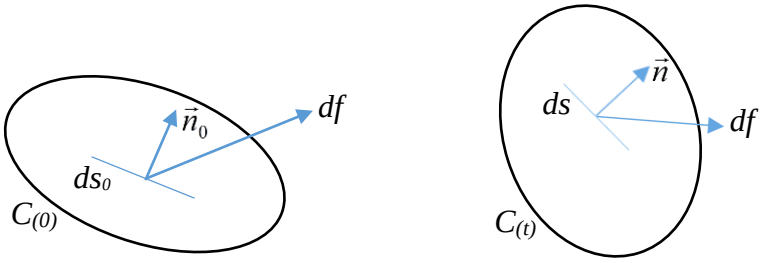

***Fig. V.5.* Internal forces configurations**

V- LARGE DISPLACEMENT STATIC AND DYNAMIC ANALYSIS

Several large displacement formulations of geometrically nonlinear finite elements analysis have been used to derive the stiffness matrix in nonlinear analysis. The main differences arise from the simplifications and assumptions imposed on the kinematic relations and the form of stress. The use of the most general large displacement formulation will render "correct" solutions, however, in many cases the use of a more restrictive formulation could be attractive because of its computational efficiency.

The first applications of the finite elements method to nonlinear structural analysis, was proposed in 1960 by [TURNER et al 1960] for a geometrically nonlinear analysis using the incremental approach, and in 1968 by [SCHMIT et al 1968] using the direct method. However, the direct method was quickly abandoned in favour of the incremental approach.

Subsequently, the incremental approach has improved and applied successfully by many authors, mainly for the elastic instability analysis: [TURNER et al 1964; FELIPPA 1966; MALLET & BERLEE 1966; ODEN 1966; GALLAGHER et al 1967; BREBBIA & CONNOR 1969; HOLAND & MOAN 1969; MARCAL 1969; DUPIUS et al 1971; WOOD 1977] and many others. It was [ARGYRIS 1965-b] who used the geometric stiffness matrix in conjunction with the updating of coordinates and an initial

displacement matrix. Later, the equations of general formulation of the geometric nonlinear analysis are established, where the principle of virtual work is used in incremental form after discretization of the displacement field in terms of nodal unknowns: [YAGHMAI 1968; HIBBIT et al 1970].

At this time, only the Total Lagrangian Formulation has been used successfully. Nevertheless, its use was limited to moderate rotations problems only: [KAWAI & YOSHIMURA 1969; ROBERTS & ASHWELL 1971; GALLAGHER 1973; BATHE et al 1975; BATOZ et al 1976]. It was not until the works of [SIMO 1985; SIMO & VU-QUOC 1986], to extend the TLF for the analysis of large rotations problems. Subsequently, several investigation and application of the TLF are presented: [CARDONA & GERADIN 1988; BUECHTER & RAMM 1992; LO 1992; SANSOUR & BUFLER 1992; IBRAHIMBEGOVIC 1995].

Considering the formulation of incremental nonlinear finite element analysis, the choice lies between using the initial configuration or the last calculated configuration as reference. The "*TLF*" presents some serious difficulties of formulation, especially with shell elements, because it requires an exact description of the finite element cinematic beside the firm representation of large rotations. In the other hand, the "ULF" was more attractive due its simplicity and effectiveness. It setback the "*TLF*" in many applications. The ULF handles large displacements and large rotations in a simple manner, by admitting the assumption of small displacements and rotations between successive configurations, and use the conventional linear theory for calculating deformations. The "*ULF*" was presented in the works of: [MURRAY & WILSON 1969; HOFMEISTER et al 1971; SHARIFI & POPOV 1971; YAGHMAI & POPOV 1971; BATHE & OZDEMIK 1975].

Subsequently, the "ULF" was extended by many authors: [BAZANT & NIMEIRI 1973; HORRIGMOE & BERGAN 1978; RAMM & OSTERRIEDER 1983; GADALA el al 1984; DVORKIN et al 1988; KEBARI & CASSELL 1992; JIANG et al 1994]. Despite simplicity and effectiveness of the Updated Lagrangian Formulation in many areas, it contains approximations that can introduce errors playing a significant role on the performance and convergence, especially with structures that exhibits highly nonlinear behaviour. A mesh fine enough and small load step must be adopted to meet the assumption of small displacements and rotations.

At the same period, dynamic nonlinear analysis was established and evolved with static nonlinear analysis based on both "*TLF*" and "*ULF*" by many authors: [ARCHER & LANGE 1965; STRICKLIN 1970; HARTZMAN & HUTCHINSON 1972; WILSON et al 1973-b; BATHE et al 1974, 1975; WU & WIRMER 1974; FELIPPA & PARK 1979; NATH 1979; BATHE & BOLOURCHI 1980; SAIGAL & YANG 1985; SIMO et al 1990].

V-1. The Updated Lagrangian Formulation

The updated Lagrangian description of motion has proven to be a very effective method in the treatment of geometric nonlinearities: [BATHE 1982]. In this formulation, the element local coordinates and local system of axes are continuously updated during movement, all static and kinematic variables are referred to the last calculated configuration. We consider large rotations and large translations here, but small strains. Rotations and displacements from two consecutive configurations may be considered small. Consequently, the quadratic terms of the derivatives of displacement are negligible. We therefore have a nonlinear analysis with large displacements and large rotations, but small strains. This approach has been considered by many authors for the nonlinear analysis of shells: [WUNDERLICH et al 1981; BATHE et al 1983]. Therefore, the linearized incremental form of the principle of virtual displacements based on the updated Lagrangian description is adopted in this work.

V-2. Finite Elements Discretization

The considered approach in this work, for the finite element approximation, is the displacement approach, in which, the displacement field is the main unknown variable. Other variables are treated as secondary quantities. Thus, the solution of algebraic equations expressing the equilibrium of a solid body by the finite element method, requires the discretization of that expression of equilibrium. This approach leads to express the displacement field over the shell finite element as a function of nodal displacements variable. Using shape functions, the displacement field is expressed in the "*ULF"* by:

$$ {}^{t}_{t}U_i = \sum N_{i\alpha}\left({}^{t}x_j\right).{}^{t}_{t}q_{i\alpha} \qquad [V\text{-}22] $$

We also must express the strain tensor as a function of discrete displacement field, which is a function of the variation of the derivative of the displacement field.

The variation of the displacement at time (*t*) inside the finite element is given by:

$$ \delta\left({}^{t}_{t}U_i\right) = \sum N_{i\alpha}\left({}^{t}x_j\right).\left(\delta\ {}^{t}_{t}q_i\right)_{\alpha} \qquad [V\text{-}23] $$

The derivation related to the current configuration is written:

$$ \frac{\partial\left(\delta_t u_i\right)}{\partial\ {}^{t}x_j} = \delta_t u_{i,j} \qquad [V\text{-}24] $$

The derivation of displacement within the finite element is given by:

$$ {}^{t}_{t}U_{i,k} = \sum N_{i\alpha,k}\left({}^{t}x_j\right).{}^{t}_{t}q_{i\alpha} \qquad [V\text{-}25] $$

V-3. Incremental Expression of the Virtual Displacement Principle in the "U.L.D"

Let us consider the motion of a solid body in a Cartesian co-ordinate system, *Fig. V.3*. In static nonlinear and implicit time integration dynamic analysis, the equilibrium of the body at time ($t+\Delta t$) is expressed and used to solve for the static and kinematic variables corresponding to time ($t+\Delta t$). The equilibrium state is characterized by a minimum of energy expressed in standard form as:

$$\delta\pi = W_{\text{int}} - W_{ext} = 0 \qquad \textit{[V-26]}$$

The discretized expression of this equation of equilibrium allows the solution of a matrix system, where the nodal displacements are the (n) unknowns to be determined. It is written:

$$^{t}[K_n]\{^{t}u_n\} = \{^{t}F_n\} \qquad \textit{[V-27]}$$

If a nonlinear behaviour is included in a FE Analysis, the set of equilibrium equations becomes nonlinear and instead of a set of linear equations, we obtain a set of nonlinear algebraic equations. In the Updated Lagrangian Formulation, all quantities are referred to the last known configuration γ^n at time (t). Considering the equilibrium of the body at time ($t+\Delta t$), the principle of virtual displacements is written related to the reference configuration γ^n in the following form:

$$\int_{^{t}v} {}^{t+\Delta t}_{t}\sigma_{ij} \cdot \delta\, {}^{t+\Delta t}_{t}e_{ij} \cdot d\,{}^{t}v = {}^{t+\Delta t}W_{ext} \qquad \textit{[V-28]}$$

Where: ${}^{t+\Delta t}W_{ext}$ is the total external virtual work.

$\delta\, {}^{t+\Delta t}_{t}e_{ij}$: is a "virtual" variation in the Cartesian components of the Green-Lagrange strain tensor in the configuration at time ($t+\Delta t$) referred to the configuration γ^n at time (t).

${}^{t+\Delta t}_{t}\sigma_{ij}$: The Cartesian components of the 2nd Piola-Kirchhoff stress tensor in the configuration at time ($t+\Delta t$) referred to the configuration γ^n at time (t).

The incremental total external virtual work due to surface forces ${}^{t+\Delta t}_{t}t_k$ and body forces ${}^{t+\Delta t}_{t}f_k$ expression is:

$${}^{t+\Delta t}W_{ext} = \int_{^{t}A} {}^{t+\Delta t}_{t}t_k \cdot \delta u_k \cdot d\,{}^{t}A + \int_{^{t}v} {}^{t+\Delta t}_{t}f_k \cdot \delta u_k \cdot d\,{}^{t}v \qquad \textit{[V-29]}$$

The term ${}^{t+\Delta t}_{t}f_k$ arise from dynamic analysis, in which the body force components are related the mass inertia ρ and acceleration $\delta\ddot{u}_k$.

Since the stresses ${}^{t+\Delta t}_{t}\sigma_{ij}$ and strains ${}^{t+\Delta t}_{t}e_{ij}$ are unknown, the following incremental decompositions of quantities that are expressed at time ($t+\Delta t$) are used:

$$ {}^{t+\Delta t}_{t}\sigma_{ij} = {}^{t}T_{ij} + {}_{t}\sigma_{ij} \qquad [V\text{-}30] $$

With: ${}^{t}_{t}\sigma_{ij} = {}^{t}T_{ij}$ and ${}^{t+\Delta t}_{t}\sigma_{ij} = {}_{t}\sigma_{ij}$.

${}^{t}T_{ij}$: is Cauchy stress tensor.

The strain increment components between times (t) and ($t+\Delta t$) can be separated into linear and nonlinear parts:

$$ \begin{cases} {}^{t+\Delta t}_{t}e_{ij} = {}_{t}\varepsilon_{ij} + {}_{t}\varepsilon^{NL}_{ij} \\ {}_{t}\varepsilon_{ij} = \dfrac{1}{2}\left({}_{t}U_{i,j} + {}_{t}U_{j,i}\right) \\ {}_{t}\varepsilon^{NL}_{ij} = \dfrac{1}{2}\left({}_{t}U_{k,i} + {}_{t}U_{k,j}\right) \end{cases} \qquad [V\text{-}31] $$

Using *Eq. [V-31] in Eq. [V-28]* yields:

$$ \int_{{}^{t}v}\left({}^{t}T_{ij} + {}_{t}\sigma_{ij}\right)\left(\delta\,{}_{t}\varepsilon_{ij} + \delta\,{}_{t}\varepsilon^{NL}_{ij}\right)d\,{}^{t}v = {}^{t+\Delta t}W_{ext} \qquad [V\text{-}32] $$

The constitutive relations with the linear elasticity Matrix C_{ijkl} can be used to relate incremental 2^{nd} Piola-Kirchhoff stresses to incremental Green-Lagrange strains:

$$ {}_{t}\sigma_{ij} = C_{ijkl} \cdot {}_{t}\varepsilon_{kl} \qquad [V\text{-}33] $$

By using *Eq. [V-33]* in *Eq. [V-32]*, and linearizing the expression of equilibrium by neglecting the product of the two incremental nonlinear strains, we finally obtain the following expression of equilibrium related to the updated configuration $C_{(t)}$:

$$ \int_{{}^{t}v}\left({}^{t}T_{ij} \cdot \delta_{t}\varepsilon^{NL}_{ij} + C_{ijkl} \cdot {}_{t}\varepsilon_{kl} \cdot \delta_{t}\varepsilon_{ij}\right)d\,{}^{t}v = {}^{t+\Delta t}W_{ext} - \int_{{}^{t}v}{}^{t}T_{ij} \cdot \delta_{t}\varepsilon_{ij} \cdot d\,{}^{t}v \qquad [V\text{-}34] $$

This incremental equation "*Eq. [V-34]"* is employed to describe equilibrium in either, static analysis or implicit time integration dynamic analysis.

Let us decompose this incremental expression of equilibrium into several parts, and find their discretized expressions:

$$ \int_{{}^{t}v} C_{ijkl} \cdot {}_{t}\varepsilon_{kl} \cdot \delta_{t}\varepsilon_{ij} \cdot d\,{}^{t}v + \int_{{}^{t}v}{}^{t}T_{ij} \cdot \delta_{t}\varepsilon^{NL}_{ij} \cdot d\,{}^{t}v = {}^{t+\Delta t}W_{ext} - \int_{{}^{t}v}{}^{t}T_{ij} \cdot \delta_{t}\varepsilon_{ij} \cdot d\,{}^{t}v \qquad [V\text{-}35] $$

$$ (A) \qquad (B) \qquad (C) \qquad (D) $$

V-3.1. Stiffness Matrix for Small Displacements in the "U.L.D"

$$(A) = \int_{{}^{t}v} C_{ijkl} \cdot {}_{t}\varepsilon_{kl} \cdot \delta\, {}_{t}\varepsilon_{ij} \cdot d\, {}^{t}v \qquad [V\text{-}36]$$

The variation of strain, written in term of nodal displacements vector is:

$$\delta\, {}_{t}\varepsilon_{ij} = {}_{t}^{t}B_{ij\alpha} \cdot \delta\, {}_{t}q_{\alpha} \qquad [V\text{-}37]$$

Then we get:

$$(A) = \int_{{}^{t}v} C_{ijkl} \cdot {}_{t}^{t}B_{kl\alpha} \cdot {}_{t}^{t}B_{ij\beta} \cdot {}_{t}q_{\alpha} \cdot \delta\, {}_{t}q_{\beta} \cdot d\, {}^{t}v \qquad [V\text{-}38]$$

$$(A) = {}_{t}^{t}K_{\alpha\beta} \cdot {}_{t}q_{\alpha} \cdot \delta\, {}_{t}q_{\beta} \qquad [V\text{-}39]$$

With: ${}_{t}^{t}K_{\alpha\beta} = \int_{{}^{t}v} C_{ijkl} \cdot {}_{t}^{t}B_{kl\alpha} \cdot {}_{t}^{t}B_{ij\beta} \cdot d\, {}^{t}v$.

${}_{t}^{t}K_{\alpha\beta}$: is the stiffness matrix for small displacements defined at time (t) with respect to the current configuration.

V-3.2. Geometric Stiffness Matrix (initial stress matrix) in the "U.L.D"

$$(B) = \int_{{}^{t}v} {}^{t}T_{ij} \cdot \delta\, {}_{t}\varepsilon_{ij}^{NL} \cdot d\, {}^{t}v \qquad [V\text{-}40]$$

Using the variation of nonlinear strain, we can write:

$$(B) = {}_{t}^{t}K_{\alpha\beta}^{\sigma} \cdot {}_{t}q_{\alpha} \cdot \delta\, {}_{t}q_{\beta} \qquad [V\text{-}41]$$

With:

$${}_{t}^{t}K_{\alpha\beta}^{\sigma} = \int_{{}^{t}v} {}^{t}T_{ij} \cdot ({}_{t}^{t}B_{ij\alpha}^{NL} \cdot {}_{t}^{t}B_{ij\beta}^{NL}) \cdot d\, {}^{t}v \qquad [V\text{-}42]$$

Stress tensor ${}^{t}T_{ij}$ is defined with respect to time (t), so it represents Cauchy stress.

${}_{t}^{t}K_{\alpha\beta}^{\sigma}$: is the initial stress matrix defined at time (t) with respect to the current configuration. It is known as geometric stiffness matrix because it results from the second order geometric strain-displacement relation.

V-3.3. External Forces in the "U.L.D"

$$(C)={}^{t+\Delta t}P_{\beta}\cdot\delta\,{}_{t}q_{\beta} \qquad [V\text{-}43]$$

${}^{t+\Delta t}P_{\beta}$: represents the vector of externally applied nodal loads at time ($t+\Delta t$).

V-3.4. Internal Forces in the "U.L.D"

$$(D)=\int_{{}^{t}v}{}^{t}T_{ij}\cdot\delta\,{}_{t}\varepsilon_{ij}\cdot d\,{}^{t}v \qquad [V\text{-}44]$$

Using *Eq. [V-37]* we get:

$$(D)={}_{t}^{t}F_{\beta}\cdot\delta\,{}_{t}^{t}q_{\beta} \qquad [V\text{-}45]$$

With:

$${}_{t}^{t}F_{\beta}=\int_{{}^{t}v}{}^{t}T_{ij}\cdot{}_{t}^{t}B_{ij\beta}\cdot d\,{}^{t}v \qquad [V\text{-}46]$$

${}_{t}^{t}F_{\beta}$: The vector of nodal forces equivalent to the internal stresses at time (t).

V-3.5. Residual Forces in "U.L.D"

Residual forces expressed in the current configuration are:

$${}_{t}^{t}R_{\alpha}={}_{t}^{t}P_{\alpha}-\int_{{}^{t}v}{}^{t}T_{ij}\cdot{}_{t}^{t}B_{ij\alpha}\cdot d\,{}^{t}v \qquad [V\text{-}47]$$

With: ${}_{t}^{t}Q_{\alpha}=\int_{{}^{t}v}{}^{t}T_{ij}\cdot{}_{t}^{t}B_{ij\alpha}\cdot d\,{}^{t}v$.

${}_{t}^{t}Q_{\alpha}$: represents internal forces defined at time (t) with respect to the current configuration.

V-3.6. Incremental Expression of Equilibrium in the "U.L.D"

Finally, the finite element discretization of the linearized incremental form of the principle of virtual displacements, gives the incremental expression of equilibrium as:

$$({}_{t}^{t}K_{\alpha\beta}+{}_{t}^{t}K_{\alpha\beta}^{\sigma}).\,{}_{t}q_{\beta}={}^{t+\Delta t}P_{\alpha}-{}_{t}^{t}F_{\alpha} \qquad [V\text{-}48]$$

With: ${}_{t}^{t}K_{\alpha\beta}^{Tg}={}_{t}^{t}K_{\alpha\beta}+{}_{t}^{t}K_{\alpha\beta}^{\sigma}$.

${}_{t}^{t}K_{\alpha\beta}^{Tg}$: represents the tangent stiffness matrix defined at time (t) with respect to the current configuration.

where: ${}_{t}^{t}K_{\alpha\beta}^{\sigma}$, is the linear strain incremental stiffness matrix; ${}_{t}^{t}K_{\alpha\beta}^{\sigma}$ is the nonlinear strain incremental (geometric) stiffness matrix; ${}^{t+\Delta t}P_{\alpha}$ is the vector of externally applied nodal loads at

time ($t+\Delta t$); ${}_t^t F_\alpha$ is the vector of nodal internal forces equivalent to the finite element's elastic stresses at time (t), and q_β is the vector of incremental nodal displacements.

The matrices in *Eq. [V-39]* and *Eq. [V-41]* are evaluated using the displacement interpolation functions of the flat shell element developed for linear small displacement analysis presented in *Chapter III*.

In dynamic analysis using implicit time integration the inertia forces corresponding to time ($t+\Delta t$) are added to the left-hand sides of *Eq. [V-34]*.

In this work, the dynamic equilibrium equation of motion is solved using the implicit Newmark's step by step integration method. Once the finite element models of geometrically nonlinear analysis and linear dynamic analysis has been created, nonlinear dynamic analysis will be obtained by combining the adopted dynamic scheme with the nonlinear scheme. The Newton-Raphson algorithm associated to the load control technique is employed for iterating within each time step increment (Δt) until equilibrium is achieved. The equilibrium equation of motion is written as:

$$M\ddot{u}_{t+\Delta t} + C\dot{u}_{t+\Delta t} + N(u)_{t+\Delta t} = R_{t+\Delta t} \qquad [V\text{-}49]$$

Where: $R_{t+\Delta t}$, is the nodal residual forces vector at time ($t+\Delta t$).

$N(u)_{t+\Delta t}$, is the equivalent internal forces vector at time ($t+\Delta t$).

We note that, in order to extend the linear dynamic scheme to taking account for geometrically nonlinear behaviour, the nodal internal (nonlinear) elastic forces vector of *Eq. [V-39]* must be taken into account, it is written as:

$$N(u)_{t+\Delta t} = \int_v [B_{t+\Delta t}]^T \{\sigma(\varepsilon)_{t+\Delta t}\} \cdot dv \qquad [V\text{-}50]$$

V-4. Tangent Stiffness Matrix for Flat Shell Elements with Drilling Rotation

As we have seen, geometrically nonlinear analysis is performed iteratively with subsequent updating of coordinates and internal stresses. Deriving the geometric stiffness matrix and computing the internal stresses constitute the main effort.

Geometric stiffness is calculated using *Eq. [V-42]* using incremental Green's strain tensor, which can be decomposed into linear and nonlinear terms $\Delta\varepsilon_{ij}$ and $\Delta\varepsilon_{ij}^{NL}$ respectively. It is calculated in relation to the reference plane related to the co-rotational reference system, which is continuously updated. Green-Lagrange strain tensor is given by:

$$\varepsilon_{ij} = \frac{1}{2}\left(\frac{\partial u_i}{\partial X_j} + \frac{\partial u_j}{\partial X_i} + \frac{\partial u_k}{\partial X_i}\frac{\partial u_k}{\partial X_j} \right) \qquad [V\text{-}51]$$

V-4.1. Plate bending geometric stiffness

Initial stress matrix is calculated using stress field resulting from the previous configuration, and quadratic terms of the nonlinear Green-Lagrange strain as:

$$[K_\sigma] = \int_A [g]^T [C][g] \cdot dA \qquad [V\text{-}52]$$

$[C]$: is the in-plane (membrane) stress tensor.

$$[C] = \begin{bmatrix} N_{xx} & N_{xy} \\ N_{yx} & N_{yy} \end{bmatrix} \qquad [V\text{-}53]$$

Quadratic terms of the nonlinear Green-Lagrange strain are written as:

$$\{\varepsilon^{NL}\} = \frac{1}{2}\{q\}[g]^T[g]\{q\} \qquad [V\text{-}54]$$

[g]: represents the slope matrix; it is expressed as a function of bending derivatives:

$$[g]\{\Delta q\} = \begin{bmatrix} \partial w/\partial x \\ \partial w/\partial y \end{bmatrix} \qquad [V\text{-}55]$$

$$[g] = \begin{bmatrix} \partial N_i/\partial x \\ \partial N_i/\partial y \end{bmatrix} \qquad [V\text{-}56]$$

Where: N_i represents shape functions of the transverse displacement field (*w*).

It is well known that "*DKQ"* and "*DKT*" plate bending elements have no explicit expression for the transverse displacement field (*w*) in the interior of the element. Therefore, the derivatives of

the transverse displacement that are required to get the geometric stiffness matrix cannot be directly obtained. To overcome this problem, we could adopt a polynomial interpolation representing the out of plane displacement field (*w*). Even though this interpolation does not represent the true displacement field of the "*DKQ"* and "*DKT*" elements, this approach gives satisfying results, see [ELKHALDI 1987].

Therefore, bi-cubic polynomial interpolation is necessary and sufficient. The adopted polynomials and the resulting shape functions are presented in appendices *B* and *C*.

V-4.2. Membrane geometric stiffness

Usually, researchers disregard the nonlinear in-plane terms of Green-Lagrange strain tensor. They take into account the nonlinear terms of plate bending elements only when deriving the geometric stiffness matrix of flat shell finite elements, even when dealing with shell elements with drilling rotation. This simplification of the kinematic relationships, assume that the in-plane displacement field components are linear, and even when they are nonlinear, they are infinitesimal so that their derivatives are small, and therefore their second order terms can be neglected according to the "von-Karman assumptions".

Hence, it is common to use the following form of the geometric stiffness matrix:

$$\left[K_\sigma\right]=\begin{bmatrix}0 & 0\\ 0 & K_\sigma^b\end{bmatrix} \qquad \textit{[V-57]}$$

K_σ^b: represents plate bending geometric stiffness.

However, geometrically nonlinear analysis of thin shell structures, involves not only large out of plane displacements, but also large in-plane displacements. The stress resultants due nonlinear in-plane strain-displacement relationship, may have a significant influence on the stiffness of the structure. In this work, since we used a higher order interpolation for the in-plane displacement field due in-plane rotations, strain tensor will contain non-negligible nonlinear terms. For a plane stress problem, quadratic terms of the nonlinear Green-Lagrange strain are written as:

$$\begin{Bmatrix}\varepsilon_x^{NL}\\ \varepsilon_y^{NL}\\ \varepsilon_{xy}^{NL}\end{Bmatrix}=\frac{1}{2}\begin{Bmatrix}\left(\frac{\partial u}{\partial x}\right)^2+\left(\frac{\partial v}{\partial x}\right)^2\\ \left(\frac{\partial u}{\partial y}\right)^2+\left(\frac{\partial v}{\partial y}\right)^2\\ \left(\frac{\partial u}{\partial x}\frac{\partial u}{\partial y}\right)+\left(\frac{\partial v}{\partial x}\frac{\partial v}{\partial y}\right)\end{Bmatrix}=\frac{1}{2}\begin{Bmatrix}\left(\frac{\partial u}{\partial x}\right)^2\\ \left(\frac{\partial u}{\partial y}\right)^2\\ \left(\frac{\partial u}{\partial x}\frac{\partial u}{\partial y}\right)\end{Bmatrix}+\frac{1}{2}\begin{Bmatrix}\left(\frac{\partial v}{\partial x}\right)^2\\ \left(\frac{\partial v}{\partial y}\right)^2\\ \left(\frac{\partial v}{\partial x}\frac{\partial v}{\partial y}\right)\end{Bmatrix} \qquad \textit{[V-58]}$$

Let us consider:

$$\begin{Bmatrix} \frac{\partial u}{\partial x} \\ \frac{\partial u}{\partial y} \end{Bmatrix} = \begin{bmatrix} \frac{\partial N_u}{\partial x} \\ \frac{\partial N_u}{\partial y} \end{bmatrix} \{q\} = [g_U]\{q\} \qquad [V\text{-}59]$$

$$\begin{Bmatrix} \frac{\partial v}{\partial x} \\ \frac{\partial v}{\partial y} \end{Bmatrix} = \begin{bmatrix} \frac{\partial N_v}{\partial x} \\ \frac{\partial N_v}{\partial y} \end{bmatrix} \{q\} = [g_V]\{q\} \qquad [V\text{-}60]$$

$$[g] = [g_U] + [g_V] \qquad [V\text{-}61]$$

$[g_u]$, and $[g_v]$ Contain shape functions derivatives for displacements *u* and *v* respectively. Using matrix notation, in-plane displacement field is written as:

$$\begin{Bmatrix} u \\ v \end{Bmatrix} = \begin{bmatrix} \overline{N}_1 \\ \overline{N}_2 \end{bmatrix} \{q\} \qquad [V\text{-}62]$$

Where: $\{q\}^T = \{u_i \quad v_i \quad \varphi_i\}$.

Shape functions of the in-plane displacement field and their derivatives are presented in appendices *D* and *E*.

As for plate bending elements, initial stress matrix of membrane elements is calculated using stress field resulting from the previous configuration, and quadratic terms of the in-plane nonlinear Green-Lagrange strain as:

$$[k_\sigma] = \int_{A^e} [G]^T [C][G] \cdot d\,{}^0A \qquad [V\text{-}63]$$

Finally, tangent stiffness matrix $[K_T]$ is written as:

$$[K_T] = [K_0] + [K_\sigma] \qquad [V\text{-}64]$$

Where: $[K_\sigma]$ represents the geometric stiffness (initial stress stiffness) matrix for the flat shell finite element with drilling rotation, it is written as:

$$[K_\sigma] = \begin{bmatrix} K_\sigma^m & 0 \\ 0 & K_\sigma^b \end{bmatrix} \qquad [V\text{-}65]$$

$[K_0]$: represents the small displacement matrix.

The linear elastic stiffness matrices of the finite elements presented in *Chapter III*, provides the linear part of the elements' tangent stiffness matrices.

VI- THE CO-ROTATIONAL APPROACH

For the conventional "*ULF*" and "*TLF*" descriptions, the reference system of axes is kept fixed. If one moves the system of reference axes with the movement of the body (translate and rotate but do not deform with the body) so as to remove the rigid body motion induced by large displacements and rotations, another Lagrangian description of a relatively simple manipulation can be defined. This description is called a Co-rotational Lagrangian Description. The new position of the system of axes, is obtained after giving the initial system of axes a rigid body displacement and rotation in order to have the closest position as possible to the current deformed configuration, *Fig .V.6.*

Indeed this would absorb large rigid body rotations and translations, so the remaining rotations can be considered small or moderate. By such a procedure, the "*CLD"* overcomes the problem of treatment of large rotations in classical Lagrangian descriptions.

As for the conventional Lagrangian descriptions, we define two specific co-rotational descriptions differentiating by choosing the appropriate configuration of reference. The co-rotational Lagrangian description can be: Total (TLCD) or Updated (ULCD). All expressions written in § *V-3*, are valid for either the "*ULD*" or the "*ULCD*". Only the reference configuration changes, where each element has its own independent reference configuration.

[WEMPNER 1969] suggested to split the motion into rigid body motion followed by a small relative deformation, so that the geometrical nonlinearities are attributed to the rigid body rotations. Thus, the co-rotational formulation, fully contains the geometric nonlinearity caused by the large rigid body motion, by a consistent transformation from the local co-rotational system to the global coordinate system. Therefore, the linear finite element formulation, can be used to calculate the stiffness matrix and internal force vector of the finite element in the local co-rotational system. The main idea of the co-rotational formulation can be summarized as:

- on the element level, define a reference system that translates and rotates with the element overall rigid-body motion;

- calculate the nodal variables in this reference system, thus the element overall rigid-body motion is excluded;

- compute the local internal force vector and element tangent stiffness matrix.

The traditional Lagrangian formulations, use the nonlinear strain-displacement relationship of a specific element to derive the tangent stiffness matrix and internal force vector. So, the geometric nonlinearity is included in the element's formulation from the beginning. However, the co-

rotational formulation, is independent of the specific local element formulation, which means that the transformation between the local and global nodal entities is independent of the assumptions made for the local element. Thus, the established process of the co-rotational finite element equations is the same for different elements with the same geometry and nodal *d.o.f.*

The co-rotational approach has been viewed as an alternative way of deriving efficient nonlinear finite elements. It has known a rapid development since it has initially presented, by: [WEMPNER 1969; ORAN 1973-a, 1973-b; BELYTSCHKO & HSIEH 1973, 1974; BATHE et al 1975; BELYTSCHKO & SCHWER 1977; ARGYRIS et al 1979; BELYTSCHKO & GLAUM 1979].

[RANKIN & BROGAN 1986] presented a concept of an element independent co-rotational formulation (EICR). The main advantage of this formulation is the complete separation of co-rotational filtering of the deformational displacements from the core element formulation. [RANKIN & NOUR-OMID 1988; NOUR-OMID & RANKIN 1991] introduced a projector matrix with 3D paramatrization of the rotation field into the (EICR) formulation in order to improve the process of the (EICR). [RANKIN et al 1994] studied the geometrically nonlinear analysis of laminated composite structures based on the EICR formulation. [CRISFIELD 1990; CRISFIELD & MOITA 1996] presented in details a unified approach for geometric nonlinear co-rotational formulation of various finite elements. Also, a unification of existing co-rotational approaches was presented by [FELIPPA & HAUGEN 2005]. [PACOSTE 1998, BATTINI & PACOSTE 2004, 2006; BATTINI 2007] introduced some modifications following the main idea of the (EICR) in order to achieve better computational efficiency. They also discussed the choice of the local coordinate system and linear triangular shell element. [IZZUDDIN 2005] presented a co-rotational formulation for a 4-node quadrilateral flat shell element with hierarchic freedoms. He used the two bisectors of the element diagonals and their cross-product to define the co-rotational framework. [KIM & LOMBOY 2006] presented a 4-node quasi-conforming stress resultant shell element for nonlinear analysis using the co-rotational formulation. He employed the polar decomposition to separate rigid-body motion from the pure element deformation.

The co-rotational formulation has been widely used in a significant numbers of works dealing with shell analysis: [CRISFIELD 1990; LIU & TO 1995; PACOSTE & ERIKSSON 1995, 1997; STOLARSKI et al 1995; BOISSE et al 1996; MEEK & RISTIC 1997; KIM et al 1998; KIM & VOYIADJIS 1999; FELIPPA 2000; HSIAO & LIN 2000; KOLAHI & CRISFIELD 2001; TABIEI & TANOV 2002; TAYLOR et al 2003; YAQUN et al 2003; THAM et al 2005; BRUNET & SABOURIN 2006; KIM et al 2007-a; KIM et al 2007-b; YANG et al 2007; KHOSRAVI et al 2008; CAI et al 2009; GARCEA et al 2009; ALMEIDA & AWRUCH 2011; AN & XU 2011; GARCEA et al 2011, 2012; ZAGARI et al 2013].

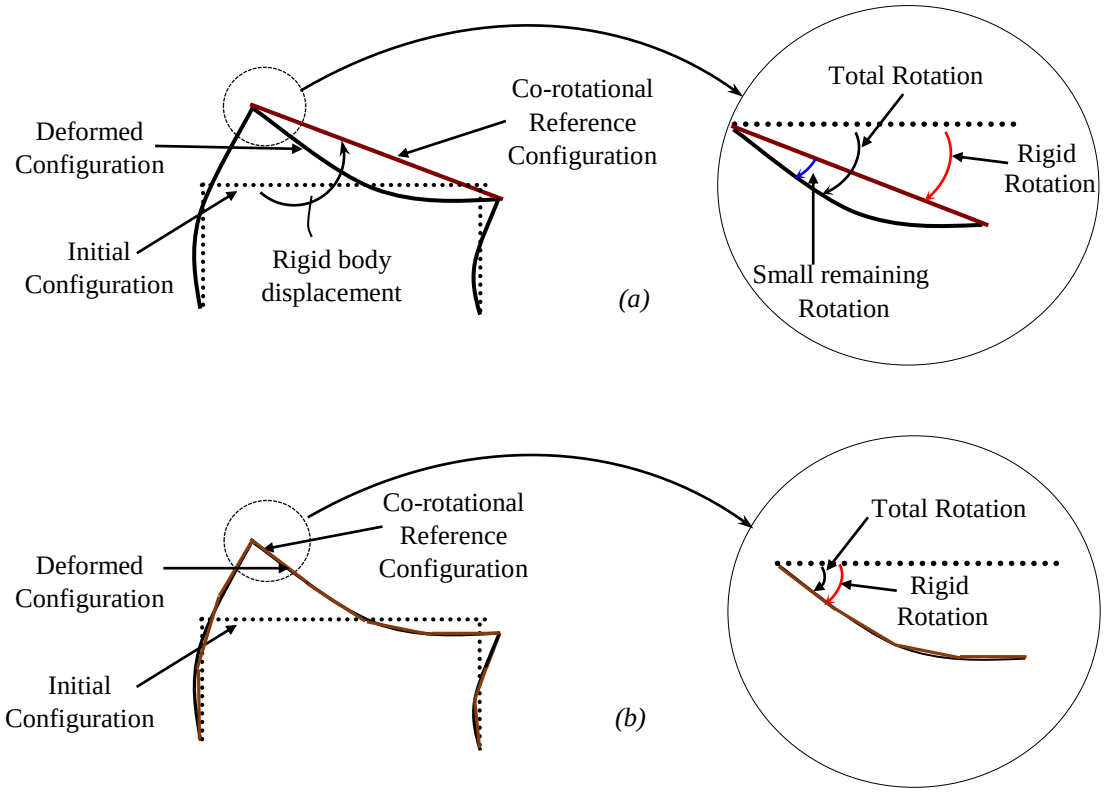

Fig. V.6. **Cinematic of the Co-rotational description**

VI-1. Handling Large Rotations

Generally, the nonlinear analysis, exhibits large displacements and large rotations. A severe difficulty stems from the fact that finite rotations are not vectorial quantities, and therefore, the extension to large rotations is not straightforward. This aspect has been discussed by [WEMPNER 1969; ARGYRIS & DUNNE 1975]. Alternative approaches to incorporate finite rotations can be found in: [BATHE & BOLOURCHI 1979; ARGYRIS 1982; SURANA 1983 ; OLIVER & ONATE 1984; BASAR 1987; HSIAO 1987; HSIAO & HUNG 1989; SIMO & FOX 1989; SALEEB et al 1990; BASAR & DING 1990, 1992; SANSOUR & BUFLER 1992; LIU & To 1995; IBRAHIMBEGOVIC 1997; WANG & THIERAUF 2001].

In this work, the treatment of finite rotations is used following the most known approach, which is based on the observation that if one can eliminate the rigid body motion from the total displacement, the remaining part of the motion is always a small quantity and only the deformational part of the rotations is accumulated. As can be seen from *Fig. V.6*. that represents the displacement of a frame structure from the initial configuration to the deformed configuration. The rigid body displacements and rotations, constitute the greatest portion of the displacement of the frame elements, while the pure deformational displacements and rotations constitute small quantities. With mesh refinement, the pure deformational displacements and rotations will become

smaller. This, will then, allow the use of the small displacement theory and thus assure the validity of vector operations. This simplified approach to circumvent the large rotation problem has also been discussed in [WEMPNER 1969; ARGYRIS & DUNNE 1975]. This method has several advantages:

• Effective treatment of large rotations;

• Easily adapt with finite elements that have rotational *d.o.f* like beams and shells:

• Decoupling of material nonlinearity and the geometric nonlinearity;

• Automatic reorientation of material by removal of the rigid body motion, avoiding the complexity of using invariants of the continuum mechanics;

• And finally, it has the advantages of exploiting the library programs in small displacements.

VI-2. Co-rotational Formulation for Triangular and Quadrilateral Flat Shell Elements with Drilling Rotational Degree of Freedom

The co-rotational description is used in order to decompose the motion of an element into small (deformational) displacement and (strain free) rigid body motion parts. After extracting rigid body displacements and rotations, the small displacement part is dealt using the linear stiffness. Such a procedure linearizes the strain-displacement and simplifies the nodal force-stress relations within the elements' co-rotational coordinates. In this case, the shell finite elements developed for linear analysis in small displacements in *chapter III*, can be applied to nonlinear dynamic analysis with large displacements and large rotations.

This is accomplished by considering a local reference system for each element also known as co-rotated frame, which is used in order to follow the rigid body motion of the element, so that only the deformational displacements and rotations are left when the element displacements are referred to this frame.

In order to captivate rigid body motion, the co-rotational reference system of axes, makes rotations and translations with the element movement. The deformation is always measured on the level of the element’s local system since large translations and large rotations are absorbed by the co-rotational system of axes, which continuously rotates and translates with the element movement. Once local deformational displacements are obtained, the finite elements based on small-strain formulation can be used to calculate quantities such as stress, internal forces and stiffness matrix in the co-rotational system.

Small deformational displacements d are defined by extracting the rigid body motion from the global displacements d_g. So, small displacements are expressed as function of global and rigid body displacements as:

$$d = d_g - d_R \qquad [V\text{-}66]$$

The objective of this section, is to present how deformational small displacements and rotations are captured from the total ones by eliminating strain-free rigid body displacements and rotations. It is important to mention that, deformational small displacements are captured at the level of the local reference system of each element after rigid-body motion is absorbed. Therefore, it is important to specify the local referential system of axes. The adopted systems for triangular and quadrilateral elements are shown in *Fig. V.7*.

VI-2.1. Reference System of Axes

All coordinates and displacements are measured in the initial local (*XY)* plane of the considered finite element. We attached the middle surface of the quadrilateral shell element to a local reference system ***oxyz***, as illustrated in *Fig. V.7*. in which, the ***x***-axis contains both points ***a***, and ***b*** located at halfway of lines (1-4, 2-3), and the ***y***-axis is perpendicular to the ***x***-axis; the two axes cross at point **o** located at halfway of the line (***a***-***b***).

We denote by ${}^0X_o$, ${}^0Y_o$ the coordinates of the central point "**o**" of the quadrilateral element at the initial configuration at time (*t=0*). They are defined as:

$${}^0X_o = \sum_1^4 {}^0X_i \big/ 4,\ {}^0Y_o = \sum_1^4 {}^0Y_i \big/ 4 \qquad [V\text{-}67]$$

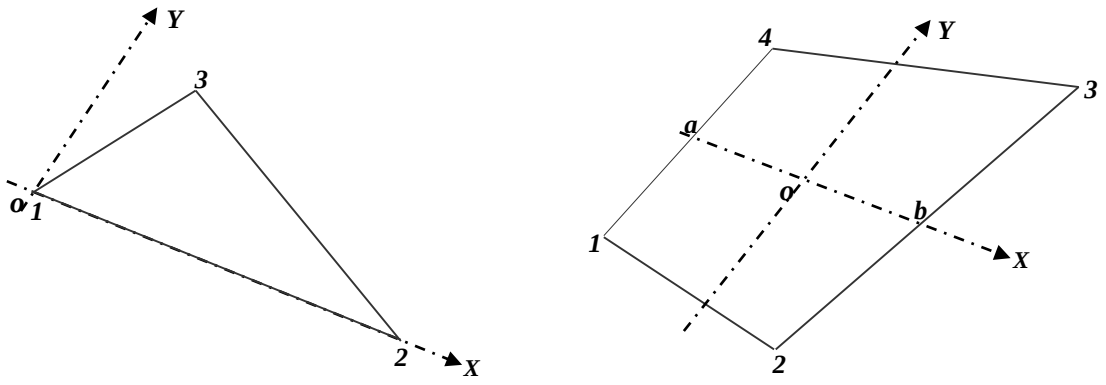

Fig. V.7. **Local system of axes**

VI-2.2. Co-rotational Formulation fore Plate Bending Elements

In addition to meshing difficulties of complex shapes, flat quadrilateral shell elements have some geometry related limitations even in linear analysis. In a four-node flat shell element case, the 4 nodes must be coplanar in the local system, so that the theory of flat shell can be validated. However, for some shells with double curvature, it may not be possible to have four nodes of the flat shell element on the same plane (warped geometries), whereas a mesh that consists of strictly flat elements may be impossible. For large deflection nonlinear analysis, this deficiency becomes more noticeable, in which, the deformed (warped) configuration $C_{(t)}$ will be used as reference to obtain the configuration $C_{(t+\Delta t)}$ when the "*ULD*" is used. Furthermore, during large bending deformations, folding may occur along the diagonals of the quadrilateral elements and result in warping, and leads to deterioration in accuracy.

Thus, even if the initial mesh satisfies the flat element restriction, the deformations can become so large that warping of the elements can be significant, which may led to some critical errors that accumulate with elements assembly. Finding ways of handling warped elements geometry is thus of fundamental importance for quadrilateral shell elements. Hence, in purpose to overcome the problems related to the probably non-planarity of the quadrilateral's nodes, we suggest to attach the middle surface of quadrilateral elements, to a local reference system ***oxyz***, as illustrated in *Fig V.8*.

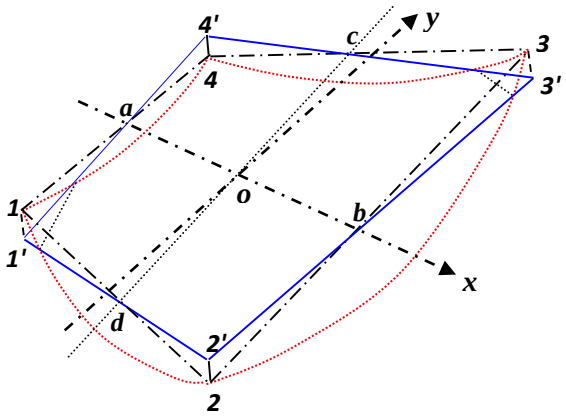

Fig. V.8. **Reference plane of the quadrilateral element**

The projection of the deformed geometry on the reference plane (1' 2' 3' 4'), minimizes the error of modeling the geometry and in calculating integration over the element area. Consequently, the geometry modeled by using this reference plane, is closer to the real deformed geometry. However the continuity between elements remains not assured.

Due to this fact, we calculate the flexional rigid rotations of the quadrilateral element, as if we had four beam elements, *Fig. V.9*. This choice is justified due to the fact that from the geometric point of view, the quadrilateral finite element is constituted from four rectilinear girders. Because rigid body translations and rotations have a geometric context, the suitable way to calculate rigid rotations is to consider the quadrilateral as a four beams assembly.

In this case, we note that the transverse displacements resulting after elimination of rigid body translations and rotations, are generally different to zero, because, the positions of the four corner nods are generally not in the same plane. That's not the case for triangular elements, where the three corner nods always make a plane, and elimination of transverse displacements is easy using a co-rotational system of axes.

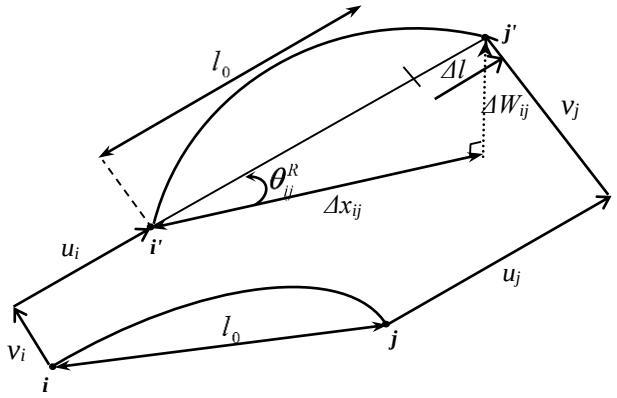

***Fig. V.9.* Out-of-plane rigid body rotations**

Then rigid body flexional rotations are written as:

$$\theta_{ij}^R = \arcsin\left(\frac{\Delta w_{ij}}{\Delta x_{ij}}\right) \qquad \textit{[V-68]}$$

The transverse displacements take the values: $\vec{w} = \overrightarrow{11} = \overrightarrow{3'3} = \overrightarrow{22'} = \overrightarrow{44'}$ as represented in *Fig. V. 8*. We can accept that these values are always small quantities after elimination of rigid body translations and rotations.

VI-2.3. Co-rotational formulation fore membrane elements

Since the local system of axes is co-rotational i.e. it makes translations and rotations following the element movement. It is important to distinguish in what position the system of axes is considered. Therefore, we denote by:

"*OXY*" the local system of axes in the initial configuration $C_{(0)}$ at time (*t=0*).

"***oxy***" the local system of axes in the current configuration $C_{(t)}$ at time (*t*).

Furthermore, we need to use an additional indication to specify in what time coordinates and displacements are expressed. We denote by:

${}^0X_i$, ${}^0Y_i$: The coordinates of a node (*i*) in the initial configuration at time (*t=0*) calculated with respect to the initial reference system, which is expressed with respect to the rotations matrix $\left[{}^0R\right]$ of the initial configuration.

${}^tX_i$, ${}^tY_i$: The coordinates of a node (*i*) in the current configuration at time (*t*) expressed with respect to the initial reference system, which is expressed with respect to the rotations matrix $\left[{}^0R\right]$.

${}^tx_i$, ${}^ty_i$: The coordinates of a node (*i*) in the current configuration at time (*t*) expressed with respect to the updated reference system, which is expressed with respect to the rotations matrix $\left[{}^tR\right]$ of the current configuration $C_{(t)}$.

With, $[R]$ is the typical rotation matrix of a flat shell element, it is defined as:

$$\left[{}^0R\right]=\begin{bmatrix}\cos(\overline{X},X) & \cos(\overline{Y},X) & \cos(\overline{Z},X)\\ \cos(\overline{X},Y) & \cos(\overline{Y},Y) & \cos(\overline{Z},Y)\\ \cos(\overline{X},Z) & \cos(\overline{Y},Z) & \cos(\overline{Z},Z)\end{bmatrix} \qquad \textit{[V-69]}$$

$$\left[{}^tR\right]=\begin{bmatrix}\cos(\overline{X},x) & \cos(\overline{Y},x) & \cos(\overline{Z},x)\\ \cos(\overline{X},y) & \cos(\overline{Y},y) & \cos(\overline{Z},y)\\ \cos(\overline{X},z) & \cos(\overline{Y},z) & \cos(\overline{Z},z)\end{bmatrix} \qquad \textit{[V-70]}$$

1- In-plane translations

For both Triangular and quadrilateral elements, the in-plane deformational small translations are taken to be the extensions along each side as presented in *Fig. V.10*. They are easily obtained by taking out the translations of the preceding state from those of the current state $C_{(t)}$ after they are placed in the reference system of axes as:

$$\begin{Bmatrix}u_i\\ v_i\end{Bmatrix}=\begin{Bmatrix}{}^tx_i-{}^0X_i\\ {}^ty_i-{}^0Y_i\end{Bmatrix} \qquad \textit{[V-71]}$$

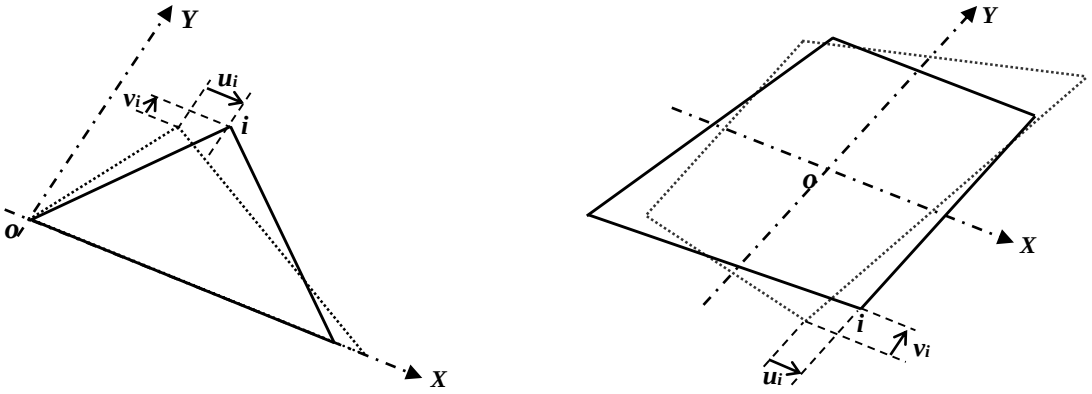

Fig. V.10. **Local deformational translations**

2- In-plane nodal rotations

Deformational small rotations denoted φ_i, are obtained by taking out the rigid in-plane rotation Φ from the total nodal rotation ϕ_i at each node independently as:

$$\varphi_i = \phi_i - \Phi \qquad [V\text{-}72]$$

A schematic of in-plane nodal rotations and their relations with in-plane rigid body rotation is shown in *Fig. V.11*, and *Fig. V.12*.

The in-plane rigid rotations Φ is taken to be the rotation of the "***x***" axis of the finite element to be considered, as could be concluded from *Fig. V.11*, and *Fig. V.12*.

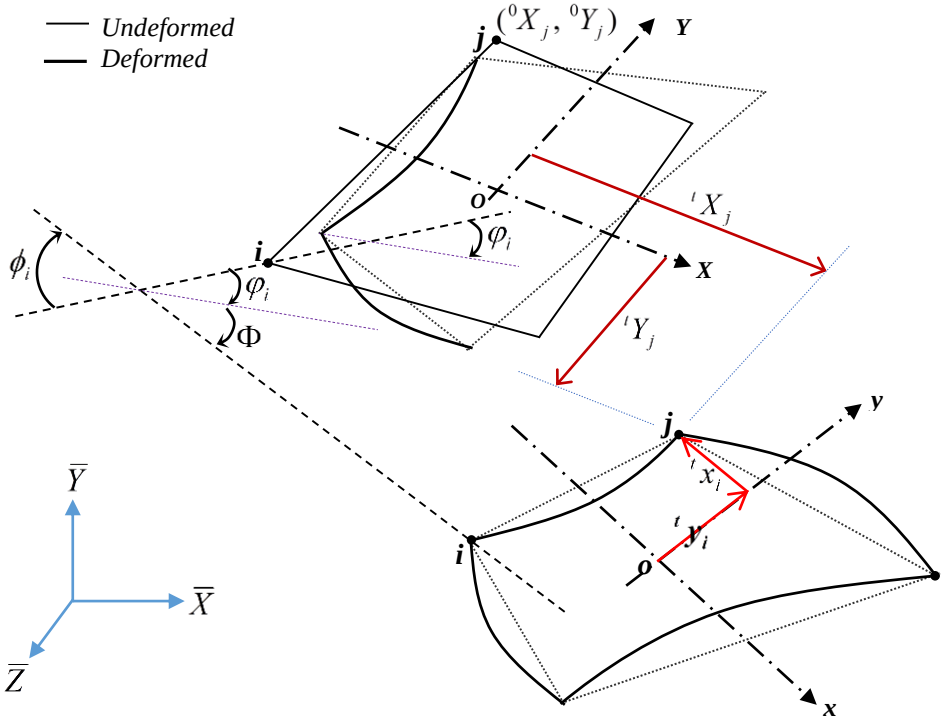

Fig. V.11. **In-plane rotations and their relations for a quadrilateral element**

We denote by:

ϕ_i : The total rotation of node (*i*).

φ_i : Small deformational rotation of node (*i*)

Φ : Rigid body in-plane rotation. For four nodded quadrilateral elements, it is calculated as*:*

$$\Phi = \arctan\left(\left(\left({}^tY_2+{}^tY_3\right)-\left({}^tY_1+{}^tY_4\right)\right)/\left(\left({}^tX_2+{}^tX_3\right)-\left({}^tX_1+{}^tX_4\right)\right)\right) \qquad [V\text{-}73]$$

For three nodded triangular elements, it is:

$$\Phi = \arctan\left(\left({}^tY_2-{}^tY_1\right)/\left({}^tX_2-{}^tX_1\right)\right) \qquad [V\text{-}74]$$

With: ${}^tX_i={}^0X_i+u_i$, and ${}^tY_i={}^0Y_i+v_i$.

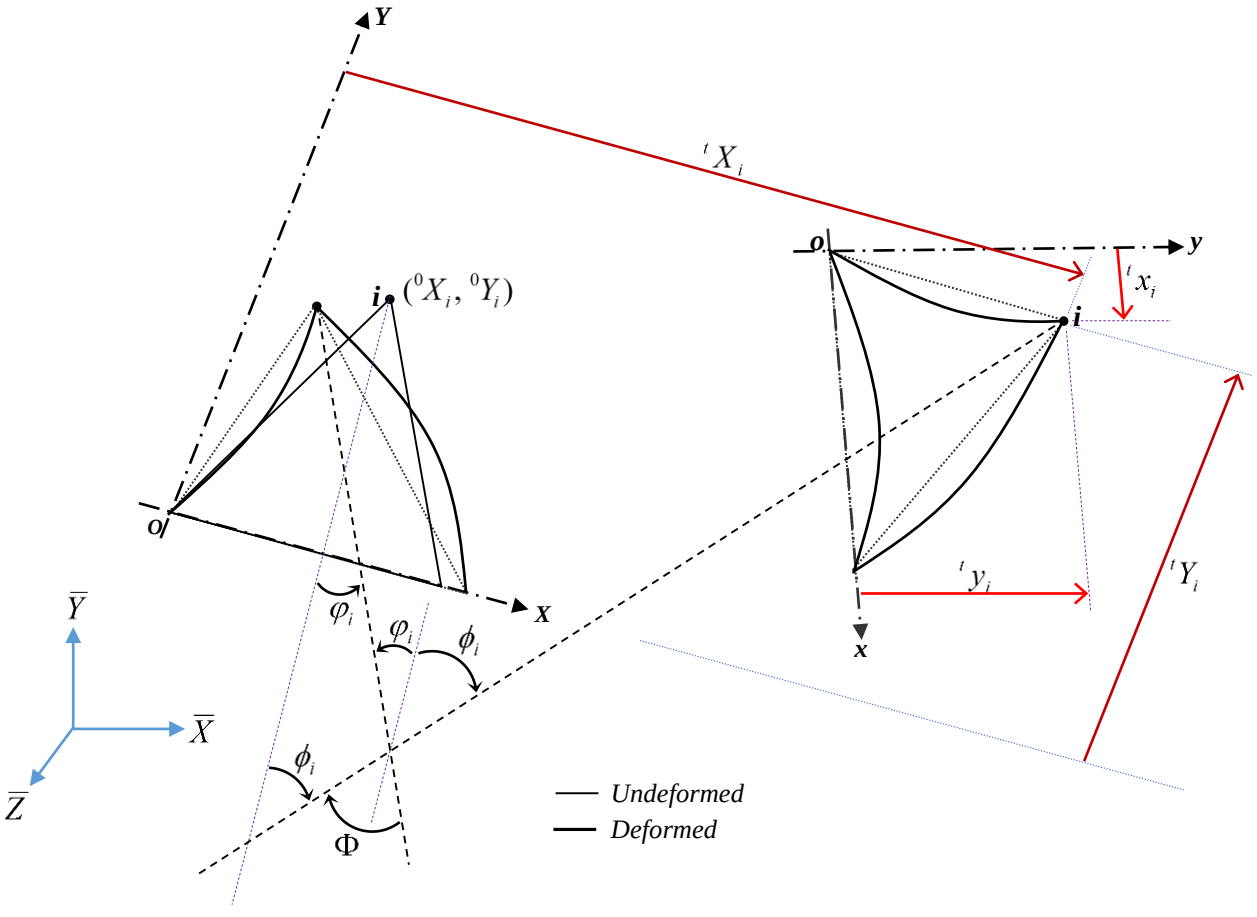

Fig. V.12. **In-plane rotations and their relations for a triangular element**

CHAPTER VI

NUMERICAL METHODS FOR NON-LINEAR ANALYSIS

I- INTRODUCTION

The finite element discretization of the equations governing the geometric nonlinear behaviour presented in previous chapters, leads to a set of non-linear algebraic equations called: Equations of residual forces. The numerical solution of this resulting nonlinear system of equations usually counts on incremental algorithms. They have become standard methods for nonlinear structural analysis. Most of these algorithms is based on the iterative Newton-Raphson method. The aim of the iterative procedure is to minimize the out-of-balance residual forces till equilibrium is achieved. For this purpose, several techniques of path-following methods, based on different approaches, have been proposed.

Apparently an effective path-following solution method should be able to trace the entire static load-displacement curve, which may include load limit points, turning points, and possibly bifurcation points. Basically, iterative methods add a constraint equation to the original non-linear governing equations, and then solve the extended system of equations by incremental-iterative procedures such as Newton-Raphson, or modified Newton Raphson to obtain the solution in discrete points along the equilibrium path. The additional constraint equation could be linear [RIKS 1979] or quadratic [CRISFIELD 1981; RAMM 1981]. Also, these algorithms differ in efficiency, and ability to handle different types of nonlinear behaviour.

To overcome the limitations of the load control and displacement control methods in vicinity of limit points and turning points respectively, a technic to switch between load and displacement controls was used by [SABIR & LOCK 1973], also a technic based on abandoning the equilibrium iterations in vicinity of limit points was used by [BERGAN et al 1978]. However, their Weakness incites the Arc-length control type algorithms in its various forms: spherical, cylindrical, and linearized versions [WEMPNER 1971; RIKS 1972, 1979; RAMM 1981; CRISFIELD 1981, 1983] to be most popular and widely used because, they simultaneously increment on both load and displacement variables. However, in some cases, difficulties in tracking equilibrium paths with various versions of the Arc-length method have been reported [CARRERA 1994; FENG et al 1996; RITTO-CORREA & CAMOTIM 2008]. It is for this reason that several algorithms and solving techniques have been developed and improved: [POWELL & SIMONS 1981; CHAN 1988; YANG & SHIEH 1990; KRENK 1995; YANG & SHIEH 1990].

In this chapter, we reviewed the existing numerical methods for solving nonlinear equilibrium equations. Detailed description will be given only for the load control and the Arc-length control methods, which are implemented in the computer programme developed during this work.

II- THE LOAD-DISPLACEMENT EQUILIBRIUM PATH

In general, static behaviour of structural systems can be characterized by a load-displacement curve, this response is plotted in a two dimensions coordinate system. The curve drawn in the load-displacement diagram is called the *equilibrium path*.

There exist a wide variety of methods of numerical resolution that are used to get the equilibrium path. The most common are iterative methods, they are based on the minimization of a residual imbalanced force after constructing a sequence of approximate solutions. Incremental solution methods can be divided into two classes:

II-1. Purely Incremental Method

Also called predictor-only method, in which the procedure used to get equilibrium path is by extrapolation. This method is the earliest nonlinear solution method. Its basic procedure is to divide the total load into a number of small load increments. In each load step, the stiffness of a structure that is determined from the last known geometry, is used to predict the displacement increment by solving the equilibrium equation relating the tangent stiffness matrix and the load increment. Once the displacement increment is obtained, the coordinates and the stiffness matrix of the structure are updated, and then the process is repeated until the desired load level is reached, [TURNER et al 1964]. The disadvantage of this method, is that the balance is not corrected, which may make the solution greatly deviated from the true equilibrium path due to accumulation of errors. The only method to minimize this error is by using a smaller load step. This could led to a higher numerical cost. More importantly, as illustrated in *Fig. VI.1*, the pure incremental method usually over-estimates the ultimate capacity of a structure, which is unsafe and undesirable in practical design.

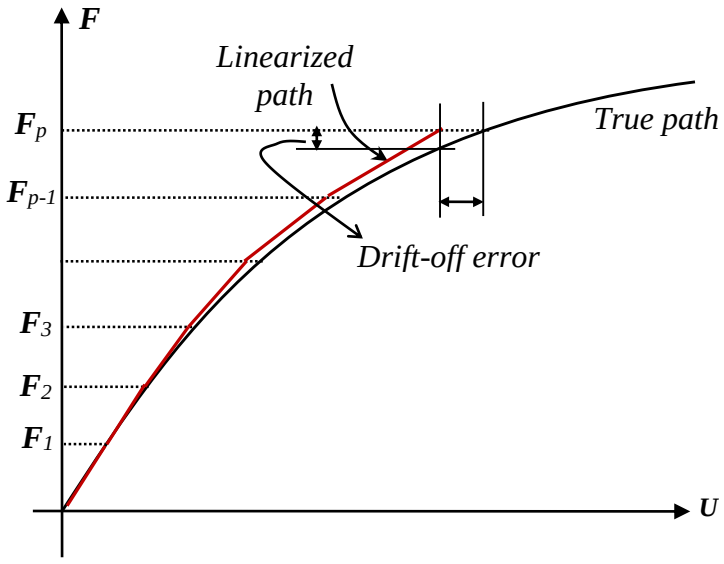

***Fig. VI.1*. Purely incremental method**

II-2. Incremental-Iterative Methods

Also called predictor-corrector methods. Unlike the pure incremental method, in which, no equilibrium check is performed, a predictor step is followed by a corrective iterations step. Its purpose is to eliminate or reduce the drift-off error also called "residual forces". The residual forces are the differences between the internal forces due existing internal strains, and the externally applied loads. By minimising the residual unbalanced forces, the solution is more accurate, and the computational time is reduced when compared to the pure incremental method.

The incremental-iterative methods consist of two parts: the increment part and the iteration part. The increment part will be discussed in the following sections. In this section, the iteration part is treated. The iteration part, is based on the minimization of the out of balance residue by the use of an iterative process for each load increment. Once convergence is achieved, the next solution step is applied. The correction of balance i.e. minimization of a residue, can be done in many iterative methods. They differ from each other mainly by the nature of the matrix used for the correction. These methods include:

II-2.1. Newton-Raphson Method

It requires the computation of the tangent stiffness matrix at every iteration, and hence, the convergence is fast, but the computer time required for each iteration is extensive. This method is well suited for analysing highly nonlinear problems, *Fig. VI.2*.

II.2.2. Modified Newton-Raphson Method

The stiffness matrix calculated at the beginning of each increment is constant for all iterations until convergence, [ODEN 1969; GERADIN et al 1980]. This leads to a significant gain in computation time, *Fig. VI.3*. However, this method needs more iterations to achieve convergence

II.2.3. Secant Method

This method uses the secant stiffness matrix within each increment to correct the balance, *Fig. VI.4*. The numerical implementation is easy but the convergence is slow.

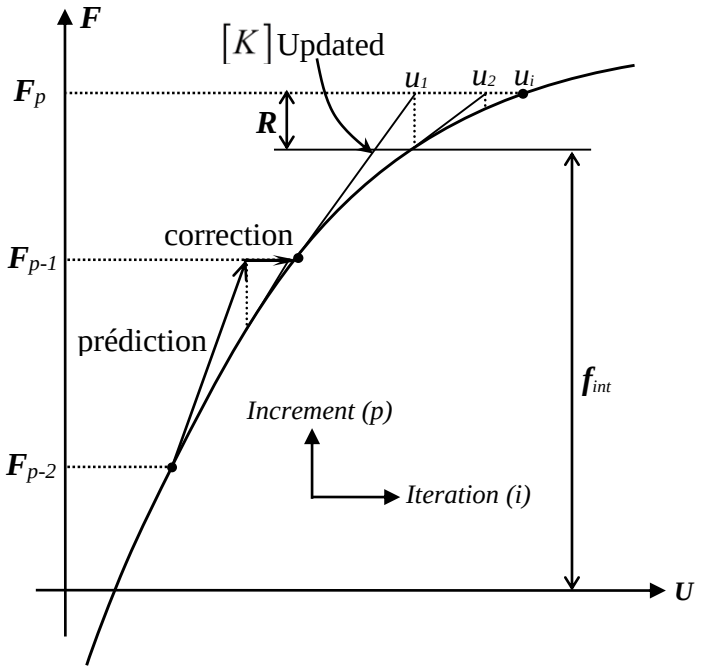

Fig. VI.2. **Newton-Raphson method**

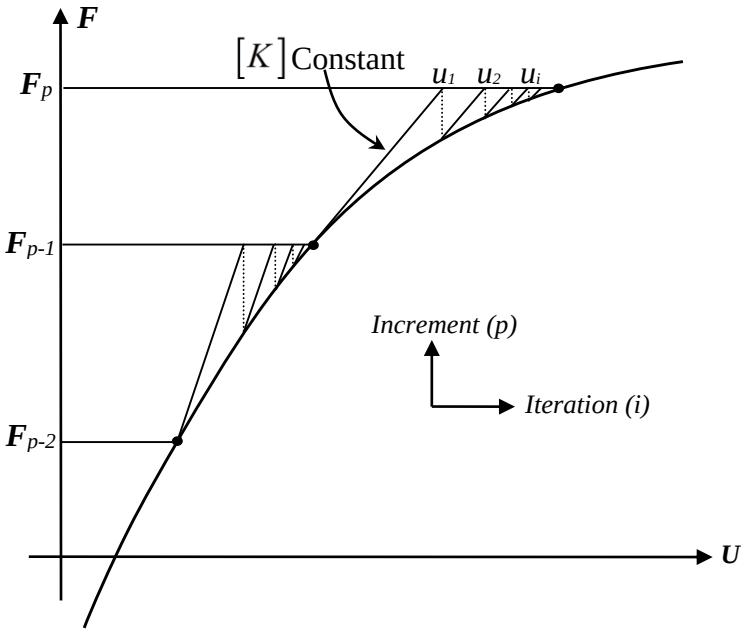

Fig. VI.3. **Modified Newton-Raphson method**

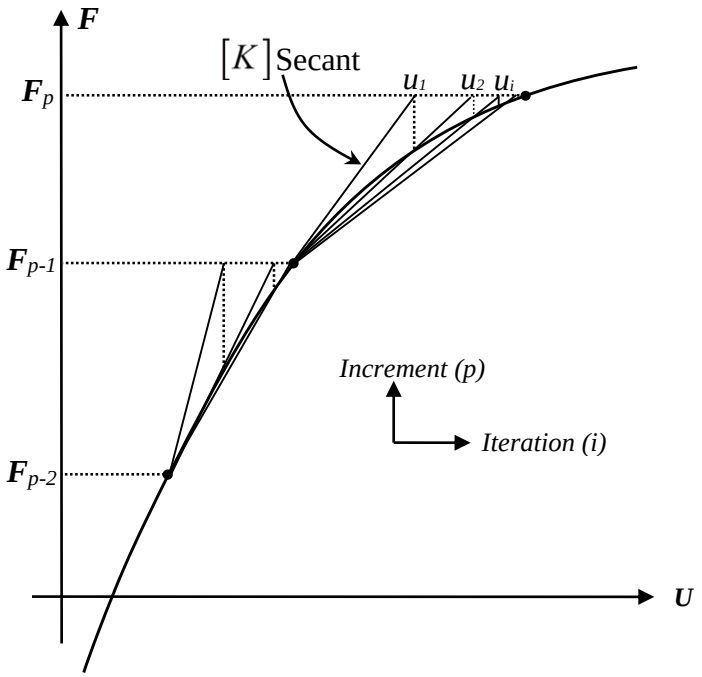

***Fig. VI.4*. Secant method**

III- INCREMENTAL-ITERATIVE PROCEDURE

An incremental iterative method has four essential aspects:

- Parameterization: the solution path is parameterized using a general scalar equation or an auxiliary surface. The aim is to find its intersection with the equation of equilibrium;
- Prediction: During the prediction phase, a linear estimation for the next point on the equilibrium path is established from a known converged solution on the equilibrium path;
- Corrector: Newton-Raphson iterations are employed during the correction phase to find a new point on the equilibrium curve;
- Convergence criterion.

III-1. Prediction

In the predictor phase, informations determined from the point previously computed (the last known geometry) are used to compute a suitable starting value for the corrector phase. In case of the updated Lagrangian formulation, it is a linear estimation of the displacement increment.

Considering an external forces load increment *{ΔP}*, the corresponding elastic solution is given by:

$$\{\Delta U\} = [K]^{-1}\{\Delta P\} \qquad [VI\text{-}1]$$

For each finite element, this solution corresponds to a strain increment such as:

$\{\Delta\varepsilon\}=[B]\ \{\Delta u\}$ *[VI-2]*

By assembling the elementary vectors, we define an equivalent nodal force vector $\{\Delta Q\}$ corresponds to the stress state calculated from the constitutive laws.

Thus, the residue is defined by:

$\{R\}=\{\Delta P\}-\{\Delta Q\}$ *[VI-3]*

If the residual is zero, this corresponds to a linear load increment, elsewhere, we must iterate seeking for a new solution of the equation $\{\Delta U\}=[K]^{-1}\{\Delta P\}$, till the residue is sufficiently close to zero. This is the purpose of the correction phase.

III-2. Correction of Equilibrium

Newton-Raphson method is based on writing, at each iteration, the residue around the preceding iteration:

$$\left\{R^{(i+1)}\right\}=\left\{R^{(i)}\right\}+\left[K^{(i)}\right]\left\{\Delta U^{(i)}\right\} \qquad \textit{[VI-4]}$$

Where: $\left\{\Delta U^{(i)}\right\}=\left\{U^{(i+1)}\right\}-\left\{U^{(i)}\right\}$ presents the correction applied to the solution at the current iteration. The correction is then, found by minimising the residue till it falls under a specified value determined by the convergence criterion. This is thru solving the following system of linear equations:

$$\left\{R^{(i)}\right\}+\left[K^{(i)}\right]\cdot\left\{\Delta U^{(i)}\right\}=\{0\} \qquad \textit{[VI-5]}$$

$\left[K^{(i)}\right]$: is the considered stiffness matrix.

In the conventional Newton-Raphson method, the tangent stiffness matrix is reformed ‘updated’ at every iteration, while for the modified Newton-Raphson method, the tangent stiffness matrix is only formed in the first iteration, and is kept constant in the subsequent iterations of each load increment. It may then be advantageous sometimes to replace the Newton-Raphson method by one of its variants, the “Modified Newton-Raphson” or the “Secant Newton-Raphson”.

The iterative process stops when satisfies the convergence criterion, which is chosen based on residual forces, or other variables (displacement, energy, strain...).

III-3. Parametrization

The incremental method is based on considering the known equilibrium configuration $C_{(t)}$ defined at time (t), and seek for the unknown configuration $C_{(t+\Delta t)}$ which is in equilibrium with the external applied loads at time ($t+\Delta t$). A proportional loading with a load factor λ is assumed. Thus, the discrete equilibrium equation is $\{Q(\{q\})\} = \{P_{ext}(\{q\}, \lambda)\}$, where the internal forces $\{Q\}$ are a function of the displacements $\{q\}$, and $\{P_{ext}\}$ is a function of $\{q\}$ and λ.

If the external and internal forces are not in equilibrium in any deformed configuration, a residual vector remains. The equation governing the nonlinear equilibrium of a structure is discretized by finite elements to the following form:

$$R(\{q\}, \lambda) = \{P_{ext}(\{q\}, \lambda)\} - \{Q(\{q\})\} = 0 \qquad \textit{[VI-6]}$$

In case, when external forces are dependent on the deformed shape of a structure (exp: hydrostatic load), the contribution of the follower forces stiffness matrix is essential. In the other case, when external forces do not depend on the deformation of the structure, follower forces stiffness matrix is zero (the case of our study), *Eq. [VI-6]* is written:

$$R(\{q\}, \lambda) = \lambda\{P_{ext}\} - \{Q(\{q\})\} = 0 \qquad \textit{[VI-7]}$$

$\{P_{ext}\}$: is the fixed external loading vector;

λ : loading level parameter that multiplies $\{P_{ext}\}$;

$\{q\}$: nodal displacement vector;

$Q(\{q\})$: internal force vector;

$\lambda\{P_{ext}\}$: the applied load level.

The iterative Newton-Raphson procedure, constructs a sequence of approximations of the equilibrium configuration trying to find a solution that satisfies the *Eq. [VI-6]*.

At each incremental step, a series of iterations is performed until convergence is achieved.

We denote here, the increment by the subscript ***p***, and the iteration by the superscript (*i)*. The incremental-iterative procedure is given by:

$$\left[K_p^{(i)}\right]\left\{\Delta q_p^{(i+1)}\right\} = \Delta\lambda_p^{(i+1)}\{p_{ext}\} + \left\{R_p^{(i)}\right\} \qquad \textit{[VI-8]}$$

Where: $\left\{R_p^{(i)}\right\} = \left\{R_p^{(i)}\left(\left\{q_p^{(i)}\right\}, \lambda_p^{(i)}\right)\right\}$, and $\left[K_p^{(i)}\right]$ is the tangent stiffness matrix.

The displacements and load factor, are computed through additive contributions from each iteration, i.e.

$$\{q_p^{(i+1)}\} = \{q_p^{(i)}\} + \{\Delta q_p^{(i+1)}\} \qquad \textit{[VI-9]}$$

$$\lambda_p^{(i+1)} = \lambda_p^{(i)} + \Delta\lambda_p^{(i+1)} \qquad \textit{[VI-10]}$$

In the (i^{th}) iteration of the $\boldsymbol{p}^{th}$ increment, the load factor is incremented by $\Delta\lambda_p^{(i+1)}$, and the resulting displacement increment $\{\Delta q_p^{(i+1)}\}$ is found. Then, the total displacement and total load factor are updated according to *Eq. [VI-9]* and *Eq. [VI-10]* respectively. The residual in *Eq. [VI-7]* is given by:

$$\{R_p^{(i)}\} = \lambda_p^{(i)}\{p_{ext}\} - \{Q_p^{(i)}(q_p^{(i)})\} \qquad \textit{[VI-11]}$$

The displacement vector $\{q\}$ contains (*n)* unknown degrees of freedom. Thus, the total number of unknowns is (*n+1*): *n* degrees of freedom $\{q\}$, and a load factor λ. Therefore, in addition to the *n* equilibrium equations of *Eq. [VI-7]*, a scalar constraint equation called the "control" or the "parameterization" equation is required. In general, it has the following form:

$$f(\{q\},\lambda) = C - \overline{C} = 0 \qquad \textit{[VI-12]}$$

This equation is used to set the incremental parameter to be imposed.

III-4. Convergence Criterion

The iterative processes will continues as long as residual forces exists, until they become negligible. A convergence criterion is therefore necessary and should be pre-determined to check the equilibrium and terminate the iterations process. Thus, the equilibrium is satisfied when the norm of the residual is sufficiently small compared to a given tolerance *ε*.

• Residual force Criterion:

$$\frac{\|R_p^1\|}{\|R_p^i\|} \le \varepsilon_r \qquad \textit{[VI-13]}$$

$\|R_p^1\|, \|R_p^i\|$ are respectively the residue at the iteration (1), and the residue at the iteration (*i*).

• Displacement criterion:

$$\frac{\|\Delta q_p^{(i)}\|}{\|\, q_p^{(i)} - q_{p-1}\|} \le \varepsilon_d \qquad \textit{[VI-14]}$$

$\left\{\Delta q_p^{(i)}\right\}$: incremental displacement at the considered iteration (*i*)

$\left\{q_p^{(i)}\right\}$: the current displacement (solution to be checked).

$\left\{q_{p-1}\right\}$: the last converged solution (at increment *p-1*).

• Energy Criterion

The above two criteria could be combined to give an energy based criteria:

The norm to be used for the residue or the displacement criteria can be selected from any one of the classic norms (Absolute, Euclidean, or maximum).

Also, a maximum number of iterations is usually set. If the convergence criterion is not satisfied after this number, the process stops, and the solution is considered as diverged.

IV- PATH FOLLOWING METHODS

The main purpose of path following techniques, is to draw the equilibrium path of a nonlinear structural analysis in the framework of a Load-displacement response diagram.

Let us consider an elastic structural system under a system of applied loading. The nonlinear response is defined by the couple ($\{q\}$, λ). Where $\{q\}$ presents the nodal displacements vector, and λ represents the load parameter intensity introduced by external forces.

The total potential energy of such a system is denoted by:

$$E = E\left(\{q\}, \lambda\right) \qquad \textit{[VI-15]}$$

The equilibrium of this structure is then determined from the stationary of function *[VI-15]* with respect to $\{q\}$. It could be expressed by the following equations:

$$R(q, \lambda) = \partial E(q, \lambda)/\partial q = 0 \qquad \textit{[VI-16]}$$

Where: *R*, presents the residual force vector.

Eq. [VI-6] represents *N*+1 relations between *N* degrees of freedoms and λ. The equilibrium paths of the structure is described by $\{q\}$ and λ together. Also, the tangent stiffness matrix of the considered structure is:

$$K^T = \frac{\partial R(q,\lambda)}{\partial q} = \frac{\partial^2 E(q,\lambda)}{\partial q^2} \qquad \textit{[VI-17]}$$

IV-1. Critical Points

Along the load-displacement response curve (the *equilibrium path)* of certain structures, appears several special states of loss of stability called *critical points*. We could state three different types of critical points. They are related to the concept of limit point, turning point, and bifurcation point.

IV-1.1. Limit Point

A limit point, is a point at which the tangent to the equilibrium curve is horizontal, i.e. parallel to the displacement axis. In the sense that the tangent stiffness matrix is zero.

Moreover, it must satisfies the condition that the equilibrium curve at this point is unique.

The elastic behaviour of a structure after passing a limit point, is associated with loss of stability called snapping. No static equilibrium exists nearby, and therefore, the structure dynamically "*snaps through"* into the next post-critical equilibrium position, as shown in *Fig. VI.5*.

* Limit points are of special importance in the Load control path following technique, see § *IV-2.1*.

IV-1.2. Turning Point

At turning point, also called displacement limit point, the tangent to the equilibrium curve is vertical, i.e. parallel to the load axis.

The elastic behaviour of a structure after passing a turning point will dynamically "*snaps back"* into the next post-critical equilibrium position, as shown in *Fig. VI.6*.

* Turning points are of special importance in the displacement control method. Besides, these points can affect the performance of the arc-length method, see § *IV-2.2,* and § *IV-2.3*.

IV-1.3. Bifurcation Point

A bifurcation point is a point in which multiple equilibrium curves intersect, *Fig. VI.7*. Such an equilibrium state is called buckling.

In this point, the equilibrium loses its uniqueness, because the relation between the loading and the associated displacement is not unique.

* These points are of special importance to the arc-length path following method, see § *IV-2.3*.

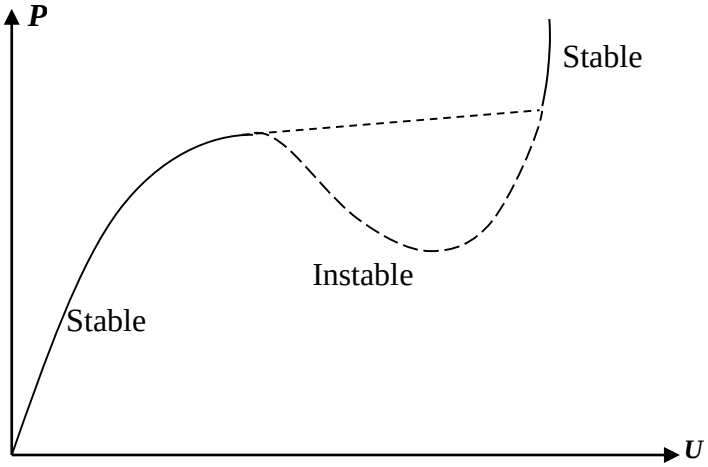

***Fig. VI.5*. Load control method in vicinity of limit point**

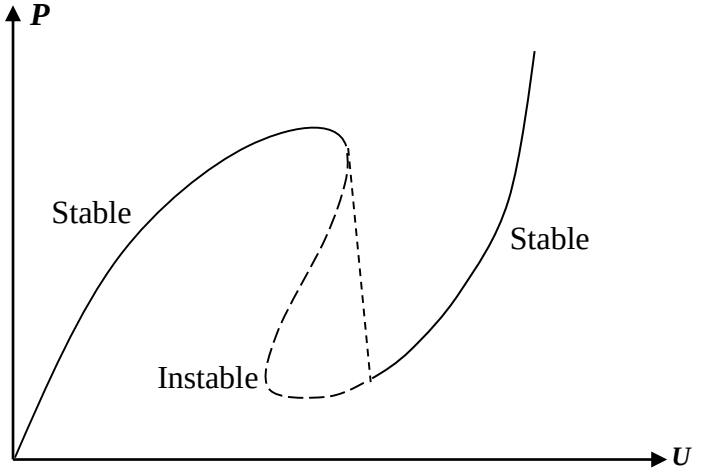

***Fig. VI.6*. Displacement control method in vicinity of turning point**

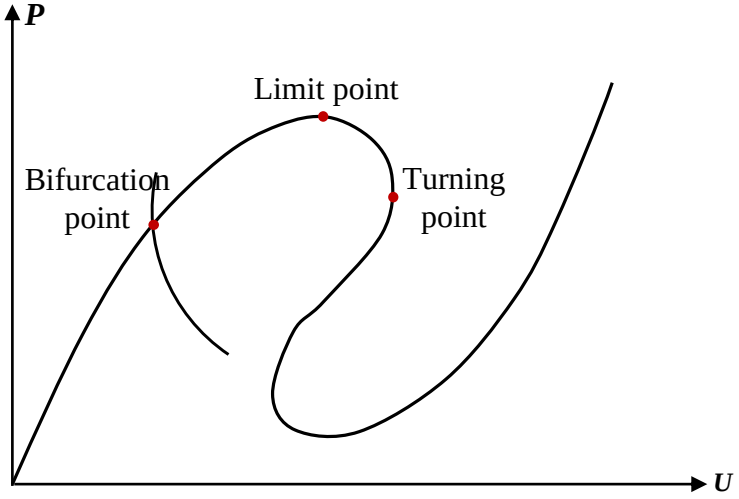

***Fig. VI.7*. Arc-length method "pass all critical points"**

IV-2. Control Function

In general, to specify a particular point on an equilibrium curve, we must add an extra scalar equation to the equilibrium equations of *Eq. [VI-7]*, called the control function. It aims to set the imposed incremental parameter. [RIKS 1972] proposed a new solution procedure based on that concept for overcoming limit points. He added to the equations of equilibrium an additional constraint equation fixing the length of the incremental load step. The applied load level becomes now an additional variable.

If this additional equation is denoted by $f(\{q\},\lambda)=0$, we can find specific equilibrium solutions by solving:

$$\begin{cases} R(\{q_p^{(i)}\},\lambda_p^{(i)})=0 \\ f(\{q_p^{(i)}\},\lambda_p^{(i)})=0 \end{cases} \qquad \textit{[VI-18]}$$

This set of equations is called the augmented system.

The constraint equation $f(\{q\},\lambda)$, also has the following form:

$$a_p^{(i)}\cdot\Delta q_p^{(i)}+b_p^{(i)}\cdot\Delta\lambda_p^{(i)}=c_p^{(i)} \qquad \textit{[VI-19]}$$

Hence, the governing system of nonlinear equations to be solved at the (i^{th}) iteration of the $\boldsymbol{p}^{th}$ incremental step is:

$$\begin{cases} \left[K_p^{T(i)}\right]\cdot\left\{\Delta q_p^{(i)}\right\}=\Delta\lambda_p^{(i)}\cdot\left\{P_{ext}\right\}+\left\{R_p^{(i)}\right\} \\ f\left(\left\{q_{p+1}\right\},\lambda_{p+1}\right)=0 \end{cases} \qquad \textit{[VI-20]}$$

The couple incremental solution ($\{\Delta q\}$, $\Delta\lambda$), is obtained after solving the above system.

Depending on the expression of the control function $f(\{q\},\lambda)$, there exist several following path control methods. Based on the bibliographic research we have done during this work, we could state seven methods as follows:

- Load control method;
- Displacement control method;
- Arc-length control method;
- Work control method;
- Generalised Displacement control method;
- Minimum Residual Displacement method;
- Orthogonal Residual Displacement method.

IV-2.1. Load Control Method

For Load control technic, the parameterization function is expressed by:

$$f\left(\{q\},\lambda\right)=\lambda-\bar{\lambda} \qquad \textit{[VI-21]}$$

With $\bar{\lambda}$ is a constant indicating the charge level.

This method is the most simple, and it has been the most popular for solving nonlinear system of equations. This can be schematically represented by a constant step load $\Delta\lambda$, as in *Fig. VI.8*. The description and convergence of this algorithm are detailed by [MONDKAR & POWELL 1978; RANNACHER 1991].

This type of algorithm breaks down in vicinity of limit points, where the tangent stiffness matrix [K^T] becomes ill-conditioned or even singular (the structure loses its load carrying capacity). Under these conditions, the algebraic system of equations becomes harder to solve using Newton-Raphson procedure. However, the solution could jumps to a distant stable configuration making it harder for a numerical method to converge, *Fig. VI.5*.

[BERGAN 1978] proposed to suppress equilibrium iterations until the limit point is passed. However, the obtained path drift from equilibrium path. [WRIGHT & GAYLORD 1968; MULLER 2007; MULLER 2008] Proposed adding a fictitious spring to stabilize the tangent stiffness matrix in the vicinity of limit points.

IV-2.2. Displacement Control Method

For the displacement control technic, unlike the load control method previously described, a constraint equation for displacement is imposed.

The associated constraint function f is defined by:

$$f\left(\{q\},\lambda\right)=\{q\}_k-\bar{q} \qquad \textit{[VI-22]}$$

Schematically, this is shown in *Fig. VI.9*.

This method does not exhibit any difficulty in passing snap-through limit points, but fails to converge beyond turning points.

[ARGYRIS 1965-c] proposed the use of the characteristic displacement increment as the control parameter. The concept of this method is to impose the displacement of a particular node (*k*) and then solve the problem of equilibrium. The disadvantage then, is related to the selection of the appropriate displacement variable. Displacement control methods assume that there exists at least

one degree of freedom with a monotonic evolution. However, such a degree of freedom may not exist, and even if it exists, selection of this displacement may not be obvious in large structures.

[MAEWAL & NACHBAR 1977] note the necessity to change the prescribed displacement variable following slow convergence or divergence of the iterative solution procedure.

Another drawback is that the augmented system of equations become non symmetric. Some modified approaches are proposed in order to preserve symmetry of the stiffness matrix [ZIENKIEWICZ 1971-b; YAMADA et al 1974] However, these approaches involved complicated procedures which become inconvenient for general use.

[BATOZ & DHATT 1979] defined a simpler technique which preserves symmetry of the stiffness matrix when using a displacement control algorithm.

Different variations of this method are presented by many authors: [NEMAT-NASSER & SHAROFF 1973; HAISLER & STRICKLIN 1977; POWELL & SIMONS 1981; THURSTON et al 1986; FUJII et al 1992-*a*, 1992-*b*; LORENTZ & BADEL 2004; ZHENG et al 2005].

IV-2.3. Arc-Length Control Method

In presence of limit points and turning points, control methods previously described fail to follow the solution curve. Hence, in order to trace the equilibrium path beyond critical points, a more general incremental control strategy is needed.

The arc-length method, has been considered to be the most effective control technique available for passing limit points. This method was initially proposed by [WEMPNER 1971] and [RIKS 1972, 1979] by introducing the constraint equation technique, in which, instead of keeping the load (or the displacement) fixed during step increment, a combined displacement-load increment called the "arc length *ΔL"* is controlled during equilibrium iterations. Both displacement $\{\Delta q\}$ and load $\Delta\lambda$ increments are controlled simultaneously (they are modified during iterations), *Fig. VI.10*.

The associated constraint function *f* is defined by:

$$f\left(\{q\},\lambda\right)=\langle\Delta q\rangle\{\Delta q\}+\ b\cdot\Delta\lambda^{2}\cdot\langle P_{ext}\rangle\{P_{ext}\}-\overline{\Delta L}^{2}=0 \qquad \textit{[VI-23]}$$

$\overline{\Delta L}$: the imposed Arc-length;

$\Delta\lambda$: incremental load parameter;

$\{\Delta q\}$: incremental movement;

b : is a scaling parameter between load and displacement.

Arc-length methods are enhanced to be suitable to a wide range of problems, mainly by [RAMM 1981; CRISFIELD 1981, 1983].

The arc length control method, is superior to both load control and displacement control methods in that it can pass snap-through and snap-back behaviour. However, Arc-length method results in unit inconsistency due the dot product of displacement in the constraint equation, because of the inclusion of both translational and rotational displacements.

Different forms and studies of the arc-length method have been proposed by many authors involving different shapes of the constraint equation [PADOVAN & TOVICHAKCHAIKUL 1982; PARK 1982; GIERLINSKI & SMITH 1985; ERIKSSON & KOUHIA 1995; QI & TIANQI 1995; DUTTA & WHITE 1997]. Further developments are presented in: [PAPADRAKAKIS 1981; RIKS 1984; BELUNI & CHULYA 1987; FELIPPA 1987; WRIGGERS et al 1988; CLARKE & HANCOCK 1990; WRIGGERS & SIMO 1990; FAFARD & MASSICOTTE 1993; CARRERA 1994; ZHOU & MURRAY 1994; ZHAO & TIANQI 1995; KRISHNAMOORTHY et al 1996; CRISFIELD et al 1997; HELLWEG & CRISFIELD 1998; NETO & FENG 1999; JORABCHI & SURESH 2011; LEE et al 2014].

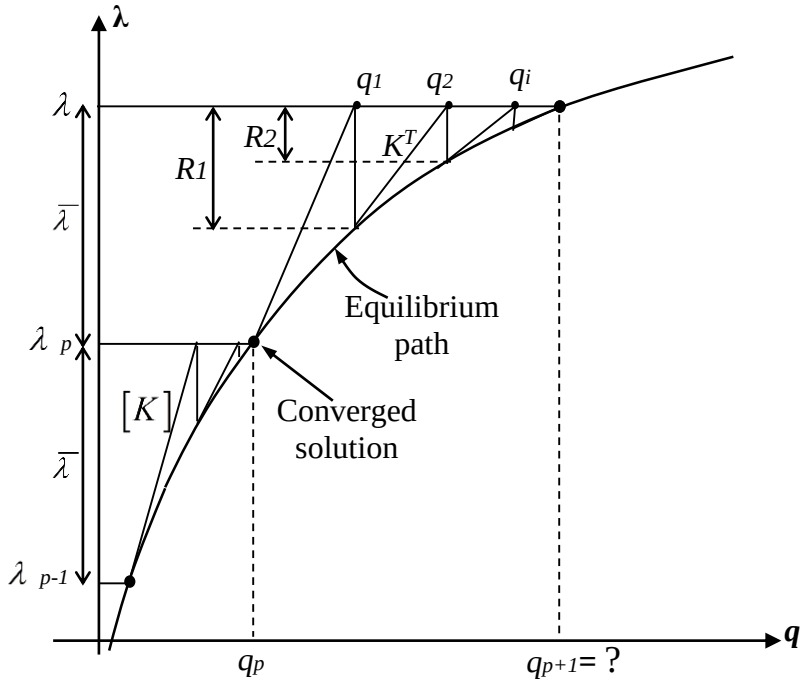

***Fig. VI.8*. Load control method**

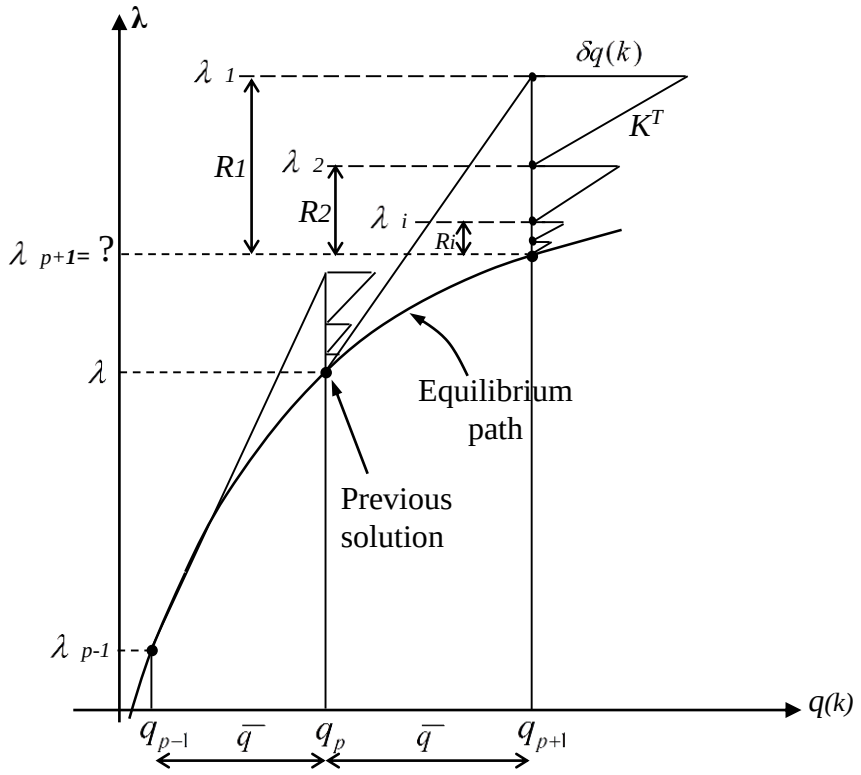

Fig. VI.9. **Displacement control method**

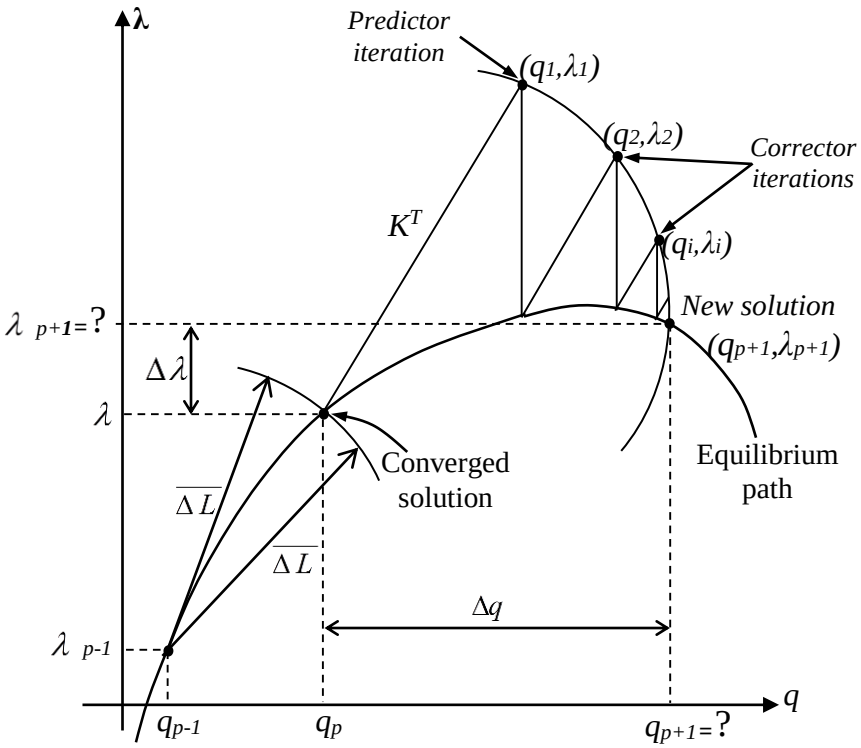

Fig. VI.10. **Arc-length control method**

IV-2.4. Constant Work Control Method

The constant work method, has the same basic idea of imposing a constraint equation to guide the incremental load, it iterates neither at a constant load nor constant displacement. This method uses a constant work increment δW, kept constant through the iterations of an incremental step (the increment of internal energy during iterations equals the amount of work done by the external loading). The concept of constant work control has been reported by many researchers including [KARAMANLIDIS et al 1981; POWELL & SIMONS 1981; BATHE & DVORKIN 1983-b; YANG & MCGUIRE 1984, 1985; CHEN & BLANDFORD 1993; LIN et al 1993; KOUHIA 2008].

$$f\left(\{q\},\lambda\right)=\Delta\lambda\left\langle P_{ext}\right\rangle\cdot\{\Delta q\}=\Delta\overline{W} \qquad \textit{[VI-24]}$$

Where: $\Delta\overline{W}$ is the prescribed work increment.

Imposing $\delta W=\delta\lambda\left\langle p_{ext}\right\rangle\cdot\{\delta q\}=0$ yields:

$$\delta\lambda_p^{(i)}=-\frac{\left\langle P_{ext}\right\rangle\left\{\delta q_p^{R(i)}\right\}}{\left\langle P_{ext}\right\rangle\left\{\delta q_p^{T(i)}\right\}} \qquad \textit{[VI-25]}$$

For the expressions of $\left\{\delta q_p^{R(i)}\right\}$ and $\left\{\delta q_p^{T(i)}\right\}$, see §*VI*.

The convergence rate of the constant work method was reported to be slow compared to that of the arc-length method. Moreover, this method fails at turning points over multiple degrees of freedom. In this case, a negative work is generated by reducing the load increment and decreasing the displacement.

IV-2.5. Generalized Displacement Control Method

To overcome numerical instability near limit points, [YANG & SHIEH 1990] proposed the generalized displacement control method. In the original formulation, the constraint equation is presented in the following form:

$$a_p^{(i)}\cdot\Delta q_p^{(i)}+b_p^{(i)}\cdot\Delta\lambda_p^{(i)}=c_p^{(i)} \qquad \textit{[VI-26]}$$

[YANG & SHIEH 1990] specified: $a_{p+1}^{(i)}=\Delta\lambda_{p+1}^{(1)}\left\{\Delta q_p^{(1)}\right\}_f$, and $b_{p+1}^{(i)}=0$

$$\begin{cases} c_{p+1}^{(i)}=\left(\Delta\lambda_1^{(1)}\right)^2\cdot\left\langle\Delta q_1^{(1)}\right\rangle_f\left\{\Delta q_1^{(1)}\right\}_f\ ; & for\ i=1 \\ c_{p+1}^{(i)}=0\ ; & for\ i\geq 2 \end{cases} \qquad \textit{[VI-27]}$$

The generalized displacement control algorithm is very successful at capturing complex nonlinear behaviour at both load and displacement limit points.

[CARDOSO & FONSECA 2007; LEON et al 2011] addressed that the generalized displacement method could be expressed as an orthogonal Arc-length. Further developments are presented in [YANG et al 2007; THAI & KIM 2009; LEON et al 2014].

IV-2.6. Minimum Residual Displacement Control Method

The basic idea of this method originally proposed by [CHAN 1988], is instead of using geometric or energy restriction, it seek to directly eliminate the residual displacement due to unbalanced forces in each iteration. The method controls the load steps by using the load factor, which follows the shortest path to obtain the solution point.

The iterative residual displacement to minimise is:

$$\{d\} = \{\delta q_p^{(i)}\} = \{\delta q_p^{R(i)}\} + \delta\lambda_p^{(i)} \cdot \{\delta q_p^{T(i)}\} \qquad \textit{[VI-28]}$$

[CHAN 1988] proposed that the condition of least square could be expressed as:

$$\frac{\partial\left(\langle \delta q_p^{(i)} \rangle \{\delta q_p^{(i)}\}\right)}{\partial \delta\lambda_p^{(i)}} = 0 \qquad \textit{[VI-29]}$$

$$\text{Then: } \delta\lambda_p^{(i)} = \frac{\langle \delta q_p^{T(i)} \rangle \{\delta q_p^{R(i)}\}}{\langle \delta q_p^{T(i)} \rangle \{\delta q_p^{T(i)}\}} = 0 \qquad \textit{[VI-30]}$$

The graphical representation of the procedure is demonstrated in *Fig. VI.11*. It can be seen that this constraint condition enforces the iteration path to follow the shortest path to arrive at the equilibrium point, which is a path normal to the load-deformation curve. In addition, the expressions for this method are simple, and it does not involve the solution of quadratic equations as in the arc-length method, see § *VI.*

IV-2.7. Orthogonal Residual Control Method

[KRENK 1995] presented the orthogonal residual method. In this method, the load is adjusted in such a way that the residual force is orthogonal to the current displacement increment. Subsequently, the magnitude of the displacement increment is optimal when the orthogonality condition is satisfied. Moreover, this approach does not need the block elimination scheme [KOUHIA 2008], see § *VI.*

The orthogonality condition is expressed as:

$$f(\{q\},\lambda)=\left\langle \Delta q_p^i \right\rangle \{R_p^i\}=0 \qquad \textit{[VI-31]}$$

However, the original formulation can break down at displacement limit points, i.e. at snap-back points, especially when the load vector contains a single point load.

Further studies are presented in: [KRENK & HEDEDAL 1995; POULSEN & DAMKILDE 1996].

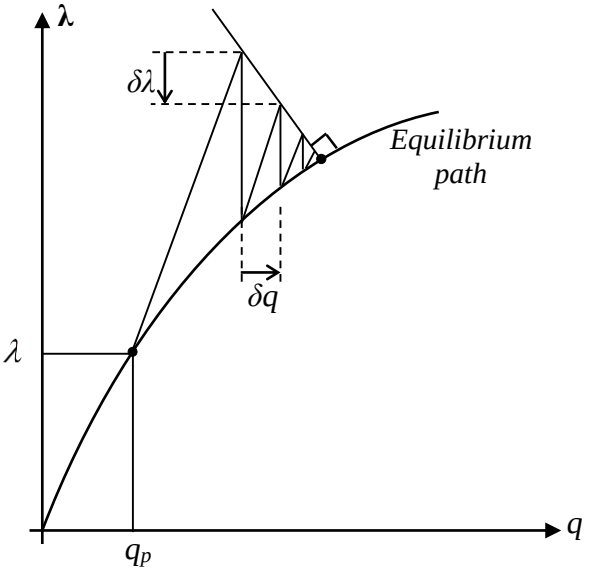

Fig. VI.11. **Minimum residual method**

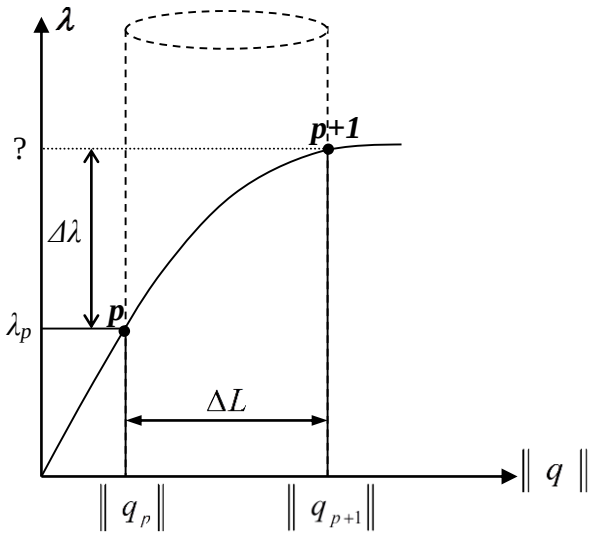

Fig. VI.12. **Cylindrical Arc-Length method**

V- THE LOAD CONTROL METHOD

The Load Control method consists of incrementing the entire applied external force $\{P_{ext}\}$ into load levels using the load multiplier λ. for each load level, a displacement is calculated. The standard load control approach is based on an equilibrium equation defined as the difference between the internal force $\{Q\}$ and a prescribed external load $\lambda\{p_{ext}\}$, such that:

$$R(\{q\})=\lambda\{P_{ext}\}-Q\{q\})=0 \qquad \textit{[VI-32]}$$

Let us consider a converged solution at the increment ***p***:

V-1.1. Parameterization

A load increment is imposed at the increment ($p+1$) as:

$$\begin{cases} f\left(\{q_{p+1}\},\lambda_{p+1}\right)=\lambda_{p+1}-\bar{\lambda} \\ \lambda_{p+1}=\bar{\lambda} \end{cases} \qquad \textit{[VI-33]}$$

$\bar{\lambda}$: is the prescribed load step.

V-1.2. Prediction

The predictor step corresponds to the first iteration (i=1).

At the first iteration (i) = 1. After constructing the tangent stiffness matrix $\left[K_{p+1}^{T(1)}\right]$, we solve:

$$\left[K_{p+1}^{T(1)}\right]\cdot\left\{\Delta q_{p+1}^{(1)}\right\}=\left(\overline{\lambda}-\lambda_p\right)\cdot\{P_{ext}\} \qquad \textit{[VI-34]}$$

The predictor solution is:

$$\begin{cases}\left\{q_{p+1}^{(1)}\right\}=\left\{q_p\right\}+\left\{\Delta q_{p+1}^{(1)}\right\}\\ \lambda_{p+1}^{(1)}=\overline{\lambda}\end{cases} \qquad \textit{[VI-35]}$$

V-1.3. Correction

- At an iteration (i) ≥ 2:

After updating the tangent stiffness matrix $\left[K_{p+1}^{T(i)}\right]$ (Newton-Raphson), the internal forces are calculated $\left\{Q_{p+1}^{i}\left(q_{p+1}^{(i-1)}\right)\right\}$. It depends on the formulation of the linear finite element.

Then the unbalanced residue is calculated as:

$$\left\{R_{p+1}^{(i)}\right\}=\overline{\lambda}\{P_{ext}\}-\left\{Q_{p+1}\right\} \qquad \textit{[VI-36]}$$

We solve the following equation for $\left\{\Delta q_{p+1}^{(i)}\right\}$:

$$\left[K_{p+1}^{T(i)}\right]\cdot\left\{\Delta q_{p+1}^{(i)}\right\}=\left\{R_{p+1}^{(i)}\right\} \qquad \textit{[VI-37]}$$

Thus, at the iteration (i) the solution is:

$$\begin{cases}q_{p+1}^{(i)}=\left\{q_{p+1}^{(i-1)}\right\}+\left\{\Delta q_{p+1}^{(i)}\right\}\\ \lambda_{p+1}^{(i)}=\overline{\lambda}\end{cases} \qquad \textit{[VI-38]}$$

This result, represented a first approximated solution. If the convergence criterion is not satisfied at this solution, we move to the next iteration till convergence is achieved, then we move to the next increment.

VI- THE ARC-LENGTH METHOD

VI-1.1. Parameterization

As we have seen, in this step, an additional constraint is added to complete the set of equations together with the equilibrium expression *Eq. [VI-7]*. Therefore, this step consists to define the function ***f*** so as to link the load and the displacement parameters via an incremental parameter. This incremental constraint is noted ΔL and called "Arc Length". So, ***f*** is explicitly defined by the following equation:

$$f(\{q\},\lambda) = \langle \Delta q \rangle \{\Delta q\} + \Delta\lambda^2 \cdot b \cdot \langle P_{ext} \rangle \{P_{ext}\} - \overline{\Delta L}^2 = 0 \qquad \textit{[VI-39]}$$

$\overline{\Delta L}$: the prescribed arc length.

$\Delta\lambda$: incremental load parameter.

$\{\Delta q\}$: incremental displacement.

b: is a scaling parameter, it determines the influence of load and displacement control in the behaviour of the arc-length method.

The arc-length method is then, aims to find the intersection of a given arc length $\overline{\Delta L}$ with the equilibrium equation, such that:

$$\{R(\overline{\Delta L})\} = \lambda(\overline{\Delta L}) \cdot \{P_{ext}\} - \{Q(\{q(\overline{\Delta L})\})\} = 0 \qquad \textit{[VI-40]}$$

The control function of the Arc-length method can take many forms depending on the author. Several forms are suggested to overcome algorithm's sensitivity to limit points and bifurcation points: [DE-BORST 1987; DUAN & MAY 1994; WEMPNER 1971; BERGAN 1980-b; RIKS 1979; RHEINBOLDT 1981; RAMM 1981; CRISFIELD 1983-b], which results with several variants of the arc-length method. For instance, we could mention:

1- *The Elliptical Arc-Length Method*

This method has the form of the most general constraint function, it is written as:

$$f(\{q\},\lambda) = \langle \Delta q \rangle \{\Delta q\} + \Delta\lambda^2 \cdot b \cdot \langle P_{ext} \rangle \{P_{ext}\} - \overline{\Delta L}^2 \qquad \textit{[VI-41]}$$

when $b > 0$ and $b \neq 1$, this equation represents an ellipsoid in three dimensional space. See also: [PARK 1982; BERGAN 1980-b; BELUNI & CHULYA 1987].

2- The Spherical Arc-Length Method

The spherical arc-length method consists of setting $b = 1$, the constraint function is written as:

$$f(\{q\},\lambda) = \langle \Delta q \rangle \{\Delta q\} + \Delta\lambda^2 \cdot \langle P_{ext} \rangle \{P_{ext}\} - \overline{\Delta L}^2 \qquad [VI\text{-}42]$$

This expression enforce the arc-length ΔL to be equal to the norm of the vector $(\{\Delta q\}, P_{ext})$.

3- The Cylindrical Arc-Length Method

In practice, for highly stiff structures, large forces are required to obtain small displacements. In this case, the term $\Delta\lambda^2 \cdot b \cdot \langle P_{ext} \rangle \{P_{ext}\}$ would tend to infinite if compared to the displacement term $\langle \Delta q \rangle \{\Delta q\}$. Therefore, the arc-length method would behave similarly to the load control and lose the ability to overcome limit points.

[CRISFIELD 1981] set the parameter *b* to be zero. This version performs well in capturing sharp turns at load limit points. Under these conditions, the stress function is:

$$f(\{q\},\lambda) = \langle \Delta q \rangle \{\Delta q\} - \overline{\Delta L}^2 \qquad [VI\text{-}43]$$

See: [DJEGHABA 1990] for further details.

This constraint equation represents a cylinder in three dimensional space, *Fig. VI.12*.

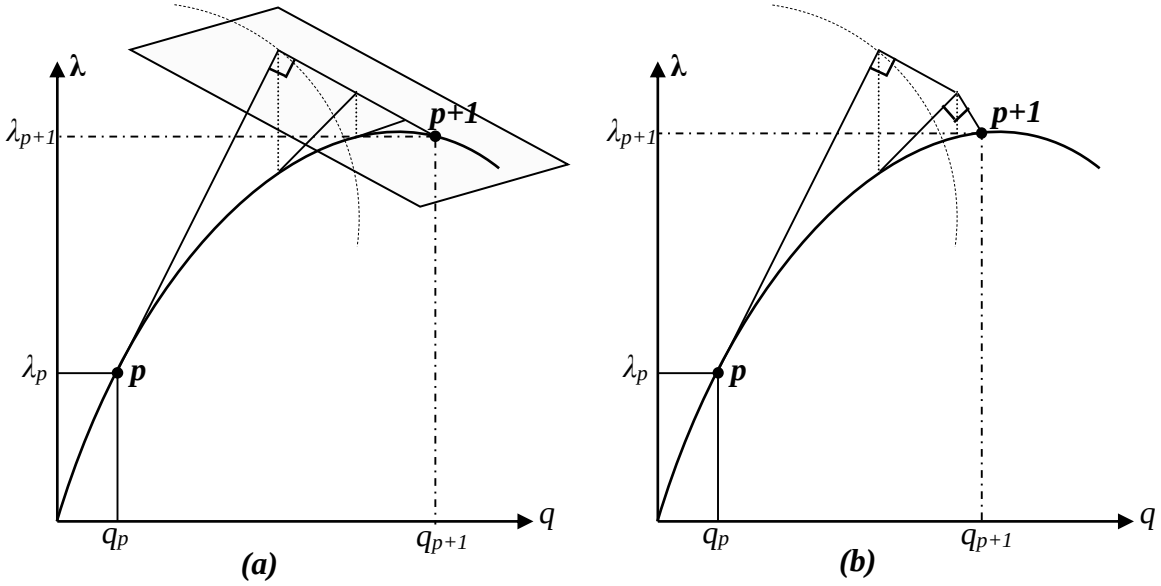

Fig. VI.13. **Linearized Arc-Length: *a.* Normal plane*; b.* Updated normal plane**

4- The Linearized Arc-Length Method

Linearized arc length method, has been introduced to overcome the problem of choosing the roots of the equation of spherical and cylindrical constraint. It was investigated by [WEMPNER 1971; RIKS 1972; RIKS 1979; CRISFIELD 1981; RAMM 1981; SCHWEIZERHOF & WRIGGERS 1986; FORDE & STIEMER 1987]. This family of methods has different variants. As example we could mention the normal plane, and the update normal plane methods, *Fig. VI.13*.

These methods are also referred to as orthogonal arc-length methods because, an orthogonality condition is imposed. The solution procedure is forced to follow a "hyperplane" that is normal to the initial or updated tangent $\{\overline{Z}_p\}$ at a distance *L* from the previous obtained solution.

$$\langle \overline{Z}_p \rangle \{Z^i_{p+1} - Z_p\} - L = 0 \qquad \textit{[VI-44]}$$

VI-1.2. Prediction

Let $(\{q_p\}, \lambda_p)$ be the previous converged solution at an increment ***p***.

At the increment ***p+1*** an arc length $\overline{\Delta L}$ is imposed such as:

$$\begin{cases} f(\{q_{p+1}\}, \lambda_{p+1}) = \langle \Delta q \rangle \{\Delta q\} + b\Delta\lambda^2 \langle p_{ext} \rangle \{p_{ext}\} - \overline{\Delta L}^2 = 0 \\ \overline{\Delta L}_{p+1} = \sqrt{\langle \Delta q \rangle \{\Delta q\} + b\Delta\lambda^2 \langle p_{ext} \rangle \{p_{ext}\}} \end{cases} \qquad \textit{[VI-45]}$$

In the following, the symbol (Δ) refers to incremental quantities while (δ) denotes iterative change.

The predictor step corresponds to the first iteration (*i*=1).

A suitable starting value for the corrector phase is using the following equation:

$$[K^{T(1)}_{p+1}](\{\delta q^{R(1)}_{p+1}\} + \Delta\lambda^{(1)}_{p+1}\{\Delta q^{(1)}_{p+1}\}) = \{R^{(1)}_{p+1}\} + \Delta\lambda^{(1)}_{p+1}\{P_{ext}\} \qquad \textit{[VI-46]}$$

for *i = 1*, we have: $\{R^{(1)}_{p+1}\} = 0$, and $\{\delta q^{R(1)}_{p+1}\} = 0$.

$$\{\Delta q_{p+1}\} = [K^T_{p+1}]^{-1}\{\Delta p_{ext}\} = \Delta\lambda_{p+1}[K^T_{p+1}]^{-1}\{p_{ext}\} = \Delta\lambda_{p+1}\{\delta q^T_{p+1}\} \qquad \textit{[VI-47]}$$

Where: $[K^T_{p+1}]$ is the tangent stiffness matrix at the beginning of the increment ***p+1***.

$\{\delta q^T_{p+1}\}$: the tangential solution.

$\{\delta q^T_{p+1}\}$, and $\{\delta q^R_{p+1}\}$ are defined as:

$$\begin{cases} \left[K_{p+1}^{T}\right]\left\{\delta q_{p+1}^{R}\right\} = \left\{R_{p+1}\right\} \\ \left[K_{p+1}^{T}\right]\left\{\delta q_{p+1}^{T}\right\} = \left\{P_{ext}\right\} \end{cases} \qquad \textit{[VI-48]}$$

Substituting *Eq. [VI-45]* into *Eq. [VI-47]*, and solving for $\Delta\lambda$, yields:

$$\Delta\lambda_{p+1}^{(1)} = \pm \frac{\overline{\Delta L}_{p+1}}{\sqrt{\left\langle \delta q^{T} \right\rangle \left\{\delta q^{T}\right\} + b\left\langle p_{ext} \right\rangle \left\{p_{ext}\right\}}} \qquad \textit{[VI-49]}$$

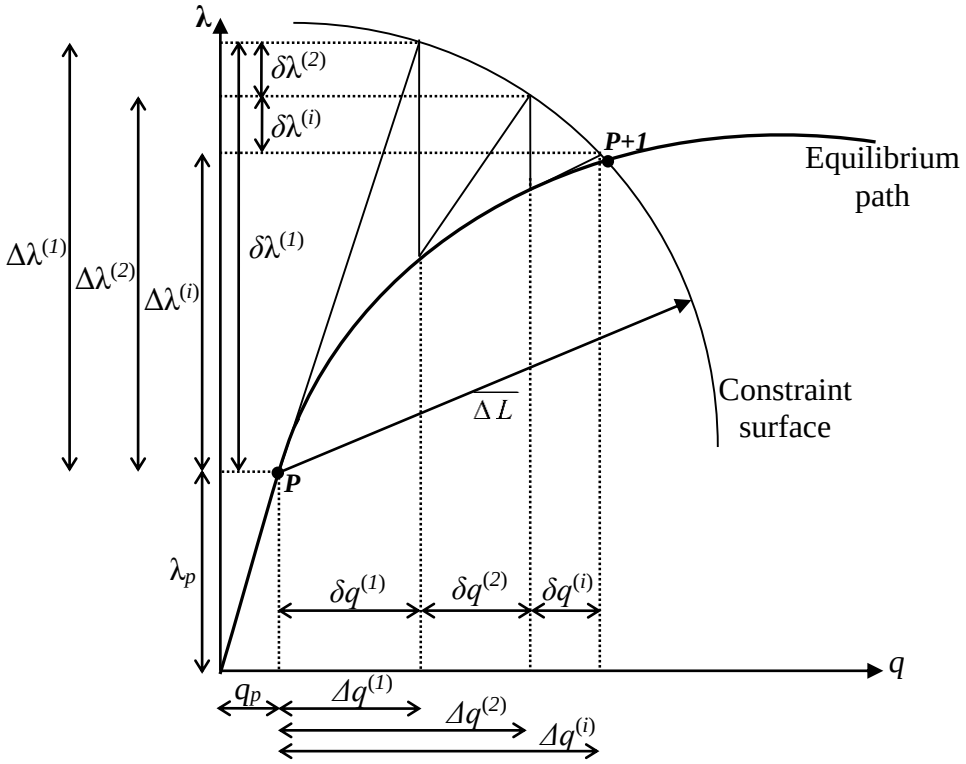

Fig. VI.14. **Arc-Length method**

Hence, two predictors with different signs are possible. The choice of the sign of the incremental load factor in the prediction phase of arc-length methods is crucial. If the wrong sign is predicted, the solution "doubles back" on the original load-deflection curve and the arc-length method fails to trace the complete path.

There exist several criterions to predict the direction of the equilibrium path (to decide if $\Delta\lambda^{(1)}_{p+1}$ is positive or negative), see [CRISFIELD 1982, 1986; KWOK et al 1985]. The most popular criterions are:

1- The Sign of the Current Tangent Stiffness Matrix Determinant

This is the most popular criterion, which was originally introduced by [CRISFIELD 1981], and it works well in the presence of limit points. However, in the presence of bifurcation, instead of

following the current path, the solution will oscillate about the bifurcation point and *fails* to get equilibrium because the sign of $det[K^T]$ cannot distinguish between limit point and bifurcation point, [FENG et al 1997]. This criterion is defined by:

$$sign(\Delta\lambda) = sign\left(\det\left[K^T\right]\right) \qquad [VI\text{-}50]$$

2- The sign of the predictor work increment

This criterion is insensitive to bifurcation points. However, it is ineffective in the descending branch of the load-deflection curve in 'snap-back' problems. This criterion is defined by:

$$sign(\Delta\lambda) = sign\left(\left\langle \delta q^T \right\rangle \{P_{ext}\}\right) \qquad [VI\text{-}51]$$

3- The sign of the internal product of the displacements

[FENG et al 1995, 1996] proposed a criterion based on the sign of the internal product between the previous converged incremental displacement $\{\Delta q\}$ and the current tangential solution $\{\delta q^T\}$

$$sign\,(\Delta\lambda) = sign\,\left(\langle \Delta q \rangle \{\delta q^T\}\right) \qquad [VI\text{-}52]$$

This criterion is insensitive to limit points, turning points and bifurcation points. Its key point is the fact that $\{\Delta q\}$ carries with it information about the history of the current equilibrium path.

VI-1.3. Correction

In the correction phase, Arc-length methods solve the augmented system of equations by applying Newton-Raphson to *Eq. [VI-20]*. This idea was first proposed by [RIKS 1972, 1979] and [WEMPNER 1979], with a different constraint equation.

A truncated Taylor series of *Eq. [VI-20]* yields:

$$\begin{cases} R^{i+1} = R^i + \dfrac{\partial r}{\partial q}\delta q^i + \dfrac{\partial r}{\partial \lambda}\delta\lambda^i = R^i + K^T\delta q^i + P_{ext}\delta\lambda^i = 0 \\ f^{i+1} = f^i + \dfrac{\partial f}{\partial q}\delta q^i + \dfrac{\partial f}{\partial \lambda}\delta\lambda^i = f^i + 2(\Delta q^i)^T\delta q^i + 2\Delta\lambda^i\delta\lambda^i b(P_{ext})^T P_{ext} = 0 \end{cases} \qquad [VI\text{-}53]$$

Where: K^T is the tangent stiffness matrix. The aim is to have $R^{i+1}(q, \lambda) = 0$ and $f^{i+1} = 0$.

For the solution of this system, there exist three phase block elimination method, which are: « The Block elimination method », « The Exterior product form algorithm », and « The Newton's method to the augmented system », see [KELLER 1983; KOUHIA 2008]. The last one is presented in what follows:

The system *[VI-53]* can be written in the following matrix form:

$$\begin{bmatrix} \{\delta q\}_{p+1}^{(i)} \\ \delta\lambda_{p+1}^{(i)} \end{bmatrix} = -\begin{bmatrix} \left[K_{p+1}^{T(i)}\right] & -\{P_{ext}\} \\ 2\langle \Delta q \rangle & 2\Delta\lambda b\langle P_{ext}\rangle\{P_{ext}\} \end{bmatrix}^{-1} \begin{bmatrix} \{R\}_{p+1}^{(i)} \\ f^{(i)} \end{bmatrix} \qquad \textit{[VI-54]}$$

- at an iteration $i \geq 2$:

After updating the stiffness matrix $\left[K_{p+1}^{T(i)}\right]$, and evaluating internal forces $Q_{p+1}^{(i)}\left(\{q_{p+1}^{i-1}\}\right)$, the residue is obtained by:

$$\left\{R_{p+1}^{(i)}\right\} = \lambda_{p+1}^{(i)} \cdot \{P_{ext}\} - \left\{Q_{p+1}^{(i)}\right\} \qquad \textit{[VI-55]}$$

We solve the following equation for $\left\{\Delta q_{p+1}^{(i)}\right\}$:

$$\begin{cases} \left[K_{p+1}^{T(i)}\right]\left\{\delta q_{p+1}^{R(i)}\right\} = \left\{R_{p+1}^{(i)}\right\} \\ \left[K_{p+1}^{T(i)}\right]\left\{\delta q_{p+1}^{T(i)}\right\} = \{P_{ext}\} \end{cases} \qquad \textit{[VI-56]}$$

Then, the resulting iterative displacement is:

$$\left\{\delta q_{p+1}^{(i)}\right\} = \left\{\delta q_{p+1}^{R(i)}\right\} + \delta\lambda_{p+1}^{(i)}\left\{\delta q_{p+1}^{T(i)}\right\} \qquad \textit{[VI-57]}$$

After obtaining $\{\delta q^i\}$, the total and incremental displacements are updated:

$$\left\{q_{p+1}^{(i)}\right\} = \left\{q_{p+1}^{(i-1)}\right\} + \left\{\delta q_{p+1}^{(i)}\right\} \qquad \textit{[VI-58]}$$

$$\left\{\Delta q_{p+1}^{(i)}\right\} = \left\{\Delta q_{p+1}^{(i-1)}\right\} + \left\{\delta q_{p+1}^{(i)}\right\} \qquad \textit{[VI-59]}$$

The Arc-length is written:

$$\overline{\Delta L}_{p+1}^{2} = \left\langle q_{p+1}^{(i)} - q_p \right\rangle \left\{q_{p+1}^{(i)} - q_p\right\} \qquad \textit{[VI-60]}$$

By combining *Eq. [VI-36]*, *Eq. [VI-37]* and *Eq. [VI-38]*, we get a second order equation of $\Delta\lambda_{p+1}^{(i)}$:

$$A \cdot \left(\delta\lambda_{p+1}^{(i)}\right)^2 + B \cdot \delta\lambda_{p+1}^{(i)} + C = 0 \qquad \textit{[VI-61]}$$

With:

$$\begin{cases} A = \left\langle \delta q_{p+1}^{T(i)} \right\rangle \cdot \left\{\delta q_{p+1}^{T(i)}\right\} + b\left\langle p_{ext}\right\rangle\{p_{ext}\} \\ B = 2\left\langle \delta q_{p+1}^{T(i)} \right\rangle \cdot \left(\left\{\delta q_{p+1}^{R(i)}\right\} + \left\{\Delta q_{p+1}^{(i)}\right\}\right) + 2\Delta\lambda_{p+1}^{(i)} b\left\langle p_{ext}\right\rangle\{p_{ext}\} \\ C = \left\langle \left\{\delta q_{p+1}^{R(i)}\right\}\left\{\Delta q_{p+1}^{(i)}\right\}\right\rangle\left(\left\{\delta q_{p+1}^{R(i)}\right\}\left\{\Delta q_{p+1}^{(i)}\right\}\right) - \overline{\Delta L}^{2} + \Delta\lambda_{p+1}^{(i)} \cdot b \cdot \left\langle p_{ext}\right\rangle\{p_{ext}\} \end{cases}$$

Where:

$$\begin{cases} \{\Delta q_{p+1}^{(i)}\} = \{q_{p+1}^{(i)}\} - \{q_p\} \\ \Delta \lambda_{p+1}^{(i)} = \lambda_{p+1}^{(i)} - \lambda_p \end{cases} \qquad \textit{[VI-62]}$$

The quadratic equation can be solved for δλ:

$$\delta\lambda_1 = \frac{-B - \sqrt{B^2 - 4AC}}{2A},\ \delta\lambda_2 = \frac{-B + \sqrt{B^2 - 4AC}}{2A}.$$

Or: $\delta\lambda = \frac{-B}{2A}$.

Finally, the load level is updated using:

$$\lambda_{p+1}^{(i)} = \lambda_{p+1}^{(i-1)} + \delta\lambda_{p+1}^{(i)} \qquad \textit{[VI-63]}$$

The solution for $\delta\lambda$ can be characterized as:

- Real roots of opposite sign: Solution process converges normally;

- Real roots of equal sign opposite to that of $\Delta\lambda^{(i-1)}$: in vicinity of a limit points;

- Real roots of equal sign same as that of $\Delta\lambda^{(i-1)}$: in vicinity of a turning points;

- Complex roots: signal a sharp turning point, a bifurcation point ==> divergent iterates.

1- Real roots

For the case of real roots with opposite sign, the correct sign of $\delta\lambda$ can be chosen according to the following criterions:

a- Positive External work criterion

$$\Delta W = \langle P_{ext} \rangle [K^T] \{P_{ext}\} \delta\lambda > 0 \qquad \textit{[VI-64]}$$

This criterion, fails at turning points and bifurcation points because ΔW=0 at these points.

b- Angle Criterion

In this criterion the selected root is the one that corresponds to the smallest change in the direction of the iterative displacement vector compared to the previous displacement vector. That implies the calculation of $\{\Delta q^i\}$ for both $\delta\lambda_1$ and $\delta\lambda_2$, and the closest to the old incremental step direction is selected. This prevent the solution from doubling back on its track.

2- Complex roots

The presence of complex solutions may occur in vicinity of bifurcation points (the arc-length ΔL is too large). A common solution [CRISFIELD 1983-b], is by reducing the arc-length ΔL by means of the so-called automatic increment cutting, in which the process is cut and re-performed starting from the last converged solution with $\Delta L^{new} = 0.5 \cdot \Delta L^{old}$.

[LAM & MORLEY 1992] have presented a methodology for treating the complex roots that can arise in the above mentioned quadratic equation.

Further contributions on root selection rules can be found in : [BATHE & DVORKIN 1983-b; BELUNI & CHULYA 1987; YANG & SHIEH 1990; KWEON & HONG 1994; CARRERA 1994; KUO & YANG 1995; FENG et al 1995; HELLWEG & CRISFIELD 1998].

VI-1.4. Step-Length Control

In the Arc-Length method, automatic incremental arc-length $\overline{\Delta L}$ is used for controlling the step length size. According to [CRISFIELD 1981], the new incremental length is found by applying:

$$\overline{\Delta L}_{p+1} = \overline{\Delta L}_p \sqrt{\frac{I_d}{I_p}} \qquad \textit{[VI-65]}$$

I_p : Number of iterations required to achieve equilibrium for the previous increment ***P***;

I_d : The desired number of iterations.

CHAPTER VII

NUMERICAL EXAMPLES

I- INTRODUCTION

In this chapter, the assessment of the proposed: flat shell finite elements with drilling rotation, co-rotational formulation, geometric stiffness, and mass matrices, for geometrically nonlinear static and dynamic analysis, is performed by comparing the numerical results from a set of usually applied benchmark problems, with similar conventional finite elements without the in-plane drilling rotational *d.o.f,* and with available reference solutions.

In the frame of this research work, the data-processing developments enabled us to have a finite elements program developed in MATLAB platform, which runs on a personal computer, devoted to the geometrically nonlinear static and dynamic analysis of shell structures. The presented flat shell finite elements were implemented in the above mentioned MATLAB program.

Using this program, analyses may carried out using one of the following finite elements:

"*Quad*": quadrilateral flat shell finite element with fictitious stiffness (DKQ + Standard Bi-linear Quadrilateral membrane element + fictitious rigidity);

"*Qdrill*": quadrilateral flat shell finite element with drilling rotation (DKQ + Quadrilateral membrane element with in-plane drilling rotational *d.o.f* presented in *chapter III,* § *III-1.2.3*);

"*Trian*": Triangular flat shell finite element with fictitious stiffness (DKT + CST membrane element + fictitious rigidity);

"*Tdrill*": Triangular flat shell finite element with drilling rotation (DKT + Triangular membrane element with in-plane rotational degrees of freedom developed in *chapter III,* § *III-1.2.3*).

In all tested examples herein, the material behaviour is taken to be isotropic linearly elastic, and the damping ratio is taken to be null. For the geometrically nonlinear analysis, a displacement convergence criteria is used where the precision criteria is taken to be: $\varepsilon = 0.001$.

Numerical comparisons are drawn between the developed elements and the existing solutions available in literature. These comparisons demonstrate the validity and reliability of the proposed approach, and the ability of the proposed shell elements with drilling rotation to describe the complete displacement field and to model planar and non-planar structures.

The first set of examples illustrates the ability of membrane elements with drilling rotation proposed herein for nonlinear dynamic analysis to handle large displacements and large rotations, and buckling problems in addition to the good representation of in plane dynamic quantities.

The second set of examples, is devoted to arbitrary plate and shell problems. These examples illustrates the ability of the proposed shell elements with drilling rotation to handle a large class of shell problems in both static and dynamic nonlinear regime. Some of those examples can be solved by the conventional shell elements, while for some others the conventional shell elements would face some modelling problems. For all presented examples, the presented shell elements with drilling rotation faces no difficulties in modelling those problems.

Note that, both shell finite elements with drilling rotation and conventional shell elements are built at the same program in the same subroutines, and work by the same way, for this reason, the comparison between these elements, has a justifiable value.

II- IN-PLANE TESTS

II-1. Linear Analysis

II-1.1. Cantilever beam under a tip load

In this example, a cantilever beam of rectangular cross-section shown in *Fig. VII.1*. is studied. The left end of the beam is fixed while the right end is subjected to a parabolic shear distribution. The dimensions and elastic properties of the beam are: $L=48$, $h=12$, $b=1$, $E = 3\times10^4$ and $\upsilon=0.25$.

To compare the accuracy of the present EAS element, the results are presented in *Tab. VII.1* against the original Allman's element, the element presented in [PILTNER & TAYLOR 2000] named "TE4" and the reference solution presented in many references [BERGAN & FELIPPA 1985; FELIPPA 2003; CEN et al 2011].

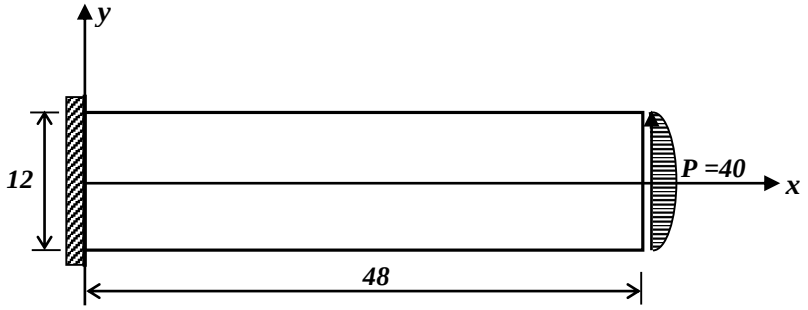

***Fig. VII.1.* Cantilever beam: geometry and loading**

Tab. VII.1. Results of the cantilever beam.

Vertical displacement at $x=48$, $y=0$				
Mesh	CST	Allman	TE4	Present
1×4	0.0907	0.2696	0.3037	0.3034
2×8	0.1984	0.3260	0.3382	0.3379
4×16	0.3056	0.3472	0.3506	0.3500
8×32	0.3421	0.3539	0.3548	0.3540
16×64	0.3531	0.3555	0.3562	0.3554
Analytic	0.3558			

II-1.2. Cook's problem

A tapered cantilever beam of unit thickness shown in *Fig. VII.2.* is clumped on one end and subjected to a distributed shear load on the other end. The elastic proprieties are: $E = 1$, $\upsilon = 0.25$. The results are compared to the best known solution which is: *23.96*, presented in many references [COOK 1974-b; LONG & XU 1994; STOLARSKI & CHEN 1995-b; FELIPPA 2003; CEN et al 2011]. The reference solution is obtained using a fine mesh of "64×64" elements, which can be considered accurate enough. The obtained results are compared to the reference solution in *Tab. VII.1.*

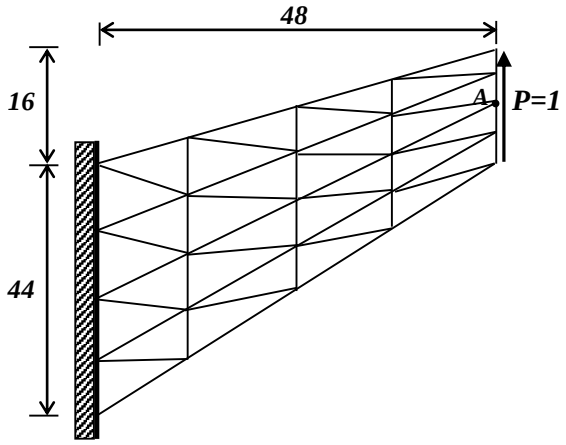

Fig. VII.2. **Cook's cantilever beam: geometry, mesh, and loading**

Tab. VII.2. Results of Cook's membrane problem.

	Vertical displacement at *point A*			
Mesh	2×2	4×4	8×8	16×16
CST	11.99	18.28	22.02	23.41
Allman	19.67	22.41	23.45	23.81
TE4	20.27	22.49	23.46	23.81
Present	20.29	22.49	23.46	23.81
Reference	23.96			

II-1.3. Clamped arch

In this example, the clamped arch depicted in *Fig. VII.3*. is subjected to a concentrated load *P=7500* located at its mid-span. The arch is modelled as a plane stress problem presented in *Fig. VII.3*. Geometrical characteristics are taken to be: *R=100*, *θ=0.707 rad*, *h=2*, and *b=1*.

The material properties are $E=10^7$, *v=0.25*.

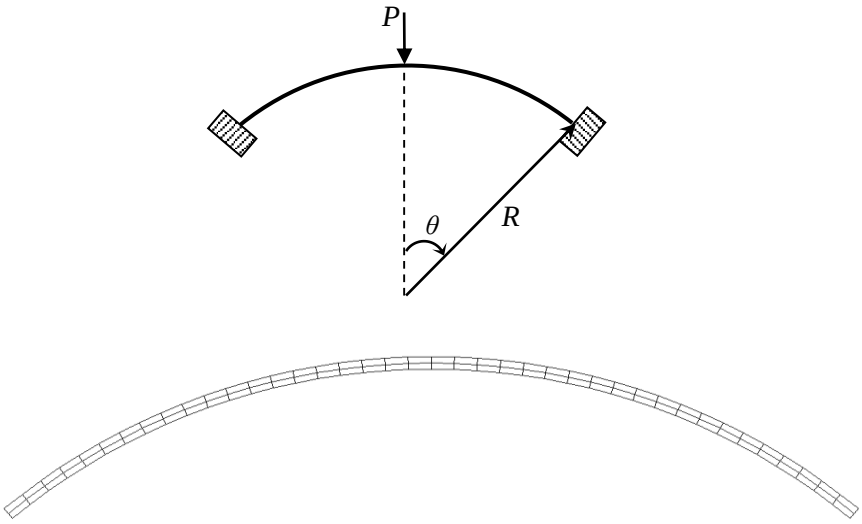

Fig. VII.3. **Clamped arch: geometry, mesh, and loading**

Tab. VII.3. Results of a clamped arch.

Vertical displacement at mid-span				
Mesh	CST	Allman	Present	Qdrill
10×2	0.01238	0.02829	0.1076	0.1278
20×2	0.02091	0.06363	0.1212	0.1467
40×2	0.040020	0.1102	0.1287	0.1519
40×4	0.042245	0.1121	0.1450	0.1536
40×8	0.042962	0.1125	0.1516	0.1542

II-2. Dynamic and Nonlinear analysis

In this section, linear and nonlinear static and dynamic responses of rectilinear and curved beams, under different loads conditions are studied in order to test the performances of the proposed developments when simulating bending by using the in-plane behaviour in both nonlinear, static and dynamic regimes.

II-2.1. Cantilever beam under distributed step loading

In this example, static and dynamic responses of a cantilever beam under distributed step load is studied. We simulated bending by using the in-plane behaviour with a mesh of "12×2" (length × thickness) quadrilateral elements, and with "32×8×2" triangular elements as presented in *Fig. VII.4*. First we tested the nonlinear response of the cantilever beam with the following geometry and material properties: $L = 10\ in$; $b = 1\ in$; $h = 0.1\ in$; $E = 12\times10^{6}\ lb/in^{2}$ and $\upsilon = 0.2$. The results shown in *Fig. VII.6*. exhibit good agreement compared to the reference solution presented in [MASSIN & AL-MIKDAD 2002].

For dynamic analysis, and in order to match the reference example presented in [KIM et al 2003], geometry and material properties are assumed to be: $L = 10\ in$; $b = 1\ in$; $h = 1\ in$; $E = 12\times10^{3}\ lb/in^{2}$, $\upsilon = 0.2$ and $\rho = 1\ lbm/in$. The Applied load is a step load of intensity $q_0 = 2.85\ lb/in$ as presented in *Fig. VII.5*. The time interval used for Newmark's integration method is $0.13512\times10^{-3}\ s$.

The results shown in *Fig. VII.7*. and *Fig. VII.8*. are compared to the reference solution for linear dynamic analysis presented in [KIM et al 2003]. For the nonlinear dynamic response, the reference solution is taken from the reference [KANT & KOMMINENI 1994].

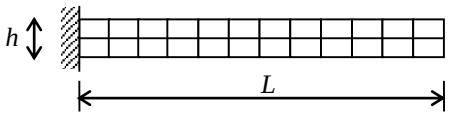

Fig. VII.4. **Cantilever beam: geometry and mesh**

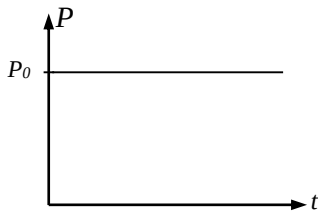

Fig. VII.5. **Step load**

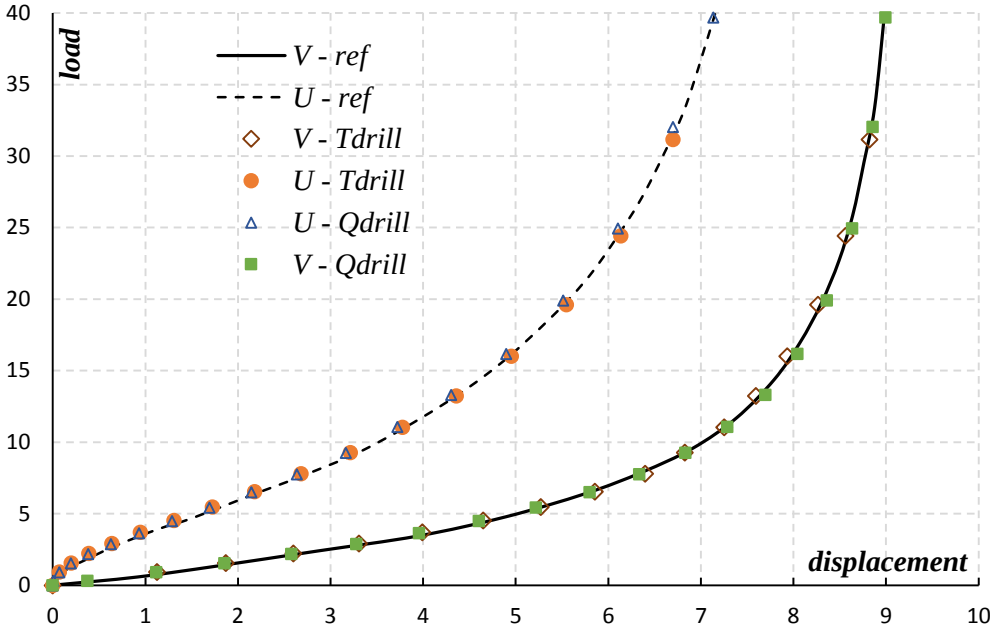

Fig. VII.6. **Load-displacement curve of the cantilever beam**

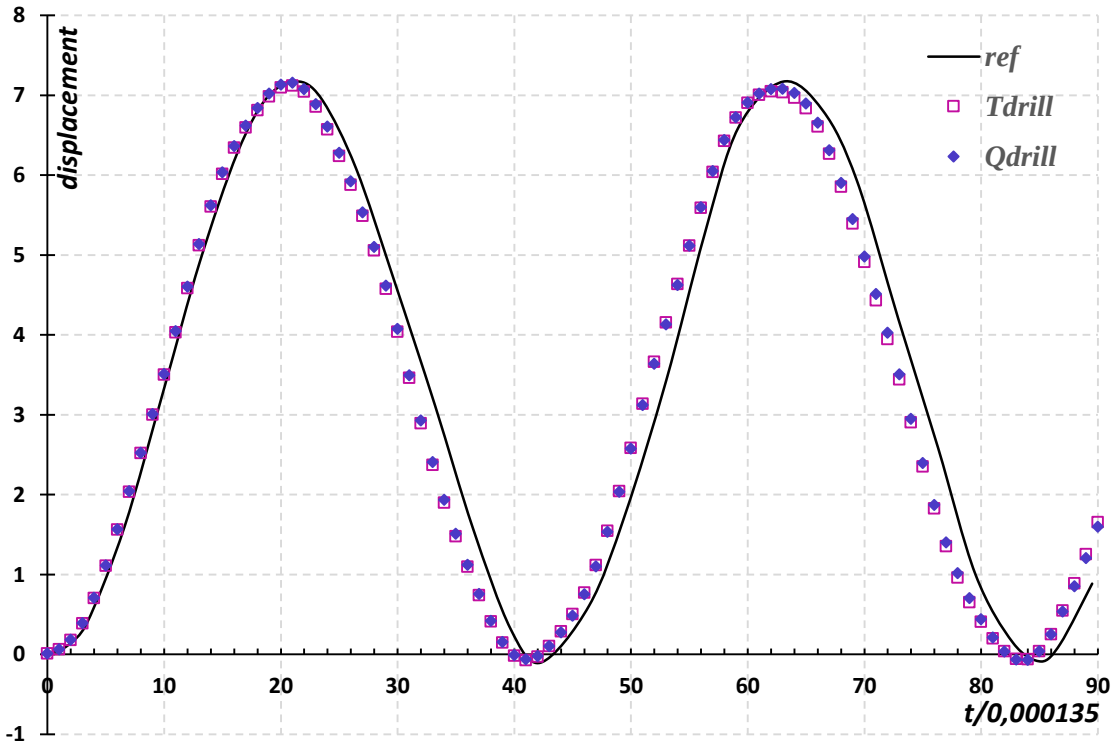

Fig. VII.7. **Linear dynamic response of the cantilever beam**

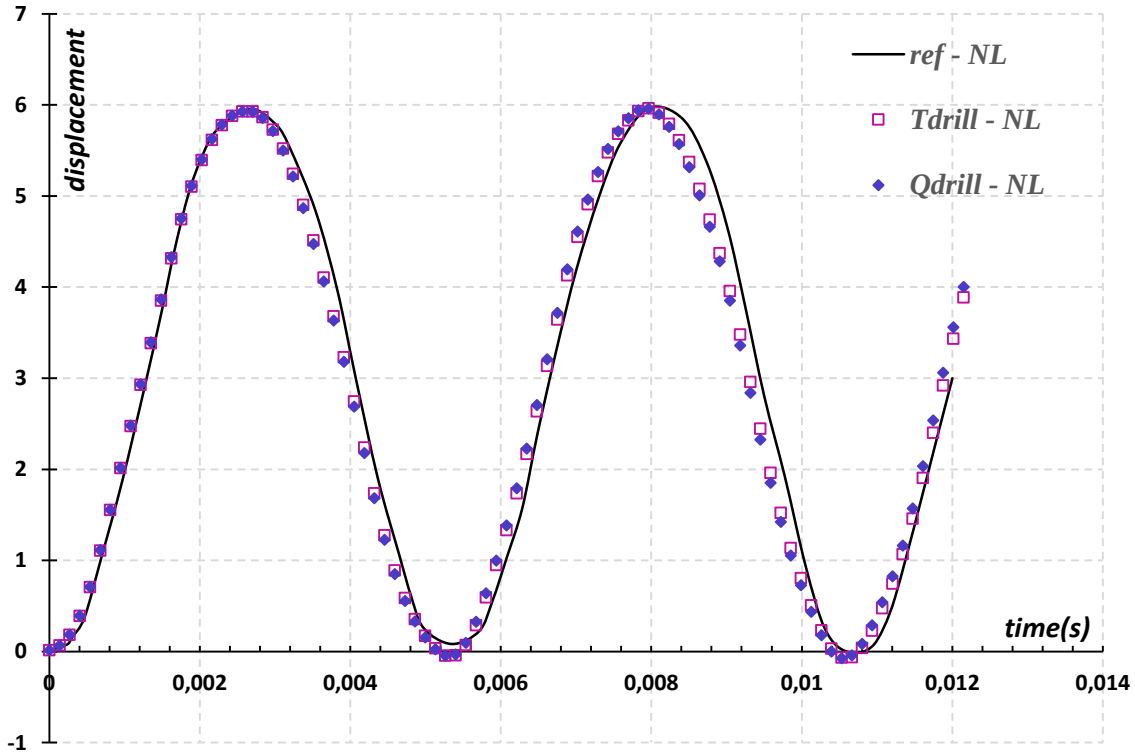

***Fig. VII.8.* Nonlinear dynamic response of the cantilever beam**

As the results show, the responses obtained by using the *"Tdrill"* and "*Qdrill"* elements associated with the proposed mass matrices for the triangular and quadrilateral elements with drilling rotation, present a good convergence compared to the reference solution. It is clear then, that the presented elements with drilling rotation exhibit true and accurate dynamic in-plane response when associated to convenient mass matrices.

II-2.2. Clamped arch

In this example, the clamped arch of *Example II-1.3* depicted in *Fig. VII.9.* is studied for nonlinear static and dynamic analysis when subjected to a concentrated step load *P* located at its mid-span. The arch is modelled as a plane stress problem with "40×2" (length × thickness) quadrilateral elements through the thickness as presented in *Fig. VII.9-c*. For the triangular element, the arch is modelled with "40×8×2" through thickness triangular elements.

Geometrical characteristics are taken to be: $R=100$, $\theta=0.707rad$, $h=2$, $b=1$, and $P=7500$. The material properties are $E=10^7$, $v=0.25$, and mass density $\rho=2.45\times10^{-4}$.
A constant time step is used for time integration: $\Delta t = 0.2\times10-3\ s$.

The static geometrically nonlinear response of the clamped arch is depicted in *Fig. VII.10.* against nonlinear beam solution.

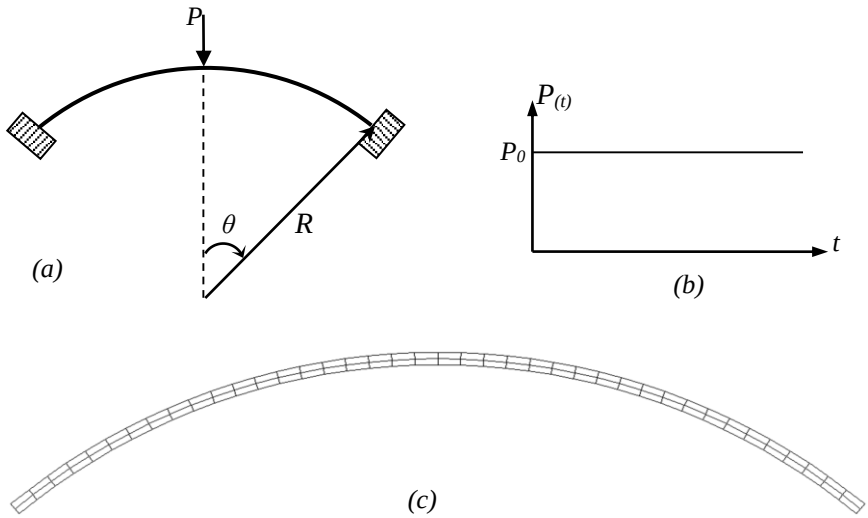

Fig. VII.9. **Clamped arch: (a) geometry, (b) load, (c) mesh**

The dynamic responses obtained by the triangular and quadrilateral membrane elements with drilling rotation representing the displacement history at the respective load point is plotted in *Fig. VII.11*. and *Fig. VII.12*. Comparing the results with numerical results of reference [DUARTE-FILHO & AWRUCH 2004] using (40×4 hexahedral elements), a very good agreement can be observed for both "*Qdrill*" and "*Tdrill*" elements.

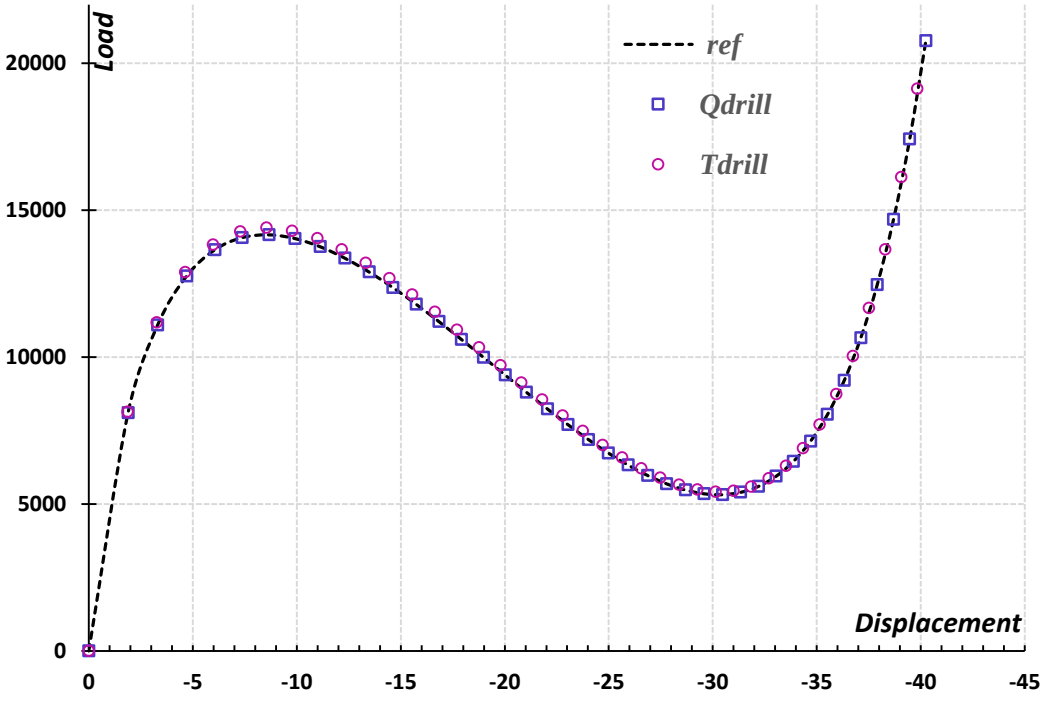

Fig. VII.10. **Nonlinear response of the clamped arch**

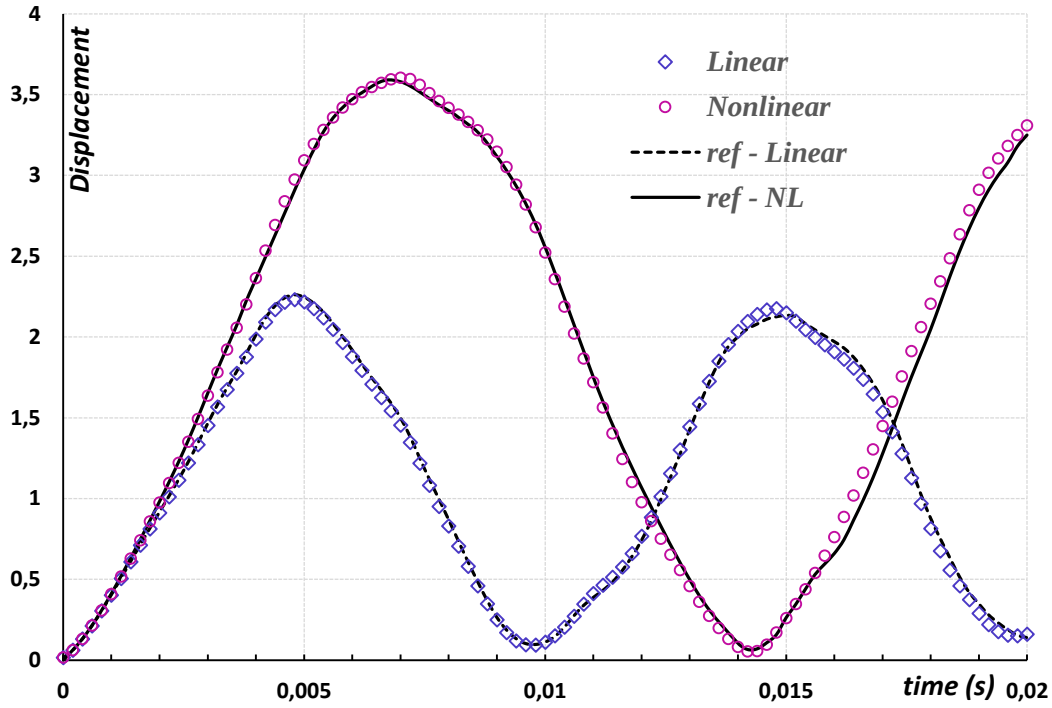

Fig. VII.11. **Dynamic response of the clamped arch using "*Qdrill*" element**

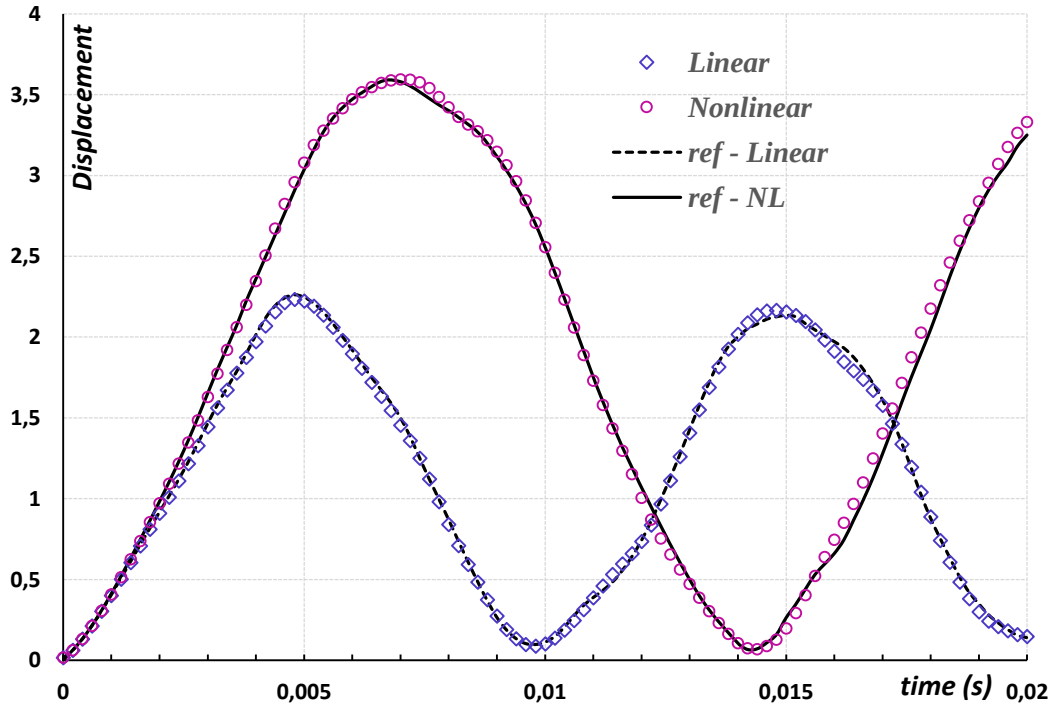

Fig. VII.12. **Dynamic response of the clamped arch using "*Tdrill*" element**

II-2.3. Cantilever beam under a concentrated end moment

In this example, a cantilever beam is subjected to a concentrated moment applied at the free end as shown in *Fig. VII.13*. The beam has a rectangular cross section with dimensions ($b \times h$) and length L. geometry and material properties are: $L = 12;\ b = 1;\ h = 0.1;\ E = 12.10^5$; *and* $\nu = 0$. $M_{max} = 50\pi/3$. The beam was discretized into "20×2" (length × thickness) quadrilateral elements.

The obtained moment-displacement curves for nonlinear static analysis are given in *Fig. VII.14*. The results show that an excellent agreement with the analytical solution taken from the reference [KUZNETSOV & LEVYAKOV 2007] was obtained.

The analytical solution corresponds to a beam rolled-up into a circular arc of radius r with $1/r = M/EI$, where M is the applied end moment. A complete circle is achieved at $M = 2\pi EI/L$.

In order to perform linear and nonlinear dynamic analysis we assume the mass density to be $\rho = 2 \times 10^{-6}$. The beam is subjected to a concentrated step moment $M=7$, applied at the free end. A constant time step $\Delta t = 0.2 \times 10^{-3} s$ is used. In this case, the time-history curves show a great convergence compared to the beam solution which is taken as the reference solution. Unfortunately, triangular elements fail to perform this example because they return wrong answer to moment loading type.

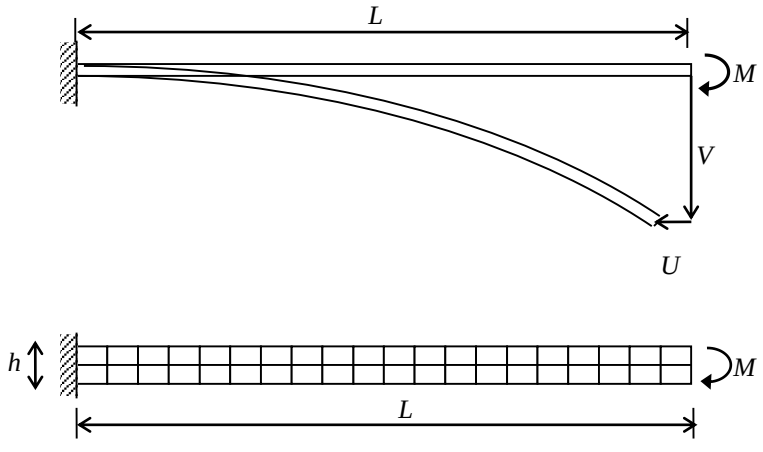

Fig. VII.13. **Cantilever beam subjected to pure bending: geometry and mesh**

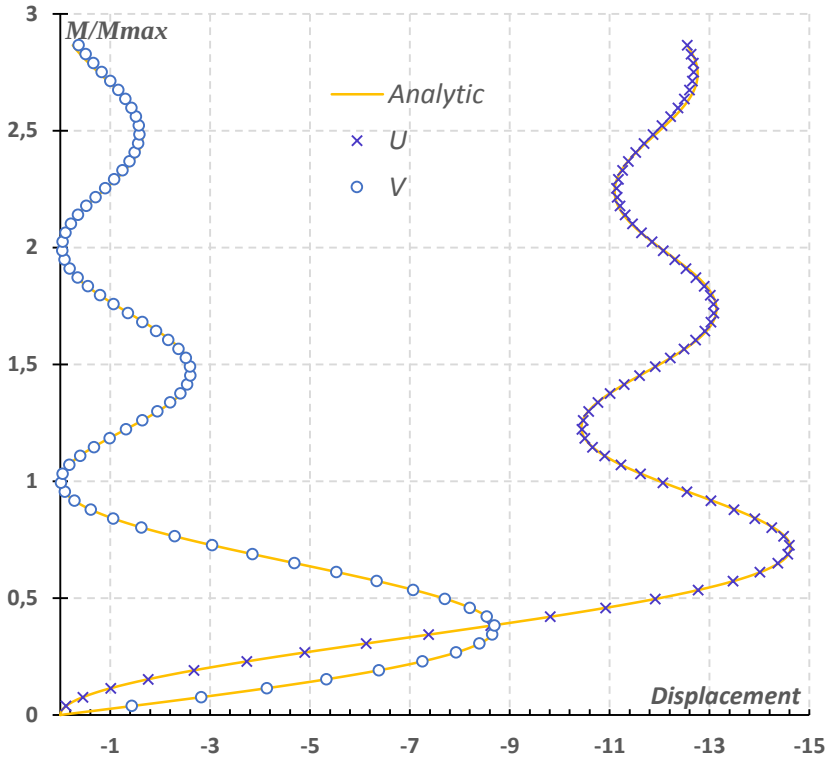

Fig. VII.14. **Cantilever beam load-displacement curve**

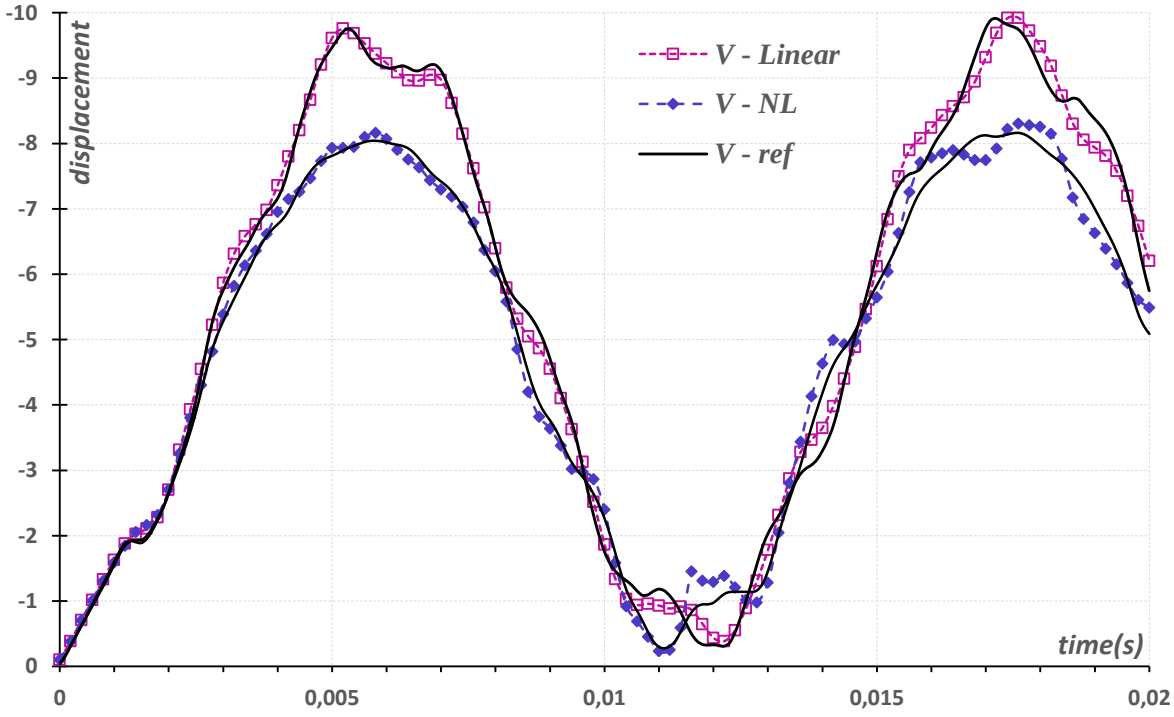

Fig. VII.15. **Cantilever beam vertical displacement time history curve**

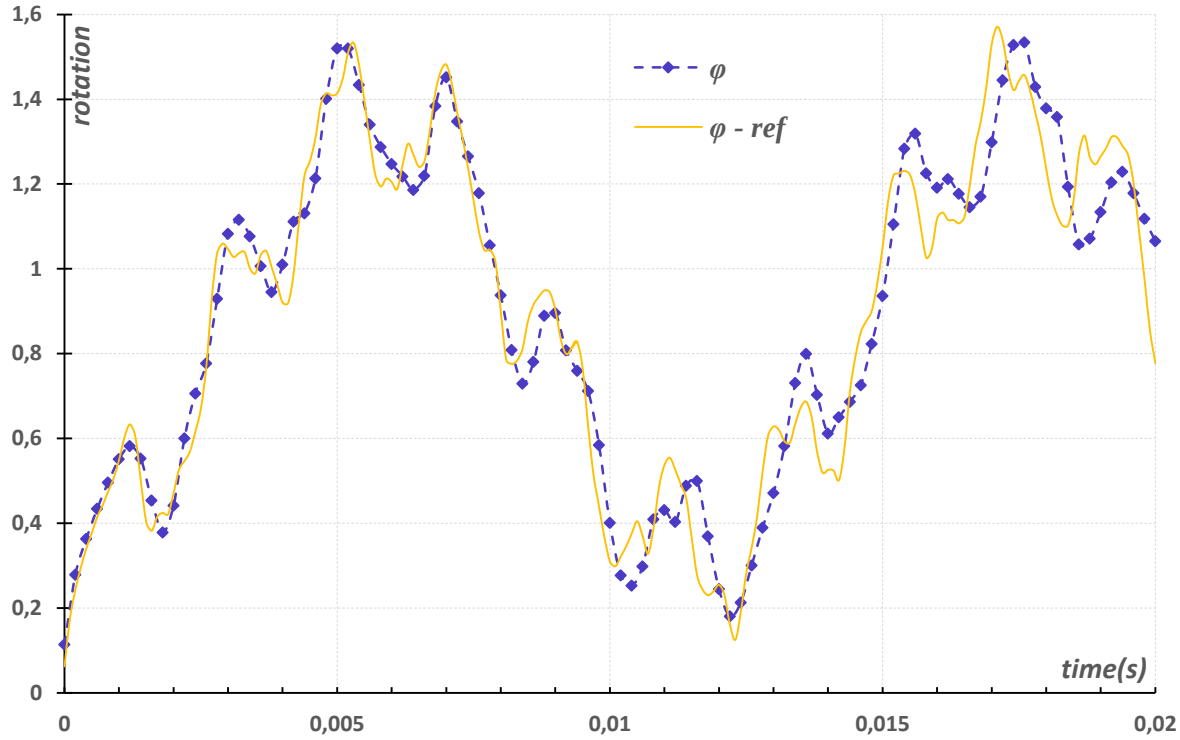

***Fig. VII.16.* Cantilever beam end rotation time history curve**

The moment-displacement curves obtained using "*Qdrill*" element given in *Fig. VII.14*. show that an excellent agreement with the analytical solution is obtained using "20×2" quadrilateral elements. These results illustrate that we have a powerful algorithm based on the updated Lagrangian co-rotational formulation for both large displacements and large rotations.

II-2.4. Lee's Frame

A hinged right angle frame with two members of uniform rectangular cross-section, is subjected to a vertical concentrated load, located on the horizontal member with a distance from the intersection point of *24 cm* as shown in *Fig. VII.17*. Both beam and column have a unified length of *120 cm*, cross section of dimensions ($20\times30\ cm^2$), and linear elastic modulus of $7.2\times10^6\ KN/m^2$. Both beam and column is discretized with "20×2" quadrilateral elements, and "20×4×2" triangular elements. This is a well-known geometric non-linear benchmark problem for its particular snap through post-buckling behaviour.

The displacements plotted against load, are the vertical and horizontal displacements of the node under the point load. An excellent agreement was found between our calculated results and the results of the reference: [NUKALA & WHITE 2004] obtained using fine mesh beam elements.

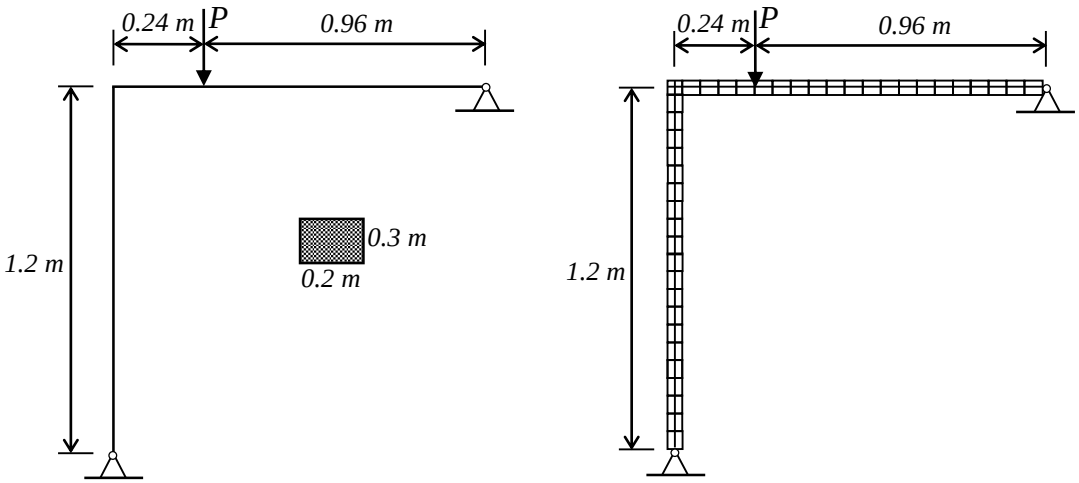

Fig. VII.17. **Lee's frame: geometry and mesh**

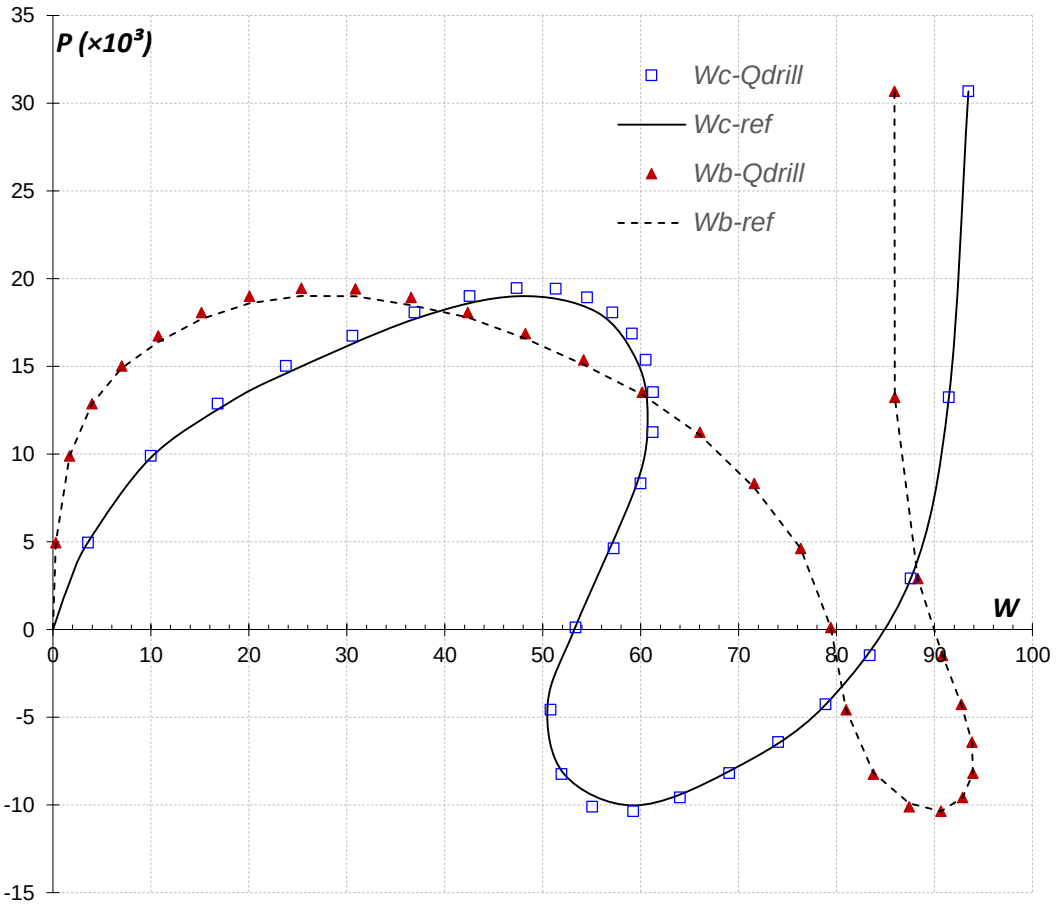

Fig. VII.18. **Lee's frame load-displacement curves using "*Qdrill*" element**

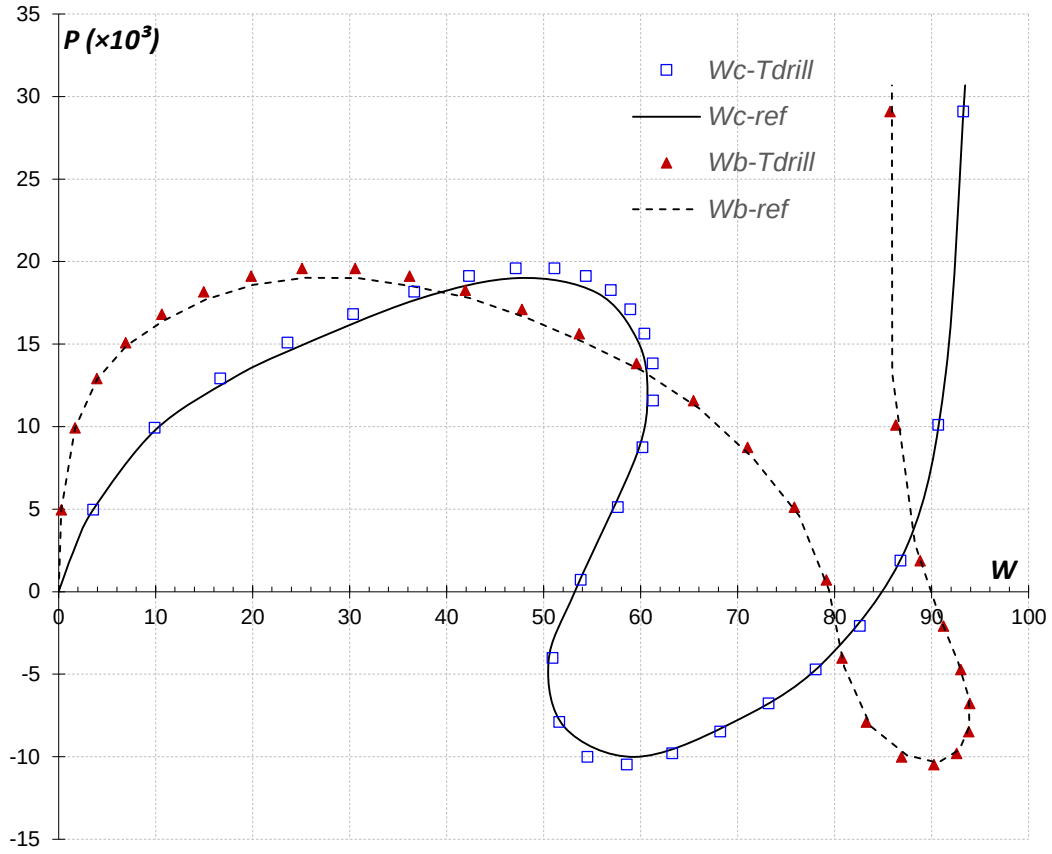

Fig. VII.19. **Lee's frame load-displacement curves using "*Tdrill*" element**

III- SHELL PROBLEMS

III-1. Geometrically Non-Linear Static Analysis

III-1.1. Cantilever beam under a concentrated moment at the free end

In this example, we studied a cantilever beam subjected to a pair of concentrated moments applied at the free end as shown in *Fig. VII.20*. This example is used as benchmark problem for large displacements and large rotations analysis. The beam was discretized here into four quadrilateral elements, and the characteristics used are as follows: $L = 12$, $b = 1$, $h = 0.1$, $v = 0$, *and* $E = 12x10^5$.

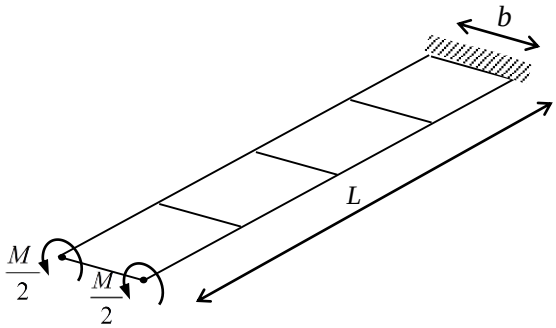

Fig. VII.20. **Geometry of the cantilever beam**

The obtained moment-displacement curves given in *Fig. VII.21.* show that an excellent agreement with the analytical solution was easily obtained using both triangular and quadrilateral elements. Several deformed configurations until the beam formed a circle are depicted in *Fig. VII.22.*

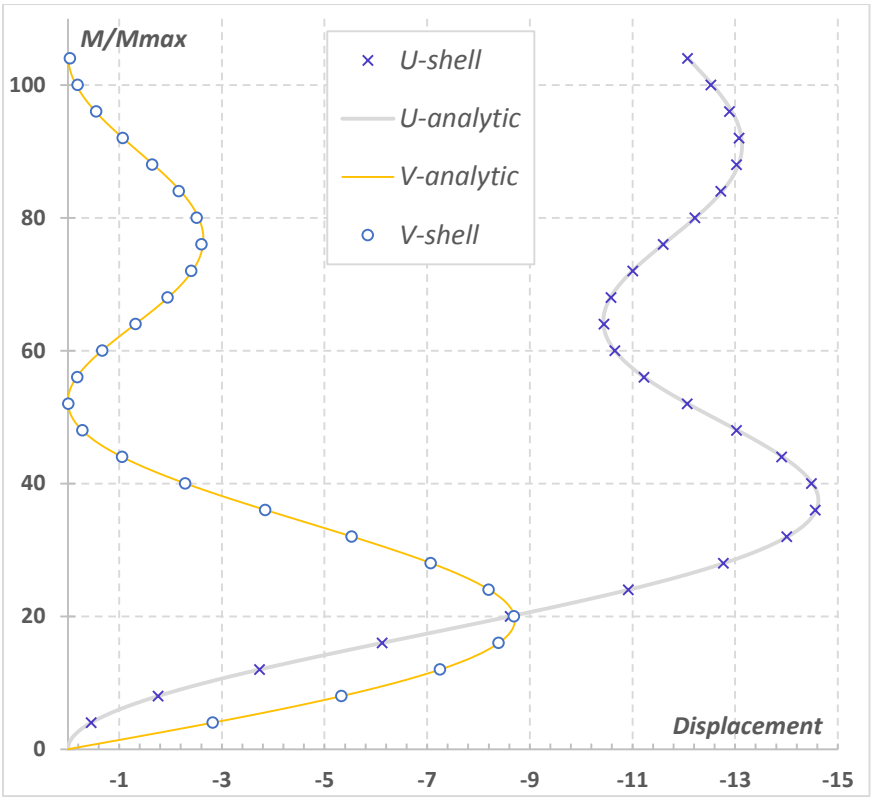

***Fig. VII.21.* Cantilever beam load-displacement curve**

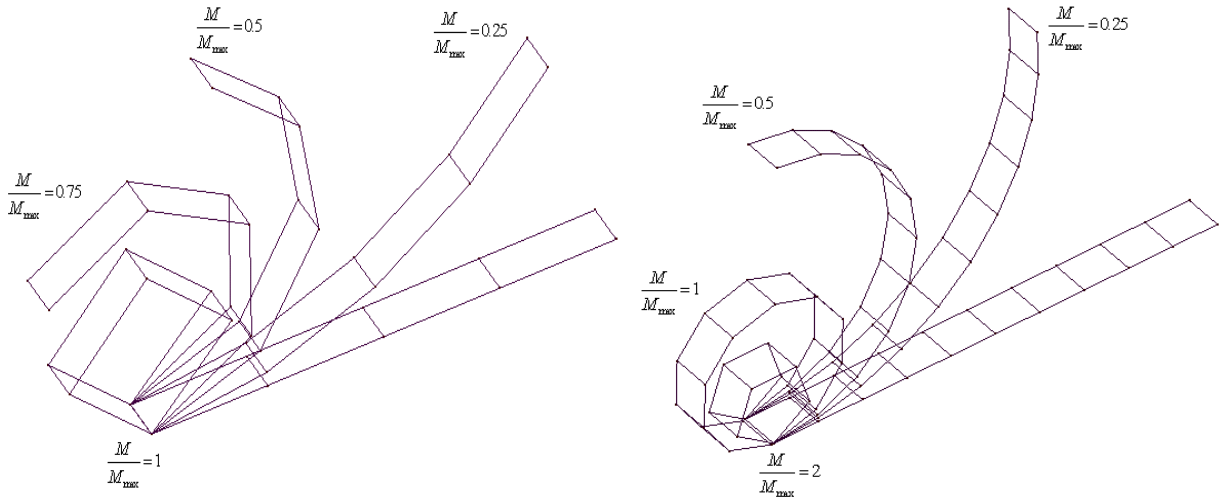

***Fig. VII.22.* Cantilever beam: deformed configurations**

III-1.2. Cylindrical shell under concentrated loading

This example is the most used to validate shell finite elements in geometrically nonlinear analysis. *Fig. VII.23*. shows a thin cylindrical shell subjected to a concentrated load applied in its center. Its curved edges are free while the straight edges are hinged. Because of the double symmetry of geometry, loading, and boundary conditions, only one quarter of the shell is modelled using "3×3" quadrilateral elements and "3×3×2" triangular elements as presented in *Fig. VII.24*.

The geometrical and mechanical characteristics are as follows: $R = 2540$ *mm*, $L = 254$ *mm*, $\theta = 0.1$ rad, $\upsilon = 0.30$, and $E = 3.10275$ *kN/mm*^{2}.

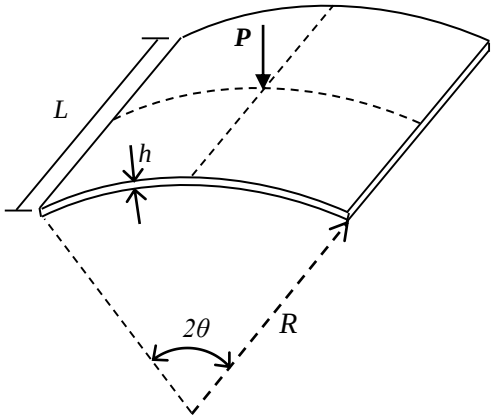

Fig. VII.23. **Geometry of the cylindrical shell**

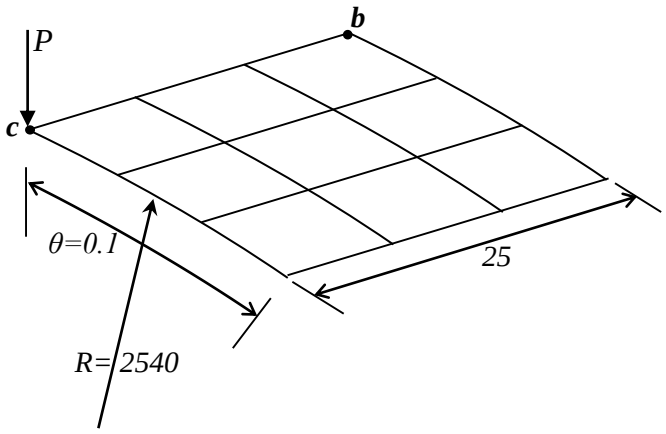

Fig. VII.24. **Mesh of one quarter of the cylindrical shell**

The analysis carried out in this work, shows the numerical difficulties that faces conventional shell elements with fictitious rigidity to undergo the unstable branch of the load-displacement curve of this example. We observed a very large number of iterations and sometimes divergence with conventional shell elements.

This analysis was carried out for two thicknesses:

* *for h=12.7 mm*: curves presented in *Fig. VII.25*. and *Fig. VII.26*.

The results obtained using the *"Qdrill"* and *"Tdrill"* elements present a precise convergence towards the reference solution by [SURANA 1983]. The total number of iterations which requires the elements with drilling rotation to plot the curve presented in *Fig. VII.25*. and *Fig. VII.26*. is 28 iterations, while the triangular element *"Trian"* and the quadrilateral *"Quad"* element require more than 30 iterations.

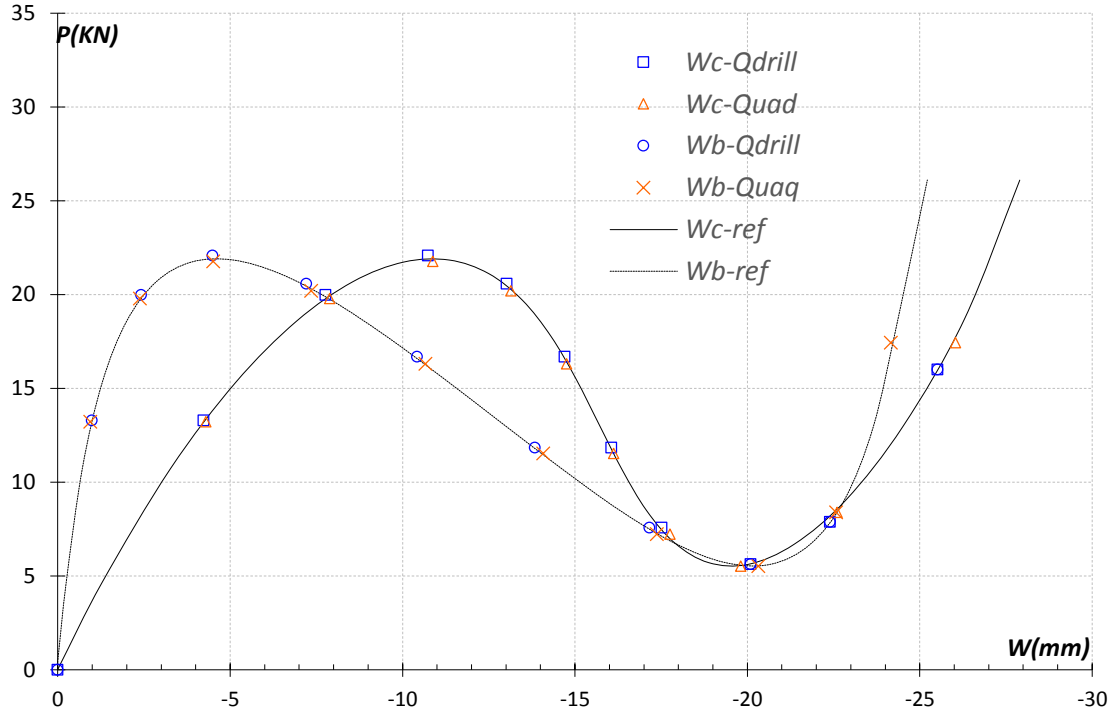

***Fig. VII.25.* Load-displacement curve using quadrilateral elements (*h=12,7 mm*)**

* *for h=6.35 mm*: curve presented in *Fig. VII.27*. and *Fig. VII.28*.

The thickness is reduced to the half. In this case the shell presents a very sensible behaviour, and a very marked snap-through is noted. For testing our results, we refer to the load-displacement curve by [RAMM 1982]. The necessary total iteration number to plot the curve *Fig. VII.27*. and *Fig. VII.28*. is 46 iterations using *"Qdrill"* element, while the "Quad" and "Trian" shell elements with fictitious stiffness require more than 60 iterations.

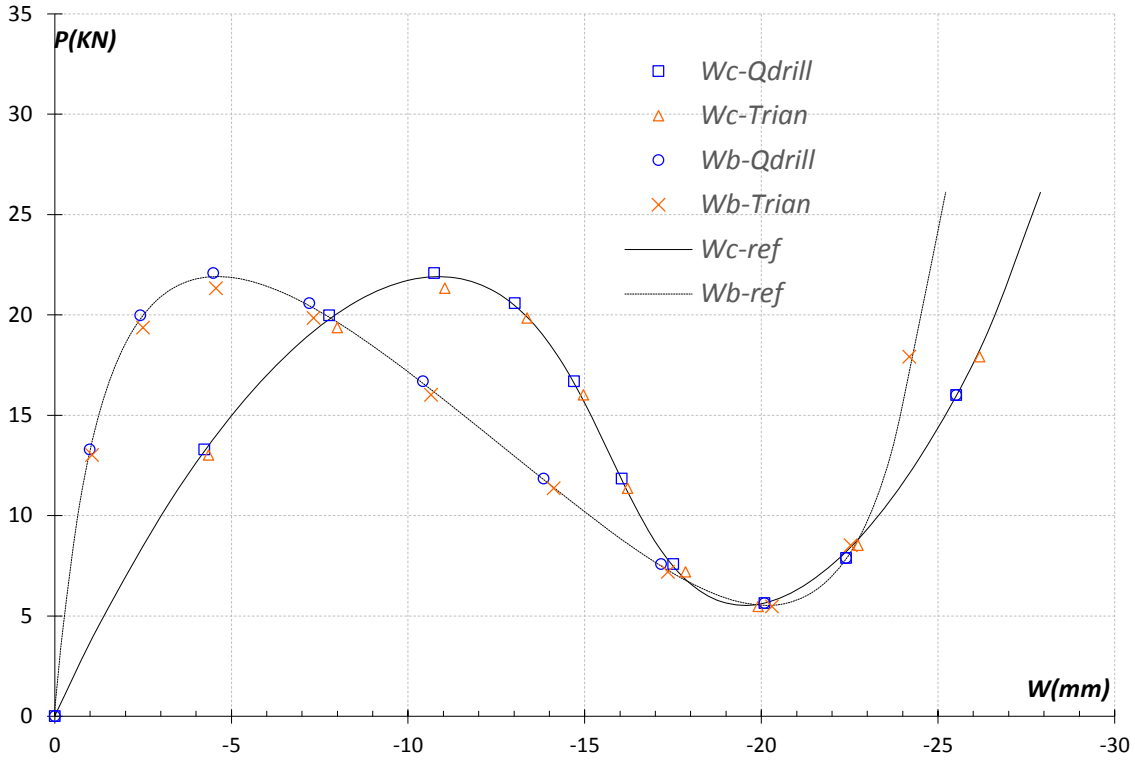

Fig. VII.26. **Load-displacement curve using triangular elements (*h=12,7 mm*)**

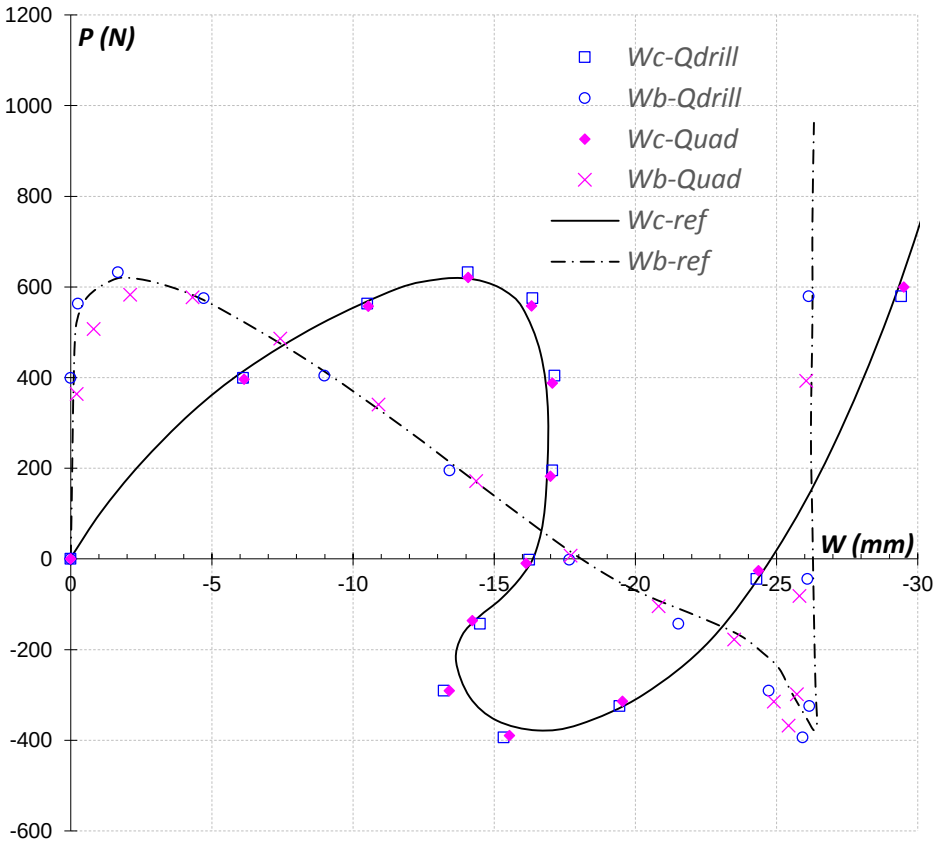

Fig. VII.27. **load-displacement curve using quadrilateral elements (*h=6,35 mm*)**

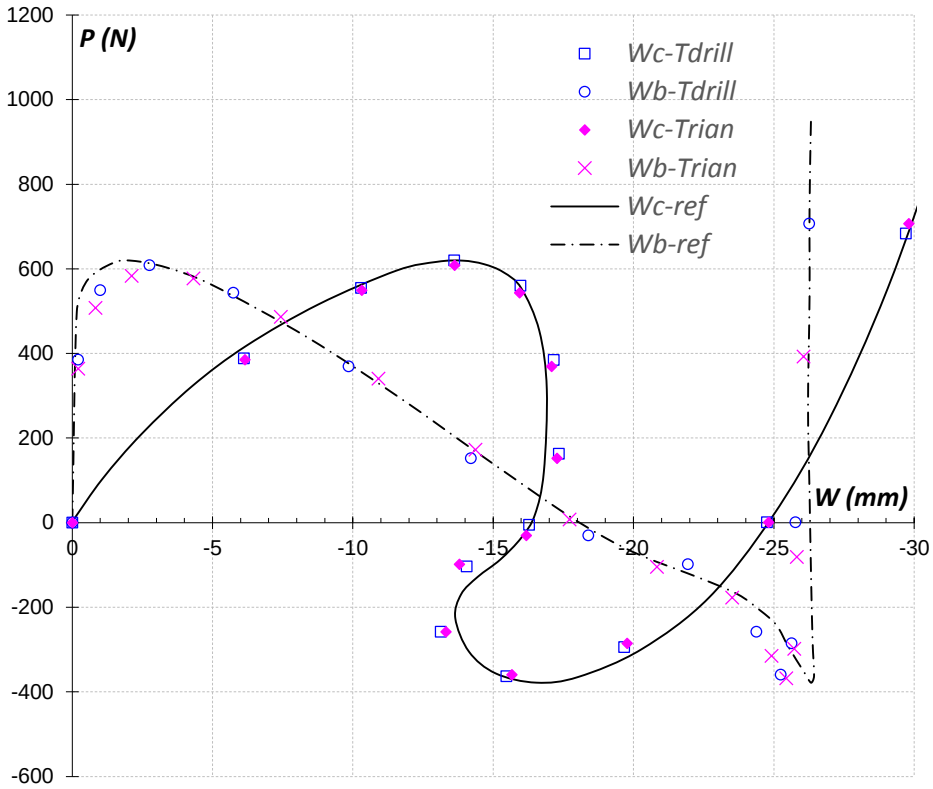

***Fig. VII.28.* load-displacement curve using triangular elements (*h=6,35 mm*)**

III-1.3. Spherical shell under concentrated loading

The presence of the double curvature is interesting for the validation of shell elements. Therefore, the example considered here is a thin spherical shell whose edges are articulated. It is subjected to a concentrated load applied at its center, *Fig. VII.29*. Because of the double symmetry of geometry, loading, and boundary conditions, only one quarter of the shell is modelled using "4×4" quadrilateral elements and "4×4×2" triangular elements. The shell characteristics are as follows: $R = 2540\ mm$; $2a = 784.90\ mm$; $h = 99.45\ mm$; $E = 68.95\ KN/mm^2$; and $\upsilon = 0.3$.

The nonlinear response of the spherical shell is illustrated by the load-displacement curve of the central point represented in *Fig. VII.30*. and *Fig. VII.31*. We refer to the analytical solution presented in the reference: [MEEK & RISTIC 1997]. The solutions obtained by using the *"Qdrill"* and *"Tdrill"* elements are in good agreement with the analytical solution for shallow shells. This can be explained by the fact that the flat shell elements with drilling rotation behaves better in the case of the double curvature.

The total number of iterations which requires *"Qdrill"* and *"Tdrill"* elements to plot the curve presented in *Fig. VII.30*. and *Fig. VII.31*. is 30 and 43 iterations respectively, while the triangular *"Trian"* and the quadrilateral *"Quad"* elements require about 60 iterations.

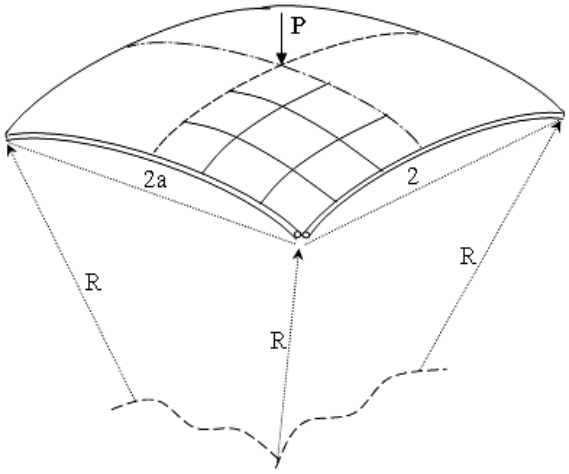

Fig. VII.29. **Geometry of the spherical shell**

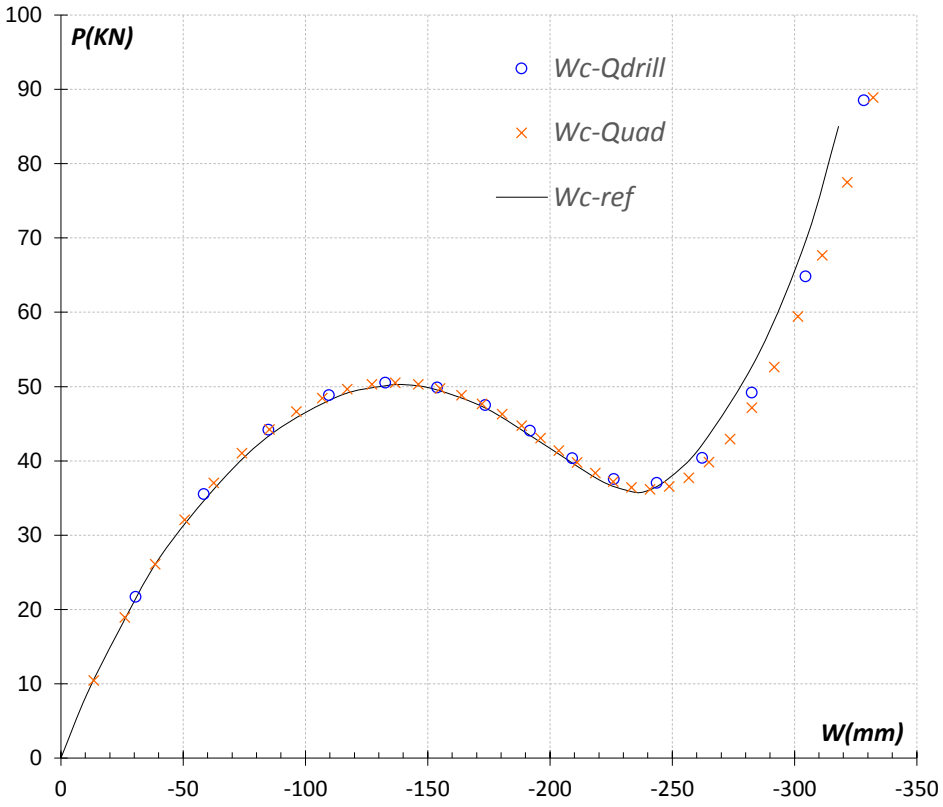

Fig. VII.30. **Load-displacement curve of the spherical shell using the quadrilateral elements**

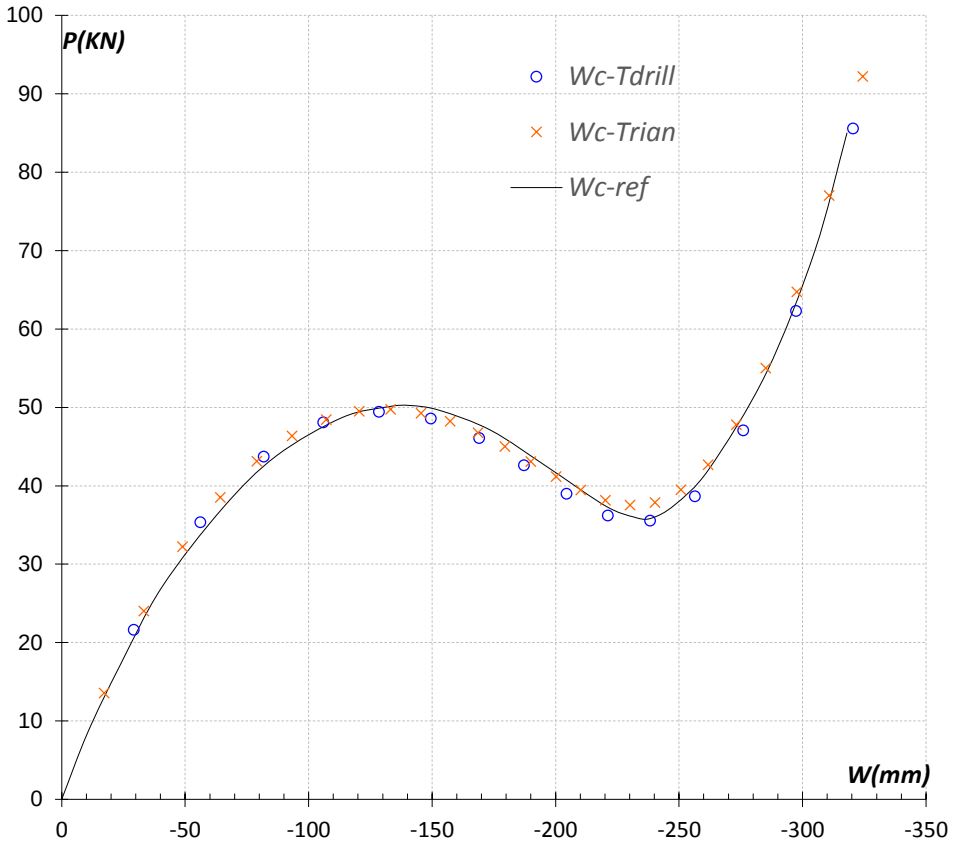

Fig. VII.31. **load-displacement curve of the spherical shell using the triangular elements**

III-2. Linear and Geometrically Non-Linear Dynamic Analysis

III-2.1. Cantilever beam under concentrated load

Fig. VII.32. represents a cantilever beam of dimensions (6"×6"×120") with a constant concentrated load applied at the free end, *Fig. VII.33*. The following material properties are used in the analysis: $E = 30x10^6$ *psi*, Poisson's ratio $\upsilon = 0.3$, and mass $m = 0.000733$ *lbm/in*. The reference solution is taken from: [OZKUL 2004]. The beam is analysed by using 6 equally sized elements with a time step of $\Delta t = 0.004s$ as used for the reference solution.

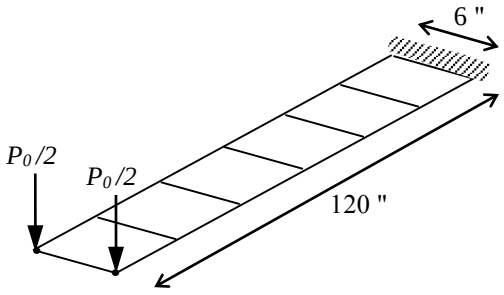

Fig. VII.32. **Geometry and mesh of the cantilever beam**

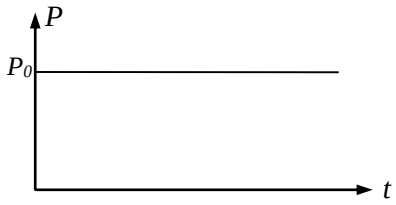

***Fig. VII.33.* Constant applied load**

The normalized vertical displacement time history of the beam tip illustrated in *Fig. VII.34.* obtained by triangular and quadrilateral elements is compared to the reference solutions given in [OZKUL 2004]. The obtained vertical displacement time history curves of the free end at the middle line show an excellent agreement with the reference solution.

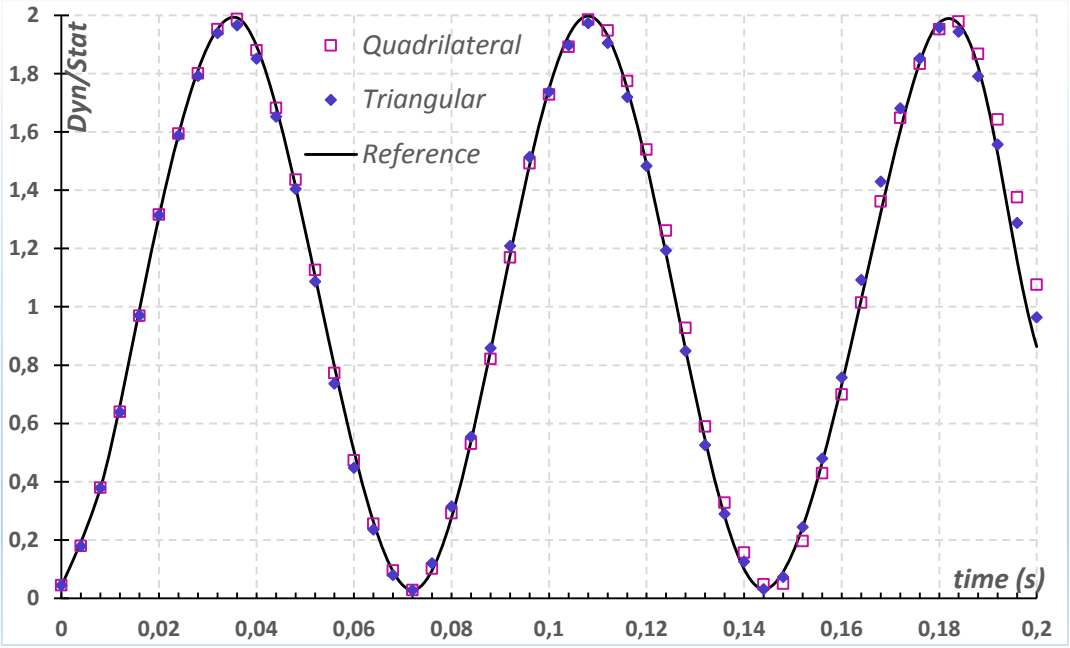

***Fig. VII.34.* Free end vertical displacement time history of the cantilever beam**

III-2.2. Simply-supported rectangular plate under concentrated step load

This example considers the linear and geometrically nonlinear dynamic analysis of a rectangular plate of dimensions: *a =1524 mm* long and *w=1016 mm* wide, with simply supported edges, as presented in *Fig. VII.35*. The plate is subject to the time-dependent concentrated load shown in *Fig. VII.36*. which is applied at the center of the plate, with $\boldsymbol{P_0 = 44.54\ N}$, and $t_0 = 0.006\ s$.

Because of the double symmetry of geometry, loading, and boundary conditions, only one quarter of the plate is required to perform the example using "8×8" elements as for the reference solution taken from: [MEEK & WANG 1998]. The thickness is taken to be *h = 25.4 mm*, Young's

modulus of elasticity is $E = 2.0955 \times 10^8\ N/m^2$, the specific weight is $\rho = 3210.05\ kg/m^3$, and the Poisson's ratio is $\upsilon = 0.25$. For direct time integration of this example, the time step size was taken to be $\Delta t = 0.004\ s$.

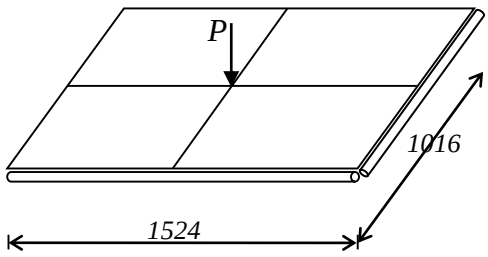

Fig. VII.35. **Geometry of the rectangular plate**

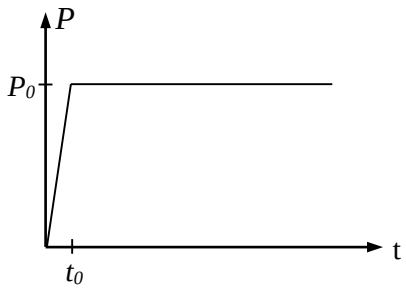

Fig. VII.36. **Time-dependent concentrated load**

The computed displacement time history of the central point, by using the two shell elements with drilling rotation "*Qdrill*" and "*Tdrill*" elements, and by using the two conventional shell elements "*Quad*" and "*Trian*" elements is shown in *Fig. VII.37*. The first observation we made is that the presented shell elements give exactly the same results in linear dynamic analyses, and a close results in geometrically nonlinear analyses. Also, it is observed that the presented shell elements give a very good accurate results accordingly to the results of [MEEK & WANG 1998] in both, linear and geometrically nonlinear dynamic analysis.

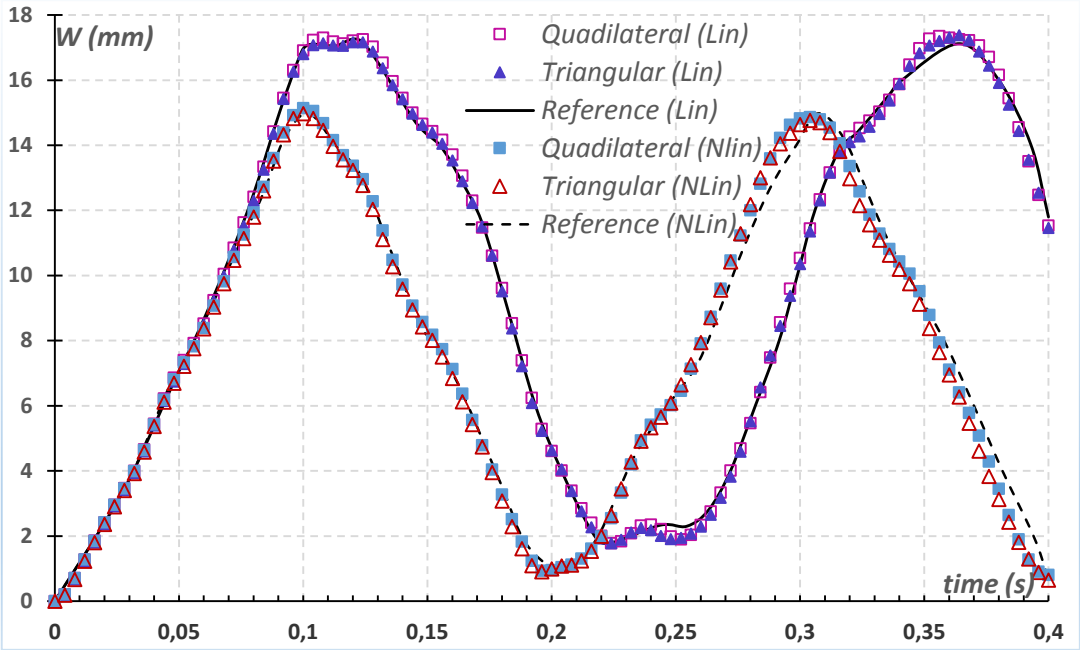

***Fig. VII.37.* Vertical displacement time history of the rectangular plate at the central point**

III-2.3. Simply-supported square plate under uniform step pressure

This example considers the square plate shown in *Fig. VII.38*. The plate is simply supported at the four edges, and subjected to a suddenly applied uniform pressure shown in *Fig. VII.39*.

The plate dimensions are: $a = 254\ mm$, $h = 12.7\ mm$, and it has the following material properties: modulus of elasticity $E = 68950\ MPa$, Poisson's ratio $\upsilon = 0.3$ and mass density $\rho = 2765.8\ kg/m^3$.

Using double symmetry, only "4×4" shell elements are used to model one quarter of the plate.

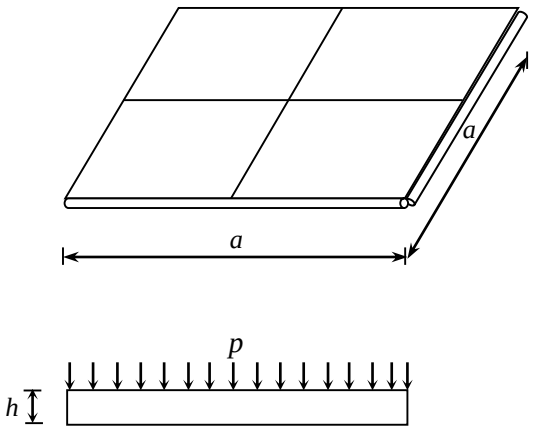

***Fig. VII.38.* Square plate: geometry and loading**

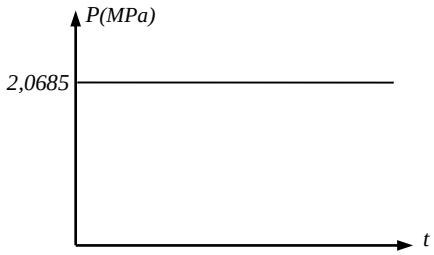

***Fig. VII.39.* Step load**

The linear and nonlinear vertical displacement time history of the central point of the plate are presented in *Fig. VII.40*. and *Fig. VII.41*. In order to check our results, we referred to the solution of [ALI & AL-NOURY 1986], where they solved the problem by finite difference method. We noticed that a close agreement was found with the results of [ALI & AL-NOURY 1986].

In this example, which is a plate structure (bending only). "*Quad*" and "*Trian*" elements with fictitious stiffness needed some extra iterations to achieve equilibrium immediately when the structure exhibits moderate nonlinearity, whereas "*Qdrill*" and "*Tdrill*" shell elements with drilling rotational *d.o.f* elements was more effective even in case when the in-plane behaviour is dominated by bending behaviour.

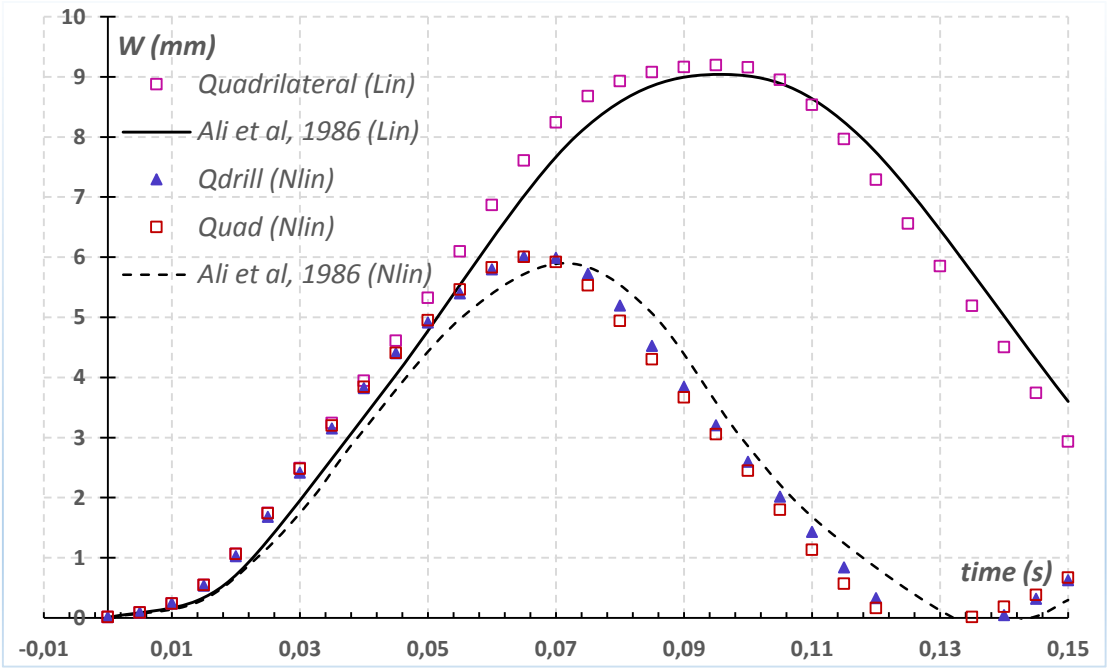

***Fig. VII.40.* Linear and nonlinear vertical displacement time history using the quadrilateral elements**

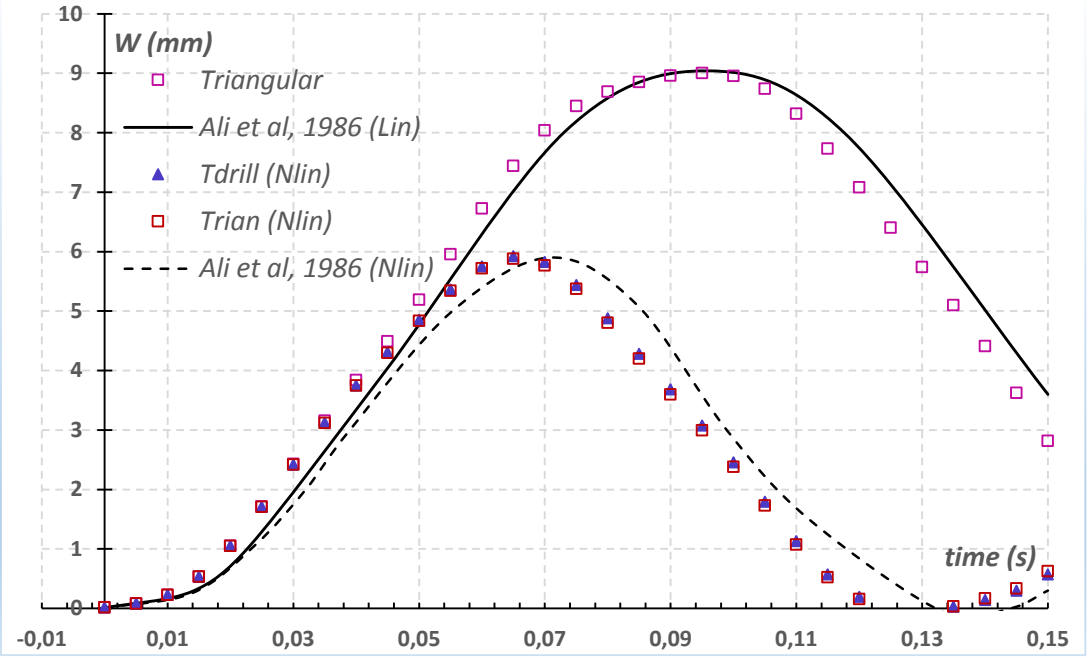

***Fig. VII.41.* Linear and nonlinear vertical displacement time history using the triangular elements**

III-2.4. Hinged cylindrical panel under concentrated load

In this example, the thin cylindrical shell of radius of curvature R, longitudinal length L, thickness h, and opening angle θ of the *Example III-1.2* is studied in linear dynamic regime. The cylindrical shell is subjected to a concentrated load applied at its center. Using double symmetry of the shell structure, only one quarter of the shell is modelled using "4×4" and "8×8" rectangular elements. The geometrical and mechanical characteristics are as follows: $R=2540\,mm$, $L=2540\,mm$; $\theta=0.1\ rad$, $h = 12.7\ mm$, $\upsilon= 0.3$, E = 0.310275 kN/mm^2, and $\rho = 3210.05\ Kg/m^3$.

The time-dependent concentrated load function is shown in *Fig. VII.42*. with $\boldsymbol{P_0} = 400\ N$, and $t_0 = 0.01s$. For dynamic integration, the time step size is taken to be: $\Delta t = 0.001s$.

The obtained vertical displacement time history curves are compared to the reference solution presented in: [MEEK & WANG 1998].

The displacement time history curves obtained using the *"Quad"* and "*Trian*" shell elements with fictitious stiffness given in (*Fig. VII.43*. *Fig. VII.44*. *Fig. VII.45*. and *Fig. VII.46*.) show that a considerable attention must be accorded to the value of the elastic constant of the fictitious stiffness *(α)* when using conventional shell elements.

In this example, several varieties of the value of the elastic constant of the fictitious stiffness *(α)* are used starting from 10^{-10} to 1.0 using both "*Quad*" and "*Trian*" elements.

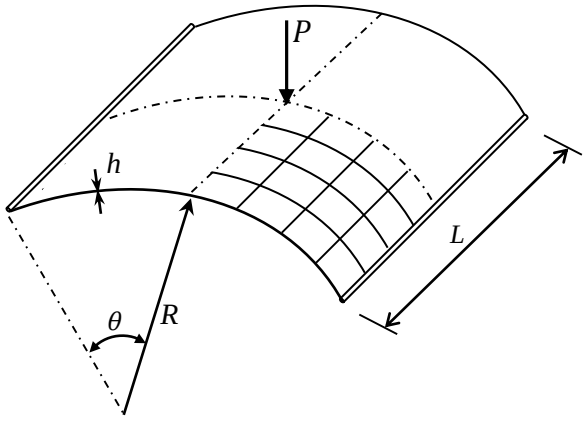

***Fig. VII.42.* Geometry of the cylindrical shell**

From displacement time history curves obtained using "8×8" '*Quad'* elements given in *Fig. VII.43*. and using "8×8×2" '*Trian*' elements given in *Fig. VII.44*. one can deduce that there is a range between $\alpha=10^{-2}$ to $\alpha=10^{-5}$ where the solutions are very close, we conclude that the value of the fictitious stiffness constant (α) must be chosen among the values of this range because values less than 10^{-5} give wrong response, and values greater than 10^{-3} also give wrong response.

When a mesh of "4×4" elements is used, the range limits are changed for the values from $\alpha=10^{-3}$ to $\alpha=10^{-6}$. The intersection of these tow ranges constitute the acceptable values of the (α) constant, which are vary from $\alpha=10^{-3}$ to 10^{-5}.

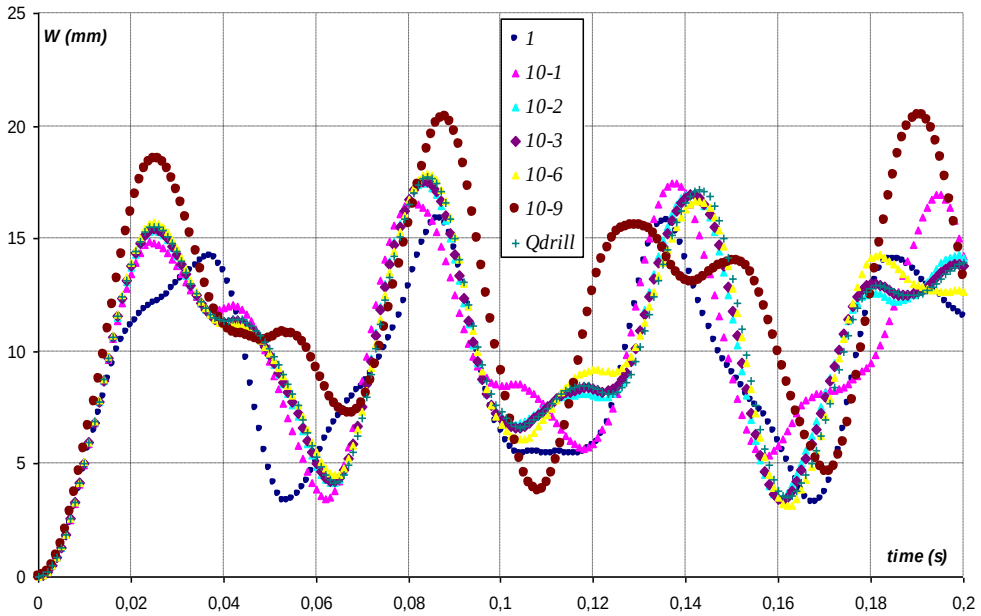

***Fig. VII.43.* Dynamic response of the cylindrical shell using 8×8 "*Quad*" elements**

It can be seen from *Fig. VII.47.* and *Fig. VII.48.* that a good convergence rate was obtained by both "*Trian*" and "*Quad*" elements using $\alpha=10^{-3}$. On the other hand, nonlinear analyses requisites the use of a bigger value of the elastic constant (α) of the fictitious stiffness to unsure numerical equilibrium and to perform the analyses with the least numerical coast.

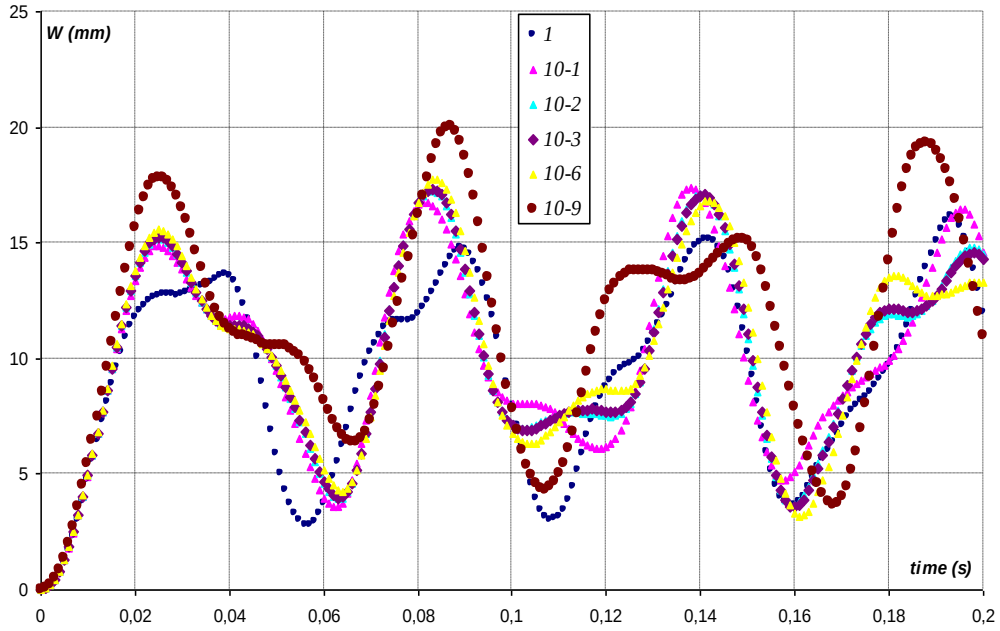

***Fig. VII.44.* Dynamic response of the cylindrical shell using 8×8 "*Trian*" elements**

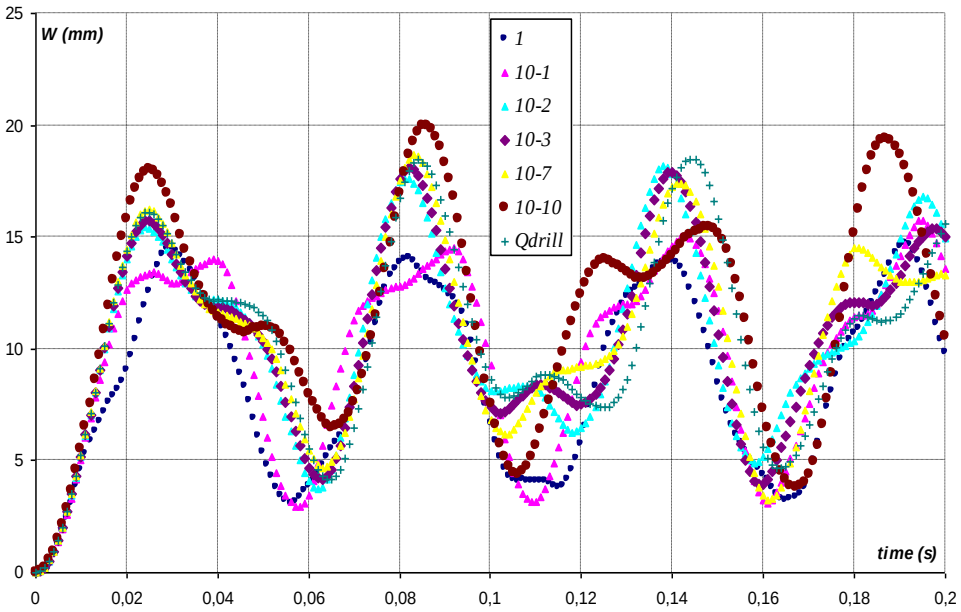

***Fig. VII.45.* Dynamic response of the cylindrical shell using 4×4 "*Quad*" elements**

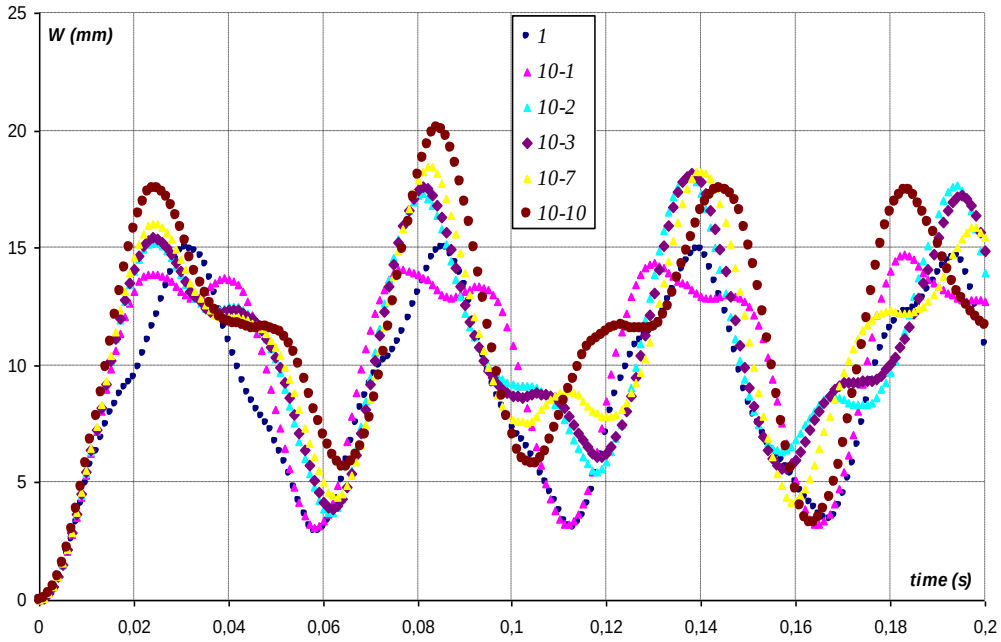

***Fig. VII.46.* Dynamic response of the cylindrical shell using 4×4 "*Trian*" elements**

In this example, the thin cylindrical shell subjected to a concentrated load applied at its center is studied in linear and geometrically nonlinear dynamic regime. The time step size is: $\Delta t = 0.002\ s$.

The time history curves of vertical displacement of point A obtained using a mesh of "8×8" quadrilateral elements is given in *Fig. VII.47.* for "*Qdrill*" shell element, and in *Fig. VII.48.* for "*Tdrill*" element. The obtained results show that an excellent agreement with the solution in the reference [MEEK & WANG 1998] is obtained using "8×8" quadrilateral meshing.

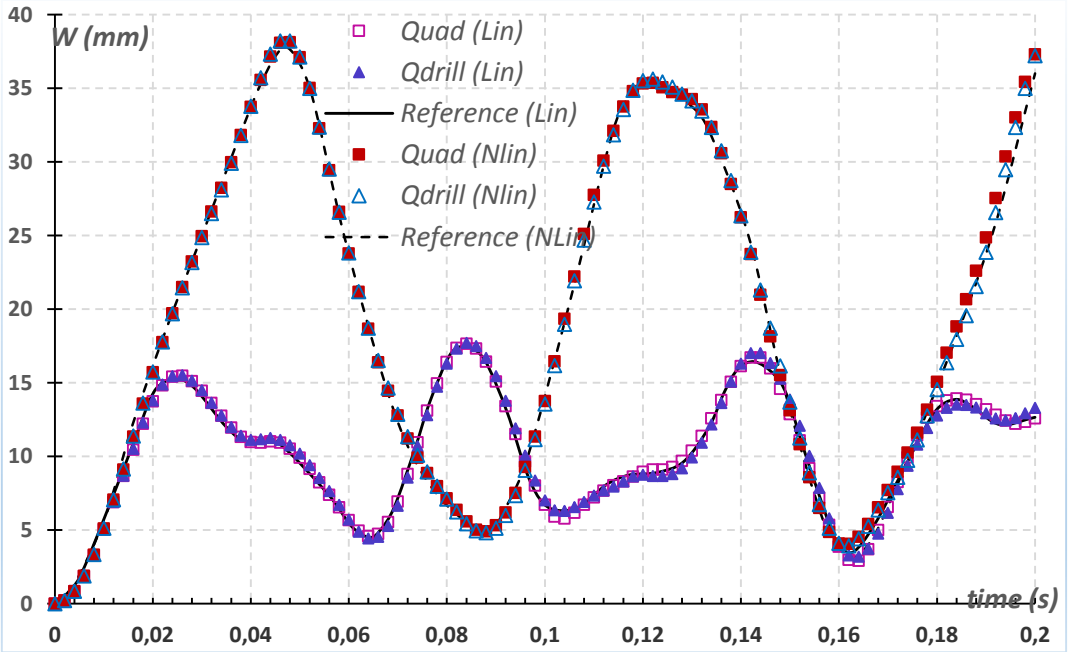

***Fig. VII.47.* Dynamic response of the cylindrical shell using Quadrilateral elements**

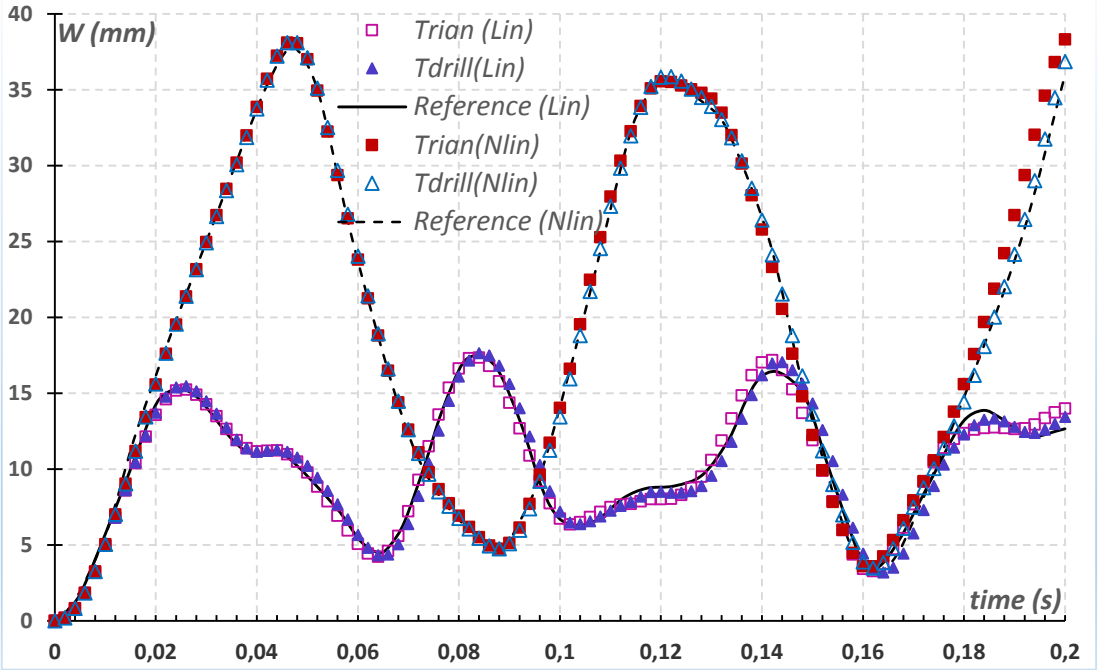

Fig. VII.48. **Dynamic response of the cylindrical shell using triangular elements**

An important factor in this example, is the number of iterations required by each one of the shell elements presented herein to perform the example. To make a comparison, the total number of iterations required to perform this example using "*Qdrill*" element is 522 iteration, while the "*Quad*" element requires 625 iteration. It is easy to see that the solution obtained using "*Qdrill*" element was very faster than the solution obtained by using "*Quad*" element. In this example it is *1.2* time faster. Also, "*Qdrill*" and "*Tdrill*" shell elements ensure more numerical stability comparison to "*Quad*" and "*Trian*" elements. As we could see, for example "*Quad*" element needed 12 iterations within time step when highly nonlinear behaviour is exhibited, which mean that, this element suffers for numerical instability, especially in regions of large nonlinearity. These numerical issues, could led the numerical solution to diverge from the exact solution. Consequently, smaller time step must be used using "*Quad*" and "*Trian*" conventional shell elements. On, the other hand, larger time step could be used safely using "*Qdrill*" and "*Tdrill*" shell elements with drilling rotation.

These results, illustrate that the presented "*Qdrill*" and "*Tdrill*" flat shell elements with drilling rotational *d.o.f*, are powerful and reliable shell elements that could be used for geometrically nonlinear dynamic analysis by direct time integration, especially when the structure response involves highly nonlinear behaviour.

III-2.4. Thin cylindrical shell under uniformly distributed half sin wave loading

A thin cylindrical shell structure having the geometry shown in *Fig. VII.49*. is studied in this example. Vertical displacement of the central point is drawn when the shell is subjected to a uniformly distributed half sinusoidal wave loading with a peak intensity of *4309.2 N/m*^{2} shown in *Fig. VII.50*. The two straight edges of the shell are free, while the curved edges are supported on rigid diaphragms against the in-plane degrees of freedom (u, w, θ_y). The shell geometrical, mechanical and physical characteristics are taken as follows: Radius of curvature $R = 15240\ mm$, longitudinal length $L = 15240\ mm$, thickness $h = 76.2\ mm$, opening angle $\theta = 20°$, poison's ratio $\upsilon = 0.3$, modulus of elasticity E=20685 *MPa*, and weight density $\rho = 1.795\ KPa$.

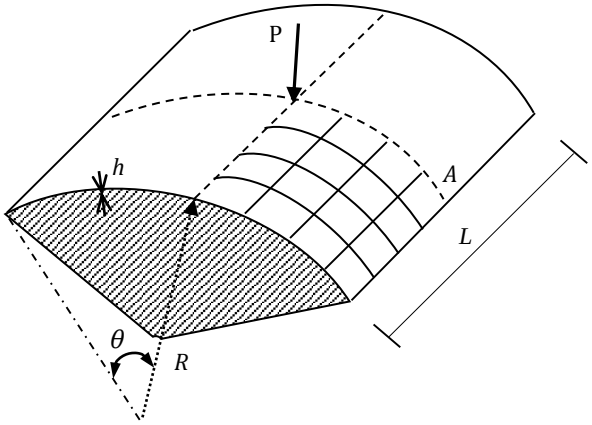

Fig. VII.49. **Cylindrical shell supported on rigid diaphragms**

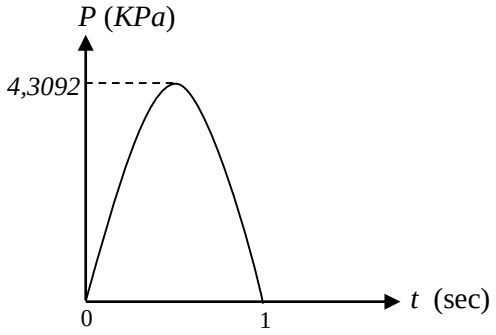

Fig. VII.50. **Half sinusoidal wave loading**

In this example, a complete study has been done. The predominance of nonlinearity has been shown over linear response. The vertical deflection time-history curves of the midpoint of the free edge (point A) are shown in *Fig. VII.51*. and *Fig. VII.52*. The results show that there is good agreement between the present solutions using "4×4" quadrilateral shell elements and the solution presented in [CLOUGH & WILSON 1971].

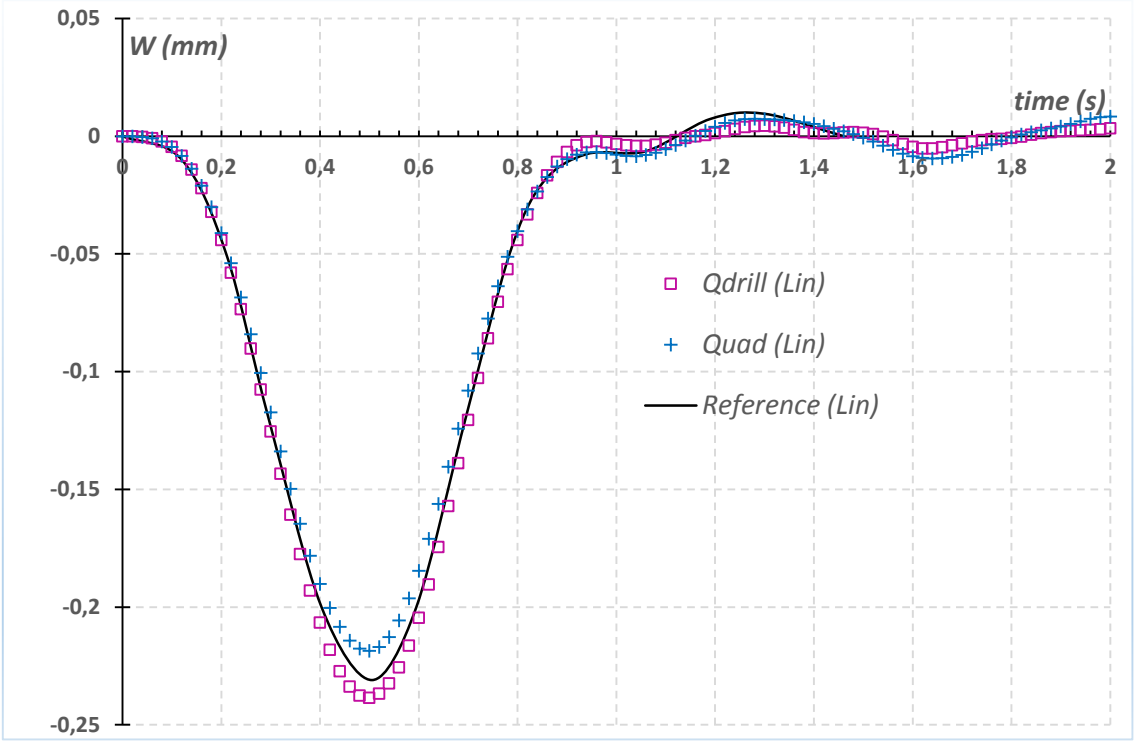

Fig. VII.51. **Linear vertical displacement time history using the quadrilateral elements**

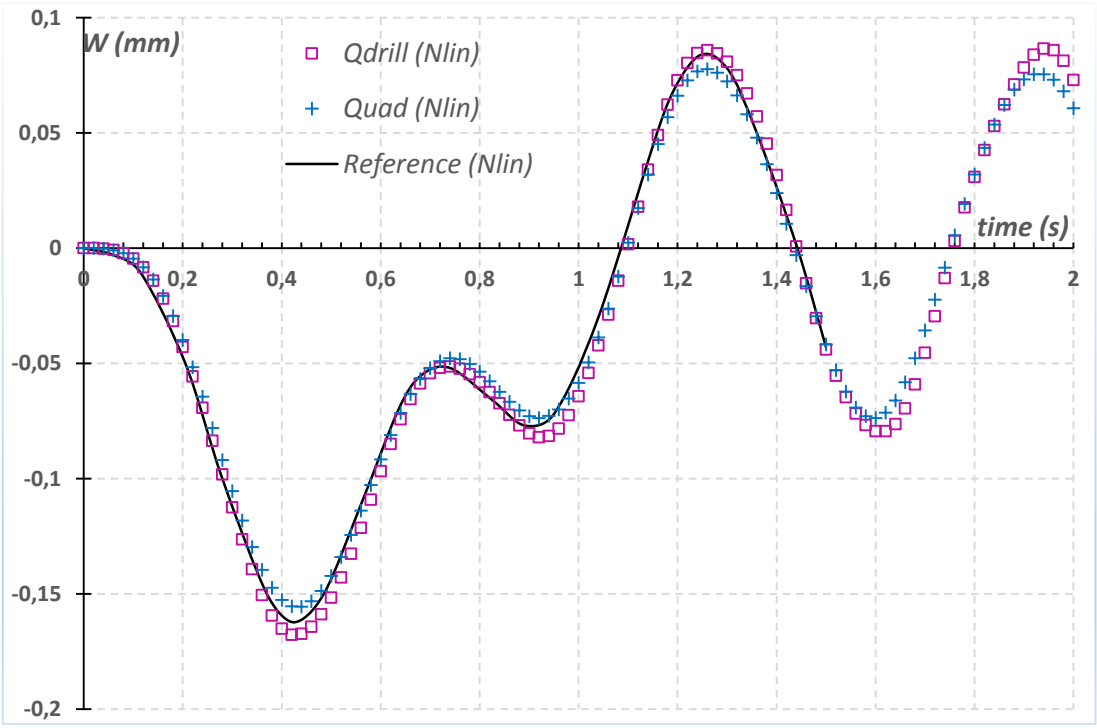

Fig. VII.52. **Nonlinear vertical displacement time history using the quadrilateral elements**

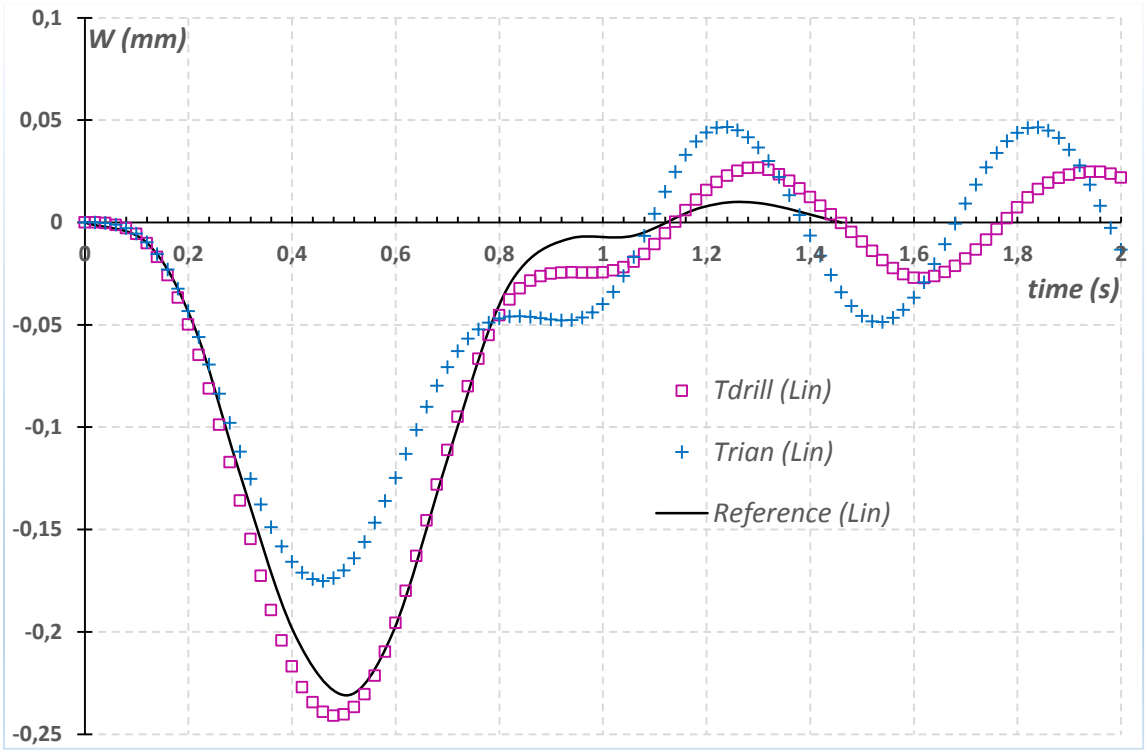

Fig. VII.53. **Linear vertical displacement time history using the triangular elements**

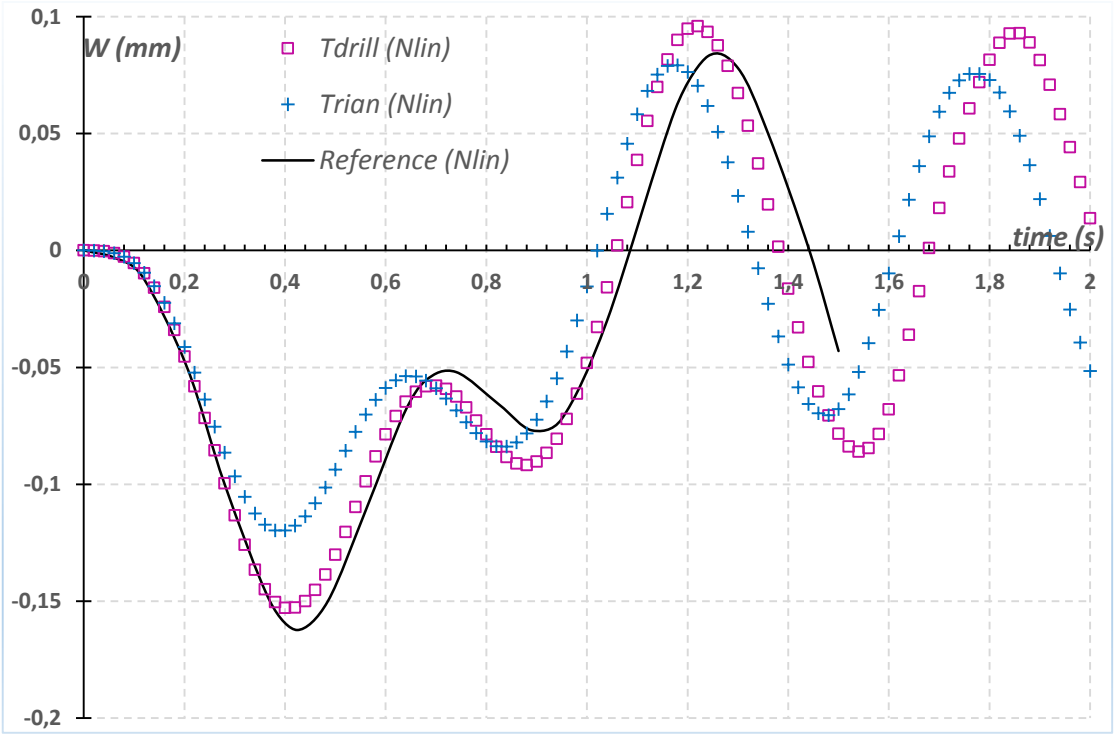

Fig. VII.54. **Nonlinear vertical displacement time history using the triangular elements**

IV- DISCUSSION

As we have seen, the co-rotational Lagrangian discerption of motion has proven to be a simple and efficient formulation to handle large in-plane rotations. When this formulation is extended to formulate a flat shell finite element with six *d.o.f,* we get a powerful shell finite element for linear and geometrically nonlinear static and dynamic analysis.

When fictitious stiffness is used, a small rotational rigidity specified by the user is added into the stiffness matrix. It's a simple solution but it has some serious disadvantages. The more important one, is that the value of that fictitious stiffness that gives accurate results is dependent on the analysis to be performed. In linear analysis, this value must be as small as possible to obtain accurate results, but big enough to avoid ill-conditioned stiffness matrix when all the elements meeting at a node are co-planar. A value of the constant $\alpha=10^{-3}$ seems to be the optimum. Also, in linear dynamic analysis, the optimum value that gives acceptable results is in order of $\alpha=10^{-3}$, which is convenient for accurate linear analysis. Unluckily, in geometrically nonlinear analysis, small values of the fictitious stiffness cannot be used safely, because in highly nonlinear problems, small value will cause serious convergence difficulties, so the fictitious stiffness value have to be increased to unsure convergence and numerical stability. A value of 10^{-3} or greater must be adopted for the constant α to perform the examples of nonlinear analysis. However, too large value may also cause the solution to diverge, or even worse, the solution may succeed, but the answers may be inaccurate.

By analysing the results obtained by "*Tdrill*" and "*Qdrill*" shell elements with drilling rotation, and those of "*Trian*" and "*Quad*" shell elements with fictitious stiffness, we can easily see that elements with drilling rotation, require less number of iterations in nonlinear static or dynamic analysis compared to the very large number of iterations and numerical instabilities that shell elements with fictitious rigidity exhibit. We think that in case of shell elements with fictitious stiffness, in-plane rotations result from the artificial stiffness can't be used in the process of correction of equilibrium by minimization of residual unbalanced forces, because in-plane stress and internal forces are related to in-plane translations only. Contrary, the natural interpolation of the in-plane rotational degree of freedom, makes it possible to calculate strain and stress due in-plane rotation, to be used in the equilibrium correction process. Thus, on one hand, shell elements with drilling rotation show a great numerical stability and less numerical cost in critical situations, even when the response involves large nonlinear behaviour. Also, they do finite in-plane rotations and they can represent true in plane dynamic response. On the other hand, one can see that the conventional membrane elements, decline the performances and capacities of convergence of the resulting flat shell finite element because of the absence of natural rotational in-plane rigidity.

CONCLUSION

CONCLUSION

This thesis, presents an investigation and contribution in linear and geometrically nonlinear static and dynamic analysis of three-noded triangular and four-noded quadrilateral membrane elements with drilling rotational degree of freedom. First, we presented the development and interpolation of a new triangular membrane element with rotational degree of freedom based on the EAS formulation. This method provides a valuable enrichment to the displacement field of the presented triangular membrane element leading to a locking free triangular element with in-plane rotation with improved behaviour. This in-plane rotational degree of freedom, however, does not represent the true drilling rotation.

The presented triangular and quadrilateral membrane elements for linear analysis have extended to perform:

- Geometrically nonlinear large displacements and large rotations analysis, by means of the co-rotational updated Lagrangian formulation. In this purpose, a new co-rotational formulation is developed and presented for both triangular and quadrilateral membrane elements with drilling rotation, also, geometric stiffness matrix that takes into account the effect of the in-plane rotational drilling degree of freedom is included.
- Linear transient dynamic analysis using the Newmark direct time integration method. In this section we developed in-plane mass matrices taking into account the in-plane rotational inertia for triangular and quadrilateral elements with drilling rotation.
- Geometrically nonlinear dynamic analysis by combining the above mentioned methods.

The proposed numerical tests for both triangular and quadrilateral membrane elements with in-plane rotational *d.o.f*, show that these elements exhibit very good performances and could return true in-plane rotational vibrational modes when using a convenient mass matrix that takes into account the in-plane rotational inertia corresponds to the drilling rotation. Furthermore, when using a well-chosen co-rotational formulation, these elements can efficiently handle finite in-plane rotations, and exhibit good performances for both nonlinear static and nonlinear dynamic analysis. The co-rotational updated Lagrangian formulation has confirmed to be very efficient for nonlinear large displacements analysis, and it has proven to be an effective formulation to handle not only moderate but also large rotations problems.

The presented membrane elements, have extended to be a part of flat shell finite elements by combining hem with the well-known “DKT” and “DKQ” thin plate bending elements. The obtained shell elements are implemented into geometrically nonlinear static and dynamic

analysis. A complete analysis of the usual strategies to introduce the in-plane rotations into the shell element's displacement field is presented, including the drilling rotation and the artificial fictitious stiffness strategy applied onto translation-only membrane formulations. The resulting shell elements providing a complete degrees-of-freedom field, which are the "*Qdrill*" and "*Tdrill*" flat shell elements with drilling rotation, and the "*Quad*" and "*Trian*" flat shell elements with fictitious stiffness, are implemented and assessed.

Several numerical examples were solved to demonstrate the accuracy of the formulation for both static and dynamic, small and large displacements and rotations analysis of plates and shells. The results were compared with those available in the existing literature.

As evidenced by the obtained results, shell elements based on the membrane formulation with drilling rotations perform significantly better relatively to the formulation without the drilling rotation component. The efficiency of the "*Qdrill*" and "*Tdrill*" flat shell elements for geometrically nonlinear analysis using the co-rotational updated Lagrangian formulation, and for linear and nonlinear transient dynamic analyses using the Newmark implicit direct time integration method has been shown.

When a flat shell element with fictitious stiffness is used for the analysis of general shells, especially in the case of problems involving large rotations, a finer mesh, large number of load steps, and small time intervals are mandatory in order to obtain a closer approximation towards the exact solution or finite element solution available in the existing literature. This is no longer required when using shell elements with drilling rotation, which leads to a computationally more efficient and economic analysis, mainly due to the extreme simplicity of the flat shell elements formulation.

Several examples have been solved with various types of geometry and loading, the obtained results show that the "*Qdrill*" and "*Tdrill*" flat shell elements exhibit very good performances in comparison to the other shell elements with fictitious stiffness. They also show a great numerical stability and less numerical cost in critical situations when the structure response involves large nonlinear behaviour, and thus, we can conclude that these elements are very powerful and much efficient for geometrically nonlinear static and dynamic analysis of general shell structures. We can see that the interpolation of the in-plane rotational *d.o.f* has a major advantage on the flat shell element response, and such flat shell element could be a good candidate for general shell structural analysis in engineering practice.

BIBLIOGRAPHY

BIBLIOGRAPHY

-A-

Adini, A., Clough, R. W., 1960. Analysis of Plate Bending by the Finite Element Method. NSF Report, Grant, G7337.

Afaq, K.S., Karama, M., Mistou S., 2003. Un nouveau modèle rafiné pour les structures multicouches. In Comptes-rendus des 13èmes Journées Nationales sur les Composites, pp. 289-292. Strasbourg, March.

Ahmad S., 1969. Curved finite element in the analysis of solid shells and plates structures. Ph.D Thesis, University of Wales, Swansea.

Ahmad, S., Irons, B.M., Zienkiewicz, O.C., 1970. Analysis of thick and thin shell structures by curved finite elements. Int. J. Num. Meth. Eng, 2: 419-451.

Ahmed, A., Sluys, L.J., 2014. Implicit/explicit elastodynamics of isotropic and anisotropic plates and shells using a solid-like shell element. European Journal of Mechanics. A/Solids, 43: 118-132.

Ali, S.A., Al-Noury, S. I., 1986. Nonlinear dynamic response of rectangular plates. Comput. Struct, 22(3): 433-437.

Allman, D.J., 1970. Triangular finite elements for plate bending with constant and linearly varying bending moments. In: Proc. IUTAM Symposium on High Speed Computing of Elastic Structures, University of Liege. pp. 105-136.

Allman, D.J., 1984. A Compatible Triangular Element Including Vertex Rotations for Plane Elasticity Analysis. Comput. Struct, 19: 1-8.

Allman, D.J., 1988-a. Evaluation of the Constant Strain Triangle with Drilling Rotations. Int. J. Num. Meth. Eng., 26: 2645-2655.

Allman, D.J., 1988-b. Quadrilateral finite elernent including vertex rotations for plane elasticity analysis. Int. J. Num. Meth. Eng, 26: 717-730.

Allman, D.J., 1988-c. The constant strain triangle with drilling rotations: a simple prospect for shell analysis. In Mathematics of Finite Elements and Applications VI, (Edited by J. R. Whiteman), pp. 233-240. Academic Press, New York.

Allman, D.J., 1991. Analysis of general shells by flat facet finite element approximation. Aeronaut. J, 95: 194-203.

Allman, D.J., 1993. Variational validation of a membrane finite element with drilling rotations. Commun. Num. Meth. Eng, 9: 345-351.

Allman, D.J., 1994. A basic flat facet finite element for the analysis of general shells. Int. J. Num. Meth. Eng, 37: 19-35.

Allman, D.J., 1996. Implementation of a flat facet shell finite element for applications in structural dynamics. Comput. Struct; 59(4): 657-663.

Allman, D.J., Morley, L.S.D., 2000. The "constant" bending moment three-noded triangle. Commun. Num. Meth. Eng, 9: 345-351.

Almeida, F.S., Awruch, A.M., 2011. Corotational nonlinear dynamic analysis of laminated composite shells. Finite. Elem. Anal. Des 47: 1131-1145.

Alvin, K., Fuente, H.M., Haugen, B., Felippa, C.A., 1992. Membrane triangles with corner drilling freedoms. I. The EFF element. Finite. Elem. Anal. Des, 12: 163-187.

Aminpour, M.A., 1992-a. An assumed-stress hybrid 4-node shell element with drilling degrees of freedom. Int. J. Num. Meth. Eng, 33: 19-38.

Aminpour, M.A., 1992-b. Direct formulation of a hybrid 4-node shell element with drilling degrees of freedom. Int. J. Num. Meth. Eng, 35: 997-1013.

An, X.M., Xu, M., 2011. An improved geometrically nonlinear algorithm and its application for nonlinear aeroelasticity. Chin. J. Theoret. Appl. Mech, 43 (1): 97-104.

Andelfinger, U., Ramm, E., 1993. EAS-elements for two-dimensional, three-dimensional, plate and shell structures and their equivalence to hr-elements. Int. J. Num. Meth. Eng, 36: 1311-1337.

Archer, R.R., Lange, C.G., 1965. Nonlinear dynamic behavior of shallow spherical shells. AIAA J, 3(12): 2313-2317.

Areias, P., Garção, J., Pires, E.B., Barbosa, J.I., 2011. Exact corotational shell for finite strains and fracture. Comput. Mech, 48: 385-406.

Argyris, J.H., 1965-a. Triangular elements in plate bending-conforming and nonconforming solutions. Proc. Conf. Matrix Meth. Struc. Mech., pages 11-190, Air Force Institute of Technology, Wright-Patterson A.F.B., Ohio.

Argyris, J.H., 1965-b. Matrix analysis of three-dimensional elastic media - small and large displacements. AIAA J, 3(1): 45-51.

Argyris, J.H., 1965-c. Continua and discontinua, in: Opening Address to the International Conference on Matrix Methods of Structural Mechanics, Dayton, OH, Wright- Patterson U.S. A.F. Base, October 26.

Argyris, J.H., 1982. An excursion into large rotations, Comp. Meth. Appl. Mech. Eng. 32; 85-155.

Argyris, J.H., Balmer, H., Doltsinis, J.St., Dunne, P.C., Haase, M., Muller, M. Scharpf, W.D., 1979. Finite Element Method- The Natural Approach. Comp. Meth. Appl. Mech. Eng, 17/18: 1-106.

Argyris, J.H., Dunne, P.C. 1975. On the application of the natural mode technique to small strain large displacement problems. World Congress on Finite Element Methods in Structural Mechanics, Bournemouth.

Argyris, J.H., Dunne, P.C., Malejanakis, G.A., Schekle, E., 1977-a. A simple triangular facet shell element with applications to linear and nonlinear equilibrium and inelastic stability. Comp. Meth. Appl. Mech. Eng, 10: 371-403.

Argyris, J.H., Fried, I., Scharpf, D.W., 1968. The TUBA family of plate elements for the matrix displacement method. Aeron. J. Roy. Aeron. Soc, 72: 701–709.

Argyris, J.H., Haase, M., Mlejnek, H.P., 1977-b. On an unconventional but natural formation of the stiffness matrix, Comp. Meth. Appl. Mech. Eng, 22: 371-403.

Argyris, J.H., Haase, M., Mlejnek, H.P., 1980. On an unconventional but natural formation of the stiffness matrix. Comp. Meth. Appl. Mech. Eng, 22: 371-403.

Argyris, J.H., Haase, M., Mlejnek, H.P., Schmolz, P.K., 1986. TRUNC for shell - an element possibly to the taste of Bruce Irons. Int. J. Num. Meth. Eng, 22: 93-115.

Argyris, J.H., Papadrakakis, M., Apostolopoulou, C., Koutsourelakis, S., 1999. The TRIC shell element: Theoretical and numerical investigation. Comp. Meth. Appl. Mech. Eng, 118: 63-119.

Argyris, J.H., Scharpf, D.W., 1968-a. The SHEBA family of shell elements for the matrix displacement method, Part I, Natural definition of geometry and strains. Aeron. J. Roy. Aeron. Soc., 72: 873–878.

Argyris, J.H., Scharpf, D.W., 1968-b. The SHEBA family of shell elements for the matrix displacement method, Part II. Interpolation scheme and stiffness matrix. Aeron. J. Roy. Aeron. Soc., 72: 878–883.

Argyris, J.H., Tenek, L., 1993. Natural triangular layered element for bending analysis of isotropic, sandwich, laminated composite and hybrid plate. Comp. Meth. Appl. Mech. Eng, 109: 197-218.

Argyris, J.H., Tenek, L., 1994. An efficient and locking free flat anisotropic plate and shell triangular element, Comp. Meth. Appl. Mech. Eng, 118: 63-119.

Argyris, J.H., Tenek, L., Olofsson, L., 1997. TRIC: a simple but sophisticated 3-node triangular element based on 6 rigid body and 12 straining modes for fast computational simulations of arbitrary isotropic and laminated composite shells. Comp. Meth. Appl. Mech. Eng, 145: 11-85.

Argyris, J.H., Tenek, L., Papadrakakis, M., Apostolopoulou, C., 1998. Postbuckling performance of the TRIC natural mode triangular element for isotropic and laminated composite shells. Comp. Meth. Appl. Mech. Eng. 166: 211-231.

Aron, H., 1874. Das Gleichgewicht und die Bewegung einer unendlich dunnen, beliebig gekrummten, elastichen schale. Zeit. Reine Angew. Math., Vol. 78.

Ashwell, D.G., Sabir, A.B., 1972. A new cylindrical shell finite element based on simple independent strain functions. Int. J. mech. Sci, 14: 171-183.

-B-

Barbero, E.J., Madeo, A., Zagari, G., Zinno, R., Zucco, G., 2014. A mixed isostatic 24 dof element for static and buckling analysis of laminated folded plates. Composite Structures, 116: 223-234.

Basar, Y., 1987. A consistent theory of geometrically nonlinear shells with an independent rotation vector. Int. J. Solids. Struct, 23: 1401-1415.

Basar, Y., Ding, Y., 1990. Finite rotation elements for the nonlinear analysis of thin shell structures. Int. J. Solids. Struct. 26: 83-97.

Basar, Y., Ding, Y., 1992. Finite rotation shell elements for the analysis of finite rotation shell problems. Int. J. Num. Meth. Eng, 34: 165-169.

Bathe, K.J., 1982. Finite Element Procedures in Engineering Analysis, Prentice-Hall, Englewood Cliffs, New Jersey.

Bathe, K.J., Baig, M.I., 2005. On a composite implicit time integration procedure for nonlinear dynamics. Comput. Struct, 83(31-32) : 2513-2524.

Bathe, K.J., Bolourchi, S., 1979. Large displacement analysis of three-dimensional beam structures. Int. J. Num. Meth. Eng, 14: 861-886.

Bathe, K.J., Bolourchi, S., 1980. A geometric and material non-linear plate and shell element. Comput. & Struct, 11: 23-48.

Bathe, K.J., Dvorkin, E.N, 1983-a. Our discrete Kirchhoff and isoparametric shell elements for nonlinear analysis. An assessment. Comput. Struct, 16: 89-98.

Bathe, K.J., Dvorkin, E.N, 1983-b. On the automatic solution of non-linear finite element equations. Comput. Struct, 17(5-6): 871-879.

Bathe, K.J., Dvorkin, E.N, 1986. A formulation of general shell elements-the use of mixed interpolation of tensorial components. Int. J. Num. Meth. Eng, 22: 697-722.

Bathe, K.J., Dvorkin, E.N., Ho, L.W., 1983. Our Discrete-Kirchhoff and Isoparametric Shell Elements for Nonlinear Analysis - An Assessment. Comput. Struct, 16: 89-98.

Bathe, K.J., Gracewski, S., 1981.On nonlinear dynamic analysis using substructig and mode superposition. Comput. Struct, 13 (5-6): 699- 707.

Bathe, K.J., Ho, L.W., 1981. A simple and effective element for analysis of general shell structures. Comput. Struct, 13: 673-681.

Bathe, K.J., Ozdemik, H., 1975. Elastic plastic large de formation static and dynamic analysis. Comput. Struct, 6: 81-92.

Bathe, K.J., Ozdemik, H., Wilson, E.L., 1974. Static and dynamic geometric and material nonlinear analysis. Technical Report UC SESM 74-4, Univ. California. Berkley.

Bathe, K.J., Ramm, E., Wilson, E.L., 1975. Finite element formulations for large deformation dynamic analysis. Int. J. Num. Meth. Eng, 9(2): 353-386.

Bathe, K.J., Wilson, E.L., 1973. Stability and accuracy analysis of direct integration methods. Eurthquake Engineering and Structural Dynamics, 1: 283-291.

Batoz, J.L., 1982. An explicit formulation for an efficient triangular plate-bending element. Int. J. Num. Meth. Eng, 18: 1077-1089.

Batoz, J.L., Bathe, K.J., Ho, L.W., 1980. A study of three-node triangular plate bending elements. Int. J. Num. Meth. Eng, 15: 1771-1812.

Batoz, J.L., Ben-Tahar, M., 1982. Evaluation of a new quadrilateral thin plate bending element. Int. J. Num. Meth. Eng, 18: 1655-1677.

Batoz, J.L., Chartopadhyay, A., Dhatt, G., 1976. Finite element large deflection analysis of shallow shells. Int. J. Num. Meth. Eng, 10(1): 39-58.

Batoz, J.L., Dhatt, G., 1972. Development of two simple shell elements. AIAA, 10: 237-238.

Batoz, J.L., Dhatt, G., 1979. Incremental displacement algorithm for nonlinear problems. Int. J. Num. Meth. Eng, 15: 1262-1267.

Batoz, J.L., Dhatt, G., 1990. Modélisation Des Structures Par Eléments Finis, Poutres et Plaques, vol.2, Hermes.

Batoz, J.L., Hammadi, F., Zheng, C., Zhong, W., 1998-b. On the linear analysis of plates and shells using a new sixteen dof flat shell element. In Advances in Finite Element Procedures and Techniques, pages 31-41, Civil-Comp Press, Edinburgh.

Batoz, J.L., Hammadi, F., Zheng, C., Zhong, W., 2000. On the linear analysis of plates and shells using a new-16 degrees of freedom flat shell element. Comput. Struct, 78: 11-20.

Batoz, J.L., Hammadi, F., Zheng, C.L., Zhong, W.X., 1998-a. A new discrete Kirchhoff 8 DOF quadrilateral element for plate bending analysis. Internal Report, UTC, LGZMS.

Batoz, J.L., Lardeur, P., 1989. A discrete shear triangular nine D.O.F. element for the analysis of thick to very thin plates. Int. J. Num. Meth. Eng, 28: 533-560.

Batoz, J.L., Zheng, C.L., Hammadi, F., 2001. Formulation and evaluation of new triangular, quadrilateral, pentagonal and hexagonal discrete Kirchhoff plate/shell elements. Int. J. Num. Meth. Eng, 52: 615-630.

Battini, J.M., 2007. A modified corotational framework for triangular shell elements. Comp. Meth. Appl. Mech. Eng., 196: 1905-1914.

Battini, J.M., Pacoste, C., 2004. On the choice of local element frame for corotational triangular shell elements. Commun Numer Methods Engrg, 20: 819-825.

Battini, J.M., Pacoste, C., 2006. On the choice of the linear element for corotational triangular shells. Comp. Meth. Appl. Mech. Eng, 195: 6362-6377.

Bazant, Z.P., Nimeiri, M.E., 1973. Large-deflection spatial buckling of thin walled beams and frames. ASCE J. Eng. Mech. Div. EM 6.

Bazeley, G.P., Cheung, Y.K., Irons, B.M., Zienkiewicz, O.C., 1966. Triangular Elements in Plate Bending, Conforming and Nonconforming Solutions", Proc. 1st Conf. 1st Conference on Matrix Methods in Structural Mechanics, pp. 547-576, Wright Patterson AF Base, Ohio.

Bazzi, G., Anderheggen, E., 1982. The p- family of algorithms for time step integration with improved numerical dissipation, Earthquake Engineering and Structural Dynamics, 10: 537-550.

Beitch, L., 1966. Shell structures solved numerically by using a network of partial panels, In Proc. AIAA/ASME Seventh Struc and Mater. Conf., pp. 35-44.

Belarbi, M.T., Bourezane, M., 2005. On improved Sabir triangular element with drilling rotation. Revue Européenne de Genie Civil, 9: 1151-1175.

Belarbi, M.T., Maalam, T., 2005. On improved rectangular finite element for plane linear elasticity analysis, Revue Européenne des Eléments Finis, 40: 985-997.

Bell, K., 1969. A Refined Triangular Plate Bending Finite Element. Int. J. Num. Meth. Eng, 1: 101-122.

Beltrami, E., 1881. Sull equilibrie delle supperficie flessibili ed inestendibili. Mem. Roy. Acad. Sci di Bologna.

BELUNI, P.X., CHULYA, A., 1987. An Improved Automatic Incremental Algorithm for the Efficient Solution of Nonlinear Finite Element Equations. Comput. Struct. 26(1/2): 99-110.

Belytschko, T., 1976. A Survey of Numerical Methods and Computer Programs for Dynamic Structural Analysis. Nuclear Engineering and Design, 37: 23-34.

Belytschko, T., Bachrach, W.E., 1985. Simple quadrilaterals with high coarse-mesh accuracy, Winter Annual Meeting of the American Society of Mechanical Engineers, Miami Beach Florida, November 17-22, 39-56. AMD-Vol. 73.

Belytschko, T., Bindeman, L.P., 1993. Assumed strain stabilization of eight node hexahedral element. Comp. Meth. Appl. Mech. Eng, 105: 225-260.

Belytschko, T., Glaum, L.W., 1979. Application of higher order corotational stretch theories to nonlinear finite element analysis. Comput. Struct, 10: 175-182.

Belytschko, T., Hsieh, B.J., 1973. Nonlinear Transient Finite Element Analysis with Coveected Co-ordinates. Int. J. Num. Meth. Eng, 7: 255-271.

Belytschko, T., Hsieh, B.J., 1974. Nonlinear Transient Analysis of Shells and Solids of Revolution by Convected Elements, AIAA J, 12(8): 1031-1035.

Belytschko, T., Leviathan, I., 1994. Physical stabilization of 4-node shell element with one-point quadrature. Comp. Meth. Appl. Mech. Eng, 113: 321-50.

Belytschko, T., Lin, J., Tsay, C.S., 1984-b. Explicit algorithms for the nonlinear dynamics of shells. Comp. Meth. Appl. Mech. Eng, 42: 225-251.

Belytschko, T., Mullen, R., 1976. Mesh partitions of explicit-implicit time integration, U.S-Germany Symp. on Formulations and Comp. Algorithms in FE Analysis, MIT, Cambridge, MA, August.

Belytschko, T., Ong, J.S.J., Liu, W.K., Kennedy, J.M., 1984-a. Hourglass control in linear and nonlinear problems. Comp. Meth. Appl. Mech. Eng, 43: 251-276.

Belytschko, T., Schwer, L., 1977. Large displacement transient analysis of space frames. Int. J. Num. Meth. Eng, 11: 65-84.

Belytschko, T., Stolarski, H., Liu, W.K., Carpenter, N., Ong, J.S.J., 1985. Stress projection for membrane and shear locking in shell finite elements. Comp. Meth. Appl. Mech. Eng, 51: 221-258.

Belytschko, T., Wong, B.L., Chiang, H.Y., 1992. Advances in one-point quadrature shell elements. Comp. Meth. Appl. Mech. Eng, 96(1): 93-107.

Belytschko, T., Wong, B.L., Stolarski, H., 1989. Assumed strain stabilization procedure for the 9-node Lagrange shell element. Int. J. Num. Meth. Eng, 28: 385-414.

Bergan, P.G., 1967. Plane stress analysis using the finite element method. Triangular element with 6 parameters at each node, Division of Structural Mechanics, The Norwegian Institute of Technology, Trondheim, Norway.

Bergan, P.G., 1978. Solution techniques for non-linear finite element problems, Int. J. Num. Meth. Eng. 12(11): 1677-1696.

Bergan, P.G., 1980-a. Finite elements based on energy orthogonal functions. Int. J. Num. Meth. Eng, 15: 1541-1555.

Bergan, P.G., 1980-b. Solution algorithms for nonlinear structural problems. Comput. Struct, 12: 497-510.

Bergan, P.G., Felippa, C.A., 1985. A Triangular Membrane Element with Rotational Degrees of Freedom. Comp. Meth. Appl. Mech. Eng, 50: 25-69.

Bergan, P.G., Hanssen, L., 1976. A new approach for deriving good finite elements. In: Whiteman JR, editor. The Mathematics of Finite Elements and Applications, vol. II, MAFELAP II Conference, Brunel University, Academic Press: London, pp. 483-497.

Bergan, P.G., Horrigmoe, G., Krakeland, B., Soreide, T.H., 1978. Solution techniques for nonlinear finite element problems. Int. J. Num. Meth. Eng, 12: 1677-1696.

Bergan, P.G., Nygård, M.K., 1981. Plate bending elements based on orthogonal functions. New Concepts in Finite Element Analysis (Edited by T. J. R. Hughes et al.), ASME, AMD, 44: 209-224.

Bergan, P.G., Nygård, M.K., 1984. Finite elements with increased freedom in choosing shape functions. Int. J. Num. Methods Eng, 20: 643-664.

Bergan, P.G., Nygård, M.K., 1986. Nonlinear shell analysis using free formulation finite element. In K.J. Bathe and W. Wunderlich (Eds.), Finite Element Method for Nonlinear Problems, Springer, Heidelberg, Germany, 317-337.

Bergan, P.G., Nygård, M.K., Wang, X., 1982. A class of quadrilateral plate bending elements. Proc. Int. Conf. On Finite Element Methods, Shangai.

Bergan, P.G., Wang, X., 1984. Quadrilateral plate bending elements with shear deformations. Comput. Struct, 19(1-2): 25-34.

Bernadou, M., Ducatel, Y., Trouvé, P., 1988. Approximation of a circular cylindrical shell by Clough-Johnson flat plate finite elements. Numer. Math, 52: 182-217.

Bernadou, M., Eiroa, P.M., Trouvé, P., 1994. On the convergence of a discrete Kirchhoff triangle method valid for shell of arbitrary shape. Comp. Meth. Appl. Mech. Eng, 118: 373-391.

Bernadou, M., Trouvé, P., 1989. Approximation of general shell problems by flat plate elements, part 2. addition of drilling degree of freedom. Comput. Mech, 6: 359-378.

Bernadou, M., Trouvé, P., Ducatel, Y., 1989. Approximation of general shell problems by flat plate elements part 1. Comput. Mech, 5: 175-208.

Bert, C.W., Stricklin, J.D., 1988. Comparative evaluation of six different numerical integration methods for non-linear dynamic systems. Journal of Sound and Vibration, 127(2): 221-229.

Bilotta, A. Casciaro, R., 2002. Assumed stress formulation of high order quadrilateral elements with an improved in-plane bending behaviour, Comp. Meth. Appl. Mech. Eng, 191(15-16): 1523-1540.

Bogner, F.K., Fox, R.L., Schmit, L.A., 1965. The Generation of Interelement Compatible Stiffness and Mass Matrices by the Use of Interpolation Formulars, Proc. Conference on Matrix Methods in Structural Mechanics, AFFDL-TR-66-80, pp. 397-444.

Bogner, F.K., Fox, R.L., Schmit, L.A., 1967. A Cylindrical Shell Discrete Element. AIAA J, 5 (4): 745-750.

Boisse, p., Gelin, J.C., Daniel, J.L., 1996. Computation of Thin Structures at Large Strains and Large Rotations Using a Simple co Isoparametric Three-Node Shell Element. Comput. Struct, 58(2): 249-261.

Bonet, J., Wood, R.D., 1997. Nonlinear Continuum Mechanics for Finite Element Analysis. Cambridge University Press.

Boot, J.C., Moore, D.B., 1984. An efficient analysis for thin plates of general quadrilateral shape subject to bending stresses. Comp. Meth. Appl. Mech. Eng, 43(1): 57-79.

Bosshard, W., 1968. Ein neues, vollvertragliches endliches Element fur Platten biegung. Internationaler Verein f¨ur Br¨uckenbau und Hochbau, Abhandlungen, 28:1.

Bottasso, C.L., Bauchau, O.A., Choi, J.Y., 2002. An energy decaying scheme for nonlinear dynamics of shells. Comp. Meth. Appl. Mech. Eng, 191: 3099-3121.

Bout, A., 1993. A displacement-based geometrically nonlinear constant stress element. Int. J. Num. Meth. Eng, 36:1161-1188.

Brank, B., Peric, D., Damjanic, B., 1995. On Implementation of Non-linear Four Node Shell Element for Thin Multilayered Elastic Shells", Comput. Mech, 16: 341-358.

Brank, B., Tonello, N., Briseghella, L., Damjanic, F.B., 1998. On non-linear dynamics of elastic shells: Implementation of the energy-momentum conserving algorithm. Int. J. Num. Meth. Eng, 42: 409-442.

Brebbia, C., Connor, J., 1969. Geometrically nonlinear finite element analysis. ASCE J. Eng. Mech. Dev, 95(EM2): 463-483.

Brunet, M., Sabourin, F., 2006. Analysis of a rotation-free 4-node shell element. Int. J. Num. Meth. Eng, 66: 1483-1510.

Bucalem, M.L., Bathe, K.J., 1993. Higher-orderMITC general elements. Int. J. Num. Meth. Eng, 36: 3729-3754.

Buchter, N., Ramm, E., Roehl, D., 1994. Three-dimensional extension of nonlinear shell formulation based on the enhanced assumed strain concept. Int. J. Num. Meth. Eng, 37: 2551-2568.

Buechter, N., Ramm, E., 1992. Shells theory versus degeneration - a comparison in large rotation finite element analysis. Int. J. Num. Meth. Eng, 34:39-59.

-C-

Cai, S.B., Shen, P.S., Hu, B.X., et al. 2009. A field consistency based co-rotational finite element procedure for 2D quadrilateral element. Eng. Mech, 26(12): 31-34.

Campello, E.M.B., Pimenta, P.M., Wriggers, P., 2003. A triangular finite shell element based on a fully nonlinear shell formulation. Comput. Mech, 31: 505-518.

Cannarozzi, A.A., Cannarozzi, M., 1995. A displacement scheme with drilling degrees of freedom for plane elements. Int. J. Num. Meth. Eng, 38: 3443-3452.

Cantin, G., Clough, R.W., 1968. A Curved Cylindrical Shell Finite Element, AIAA J, Vol. 6, No.6, June.

Cardona, A., Geradin, M., 1988. A beam finite element non-linear theory with finite rotations. Int. J. Num. Meth. Eng, 26: 2403-2438.

Cardoso, E.L., Fonseca, J.S.O., 2007. The GDC method as an orthogonal arc-length method. Commun. Num. Meth. Eng, 23: 263-271.

Cardoso, R.P.R., Yoon, J.W., Mahardika, M., Choudhry, S., De-Sousa, R.J., Valente, F.R.A., 2007. Enhanced assumed strain (EAS) and assumed natural strain (ANS) methods for one-point quadrature solid-shell elements. Int. J. Num. Meth. Eng, 69: 627-663.

Carpenter, N., Stolarski, H., Belytschko, T., 1985. A flat triangular shell element with improved membrane interpolation. Commun. App. Num. Meth, 1:161-168.

Carpenter, N., Stolarski, H., Belytschko, T., 1986. Improvements in 3-node triangular shell elements. Int. J. Num. Meth. Eng, 23: 1643-1667.

Carrera, E., 1994. A study of arc-length-type methods and their operation failures illustrated by a simple model. Comput. Struct, 50(2): 217-229.

Caylak, I., Mahnken, R., 2011. Mixed finite element formulations with volume bubble functions for triangular elements. Comput. Struct, 89: 1844-1851.

Cazzani, A., Atluri, S.N., 1993. Four-noded mixed finite elements, using unsymmetric stresses, for linear analysis of membranes. Comput Mech, 11: 229-51.

Cen, S., Zhou, M.J., Fu, X.R., 2011. A 4-node hybrid stress-function (HS-F) plane element with drilling degrees of freedom less sensitive to severe mesh distortions. Comput. Struct, 89: 517-528.

Chan, S.L., 1988. Geometric and Material Non-linear Analysis of Beam-Columns and Frames Using the Minimum Residual Displacement Method. Int. J. Num. Meth. Eng, 26: 2657-2699.

Chang, C., Mohraz, B., 1990. Modal analysis of nonlinear systems with classical and non-classical damping. Comput. Struct, 36(6): 1067-1080.

Chang, H., Harder, R.L., Hoff, C.C., et al., 2003. Practical finite element modeling of assembled shell structures. In: Proceedings of the NAFEMS World Congress 2003, Orlando, FL.

Chen, H., Blandford, G. E., 1993. Work-Increment-Control Method for Non-Linear Analysis. Int. J. Num. Meth. Eng, 36(6): 909-930.

Chen, H.C., 1992. Evaluation of Allman triangular membrane element-used in general shell analysis. Comput. Struct, 43(05): 881-887.

Chen, K.K., 1979. A triangular plate finite element for large displacement elastic plastic analysis of automobile structural components. Comput. Struct, 10: 203-215.

Chen, W., Cheung, Y.K., 1987. A new approach for the hybrid element method. Int. J. Num. Meth. Eng, 24: 1697-1709.

Chen, W.J., Cheung, Y.K., 1999. Refined non-conforming triangular elements for analysis of shell structures. Int. J. Num. Meth. Eng, 46: 433-455.

Chen, W.J., Tang, L.M., 1981. Isoparametric quasi-conforming element. J Dalian Univ Tech, 20(1): 63-74.

Chen, X.M., Cen, S., Long, Y.Q., Yao, Z.H., 2004. Membrane elements insensitive to distortion using the quadrilateral area coordinate method. Comput. Struct, 82: 35-54.

Chen, Y.I, Wu, G.Y., 2004. A mixed 8-node hexahedral element based on the Hu-Washizu principle and the field extrapolation technique. Structural Engineering and Mechanics, 17: 113-140.

Chen, Y.L., Cen, S., Yao, Z.H., Long, Y.Q., Long, Z.F., 2003. Development of triangular flat-shell element using a new thin-thick plate bending element based on semiloof constraints. Structural Engineering and Mechanics, 15(1): 83-114.

Cheung, Y.K., Chen, W.J., 1995. Refined nine-parameter triangular thin plate bending element by using refined direct stiffness method. Int. J. Num. Meth. Eng, 38: 283-298.

Chevalier, L., 1996. Mécanique des Systèmes et des Milieux Déformables. Ellipses / Edition Marketing S.A.

Chin, C. K., Al-Bermani, F. G. A., Kitipornchai, S., 1994. Non-linear analysis of thin-walled structures using plate elements. Int. J. Num. Meth. Eng, 37: 1697-1711.

Chinosi, C., 1994. Shell elements as a coupling of plate and "drill" elements. Comput. Struct, 57(5): 893-902.

Chinosi, C., Comodi, M.I., Sacchib, G., 1997. A new finite element with 'drilling' d.o.f. Comp. Meth. Appl. Mech. Eng, 143: 1-11.

Cho, C., Park, H.C., Lee, S.W., 1998. Stability analysis using a geometrically nonlinear assumed strain solid shell element model. Finite. Elem. Anal. Des, 29: 121-135.

Choi, C.K., Lee, P.S., Park, Y.M., 1999. Defect-free 4-node flat shell element: NMS-4F element. Struct. Engrg. Mech, 8: 207-231.

Choi, C.K., Lee, T.Y., 2003. Efficient remedy for membrane locking of 4-node flat shell elements by non-conforming modes. Comp. Meth. Appl. Mech. Eng, 192: 1961-1971.

Choi, N., Choo, Y.S., Lee, B.C., 2006. A hybrid Trefftz plane elasticity element with drilling degrees of freedom. Comp. Meth. Appl. Mech. Eng, 195: 4095-4105.

Choo, Y.S., Choi, N., Lee, B.C., 2006. Quadrilateral and triangular plane elements with rotational degrees of freedom based on the hybrid Trefftz method. Finite. Elem. Anal. Des, 42: 1002-1008.

Chroscielewski, J., Makowski, J., Stumpf, H., 1992. Genuinely resultant shell finite elements accounting for geometric and material non-linearity. Int. J. Num. Meth. Eng, 35: 63-94.

Chroscielewski, J., Makowski, J., Stumpf, H., 1997, Finite element analysis of smooth, folded and multi-shell structures. Comp. Meth. Appl. Mech. Eng, 141: 1-46.

Chu, T.C., Schnobrich, W.C., 1970. Finite Element Analysis of Translational Shells. J Civil Engineering Studies, Structural Research Series No. 368, University of Illinois, Urbana, Illinois, November.

Chu, T.C., Schnobrich, W.C., 1972. Finite Element Analysis of Translational Shells. Comput. Struct, 2: 197-222.

Chung, J., Hulbert, G., 1993. A time integration algorithm for structural dynamics with improved numerical dissipation: the generalized alpha method. J. Appl. Mech, 60: 371-375.

Clarke, J.M., Hancock, G.J., 1990. A study of incremental-iterative strategies for non- linear analyses. Int. J. Num. Meth. Eng, 29(7): 1365-1391.

Clough, G.J., Johnson, C.P., 1968. A finite element approximation for the analysis of thin shells. Iny. J. Solids. Struct, 4: 43-60.

Clough, R. W., Felippa, C. A., 1968. A Refined Quadrilateral Element for Analysis of Plate Bending, Proc. Conference (2nd) on Matrix Methods in Structural Mechanics, Wright-Patterson AFB, Ohio.

Clough, R.W. Tocher, J.L., 1965. Finite Element Stiffness Matrices for Analysis of Plate Bending, Proc. Conference on Matrix Methods in Structural Mechanic, WPAFB, Ohio, pp. 515-545.

Clough, R.W., Wilson, E.L., 1971. Dynamic Finite Element Analysis of Arbitrary Thin Shells. Comput. Struct, 1: 33-56.

Cocchetti, G., Pagani, M., Perego, U., 2013. Selective mass scaling and critical time-step estimate for explicit dynamics analyses with solid-shell elements. Comput. Struct, 127:39-52.

Connor, J.J., Brabbia, C., 1967. Stiffness Matrix for Shallow Rectangular Shell Elements, J. Eng. Mech. Div., ASCE, 93(EM5): 43-65.

Cook, R.D., 1974-a. Concepts and Applications of Finite Element Analysis, Wiley.

Cook, R.D., 1974-b. Improved two-dimensional finite element. J. struct. Div. ASCE 100 (ST9), Proc. Paper 10808, pp. 1851-1863.

Cook, R.D., 1975. Avoidance of parasitic shear in plane element. J. Struct. Div., AXE l0l (ST6), 1239-1253.

Cook, R.D., 1986. On The Allman Triangle and Related Quadrilateral Element. Comput. Struct, 22: 1065-1067.

Cook, R.D., 1987. A plane hybrid element with rotational d.o.f. and adjustable stiffness. Int. J. Num. Meth. Eng, 24: 1499-1508.

Cook, R.D., 1990. Some Options for Plane Triangular Elements with Rotational Degrees of Freedom. Finite. Elem. Anal. Des, 6: 245-249.

Cook, R.D., 1991. Modified formulations for nine-d.o.f. plane triangles that include vertex rotations. Int. J. Num. Meth. Eng, 31: 825-835.

Cook, R.D., 1993. Further development of a three-node triangular shell element. Int. J. Num. Meth. Eng, 36(8): 1413-1425.

Cook, R.D., 1994. Four-node `flat' shell element: drilling degrees-of-freedom, membrane-bending coupling, warped geometry, and behavior. Comput. Struct, 50: 549-455.

Cook, R.D., Al-Abdulla, J.K., 1969. Some plane quadrilateral 'hybrid' finite elements. AIAA J, 7(11): 2184-2185.

Cook, R.D., Malkus, D.S., Plesha, M.E., Witt, R.J., 2002. Concepts and applications of finite element analysis. John Wiley and Sons, New York.

Crisfield, M.A., 1981. A fast incremental/iterative solution procedure that handles snap-through. Comput. Struct, 13: 55-62.

Crisfield, M.A., 1982. Variable step-lengths for nonlinear structural analysis. TRR. Lab., Rep. 1049.

Crisfield, M.A., 1983-a. A four-noded thin plate bending element using shear constraints - a modified version of Lyons' element. Comp. Meth. Appl. Mech. Eng, 39: 93-120.

Crisfield, M.A., 1983-b. An arc-length method including line search and accelerations. Int. J. Num. Meth. Eng, 19: 1269-1289.

Crisfield, M.A., 1990. A consistent co-rotational formulation for non-linear, three dimensional, beam-elements. Comp. Meth. Appl. Mech. Eng, 81: 131-150.

Crisfield, M.A., 1990. A consistent co-rotational formulation for non-linear, three- dimensional, beam-elements, Comp. Meth. Appl. Mech. Eng, 81: 131-150.

Crisfield, M.A., Jelenic, G., Mi, Y., Zhong, H.G., Fan, Z., 1997. Some aspects of the nonlinear finite element method, Finite Element in Analysis and Design, 27(1): 19-70.

Crisfield, M.A., Moita, G.F., 1996. A unified co-rotational for solids, shells and beams. Int. J. Solids. Struct, 33: 2969-2992.

Crisfield, M.A., Shi, J., 1994. A co-rotational element/time-integration strategy for non-linear dynamics. Int. J. Num. Meth. Eng, 37(11): 1897-1913.

Crisfield, M.A., Tan, D., 2001. Large-strain elasto-plastic shell analysis using low-order elements. Eng Comput, 18(1/2): 255-86.

-D-

Dawe, D.J., 1972. Shell analysis using a simple facet element. J. Strain. Anal, 7: 226-270.

Debongnie, J.F., 1979. Physical interpretation and generalization of Marguerre's shallow shell. Int. Jour. Engng. Sci, 17(4): 387-399.

De-Borst, R., 1987. Computation of post-bifurcation and post-failure behaviour of strain-softening solids. Comput. Struct, 25: 823-829.

Destuynder, Ph. Salaün, M., 1998. Approximation of shell geometry for non-linear analysis. Comp. Meth. Appl. Mech. Eng, 152: 393-430.

De-Veubeke, B.F., 1965. Displacement and equilibrium models in the finite element method, in: O.C. Zienkiewicz and G.S. Holister, eds., Stress Analysis, Wiley, London, 145-196.

De-Veubeke, B.F., 1968. A conforming finite element for plate bending, Int. J. Solids. Struct, 4: 95-108.

Dhatt, G.S., 1969. Numerical analysis of thin shells by curved triangular elements based on discrete Kirchhoff hypothesis. In Proc. Conference on Application of Finite Element Method in Civil Engineering, pp. 255-278. Vanderbilt University, Nashville, TN.

Dhatt, G.S., 1970. An efficient triangular shell element. AIAA J, 8(11): 2100-2102.

Dhatt, G.S., Marcotte, L., Matte, Y., 1986. A New Triangular Discrete Kirchhoff Plate Shell Element. Int. J. Num. Meth. Eng, 23: 453-470.

Di, S., Ramm, E., 1994. On alternative hybrid stress 2D and 3D elements. Engineering and Computers, 11: 49-68.

Djeghaba, K., 1990. Contribution à l'analyse non linéaire géométrique des coques minces en théorie de Marguerre, INSA de Lyon, Thèse de doctorat.

Dohrmann, C.R., Heinstein, M.W., Jung, J., Key, S.W., Witkowski, W.R., 2000. Node-based uniform strain elements for three-node triangular and four-node tetrahedral meshes. Int. J. Num. Meth. Eng. 47: 1549-68.

Dokainish, M.A., Subbaraj, K., 1989. A survey of direct time-integration methods in computational structural dynamics-i. explicit methods. Comput. Struct, 32(6): 1371-1386.

Doll, S., Schweizerhof, K., Hauptmann, R., Freischlager, C., 2000. On volumetric locking of low order solid and solid-shell elements for finite elastoviscoplastic deformations and selective reduced integration. Engrg. Comput, 17: 874-902.

Dong, S.B., 1966. Analysis of laminated shells of revolution, J. Engng. Mech. Div, ASCE, 9(6): 135-155.

Du, Y., Cen, S., 2008. Geometrically nonlinear analysis with a 4-node membrane element formulated by the quadrilateral area coordinate method. Finite. Elem. Anal. Des, 44: 427-438.

Duan, Y., May, I.M., 1994. A local arc-length procedure for strain softening. ACME Proc. Computational Mechanics in UK-1994, ed. Geotechnical Engineering Group, Department of Mechanical Engineering Manchester and UK, pp. 65-68.

Duarte-Filho, L.A., Awruch, A.M., 2004. Geometrically nonlinear static and dynamic analysis of shells and plates using the eight-node hexahedral element with one-point quadrature. Finite. Elem. Anal. Des, 40: 1297-1315.

Dungar, R., Severn, R.T., 1969. Triangular finite elements of variable thickness and their application to plate and shell problems. J. Strain. Anal, 4: 10-21.

Dupius, G.A., Hibbit, H.D., McNamara, S.F., Marcal, P.V., 1971. Non-linear material and geometric behaviour of shell structures. Comput. Struct, 1: 223-239.

Dupuis, G., Goel, J.J., 1969. A Curved Finite Element for Thin Elastic Shells. Brown university Providence, Technical Report No. 4. December I969.

Dutta, A., White, D.W., 1997. Automated solution procedures for negotiating abrupt non-linearities and branch points. Eng Comput, 14(1): 31-56.

Dvorkin, E. Onate, E. Olivier, J., 1988. On a non-linear formulation for curved timoshenko beam elements considering large displacement/rotation increments. Int. J. Num. Meth. Eng, 26: 1597-1613, 1988.

Dvorkin, E., Bathe, K.J., 1984. A continuum mechanics based four-node shell element for general non-linear analysis. Engng. Comp, 1: 77-88.

-E-

Edem, I.B., Gosling, P.D., 2013. Physically stabilised displacement-based ANS solid-shell element. Finite. Elem. Anal. Des, 74: 30-40.

El-Khaldi, F., 1987. Contrbution au Traitement des Phénomènes de Blocage de Membrane et Cisaillement dans le Modelisation des arcs et des coques minces en Théorie de Margueurre. Thése de Doctorat. Institut National des Sciences Appliquées de LYON, p 305.

Ergatoudis, J., Irons, B.M., Zienkiewicz, O. C., 1968. Three Dimensional Stress Analysis of Arch Dams and Their Foundations, Proc. Symp. on Arch Dams, 37-50, Inst. of Civil Eng., London.

Ergatoudis, J., Irons, B.M., Zienkiewicz, O.C., 1966. Three Dimensional Stress Analysis of Arch Dams by the Finite Element Method, Reports AD/1935 and AD/1745, Inst. of Civil Eng., London.

Eriksson, A. Pacoste, C., 2002. Element formulation and numerical techniques for stability problems in shells, Comp. Meth. Appl. Mech. Eng, 191: 3775-3810.

Eriksson, A., Kouhia, R., 1995. On step size adjustments in structural mechanics. Comput. Struct, 55(3): 495-506.

Ertas, A., Krafcik, I.T., Ekwaro-Osire, S., 1992. Performance of an anisotropic Allman/DKT 3-node thin triangular flat shell element. Comp. Eng, 2: 269-280.

-F-

Fafard, M., Dhatt, G., Batoz, J.L., 1989. A New Discrete Kirchhoff Plate-Shell Element with Updated Procedures. Comput. Struct, 31: 591-606.

Fafard, M., Massicotte, B., 1993. Geometrical Interpretation of the Arc-Length Method. Comput. Struct, 46(4): 603-615.

Fan, S.C., Fung, T.C., Sheng, G., 1997. A comprehensive unified set of single-step algorithms with controllable dissipation for dynamics Part II. Algorithms and analysis. Comp. Meth. Appl. Mech. Eng, 145: 99-107.

Felippa, C.A., 1966. Refined finite element analysis of linear and nonlinear two dimensional structures. Technical Report SESM 66-22, Univ. California, Berkeley.

Felippa, C.A., 1987. Penalty spring stabilization of singular Jacobians. J. Appl. Mech Transactions, ASME, 54(3): 728-729.

Felippa, C.A., 2000. A systematic approach to the element-independent corotational dynamics of finite elements. In Int. Conf. Computational Methods for Shell and Spatial Structures, Papadrakakis, M., Samartin, A. and Onate, E. (Eds.) ISASR-NTUA, Athens, Greece. IASS-IACM.

Felippa, C.A., 2003. Study of optimal membrane triangles with drilling freedoms. Comp. Meth. Appl. Mech. Eng, 192: 2125-2168.

Felippa, C.A., 2006. Supernatural Quad4: a template formulation. Comp. Meth. Appl. Mech. Eng, 195(41-43): 5316-5342.

Felippa, C.A., 2007. Nonlinear finite element methods (NFEM). Lecture note, University of Colorado at Boulder.

Felippa, C.A., Alexander, S., 1992. Membrane triangles with corner drilling freedoms III. Implementation and performance evaluation. Finite. Elem. Anal. Des, 12: 203-239.

Felippa, C.A., Bergan, P.G., 1987. A Triangular Bending Element Based on Energy Orthogonal Free Formulation. Comp. Meth. Appl. Mech. Eng, 61: 129-160.

Felippa, C.A., Haugen, B., 2005. A unified formulation of small-strain corotational finite elements: I. theory. Comp. Meth. Appl. Mech. Eng, 194: 2285-2335.

Felippa, C.A., Militello, C., 1992. Membrane triangles with corner drilling freedoms II. The ANDES element. Finite. Elem. Anal. Des, 12: 189-201.

Felippa, C.A., Park, K.C., 1979. Direct Time Integration Methods in Nonlinear Structural Dynamics. Comp. Meth. Appl. Mech. Eng, 17/18: 277-313.

Feng, Y.T., Owen, D.R.J., Peric, D., 1997. On the sign of the determinant of the structural stiffness matrix for determination of loading increment in arc-length methods. Comm. Num. Mech. Eng, 13: 47-49.

Feng, Y.T., Peric, D., Owen, D.R.J., 1995. Determination of travel directions in path-following methods. Math. Comput. Modelling, 21: 43-59.

Feng, Y.T., Peric, D., Owen, D.R.J., 1996. A new criterion for determination of initial loading parameter in arc-length methods. Comput. Struct, 58: 479-485.

Fish, J., Belytschko, T., 1992. Stabilized rapidly convergent 18-degrees-of-freedom flat shell triangular element. Int. J. Num. Meth. Eng, 33: 149-62.

Flanagan, D.P., Belytschko, T., 1981. A uniform strain hexahedron and quadrilateral with orthogonal hourglass control. Int. J. Num. Meth. Eng, 17: 679-706.

Flugge, W., 1934. Statik und Dynamik der Schalen. Springer-Verlag, Berlin.

Flugge, W., 1960. Stresses in Shells. Springer, New York.

Fonder, G.A., Clough, R.W., 1973. Explicit addition of rigid body motions in curved finite elements. AIAA J, 11: 305-312.

Forde, B.W.R., Stiemer, S.F., 1987. Improved Arc Length Orthogonality Methods For Nonlinear Finite Element Analysis. Comput. Struct, 27(5): 625-632.

Forest, S., Amestoy, M., Cantournet, S., Damamme, G., Kruch, S., 2006. Mécanique des Milieux Continues. Ecole des Mines de Paris.

Fox, D.D., Simo, J.C., 1992. Drill rotation formulation for geometrically exact shells. Comp. Meth. Appl. Mech. Eng, 98: 329-343.

Freischläger, C., Schweizerhof, K., 1996. On a systematic development of trilinear three-dimensional solid elements based on Simo's enhanced strain formulation. Int. J. Solids. Struct, 33(20-22): 2993-3017.

Frey, F., 1989. Shell finite elements with six degrees of freedom per node. ASME Winter Annual Meeting, San Francisco, December.

Fried, I., 1973. Shear in Co and C' plate bending elements. Int. J. Solids. Struct, 9: 449-460.

Fried, I., 1974. Residual energy balancing technique in the generation of plate bending finite elements. Comput. Struct, 10: 771-778.

Fried, I., Yang, S.K., 1973. Triangular nine degree-of-freedom C^o plate bending element of quadratic accuracy. Q. appl. Math, 31: 303-312.

Fujii, F., Choung, K.K., Gong, S.X., 1992-b. Variable Displacement Control to Overcome Turning Points of Nonlinear Elastic Frames. Comput. Struct, 44(1/2): 133-136.

Fujii, F., PEREZ, B.C., Choung, K.K., 1992-a. Selection of the Control Parameter in Displacement Incrementation. Comput. Struct, 42(2): 167-174.

Fulton, R.E., Eppnik, R.T., Walz, J.E., 1966. The accuracy of finite element methods in continuum problems, In Proc. Fifth U.S. Congress of Applied Mech., ASME.

-G-

Gadala, M.S., Dokainish, M.A., Oravas, G.A., 1984. Formulation methods of geometric and material nonlinearity problems. Int. J. Num. Meth. Eng, 20: 887-914.

Gallagher, R.H., 1973. The finite element method in shell. Comput. Struct, 3(3): 543-557.

Gallagher, R.H., 1975. Finite Element Analysis: Fundamentals, Prentice Hall, Inc.

Gallagher, R.H., 1976. Finite element representations for thin shell analysis. In Buckling of Structures (Edited by B. Budiansky), Springer-Verlag, New York.

Gallagher, R.J., Gellatly, R.A., Padlog, J., Mallet, R.H., 1967. A discrete element procedure for thin shell instability analysis. Am. Inst. Aero. & Astro. J, 5(1): 138-145.

Garcea, G., Madeo, A., Casciaro, R., 2011. The implicit corotational method and its use in the derivation of nonlinear structural models for beams and plates. J Mech Mater Struct, 7(6): 509-38.

Garcea, G., Madeo, A., Casciaro, R., 2012. Nonlinear FEM analysis for beams and plate assemblages based on the implicit corotational method. J Mech Mater Struct, 7(6): 539-74.

Garcea, G., Madeo, A., Zagari, G., Casciaro, R., 2009. Asymptotic post-buckling FEM analysis using corotational formulation. Int. J. Solids. Struct, 46(2): 377-97.

Garnet, H., Pifko, A., 1983. An efficient triangularplate bending finite element for crash simulation. Comput. Struct, 16: 371-379.

Geradin, M., Idelsohn, S., Hogge, M., 1980. Computational strategies for the solution of large nonlinear problems via Quasi-Newton methods. Comput. Struct, 13: 73-81.

Geschwindner, L. F., 1981. ASCE, Nonlinear dynamic analysis by modal superposition, Jornal of structural engineering, 107(12): 2325-2336.

Geyer, S., Groenwold, A.A., 2002. Two hybrid stress membrane finite element families with drilling rotations, Int. J. Num. Meth. Eng, 53: 583-601.

Geyer, S., Groenwold, A.A., 2003. On reduced integration and locking of flat shell finite elements with drilling rotations. Commun. Num. Meth. Eng, 19: 85-97.

Gierlinski, J.T., Smith, G.T.R., 1985. A variable load iteration procedure for thin-walled structures. Comput. Struct, 21(5): 1085-94.

Gopalacharyulu, S., 1973. A Higher Order Conforming Rectangular Plate Element", Int. J. Num. Meth. Eng, 6: 305-308.

Gotsis, P. K., 1994. Structural optimization of shell structures", Comput. Struct, 50(4): 499-507.

Grafton, P.E., Strome, D.R., 1963. Analysis of axysymmetric shells by the direct stiffness method, AIAA J, 1: 2342-2347.

Greene, B.E., Jones, R.E., Stome, D.R., 1968. Dynamic Analysis of Shell Using Doubly Curved Finite Elements, Proc. 2nd Cong, on Matrix Methods in Struct. Mech., Wright-Patterson Air Force Base, Ohio.

Greene, B.E., Strome, D.R., Weikel, R.C., 1961. Application of the stiffness method to the analysis of shell structures, in the proc. Aviation Conf. of ASME, Los Angeles, CA, March.

Groenwold, A.A., Stander. N., 1995. An efficient 4-node 24 d.o.f. thick shell finite element with 5-point quadrature. Engrg. Comput, 12: 723-748.

Groenwold, A.A., Xiao, Q.Z., Theron, N.J., 2004. Accurate solution of traction free boundaries using hybrid stress membrane elements with drilling degrees of freedom. Comput. Struct, 82: 2071-2081.

Gruttmann, F., Wagner, W., Wriggers, P., 1992. A nonlinear quadrilateral shell element with drilling degrees of freedom. Archive of Applied Mechanics, Archive. Appl. Mech, 62: 474-486.

Guo, Y.Q., Gati, W., Naceur, H., Batoz, J.L., 2002. An efficient DKT rotation free shell element for springback simulation in sheet metal forming. Comput. Struct, 80: 2299-312.

-H-

Haisler, W.E., Stricklin, J.A., 1977. Displacement incrementation in nonlinear structure analysis by the self-correcting method. Int. J. Num. Meth. Eng, 11: 3-10.

Hajlaoui, A., Jarraya, A., 2012. Buckling analysis of a laminated composite plate with delaminations using the enhanced assumed strain solid shell element. Journal of Mechanical Science and Technology.

Hamadi, D.J., Belarbi, M.T., 2006. Integration solution routine to evaluate the element stiffness matrix for distorted shapes. Asian Journal of Civil Engineering, 7: 525-549.

Hammerand, D.C., Kapania, R.K., 2000. Geometrically nonlinear shell element for hygrothermorheologically simple linear viscoelastic composites. AIAA J, 38(12): 2305-2319.

Han, S.C., Ham, H.D., Nukulchai, W.K., 2008. Geometrically non-linear analysis of arbitrary elastic supported plates and shells using an element-based Lagrangian shell element. Int. J. Nonlinear. Mech, 43: 53-64.

Harbord, R., 1973. Berechnung von Schalen mit endlichen Verschiebungen - Gemischte finite Elemente Inst. Statik, Techn. Univ. Braunschweig, Bericht Nr. 72-7.

Harnau, M., Schweizerhof, K., 2002. About linear and quadratic ‘‘Solid-Shell’’ elements at large deformation. Comput. Struct, 80: 805-817.

Harris, J.C., Bartholomew, P., 1989. Cubic triangular membrane element with drilling rotation freedom. RAE Technical Report 89042.

Hartzman, M., Hutchinson, J.R., 1972. Nonlinear Dynamics of Solids by the Finite Element Method. Comput. Struct, 2: 47-77.

Hauptmann, R., Doll, S., Harnau, M., Schweizerhof, K., 2001. Solid-shell elements with linear and quadratic shape functions at large deformations with nearly incompressible materials. Comput. Struct, 79: 1671-1685.

Hauptmann, R., Schweizerhof, K., 1998. A systematic development of ‘solid-shell’ element formulations for linear and non-linear analyses employing only displacement degrees of freedom. Int. J. Num. Meth. Eng, 42:49-69.

Hauptmann, R., Schweizerhof, K., Doll, S., 2000. Extension of the ‘solid-shell’ concept for application to large elastic and large elastoplastic deformations. Int. J. Num. Meth. Eng, 49: 1121-1131.

Hellan, K., 1967. Analysis of elastic plates in flexure by a simplified finite element method. Civ. Engrg. Bldg. Construction Ser. No. 46. Acta Polytechnica Scandinavica.

Hellweg, H.B., Crisfield, M.A., 1998. A New Arc-Length Method for Handling Sharp Snap-Backs. Comput. Struct, 66(5): 705-709.

Herrmann, L.R., 1965. Elasticity equations for nearly incompressible materials by a variational theorem, AIAA J. 3(10): 1896-1900.

Herrmann, L.R., 1967. Finite element bending analysis of plates. J. Eng. Mech. Div. ASCE, 93(5): 13-25.

Herrmann, L.R., Campbell, D.M., 1968. A finite element analysis of thin shell. AIAA J., 6: 1842-1846.

Hibbit, H.D., Marcal, P.V., Rice, J.R., 1970. A finite element formulation for problems of large strain and large displacement. Int. J. Solids. Struct, 6(8): 1069-1086.

Hilber, H.M., Hughes, T.J.R., 1978. Collocation, dissipation and 'overshoot' for time integration schemes in structural dynamics, Earthquake Engineering and Structural Dynamics, 6: 99-118.

Hilber, H.M., Hughes, T.J.R., Taylor R.L., 1977. Improved numerical dissipation for time integration algorithms in structural dynamics, Earthquake Engineering and Structural Dynamics, 5: 283-292.

Hildebrand, F.B., Reissner, E., Thomas, G.B., 1949. Note on the foundations of the theory of small displacements of orthotropic shells. NACA TN-1833.

Ho, P.T.S., 1992. Comparison of Performance of a Flat Faceted Shell Element and a Degenerated Superparametric Shell Element. Comput. Struct, 44(4): 895-904.

Hoff, C., Pahl, P.J., 1988. Development of an Implicit Method with Numerical Dissipation from a Generalized Single-Step Algorithm For Structural Dynamics. Comp. Meth. Appl. Mech. Eng, vol. 67: 367-385.

Hofmeister, L.D., Greenbaum, G.A., Evensen, D.A., 1971. Large strain elasteplastic finite element analysis. AIAA J, 9(7): 1248-1254.

Holand, I., Bergan, P.G., 1968. Higher order finite element for plane stress, Discussion. Proc. ASCE, Journal of the Engineering Mechanics Division, 94(EM2): 698-702.

Holand, I., Moan, T., 1969. The finite element in plate buckling. Finite Element Meth. in Stress Analysis, ed. I. Holand et al., Tapir.

Horrigmoe, G., 1976. Large displacement analysis of shells by a hybrid stress finite element method, IASS World Congress on Space Enclosures, Montreal, Jul. 489-499.

Horrigmoe, G., 1977. Finite element instability analysis of free-form shells, (Div. Struct. Mech., Norwegian Inst. Tech., Trondheim, Report No. 77-2, May.

Horrigmoe, G., 1978. Hybrid stress finite element model for nonlinear shell problems. Int. J. Num. Meth. Eng, 12: 1819-1839.

Horrigmoe, G., Bergan, P.G., 1978. Nonlinear analysis of free form shells by flat elements. Comp. Meth. Appl. Mech. Eng, 16: 11-35.

Houbolt, J.C., 1950. A recurrence matrix solution for the dynamics response of elastic aircraft. Journal of the Aeronautical Sciences, 17: 540-550.

Hsiao, K.M., 1987. Nonlinear analysis of general shell structures by flat triangular shell element. Comput. Struct, 25: 665-675.

Hsiao, K.M., Hung, H.C., 1989. Large deflection analysis of shell structure by using corotational total Lagrangian formulation. Comp. Meth. Appl. Mech. Eng, 73: 209-225.

Hsiao, K.M., Lin, W.Y., 2000. A co-rotational finite element formulation for buckling and postbuckling analyses of spatial beams. Comp. Meth. Appl. Mech. Eng, 188: 567-594.

Huang, H.C., Hinton, E., 1986-a. A new nine-node degenerate shell element with enhanced membrane and shear interpolation. Int. J. Num. Meth. Eng, 22: 73-92.

Huang, H.C., Hinton, E., 1986-b. Lagrangian and serendipity plate and shell elements through thick and thin. In: Finite Element Methods for Plate and Shell Structures, ed. Hughes, T.J.R. and Hinton, E., Pineridge Swansea, pp. 46-61.

Huang, M., Zhao, Z., Shen, C., 2010. An effective planar triangular element with drilling rotation, Finite Element in Analysis and Design, 46: 1031-1036.

Hughes, T.J.R., Brezzi, F., 1989. On drilling degrees of freedom. Comp. Meth. Appl. Mech. Eng, 72: 105-121.

Hughes, T.J.R., Brezzi, F., Masud, A., Harari, I., 1989. Finite Elements with Drilling Degrees of Freedom: Theory and Numerical Evaluations, Proceedings of the Fifth International Symposium on Numerical Methods in Engineering, Computational Mechanics Publications, Ashurst, U.K., pp 3-17.

Hughes, T.J.R., Cohen, M., Haroun, 1978. Reduced and selective integration techniques in finite element analysis of plates. Nuclear Engineering Design, 46: 203-222.

Hughes, T.J.R., Liu, W.K., 1978-a. Implicit-explicit finite elements in transient analysis: implementation and numerical examples, J. Appl. Mech. ASME, 45: 375-378.

Hughes, T.J.R., Liu, W.K., 1978-b. Implicit-explicit finite elements in transient analysis: stability theory. J. Appl. Mech. ASME, 45: 371-374.

Hughes, T.J.R., Liu, W.K., 1981. Nonlinear finite element analysis of shells: Part I. Three-dimensional shells. Comp. Meth. Appl. Mech. Eng, 26: 331-362.

Hughes, T.J.R., Masud, A., Harari, I., 1995. Dynamic analysis and drilling degrees of freedom, Int. J. Num. Meth. Eng. 38: 3193-3210.

Hughes, T.J.R., Pister, K.S., Taylor, R.L., 1979. Implicit-explicit finite elements in nonlinear transient analysis, Comp. Meth. Appl. Mech. Eng, 17/18: 159-182.

Hughes, T.J.R., Taylor, R.L. Nukulchai, W.K., 1977. A simple and efficient element for plate bending. Int. J. Num. Meth. Eng, 11: 1529-1543.

-I-

Ibrahimbegovic, A., 1990. A novel membrane finite element with an enhanced displacement interpolation, Finite. Elem. Anal. Des, 7: 167-179.

Ibrahimbegovic, A., 1993. Mixed finite element with drilling rotations for plane problems in finite elasticity. Comp. Meth. Appl. Mech. Eng, 107: 225-238.

Ibrahimbegovic, A., 1994. Stress resultant geometrically nonlinear shell theory with drilling rotations-Part I. A consistent formulation. Comp. Meth. Appl. Mech. Eng, 118: 265-284.

Ibrahimbegovic, A., 1995. On finite element implementation of geometrically nonlinear reissner's beam theory: three-dimensionai curved beam elements. Comp. Meth. Appl. Mech. Eng, 26: 11-26.

Ibrahimbegovic, A., 1997. Stress resultant geometrically exact shell theory for finite rotations and its finite element implementation. Appl. Mech. Rev, 50(4): 199-226.

Ibrahimbegovic, A., Frey, F., 1992. Quadrilateral membrane elements with rotational degrees of freedom. Engrg. Fract. Mech, 43: 13-24.

Ibrahimbegovic, A., Frey, F., 1993. Geometrically nonlinear method of incompatible modes in application to finite elasticity with independent rotations. Int. J. Num. Meth. Eng, 36: 4185-4200.

Ibrahimbegovic, A., Frey, F., 1994. Stress resultant geometrically nonlinear shell theory with drilling rotations-Part II. Computational aspects. Comp. Meth. Appl. Mech. Eng, 118: 285-308.

Ibrahimbegovic, A., Frey, F., 1995. Variational principles and membrane finite elements with drilling rotations for geometrically nonlinear elasticity. Int. J. Num. Meth. Eng, 38: 1885-1900.

Ibrahimbegovic, A., Mamouri, S., 2002. Energy conserving/decaying implicit time-stepping scheme for nonlinear dynamics of three-dimensional beams undergoing finite rotations. Comp. Meth. Appl. Mech. Eng, 191: 4241-4258.

Ibrahimbegovic, A., Taylor, R.L., Wilson, E. L., 1990. A robust quadrilateral membrane finite element with drilling degrees of freedom. Int. J. Num. Meth. Eng, 30: 445-457.

Ibrahimbegovic, A., Wilson, E.L., 1991-a. A Unifed Formulation for Triangular and Quadrilateral Flat Shell Finite Element with Six Nodal Degrees of Freedom. Commun. App. Num. Meth, 7: 1-9.

Ibrahimbegovic, A., Wilson, E.L., 1991-b. A modified method of incompatible modes. Commun. App. Num. Meth, 7: 187-94.

Idelsohn, S.R, 1981. On the use of deep, shallow or flat shell finite elements for the analysis of thin shell structures. Comp. Meth. App. Mech. Eng, 26: 321-330.

Idelsohn, S.R., Cardona, A., 1985. A reduction method for nonlinear structural dynamic analysis. Comp. Meth. Appl. Mech. Eng: 49(3): 253-279.

Idlbi, A., Karama, M., Touratier, M., 1997. Comparaison of various laminated plate theories. Composite Structures, 37: 173-784.

Irons, B.M., 1966. Engineering applications of numerical integration in stiffness methods. AIAA J, 4: 2035-2037.

Irons, B.M., 1973. Comment on a Higher Order Conforming Rectangular Plate Element by S. Gopalacharyulu. Int. J. Num. Meth. Eng, 6: 308-309.

Irons, B.M., 1974. The Semiloof shell element. Conf. on finite elements applied to thin shells and curved members, University College, Cardiff. May, 1974.

Irons, B.M., Razzaque, A., 1972. Experience with the patch test for convergence of finite elements, in mathematical foundation of the finite element method (New York: Academic Press) pp 557-587.

Irons, B.M., Razzaque, A., 1976. The Semiloof shell element. Finite elements for thin shells and curved members, Edit. Ashwell and Gallagher, Wiley, pp 197-222.

Iura, M., Atluri, S.N., 1992. Formulation of a membrane finite element with drilling degrees of freedom. Comput. Mech, 96: 417-428.

Izzuddin, B.A., 2005. An enhanced co-rotational approach for large displacement analysis of plates. Int. J. Num. Meth. Eng, 64: 1350-1374.

-J-

Jaamei, S. Frey, F., Jetteur, Ph., 1987. Nonlinear thin shell finite element with six degrees of freedom per node, in: Seventh International Symposium on Computing methods in Applied Science and Engineering, Versailles.

Jaamei, S., 1988. 'Jet' thin shell finite element with drilling rotations. IREM Internal Report 88/7, Ecole Polytechnique Fédérale de Lausanne.

Jaamei, S., Frey, F., Jetteur, Ph., 1988. Numerical tests with JET shell element. Part III: JET shell tests. IREM Internal Report 88/8, Départment de Génie Civil, Institut de Statique et Structures, Ecole Polytechnique Fédérale de Lausanne, August.

Jaamei, S., Frey, F., Jetteur, Ph., 1989. Nonlinear thin shell finite element with six degrees of freedom per node. Comp. Meth. Appl. Mech. Eng, 75: 251-266.

Javaherian, H., Dowling, P.J., Lyons, L.P.R., 1980. Nonlinear Finite Element Analysis of Shell Structures Using the Semi-Loof Element. Comput. Struct, 12: 147-159.

Jetteur, Ph., 1986. A shallow shell element with in-plane rotational degrees of freedom. IREM Internal Report 86/3, Département de Génie Civil, Institut de Statique et Structures, Ecole Polytechnique Fédérale de Lausanne.

Jetteur, Ph., 1987. Improvement and large rotations of the JET shell element in nonlinear analysis. IREM Internal Report 87/4, Département de Génie Civil, Institut de Statique et Structures, Ecole Polytechnique Fédérale de Lausanne.

Jetteur, Ph., Frey, F., 1986. A four node Marguerre element for non-linear shell analysis. Engrg. Comput, 3: 276-282.

Jeyachandrabose, C., Kirkhope, J., 1986. Construction of new efficient three-node triangular thin plate bending elements. Comput. Struct, 23: 587-603.

Jeyachandrabose, C., Kirkhope, J., Babu, C.R., 1985. An alternative explicit formulation for the DKT plate-bending element. Int. J. Num. Meth. Eng, 21: 1289-1293.

Jeyachandrabose, C., Kirkhope, J., Meekisho, L., 1987. An improved discrete Kirchhoff quadrilateral thin-plate bending element. Int. J. Num. Meth. Eng, 24: 635-654.

Jiang, L., Chernuka, M.W. Pegg, N.G., 1994. A corotational, updated lagrangian formulation for geometricall- nonlinear finite element analysis of shell structures- Finite. Elem. Anal. Des, 18: 129-140.

Jiang, L., Chernuka, W., 1994. A simple four-noded co-rotational shell element for arbitrarily large rotations. Comput. Struct, 53(5): 1123-1132.

Jin, W.G., Cheung, Y.K., Zienkiewicz, O.C., 1990. Application of the Trefftz method in plane elasticity problems. Int. J. Num. Meth. Eng, 30: 1147-1161.

Jintai, Ch., Gregory, M.H., 1994. A family of single-step Houbolt time integration algorithms for structural dynamics. Comp. Meth. Appl. Mech. Eng, 118: 1-11.

Jirousek, J., Venkatesh, A., 1992. Hybrid Trefftz plane elasticity elements with p-method capabilities. Int. J. Num. Meth. Eng, 35: 1443-1472.

Jones, R.E., Strome, D.R., 1966. Dircet stiffness method analysis of shells of revolution utilizing curved elements, AIAA J, 4: 1519-1525.

Jorabchi, K., Suresh, K., 2011. A robust continuation method to pass limit-point instability. Finite. Elem. Anal. Des, 47: 1253-1261.

-K-

Kang, L., Zhang, Q., Wang, Z., 2009. Linear and geometrically nonlinear analysis of novel flat shell elements with rotational degrees of freedom. Finite. Elem. Anal. Des, 45: 386-392.

Kant, T., Kommineni, J. R., 1994. Geometrically non-linear transient analysis of laminated composite and sandwich shells with a refined theory and C0 finite elements. Comput. Struct, 52(6): 1243-1259.

Kant, T., Swaminathan, K., 2002. Analytical solutions for the static analysis of laminated composite and sandwich plates based on a higher order refined theory. Composite Structures, 56: 329-344.

Kapania, R.K., Mohan P., 1996. Static, free vibration and thermal analysis of composite plates and shells using a flat triangular shell element. Comput. Mech, 17: 343-357.

Karaköse, Ü.H.C., Askes, H., 2010. Static and dynamic convergence studies of a four-noded membrane finite element with rotational degrees of freedom based on displacement superposition. Int. J. Numer. Methods. Biomed. Eng, 26: 1263-1275.

Karamanlidis, D., Honecher, A., Knothe, K., 1981. Large deflection finite element analysis of pre and post critical response of thin elastic frames, in Nonlinear Finite Element Analysis in Structural Mechanics, Edited by Wunderlich, W., Stein, E. and Bathe, K.J., Springer-Verlag, Berlin Heidelberg, N.Y.

Katili, I., 1993-a. A new discrete Kirchhoff-Mindlin element based on Mindlin-Reissner plate theory and assumed shear strain fields—Part I: an extended DKT element for thick-plate bending analysis. Int. J. Num. Meth. Eng, 36: 1859-1883.

Katili, I., 1993-b. A new discrete Kirchhoff-Mindlin element based on Mindlin-Reissner plate theory and assumed shear strain fields-Part II: an extended DKQ element for thick-plate bending analysis. Int. J. Num. Meth. Eng, 36: 1885-1908.

Kawai, T., Yoshimura, S., 1969. Analysis of large deflection of plates by the finite element method. Int. J. Num. Meth. Eng, 1: 123-133.

Kebari, H., Cassell, A.C., 1992. A stabilized 9-node non-linear shell element. Int. J. Num. Meth. Eng, 35: 37-61.

Keller, H.B., 1983. The bordering algorithm and path following near singular points of higher nullity, SIAM J. Sci. Stat. Comput, 4: 573-582.

Keulen, V.F., Booij, J., 1996. Refined consistent formulation of a curved triangular finite rotation shell element. Int. J. Num. Meth. Eng, 39: 2803-2820.

Keulen, V.F., Bout, A., Ernst, L., 1993. Nonlinear thin shell analysis using a curved triangular element. Comp. Meth. Appl. Mech. Eng, 103: 315-343.

Khare, R.K., Kant, T., Garg, A.K., 2004. Free vibration of composite and sandwich laminates with a higher-order facet shell element. Composite Structures, 65: 405-418.

Khosravi, P., Ganesan, R., Sedaghati, R., 2007. Corotational nonlinear analysis of thin and moderately thick laminated composite structures. Int. J. Num. Meth. Eng, 69: 859-885.

Khosravi, P., Ganesan, R., Sedaghati, R., 2008. An efficient facet shell element for corotational nonlinear analysis of thin plates and shells using a new shell element. Comput. Struct, 86: 850-858.

Khudada, A.E., Geschwindner, L.F., 1997. Nonlinear dynamic analysis of steel frames by modal superposition. ASCE, Journal of structural engineering, 123(11): 1519-1527.

Kikuchi, F., 1984. Error analysis of flat plate element approximation of circular cylindrical shells. Theor. Appl. Mech, 32: 469-484.

Kim, D.N., Bathe, K.J., 2008. A 4-node 3D-shell element to model shell surface tractions and incompressible behavior. Comput. Struct, 86(21–22): 2027-2041.

Kim, J.H., Kim, Y.H., 2002. A three-node C0 ANS element for geometrically non-linear structural analysis. Comp. Meth. Appl. Mech. Eng, 191: 4035-4059.

Kim, K., Voyiadjis, G.Z., 1999. Non-linear finite element analysis of composite panels. Composites, Part B, 30: 365-381.

Kim, K.D., Lee, C.S., Han, S.C., 2007-a. A 4-node co-rotational ANS shell element for laminated composite structures. Composite Structures. 80: 234-252.

Kim, K.D., Han, S.C., Suthasupradita, S., 2007-b. Geometrically non-linear analysis of laminated composite structures using a 4-node co-rotational shell element with enhanced strains. Int. J. Non-Linear. Mech, 42: 864-881.

Kim, K.D., Liu, G.Z., Han, S.C., 2005. A resultant 8-node solid-shell element for geometrically nonlinear analysis. Comput. Mech, 35: 315-331.

Kim, K.D., Lomboy, G.R., 2006. A co-rotational quasi-conforming 4-node resultant shell element for large deformation elasto-plastic analysis. Comp. Meth. Appl. Mech. Eng, 195: 6502-6522.

Kim, K.D., Lomboy, G.R., Voyiadjis, G.Z., 2003. A 4-node assumed strain quasi-conforming shell element with 6 degrees of freedom. Int. J. Num. Meth. Eng, 58: 2177-2200.

Kim, K.D., Park, T., Voyiadjis, G.Z., 1998. Postbuckling analysis of composite panels with imperfection damage. Comput. Mech, 22: 375-387.

Kirchhoff, G., 1850. Uber das gleichgewicht und die bewegung einer elastischen scheibe. Journal fur reine und angewandte Mathematik, 40: 51-88.

Kirchhoff, G., 1876. Vor1esungen uber Hathematische Physik, Mechanik, Vol. 1.

Klein, S., Trujillo, D.M., 1983. An unconditionally stable finite element analysis for nonlinear structures. Comput. Struct, 16: 187-197.

Klinkel, S., Gruttmann, F., Wagner, W., 1999. A continuum based 3D-shell element for laminated structures. Comput. Struct, 71: 43-62.

Klinkel, S., Gruttmann, F., Wagner, W., 2006. A robust non-linear solid shell element based on a mixed variational formulation. Comp. Meth. Appl. Mech. Eng, 195: 179-201.

Klinkel, S., Wagner, W., 1997. A geometrical non-linear brick element based on the EASmethod. Int. J. Num. Meth. Eng, 40: 4529-4545.

Knight, N.F., 1997. Raasch challenge for shell elements. AIAA J, 35(2): 375-381.

Knowles, N.C., Razzaque, A., Spooner, J.B., 1976. Experience of finite element analysis of shell structures. In Finite Elements for Thin Shells and Curved Members (Edited by R. H. Gallagher and D. G. Ashwell), pp. 245-262. John Wiley, New York.

Koiter, W.T., 1960-a. A consistent first approximation in the general theory of thin elastic shells. In Proceedings of the IUTAM Symposium on the Theory of Thin Elastic Shells, pages 12-33, Delft, August 1959. North-Holland Publishing Company, Amsterdam.

Koiter, W.T., 1960-b, Theory of thin elastic shells, Proceedings of First IUTAM Symposium, Delft 1959, North Holland.

Kolahi, A.S., Crisfield, M.A., 2001. A large-strain elasto–plastic shell formulation using the Morley triangle. Int. J. Num. Meth. Eng, 52: 829-849.

Kouhia, R., 2008. Stabilized forms of orthogonal residual and constant incremental work control path following methods. Comp. Meth. Appl. Mech. Eng, 197: 1389-1396.

Krakeland, B., 1977. Large displacement analysis of shells considering elasto-plastic and elasto-viscoplastic materials, Div. Struct. Mech., Norwegian. Inst. Tech, Trondheim, Report No. 7776.

Krenk, S. 1995. An orthogonal residual procedure for non-linear finite element equations. Int. J. Num. Meth. Eng, 38(5): 823-839.

Krenk, S., Hededal, O., 1995. A Dual Orthogonality Procedure for Non-Linear Finite Element Equations. Comp. Meth. Appl. Mech. Eng, 123(1-4): 95-107.

Krishnamoorthy, C.S., Ramesh, G., Dinesh, K.U., 1996. Post-buckling analysis of structures by three-parameter constrained solution techniques, Finite Element in Analysis and Design, 22(2): 109-142.

Kuan-Jung, J., Wilson, E.L., 1988. An Adaptive Finite Element Technique for Structural Dynamic Analysis. Comput. Struct, 30(6): 1319-1339.

Kugler, S., Fotiu, P., Murin, J., 2010. A highly efficient membrane finite element with drilling degrees of freedom. Acta Mech, 213: 323-348.

Kugler, S., Fotiu, P.A., Murin, J., 2011. Advances in quadrilateral shell elements with drilling degrees of freedom, in: H. Altenbach, V. Eremeyev (Eds.), Shell-Like Structures-Advanced Structured Materials, 15: 307-328.

Kuhl, D., Crisfield, M., 1999. Energy conserving and deaying algorithms in non-linear structural dynamics. Int. J. Num. Meth. Eng, 45: 569-599.

Kuhl, D., Ramm, E., 1996. Constraint Energy Momentum Algorithm and its application to non-linear dynamics of shells. Comp. Meth. Appl. Mech. Eng, 136: 293-315.

Kuhl, D., Ramm, E., 1999. Generalized Energy-Momentum Method for non-linear adaptive shell dynamics. Comp. Meth. Appl. Mech. Eng, 178: 343-366.

Kuo, S.R., Yang, Y.B., 1995. Tracing postbuckling paths of structures containing multi-loops. Int. J. Num. Meth. Eng, 38: 4053-75.

Kutta, W., 1901. Zeitschrift fur Mathematik und Physik 46,435-453. Beitrag zur naherungsweisen Integration totaler Differentialgleichungen.

Kuznetsov, V.V., Levyakov, S.V., 2007. Phenomenological invariant-based finite-element model for geometrically nonlinear analysis of thin shells. Comp. Meth. Appl. Mech. Eng, 196: 4952-4964.

Kweon, J.H., Hong, C.S., 1994. An improved arc-length method for postbuckling analysis of composite cylindrical panels. Comput. Struct, 53(3): 541-9.

Kwok, H.H., Kamat M.P., Watson, L.T., 1985. Location of stable and unstable equilibrium configurations using a model truss region quasi-Newton method and tunnelling. Comput. Struct, 21: 909-916.

Kwon, Y.W., 2013. Analysis of Laminated and Sandwich Composite Structures Using Solid-like Shell Elements. Applied Composite Materials.

-L-

Lam, W.F., Morley, C.T., 1992. Arc-length method for passing limit points in structural calculation. Journal of Structural Engineering, 118(1): 169-185.

Lame, G., Clapeyron, B.P.E., 1833. Memoire Sur lequilibre interieur des corps solides, Hem. Pres. Par Div. Savants, Vol. 4.

Lee, K., Han, S.E., Hong, J.W., 2014. Post-buckling analysis of space frames using concept of hybrid arc-length methods. Int. J. Nonlinear Mech, 58: 76-88.

Lee, N.S., Bathe, K.J., 1993. Effects of element distortions on the performance of isoparametric elements. Int. J. Num. Meth. Eng, 36(20): 3553-76.

Lee, S.C., Yoo, C.H.H., 1988. A novel shell element including in plane torque effect. Comput. Struct, 28: 505-522.

Lee, S.J., Nukulchai, W.K., 1998. A Nine-Node Assumed Strain Finite Element for Large-Deformation Analysis of Laminated Shells. Int. J. Num. Meth. Eng, 42: 777-798.

Lee, S.Y., Wooh, S.C., 2004. Finite element vibration analysis of composite box structures using the high order plate theory. Journal of Sound and Vibration, 277: 801-814.

Lee, W.J., Lee, B.C., 2001. An Effective Finite Rotation Formulation for Geometrical Non-linear Shell Structures. Comput. Mech, 27: 360-368.

Leon, S.E., Lages, E.N., De-Araújo, C.N., Paulino, G.H., 2014. On the effect of constraint parameters on the generalized displacement control method. Mechanics Research Communications, 56: 123-129.

Leon, S.E., Paulino, G.H., Pereira, A., Menezes, I.F.M., Lages, E.N., 2011. A unified library of nonlinear solution schemes. Applied Mechanics Reviews 64, 040803.

Leontyev, V.A., 2010. Direct Time Integration Algorithm With Controllable Numerical Dissipation For Structural Dynamics: Two-Step Lambda Method. Applied Numerical Mathematics, 60: 277-292.

Li, L.M., Li, D.Y., Peng, Y.H., 2011-b. The simulation of sheet metal forming processes via integrating solid-shell element with explicit finite element method. Engineering with Computers.

Li, L.M., Peng, Y.H., Li, D.Y., 2011-a. A stabilized underintegrated enhanced assumed strain solid-shell element for geometrically nonlinear plate/shell analysis. Finite. Elem. Anal. Des, 47(5): 511-518.

Li, M., Zhan, F., 2000. The finite deformation theory for beam, plate and shell. Part V. The shell element with drilling degree of freedom based on Biot strain. Comp. Meth. Appl. Mech. Eng, 189: 743-759.

Li, Z.X., Izzuddin, B.A., Vu-Quoc, L., 2008. A 9-node co-rotational quadrilateral shell element. Comput Mech, 42: 873-884.

Liberscu, L., 1967. On the theory of anisotropic elastic shell and plates. Int. J. Solids. Struct, 3: 53-68.

Lin, H., Tang, L.M., Lu, H.X., 1990. The quasi-conforming plane element with rotational degree of freedom. Comput. Struct. Mech. Applic, 7: 23-31.

Lin, T.W., Yang, Y.B., Shiau, H.T., 1993. A Work Weighted State Vector Control Method for Geometrically Nonlinear Analysis. Comput. Struct, 46(4): 689-694.

Liu, J., Riggs, H.R., Tessler, A., 2000. A four-node, shear-deformable shell element developed via explicit Kirchhoff constraints. Int. J. Num. Meth. Eng, 49: 1065-1086.

Liu, M.L., To, C.W.S., 1995. Hybrid strain based three node flat triangular shell elements I: nonlinear theory and incremental formulation. Comput. Struct, 54(6): 1031-1056.

Lo, K.H., Christensen, R.M., 1977-a. A high-order theory of plate deformation. Part 1: Homogeneous plates. J. Appl. Mech, 44(4): 663-668.

Lo, K.H., Christensen, R.M., 1977-b. A high-order theory of plate deformation. Part 2: laminated plates. J. Appl. Mech, 44: 669-676.

Lo, S.H., 1992. Geometrically nonlinear formulation of 3D finite strain beam element with large rotations. Comput. Struct, 44: 147-157.

Lomboy, G.R., Suthasupradit, S., Kim, K.D., Oñate, E., 2009. Nonlinear Formulations of a Four-Node Quasi-Conforming Shell Element. Arch. Comp. Meth. Eng, 16: 189-250.

Long, C.S., Geyer, S., Groenwold, A.A., 2006. A numerical study of the effect of penalty parameters for membrane elements with independent rotation fields and penalized equilibrium. Finite Element in Analysis and Design, 42: 757-765.

Long, C.S., Loveday, Ph.W., Groenwold, A.A., 2009. Effects of finite element formulation on optimal plate and shell structural topologies. Finite. Elem. Anal. Des, 45: 817-825.

Long, Y.Q. Li, J.X., Long, Z.F., Cen, S., 1999-a. Area coordinates used in quadrilateral elements. Commun. Num. Meth. Eng, 15(8): 533-545.

Long, Y.Q., Xu, Y., 1994. Generalized conforming triangular membrane element with vertex rigid rotation al freedom. Finite Elem Anal Des, 17: 259-71.

Long, Z.F., Li, J.X., Cen, S., Long, Y.Q., 1999-b. Some basic formulae for area coordinates used in quadrilateral elements. Commun. Num. Meth. Eng, 15(12): 841-852.

Lorentz, E., Badel, P., 2004. A new path-following constraint for strain-softening finite element simulations. Int. J. Num. Meth. Eng, 60(2): 499-526.

Love, A.E.H., 1888. On the Small Vibrations and Deformations of Thin Elastic Shells, Phil. Trans. Roy. Sci., Vol. 179, p. 491.

Love, A.E.H., 1944. A treatise on the mathematical theory of elasticity, 4th. edn, Dover, New York.

Lyons, L.P.R., 1970. Elastic plane stress analysis of twodimensional pierced shear walls by finite element idealisation, CIRIA Report.

-M-

MacLeod, I.A., 1969. New rectangular finite element for shear wall analysis. J. Struct. Div, Proc. ASCE, 95: 399-409.

Macneal, R.H., 1978. A simple quadrilateral shell element. Comput. Struct, 8: 175-183.

MacNeal, R.H., 1982. Derivation of element stiffness matrices by assumed strain distribution. J. Nucl. Engrg. Des, 70: 3-12.

MacNeal, R.H., 1987. A theorem regarding the locking of tapered four-noded membrane elements. Int. J. Num. Meth. Eng. 24(9): 1793-1799.

MacNeal, R.H., 1989. Toward a defect-free four nodded membrane element. Finite. Elem. Anal. Des, 5: 31-37.

MacNeal, R.H., Harder, R.L., 1988. A refined four-node membrane element with rotational degrees of freedom. Comput. Struct, 28(1): 75-84.

Madenci, E., Barut, A., 1994. A free formulation flat shell element for non-linear analysis of thin composite structures. Int. J. Num. Meth. Eng, 37: 3825-3842.

Madeo, A., Zagari, G. Casciaro, R., 2012. An isostatic quadrilateral membrane finite element with drilling rotations and nospurious modes. Finite. Elem. Anal. Des, 50: 21-32.

Maewal, A., Nachbar, W., 1977. Stable postbuckling equilibria of axially compressed elastic circular cylindrical shells: a finite element analysis and comparison with experiments. J. Appl. Mech, 44: 475-481.

Malkus, D.S., Hughes, T.J.R. 1978. Mixed finite element methods-reduced and selective integration techniques: a unification of concepts. Comp. Meth. Appl. Mech. Eng, 15: 63-81.

Mallet, R.H., Berlee, L., 1966. Automated method for the large deflection and instability analysis of 3-dimensional truss and frame assemblies, AFF DL-TR- 66-102.

Marcal, P.V., 1969. Finite element analysis of combined problems of non-linear material and geometric behaviour. Proc. Am. Soc. Mech. Conf. on Comp. Approaches in Appl. Mech.

Marguerre, K., 1950. Knick-und Beulvorgängne - Einführung in die Theorie der elastichen Stabilität. Chapitre VI de: Neuere Festigkeitsprobleme des Ingenieurs, herausgegeben von K. Marguerre, Springer-Verlag.

Massin, P., Al-Mikdad, M., 2002. Nine node and seven node thick shell elements with large displacements and rotations. Comput. Struct, 80: 835-847.

Meek, J.L., Ristic, S., 1997. Large displacement analysis of thin plates and shells using a flat facet finite element formulation. Comp. Meth. Appl. Mech. Eng, 145: 285-299.

Meek, J.L., Tan, H.S., 1985. A Discrete Kirchhoff Plate Bending Element with Loof Nodes. Comput. Struct, 21: 1197-1212.

Meek, J.L., Tan, H.S., 1986-a. A faceted shell element with loof nodes. Int. J. Num. Meth. Eng, 23: 49-67.

Meek, J.L., Tan, H.S., 1986-b. Instability analysis of thin plates and arbitrary shells using a faceted shell element with loof nodes. Comp. Meth. Appl. Mech. Eng, 57: 143-170.

Meek, J.L., Wang, Y., 1998. Nonlinear static and dynamic analysis of shell structures with finite rotation. Comp. Meth. Appl. Mech. Eng, 162: 301-315.

Melosh, R. J., 1961. A Stiffness Matrix for the Analysis of Thin Plates in Bending. Journa1 of Aerospace Science, 28(1): 34-42.

Melosh, R.J., 1965. A flat triangular shell element stiffness matrix. Proc. of the Conference on Matrix Methods in Structural Eng., Wright-Patterson Air Force Base, 503-514.

Mengfu, W., Au, F.T.K., 2006. Assessment and improvement of precise time step integration method. Comput. Struct, 84: 779-786.

Miehe, C., 1998. A theoretical and computational model for isotropic elastoplastic stress analysis in shells at large strains. Comp. Meth. Appl. Mech. Eng, 155: 193-233.

Milford, R.V., Schnobrich, W.C., 1986. Degenerated isoparametric finite elements using explicit integration. Int. J. Num. Meth. Eng, 23: 133-154.

Militello, C., Felippa, C.A., 1991. The first ANDES elements: 9-dof plate bending triangles. Comp. Meth. Appl. Mech. Eng, 93(2): 217-246.

Mindlin, R.D., 1951. Influence of rotatory inertia and shear on flexural motions of isotropic elastic plates. J. Appl. Mech, 18: 31-38.

Mohammadi, S., Owen, D.J.R., Peric, D., 1999. Performance of the anisotropic Morley shell element in dynamic large deformation analysis. Commun. Num. Meth. Eng, 15: 445-455.

Mohan, P., Kapania, R.K., 1997. Geometrically nonlinear analysis of composite plates and shells using a flat triangular shell element. 38th AAIA/ASME/ASCE/AHS/ASC Structures, Structural Dynamics and Materials Conference, Kissimmee, FL, Paper 97-1233, 2347-2361.

Mohan, P., Kapania, R.K., 1998. Updated Lagrangian formulation of a flat triangular element for thin laminated shells. AIAA J, 36(2): 273-281

Mohr, G.A., 1982. Finite element formulation by nested interpolations: application to the drilling freedom problem. Comput. Struct, 15: 185-190.

Mohraz, B., Elghadamsi, F.E., Chang, C., 1991. An incremental mode-superposition for nonlinear dynamic analysis. Earthquake Engineering & Structural Dynamics, 20(5): 471-481.

Mondkar, D.P., Powell, G.H., 1978. Evaluation of Solution Schemes for Nonlinear Structures. Comput. Struct, 9(3): 223-236.

Moreira, R.A.S. Rodrigues, J.D., 2011. A non-conforming plate facet-shell finite element with drilling stiffness. Finite. Elem. Anal. Des, 47: 973-981.

Morley, L.S.D. 1971. On the constant-moment plate bending element. J. Strain. Anal, 6: 20-24.

Morley, L.S.D., Mould, M.P., 1987. The role of bending in the finite element analysis of thin shells. J Finite Elements Anal Des, 3: 213-240.

Morris, N.F., 1977. The use of modal superposition in nonlinear dynamics. Comput. Struct, 7(1): 65-72.

Mostafa, M., Sivaselvan, M.V., Felippa, C.A., 2013. Reusing linear finite elements in material and geometrically nonlinear analysis-Application to plane stress problems. Finite. Elem. Anal. Des, 69: 62-72.

Mousa, A.I., Sabir, A. B., 1994. Finite Element Analysis of Fluted Conical Shell Roof Structures, Civil-Comp-Ltd, Edinburgh, Scotland, Computational Structural Engineering for Practice, pp. 173-181.

Muller, M., 2007. Passing of instability points by applying a stabilized Newton-Raphson scheme to a finite element formulation: comparison to arc-length method. Comput. Mech, 40(4): 683-705.

Muller, M., 2008. Post buckling analysis stabilized by penalty springs and intermediate corrections. Comput. Mech, 42(5): 631-654.

Murray, D.W., Wilson, E.L., 1969. Finite element large deflection analysis of plates. ASCE, J. Engng. Mech. Div. 95, 23: 143-165.

Murthy, M.V.V., 1994. On improving the membrane capability of a Four-noded quadrilateral element. Comput. Struct, 53(4): 787-799.

Murthy, S.S., Gallagher, R.H., 1983. Anisotropic cylindrical shell element based on discrete Kirchhoff theory. Int. J. Num. Meth. Eng, 19: 1805-1823.

-N-

Naceur, H., Shiri, S., Coutellier, D., Batoz, J.L., 2013. On the modeling and design of composite multilayered structures using solid-shell finite element model. Finite. Elem. Anal. Des, 70–71: 1-14.

Naghdi, P.M., 1963. Foundations of elastic shell theory. In Sneddon, I. N. and Hill, R., editors, Progress in Solid Mechanics, volume IV, pages 1-90. North-Holland Publishing Company, Amsterdam.

Nath, Y. 1979. Nonlinear dynamic response of rectangular plates subjected to transient loads. J. Sound Vibr, 63: 179-188.

Navaratna, D.R., 1966. Computation of stress resultants in finite element analysis, AIAA. J, 4: 2058-2060.

Nelson, R.B. Lorch, D.R., 1974. A refined theory for laminated orthotropic plates. ASME J. Appl. Mech, 41: 177-183.

Nemat-Nasser, S., S. Sharoff, S., 1973. Numerical analysis of pre and post-critical response of elastic continua at finite strains. Comput. Struct, 3(5): 983-999.

Neto, E.A.S., Feng, Y.T., 1999. On the determination of the path direction for arc-length methods in the presence of bifurcations and 'snap-backs'. Comp. Meth. Appl. Mech. Eng, 179: 81-89.

Neto, M.A., Leal, R.P., Yu, W., 2012. A triangular finite element with drilling degrees of freedom for static and dynamic analysis of smart laminated structures. Comput. Struct, 108-109: 61-74.

Newmark, N.M., 1959. A method of computational for structural dynamics. ACSE, Journal of Engineering Mechanics Division, 8: 67-94.

Nguyen-Van, H., Mai-Duy, N., Karunasena, W., Tran-Cong, T., 2011. Buckling and vibration analysis of laminated composite plate/shell structures via a smoothed quadrilateral flat shell element with in-plane rotations. Comput. Struct, 89: 612-625.

Nguyen-Van, H., Mai-Duy, N., Tran-Cong, T., 2009. An improved quadrilateral flat element with drilling degrees of freedom for shell structural analysis. CMES: Comput Model Eng Sci, 49(2): 81-112.

Nguyen-Van, H., Nguyen-Hoai, N., Chau-Dinh, T., Nguyen-Thoi, T., 2014. Geometrically nonlinear analysis of composite plates and shells via a quadrilateral element with good coarse-mesh accuracy. Composite Structures, 112: 327-338.

Nickell, R.E., 1976. Nonlinear dynamics by mode superposition. Comp. Meth. Appl. Mech. Eng, 7(1): 107-129.

Noor-Omid, B., Rankin, C.C., 1991. Finite rotation analysis and consistent linearization using projectors. Comp. Meth. Appl. Mech. Eng, 93: 353-384.

Nour-Omid, B. Rankin, C.C., 1991. Finite rotation analysis and consistent linearization using projectors. Comp. Meth. Appl. Mech. Eng, 93: 353-384.

Novozhilov, V.V., 1959. The theory of thin-shells. Groningen: P. Noordhoff.

Novozhilov, V.V., 1961. Theory of Elasticity. Pergamon Press, Oxford.

Nukala, P.K.V., White, D.W., 2004. A mixed finite element for three-dimensional nonlinear analysis of steel frames. Comp. Meth. Appl. Mech. Eng, 193: 2507-2545.

Nukulchai, W.K., 1979. A simple and efficient finite element for general shell analysis. Int. J. Num. Meth. Eng, 14: 179-200.

Nukulchai, W.K., Wong, W.K., 1988. Element-Based Lagrangian Formulation for Large Deformation Analysis. Comput. Struct, 30(4): 967-974.

-O-

Oden, J.T., 1966. Calculation of geometric stiffness matrices for complex structures. AIAA J, 4(8): 1480-1482.

Oden, J.T., 1969. Finite Element Applications in nonlinear structural analysis, Proc. Conf. On Finite Element Method, Vanderbilt Univ., Tennessee.

Oliver J., Onate, E., 1984. A total lagrangian formulation for the geometrically nonlinear analysis of structures using finite element. Part I. two-dimensional problems: shell and plate structures. Int. J. Num. Meth. Eng, 20: 2253-2281.

Olson, M.D., Bearden, T.W., 1979. A simple triangular shell element revisited. Int. J. Num. Meth. Eng, 14: 5l-68.

Onãte, E., 1994. A review of some finite element families for thick and thin plate and shell analysis. In: Hughes TJR, Onate E, Zienkiewicz OC, editors. Recent Developments in Finite Element Analysis, CIMNE, Barcelona, Spain. p. 98-111.

Onãte, E., Cendoya, P., Miquel, J., 2002. Non-linear explicit dynamic analysis of shells using the BST rotation-free triangle. Engrg. Comput, 19: 662-706.

Onãte, E., Hinton, E., Glover, N., 1978. Techniques for improving the performance of Ahmad shell elements. C/R/313/78, Department of Civil Engineering, University of Wales, Swansea.

Onãte, E., Zárate, F., 2000. Rotation-free triangular plate and shell elements. Int. J. Num. Meth. Eng, 47: 557-603.

Oral, S., Barut, A., 1991. A Shear-Flexible Facet Shell Element for Large Deflection and Instability Analysis. Comp. Meth. Appl. Mech. Eng, 93: 415-431.

Oran, C., 1973-a. Tangent stiffness in plane frames. J Struct Div ASCE, 99(ST6): 973-985.

Oran, C., 1973-b. Tangent stiffness in space frames. J Struct Div ASCE, 99(ST6): 987-1001.

Ozkul, T.A., 2004. A finite element formulation for dynamic analysis of shells of general shape by using the Wilson-h method. Thin-Walled Structures, 42: 497-513.

-P-

Pacoste, C., 1998. Co-rotational flat facet triangular elements for shell instability analysis. Comp. Meth. Appl. Mech. Eng, 156: 75-110.

Pacoste, C., Eriksson, A., 1995. Element behaviour in post-critical plane frame analysis. Comp. Meth. Appl. Mech. Eng, 125: 319-343.

Pacoste, C., Eriksson, A., 1997. Beam elements in instability problems. Comp. Meth. Appl. Mech. Eng, 144: 163-197.

Padovan, J., Tovichakchaikul, S., 1982. Self-adaptive predictor-corrector algorithm for static nonlinear structural analysis. Comput. Struct, 15: 365-377.

Pajand, M.P., Karkon, M., 2013. An effective membrane element based on analytical solution. European Journal of Mechanics A/Solids, 39: 268-279.

Papadrakakis, M., 1981. Post-buckling analysis of spatial structures by vector iteration methods. Comput. Struct, 14, 393-402.

Parisch, H., 1978. Geometrical nonlinear analysis of shells. Comp. Meth. Appl. Mech. Eng, 14: 159-178.

Parisch, H., 1979. A critical survey of the 9-node degenerated shell element with special emphasis on thin shell application and reduced integration. Comp. Meth. Appl. Mech. Eng, 20: 323-350.

Parisch, H., 1981. Large displacements of shells including material nonlinearities. Comp. Meth. Appl. Mech. Eng, 27: 183-214.

Parisch, H., 1991. An Investigation of a Finite Rotation Four Node Assumed Strain Shell Element. Int. J. Num. Meth. Eng, 21: 127-150.

Park, D.W., Oh, S.I., 2004. A four-node shell element with enhanced bending performance for springback analysis. Comp. Meth. Appl. Mech. Eng, 193: 2105-2138.

Park, K.C., 1982. A family of solution algorithms for nonlinear structural analysis based on the relaxation equations. Int. J. Num. Meth. Eng, 18: 1337-47.

Park, K.C., Stanley, G.M., 1986. A curved C° shell element based on assumed natural-coordinate strains. J. Appl. Mech, 53: 51-54.

Park, T., Kim, K., Han, S., 2006. Linear static and dynamic analysis of laminated composite plates and shells using a 4-node quasi-conforming shell element. Composites Part B: Engineering, 37(2-3): 237-248.

Pawsey, S.F., Clough, R.W., 1971. Improved numerical integration for thick slab finite elements. Int. J. Num. Meth. Eng, 3: 575-586.

Peng, X., Crisfield, M.A., 1992. A consistent co-rotational formulation for shell using the constant stress/constant moment triangle. Int. J. Num. Meth. Eng, 35: 1829-1847.

Percy, J.H., Pian, T.H., Klein, S., Navaratna, D.R., 1965. Application of the matrix displacement method of linear elastic analysis of shells of revolution, AIAA J, 3: 2138-2145.

Peric, D., Owen, D.R.J., 1991. The Morley thin shell finite element for large deformations problem: simplicity versus sophistication. In: Proc. of the International Conference on nonlinear Engineering Computations, Pineridge, Swansea, Wales, U.K. pp. 121-142.

Pian, T.H.H., 1964. Derivation of element stiffness matrices by assumed stress distributions. AIAA J, 2(7): 1333-1336.

Pian, J.H.H., Sumihara, K., 1984. Rational approach for assumed stress finite elements. Int. J. Num. Meth. Eng, 20: 1685-1695.

Piancastelli, L., 1992. Some considerations on a four-node finite element for composites with the drilling degrees of freedom. Comput. Struct, 43(2): 337-342.

Piltner, R. Taylor, R.L., 1995. A quadrilateral mixed finite element with two enhanced strain modes. Int. J. Num. Meth. Eng, 38: 1783-1808.

Piltner, R., Taylor, R.L., 1999. A systematic construction of b-bar functions for linear and non-linear mixed-enhanced finite elements for plane elasticity problems. Int. J. Num. Meth. Eng, 44(5): 615-639.

Piltner, R., Taylor, R.L., 2000. Triangular finite elements with rotational degrees of freedom and enhanced strain modes. Comput. Struct, 75: 361-368.

Piltner, R., Taylor, R.L., 2005. A quadrilateral mixed finite element with two enhanced strain modes. Int. J. Num. Meth. Eng, 38(11): 1783-1808.

Pimenta, P.M., Campello, E.M.B., Wriggers, P., 2004. A fully nonlinear multi-parameter shell model with thickness variation and a triangular shell finite element. Comput. Mech, 34: 181-193.

Pimpinelli, G., 2004. An assumed strain quadrilateral element with drilling degrees of freedom. Finite. Elem. Anal. Des, 41: 267-283.

Popov, E.P., Penzien, J., Lu, Z.A., 1964. Finite element solutions for axisymmetric shells. J. Engng. Mech. Div, ASCE, 90(5): 119-145.

Popov, E.P., Sharifi, P., 1971. A Refined Curved Element for Thin Shells of Revolution. Int. J. Num. Meth. Eng, 3: 495-508.

Poulsen, P.N., Damkilde, L., 1996. A Flat Triangular Shell Element with Loof Nodes. Int. J. Num. Meth. Eng, 39(22): 3867-3887.

Powell, G., Simons, J., 1981. Improved iteration strategy for nonlinear structures. Int. J. Num. Meth. Eng, 17: 1455-1467.

Prathap, G., 1984. An optimally constrained 4 node quadrilateral thin plate bending element. Comput. Struct, 18(5): 789-794.

Prathap, G., 1985. The poor bending response of the four-node plane stress quadrilateral. Int. J. Num. Meth. Eng, 21: 825-835.

Prathap, G., Senthilkumar, V., 2008. Making sense of the quadrilateral area coordinate membrane elements. Comp. Meth. Appl. Mech. Eng, 197: 4379-4382.

Providas, E., Kattis, M.A., 1999. A simple finite element model for the geometrically nonlinear analysis of thin shells. Comput. Mech, 24: 127-37.

Providas, E., Kattis, M.A., 2000. An assessment of two fundamental flat triangular shell elements with drilling rotations. Comput. Struct, 77: 129-139.

Pugh, E.D.L., Hinton, E., Zienkiewicz, O.C., 1978. A study of quadrilateral plate bending elements with reduced integration. Int. J. Numer. Meth. Eng, 12: 1059-1079.

Puso, M.A., 2000. A highly efficient enhanced assumed strain physically stabilized hexahedral element. Int. J. Num. Meth. Eng, 49: 1029-1064.

-Q-

Qi, Z., Tianqi, Y., 1995. The adaptative parameter incremental method for the analysis of snapping problems. Appl Math Mech, 16(9): 851-8.

-R-

Rah, K., Paepegem, W.V., Degrieck, J., 2013-a. A novel versatile multilayer hybrid stress solid-shell element. Comput. Mech.

Rah, K., Paepegem, W.V., Habraken, A.M., Degrieck, J., 2011. A partial hybrid stress solid-shell element for the analysis of laminated composites. Comp. Meth. Appl. Mech. Eng, 200(49–52): 3526-3539.

Rah, K., Paepegem, W.V., Habraken, A.M., Degrieck, J., 2013-b. Optimal low-order fully integrated solid-shell elements. Comput. Mech.

Rajendran, S., 2010. A technique to develop mesh-distortion immune finite elements. Comp. Meth. Appl. Mech. Eng, 199: 1044-1063.

Ramm, E., 1981. Strategies for tracing the nonlinear response near limit points. In Nonlinear Finite Element Analysis in Structural Mechanics (Edited by Wunderlich et al.), pp. 63-89. Springer, NY.

Ramm, E., 1982. The Riks/Wempner approach - An extension of the displacement control method in nonlinear analyses. Recent Advances in nonlinear Computational Mechanics, university of Swansea, England, pp. 63-89.

Ramm, E., Osterrieder, P., 1983. Ulimate load analysis of three-dimensional beam structures with thin-walled cross sections using finite elements. In Proc. Third Int. Colloquium. Stability of metal stuctures. CTICM, Paris, Nov.

Rankin, C.C., Brogan, F.A., 1986. An element independent corotational procedure for the treatment of large rotations. Journal of Pressure Vessel Technology, 108: 165-174.

Rankin, C.C., Brogan, F.A., Loden, W.A., Cabiness, H.D., 1994. Stags user manual, Lockheed Martin Missiles and Space Co. Inc. Advanced Technology Center, Version 3.0, Report P032594.

Rankin, C.C., Nour-Omid, B., 1988. The use of projectors to improve finite element performance. Comput. Struct, 30: 257-267.

Rannacher, R., 1991. On the convergence of the Newton-Raphson method for strongly nonlinear equations. In P. Wriggers and W. Wagner, editors, Nonlinear. Com. Mech, pp. 11-30.Springer-Verlag.

Rebiai, C., Belounar, L., 2013. A new strain based rectangular finite element with drilling rotation for linear and nonlinear analysis, Archives of Civil and Mechanical Engineering, 13(1): 72-81.

Rebiai, C., Belounar, L., 2014. An effective quadrilateral membrane finite element based on the strain approach. Measurement, 50: 263-269.

Reddy, J.N., 1984. A simple higher-order theory for laminated composite plates. J. Appl. Mech, 51: 745-752.

Reese, S., 2007. A large deformation solid-shell concept based on reduced integration with hourglass stabilization. Int. J. Num. Meth. Eng, 69: 1671-1716.

Reese, S., Wriggers, P., Reddy, B.D., 2000. A new locking-free brick element technique for large deformation problems in elasticity. Comput. Struct, 75:291-304.

Reissner, E., 1945. The effect of transverse shear deformations on the bending of elastic plates. J. Appl. Mech, 12: 69-77.

Reissner, E., Stavsky, Y., 1961. Bending and stretching of certain types of heterogeneous aelotropic elastic plate. J. Appl. Mech, 28: 402-408.

Rengarajan, G., Aminpour, M.A., Knight, N.F., 1995. Improved assumed-stress hybrid shell element with drilling degrees of freedom for linear stress, buckling and free vibration analyses. Int. J. Num. Meth. Eng, 38: 1917-1943.

Rheinboldt, W.C., 1981. Numerical analysis of continuation methods for nonlinear structural problems. Comput. Struct, 13: 103-113.

Riks, E., 1972. The application of Newton's method to the problem of elastic stability. J. Appl. Mech. 39: 1060-1066.

Riks, E., 1979. An incremental approach to the solution of snapping and buckling problems. Int. J. Solids. Struct, 15: 529-551.

Riks, E., 1984. Some computational aspects of the stability analysis of nonlinear structures, Comp. Meth. Appl. Mech. Eng, 47(3): 219-259.

Ritto-Correa, M., Camotim, D., 2008. On the arc-length and other quadratic control methods: established, less known and new implementation procedures. Comput. Struct, 86(11-12): 1353-1368.

Roberts, T.M., Ashwell, D.G., 1971. The use of the finite mid-increment stiffness matrices in the post-buckling analysis of imperfect structures. Int. J. Solids. Struct, 7(7): 805-823.

Robinson, J., 1980. Four-node quadrilateral stress membrane element with rotational stiffness. Int. J. Num. Meth. Eng, 16: 1567-1569.

Robinson, J., Haggenmacher, G.W, 1979. Lora - an accurate four nodes stress plate bending element, Int. J. Num. Meth. Eng, 14(2): 296-306.

Robinson, J., Haggenmacher, G.W., 1979. Some new developments in matrix force analysis. In Recent Advances in Matrix Method of Structural Analysis and Design, pp. 183-228. Univof Alabama Press.

Runge, C., 1895. Muthematische Annalen. Uber die numerische Auflosung von Differentialgleichungen, 46: 167-178.

-S-

Sabir A.B., 1985. A rectangular and triangular plane elasticity element with drilling degrees of freedom, Chapter 9 in proceeding of the 2nd international conference on variational methods in engineering, Southampton University, Springer-Verlag, Berlin, pp. 17-25.

Sabir, A. B., 1983. Strain Based Finite Elements for the Analysis of Cylinders with Holes and Normally Intersecting Cylinders. Nuclear Eng. And Design, 76: 111-1210.

Sabir, A. B., 1987. Strain Based Shallow Spherical Shell Element, Proc. Of Int. Conf. on the Mathematics of Finite Elements and Applications, Bunel University.

Sabir, A.B., Charchafchi, T.A., 1982. Curved Rectangular and General Quadrilateral Shell Element for Cylindrical Shells, The Math. of Finite Element and Applications II, Academic Press, pp. 213-239.

Sabir, A.B., Lock, A.C., 1972. A curved cylindrical shell finite element, Int. J. mech. Sci. 14: 125 - 135.

Sabir, A.B., Lock, A.C., 1973. The application of finite elements to the large deflection geometrically non-linear behaviour of cylindrical shells. In Variational Methods in Engineering (Edited by C. A. Brebbia and H. N. Totenham), 7/66-7/7X Southampton University Press.

Sabir, A.B., Ramadanhi, F., 1985. A Shallow Shell Finite Element for General Shell Analysis, Proc. of Sec. Int. Conf. On Variational Methods in Eng., Univ. of Southampton, pp. 5-3 to -13.

Sabir, A.B., Salhi, H.Y., 1986. A strain based finite element for general plane elasticity in polar coordinates. RES, 19: 1-16.

Sabir, A.B., Sfendji, A., 1995. Triangular and rectangular plane elasticity finite element. Thin-Walled Structures, 21: 225-232.

Sabourin, F., Brunet, M., 1995. Analysis of plates and shells with a simplified three node triangular element. Thin-Wall Struct, 21: 209-23.

Saigal, S., Yang, T.Y., 1985. Nonlinear dynamic analysis with a 48 D.O.F. curved thin shell element. Int. J. Num. Meth. Eng, 21: 1115-1128.

Saleeb, A.F., Chang, T.Y., Graf, W., Yingyeunyong, S., 1990. A hybrid/mixed model for non-linear shell analysis and its applications to large rotation problems. Int. J. Num. Meth. Eng, 29: 407-446.

Samanta, A., Mukhopadhyay, M., 1999. Finite element large deflection static analysis of shallow and deep stiffened shells. Finite. Elem. Anal. Des, 33: 187-208.

Sanders, J.L., 1959. An improved first approximation theory of thin shells. NASA Report 24.

Sansour, C., Bufler, H., 1992. An exact finite rotation shell theory, its mixed variational formulation and its finite element implementation. Int. J. Num. Meth. Eng, 34: 73-115.

Sansour, C., Wriggers, P., Sansour, J., 1997. Nonlinear dynamics of shells: theory finite element formulation and integration schemes. Nonlinear Dyn, 13: 279-305.

Schmir, L.A., Bognor, F.K., Fox, R.L., 1968. Finite deflection structural analysis using plate and shell discrete elements. AIAA J, 6(5): 781-791.

Schmit, L.A., Bognor, F.K., Fox, R.L., 1968. Finite deflection structural analysis using plate and shell discrete elements. AIAA J, 6(5): 781-791.

Schoop, H., 1986-a. Oberflachennorientierte endlicher Verdchiebungen, Ing. Arch, 56: 427-437.

Schoop, H., 1986-b. Postbuckling and snap through of thin elastic shells with a double surface theory. In Postbuckling of Elastic Structures, J. Szabo (Ed.), 321-337, Elsevier, Amsterdam.

Schoop, H., 1989. A simple nonlinear flat element for large displacement structures. Comput. Struct, 32(2): 379-385.

Schweizerhof, K.H., Wriggers, P., 1986. Consistent linearization for path following methods in nonlinear FE analysis. Comp. Meth. Appl. Mech. Eng, 59: 261-279.

Senjanovic, I., 1984. Harmonic acceleration method for dynamic structural analysis. Comput. Struct, 18: 71-80.

Seshu, P., Ramamurti, V., 1989. Effect of fictitious rotational stiffness coefficient on natural frequencies. Journal of Sound and Vibration, 133(l): 177-179.

Sharifi, P., Popov, E.P., 1971. Nonlinear buckling analysis of sandwich arches. ASCE J. Eng. Mech. Div, 97: 1397-1411.

Shin, C.M., Lee, B.C., 2014. Development of a strain-smoothed three-node triangular flat shell element with drilling degrees of freedom. Finite. Elem. Anal. Des, 86: 71-80.

Simo J.C., Fox D.D., Rifai MS. 1989. On a stress resultant geometrically exact shell model Part II: The linear theory; computational aspects. Comp. Meth. Appl. Mech. Eng, 73: 53-92.

Simo, J.C., 1985. A finite strain beam formulation. the three-dimensional dynamic problem. part i. Comp. Meth. Appl. Mech. Eng, 49: 53-70.

Simo, J.C., Armero, F., 1992. Geometrically nonlinear enhanced-strain mixed methods and the method of incompatible modes. Int. J. Num. Meth. Eng, 33: 1413-1449.

Simo, J.C., Fox, D.D., 1989. On a stress resultant aeometriclaly exact shell model. Part I: formulation and optimal parametrization. Comp. Meth. Appl. Mech. Eng, 72: 267-304.

Simo, J.C., Fox, D.D., Hughes, T.J.R., 1992-a. Formulation of finite elasticity with independent rotations. Comp. Meth. Appl. Mech. Eng, 95: 277-288.

Simo, J.C., Fox, D.D., Rifai, M.S., 1992-b. On a stress resultant geometrically exact shell model. Part VI: Conserving algorithms for nonlinear dynamics. Int. J. Num. Meth. Eng, 34: 117-164.

Simo, J.C., Hughes, T.J.R., 1986. On the variational foundations of assumed strain methods, J. Appl. Mech. ASME, 53: 51-54.

Simo, J.C., Rifai, M.S., 1990. A class of mixed assumed strain methods and the method of incompatible modes. Int. J. Num. Meth. Eng, 29: 1595-638.

Simo, J.C., Rifai. M.S., Fox, D.D., 1990. On a stress resultant geometrically exact shell model. part vi: Nonlinear dynamics and conserving algorithms. Int. J. Num. Meth. Eng, 34: 117-164.

Simo, J.C., Tarnow, N., 1994. A new energy and momentum conserving algorithm for the nonlinear dynamics of shells. Int. J. Num. Meth. Eng, 37: 2527-2549.

Simo, J.C., Vu-Quoc, L., 1986. A three-dimensional finite strain rod model. part ii: cornpucational aspects. Comp. Meth. Appl. Mech. Eng, 58: 79-116.

Specht, B., 1988. Modified Shape Functions for the Three Node Plate Bending Element Passing the Patch Test. Int. J. Num. Meth. Eng, 26: 705-715.

Stanley, G.M., Park, K.C., Hughes, T.J.R., 1986. Continuum-based resultant shell elements. In: Finite Element Methods for Plate and Shell Structures, ed. Hughes, T. J. R. and Hinton, E., Pineridge, Swansea, pp. 1-45.

Stolarski, H., Belytschko, T., 1983. Shear and membrane locking in curved C^0 elements. Comp. Meth. Appl. Mech. Eng, 41: 279-296.

Stolarski, H., Belytschko, T., Carpenter, N., Kennedy, J.M., 1984. A simple triangular curved shell element. Engng. Comput, 1: 210-218.

Stolarski, H., Belytschko, T., Lee, S.H., 1995. Review of shell finite elements and corotational theories. Comput Mech Adv, 2: 125-212.

Stolarski, H.K., Chen, Y.I., 1995-a. Assumed strain formulation for the four-node quadrilateral with improved in-plane bending behaviour. Int. J. Num. Meth. Eng, 38(8): 1287-1305.

Stolarski, H.K., Chen, Y.I., 1995-b. Extrapolated fields in the formulation of the assumed strain elements Part 1: Two-dimensional problems. Comp. Meth. Appl. Mech. Eng, 123: 247-262.

Strickland, G.E., Loden, W.A., 1968. A Doubly-Curved Triangular Shell Element, Proc. 2nd Conf. on Matrix Methods in Struct. Mech., Wright-Patterson Air Force Base, Ohio.

Stricklin, J.A., 1970. Geometrically nonlinear static and dynamic analysis of shells of revolution, High speed computing of elastic structures, Proc. Symp. IUTAM, University of Liege, pp. 383-411 (August).

Stricklin, J.A., Haisler, W.E., Tisdale, P.R., Gunderson, R., 1969. A rapidly converging triangular plate element. AIAA J, 7: 180-181.

Subbaraj, K., Dokainish, M.A., 1989. A survey of direct tome-integration methods in computational structural dynamics-ii. implicit methods. Comput. Struct, 32(6): 1387-1401.

Sun, S.L., Yuan, M.W., Chen, P., 1997. A practical quadrilateral membrane element with drilling degrees of freedom. Acta Mechanica Solida Sinica, 10(2): 179-188.

Surana, K.S., 1983. Geometrically nonlinear formulation for curved shell elements. Int. J. Num. Meth. Eng, 19: 581-615.

Swaminathan, K., Ragounadin, D., 2004. Analytical solutions using a higher-order refined theory for the static analysis of antisymmetric angle-ply composite and sandwich plates. Composite Structures, 64: 405-417.

Sydenstricker, R.M., Landau, L., 1996. A survey in the definition of transverse displacement for discrete Reissner/Mindlin elements. The third international conference on computational structures technology, Budapest.

Sydenstricker, R.M., Landau, L., 2000. A study of some triangular discrete Reissner-Mindlin plate and shell elements. Comput. Struct, 78: 21-33.

Sze, K.Y., Chan, W.K., Pian, T.H.H., 2002. An 8-node hybrid-stress solid-shell element for geometric nonlinear analysis of elastic shells. Int. J. Num. Meth. Eng, 55: 853-878.

Sze, K.Y., Ghali, A., 1993. Hybrid plane quadrilateral element with corner rotations. ASCE Journal of Structural Engineering, 119: 2552-2572.

Sze, K.Y., Ghali, A., 2000. On immunizing five-beta hybrid stress elements from trapezoidal locking in practical analyses. Int. J. Num. Meth. Eng, 47(4): 907-920.

Sze, K.Y., Wanji, C., Cheung, Y.K., 1992. An efficient quadrilateral plane element with drilling degrees of freedom using orthogonal stress modes. Comput. Struct, 42(5): 695-705.

Sze, K.Y., Yao, L.Q., 2000. A hybrid stress ANS solid-shell element and its generalization for smart structure modelling. Part I-solid-shell element formulation. Int. J. Num. Meth. Eng, 48: 545-564.

-T-

Tabiei, A., Tanov, R., 2002. Sandwich shell finite element for dynamic explicit analysis. Int. J. Num. Meth. Eng, 54: 763-787.

Taig, I.C., 1961. Structural analysis by the matrix displacement method. English Electric Aviation report No. 5017.

Taig, I.C., Kerr, R., 1964. Some problems in the discrete element representation of aircraft structure. Matrix method of the structural analysis. Pergamon: London, p. 267-315.

Talbot, M., Dhatt, G., 1987. Three Discrete Kirchhoff elements for shell analysis with large geometrically non-linearities and bifurcations. Engrg. Comput, 4: 15-22.

Tan, X.G., Vu-Quoc, L., 2005. Efficient and accurate multilayer solid-shell element: Non-linear materials at finite strain. Int. J. Num. Meth. Eng, 63: 2124-2170.

Tang, L.M., Chen, W.J., Liu, Y.X., 1984. Formulation of quasiconforming element and Hu-Washizu principle. Comput. Struct, 19: 247-250.

Taylor, R.L., Beresford, P.J., Wilson, E.L., 1976. A nonconforming element for stress analysis. Int. J. Num. Meth. Eng, 10: 1211-1219.

Taylor, R.L., Filippou, F.C., Saritas, A., Auricchio, F., 2003. A mixed finite element method for beam and frame problems. Comput. Mech, 31: 192-203.

Taylor, R.L., Simo, J.C., 1985. Bending and Membrane Elements for the Analysis of Thick and Thin Shells, Proceedings of the NUMEETA-85 Conference, Swansea, January.

Tenek, L.H., Hagiwara, I., 1994. Optimal rectangular plate and shallow shell topologies using thickness distribution or homogenization. Comp. Meth. Appl. Mech. Eng, 115: 111-124.

Tessler, A., 2000. Comparison of Interdependent Interpolations for Membrane and Bending Kinematics in Shear-Deformable Shell Elements, Proceedings of Intern. Conf. on Computational Engineering Science (ICES2K), Los Angeles, CA.

Tessler, A., Hughes, T.J.R., 1985. A Three-node Mindlin Plate Element with Improved Transverse Shear. Comp. Meth. Appl. Mech. Eng, 50: 71-101.

Tessler, A., Mohr, J.W., 2000. A three-node shell element with drilling degrees of freedom for thick composite and sandwich structures, Proceedings of IASS-IACM 2000 Colloquium on Computation of Shell and Spatial Structures, Athens, Greece.

Thai, H.T., Kim, S.E., 2009. Large deflection inelastic analysis of space trusses using generalized displacement control method. Journal of Constructional Steel Research, 65: 1987-1994.

Tham, C.L., Zhang, Z., Masud, A., 2005. An elasto-plastic damage model cast in a co-rotational kinematic framework for large deformation analysis of laminated composite shells. Comp. Meth. Appl. Mech. Eng, 194: 2641-2660.

Thomas, G.R., Gallagher, F.H., 1975. A triangular thin shell element: nonlinear analysis (Cornell Univ. Ithaca, NY, NASA CR No. 2483, Jul).

Thurston, G.A., Brogan, F.A., Stehlin, P., 1986. Postbuckling analysis using a general purpose code. AIAA J, 24(6): 1013-1020.

Tian, R., Yagawa, G., 2007. Allman's triangle, rotational DOF and partition of unity. Int. J. Num. Meth. Eng, 69: 837-858.

To, C.W.S., Liu, M.L., 1994. Hybrid strain based three-node flat triangular shell elements. Finite. Elem. Anal. Des, 17: 169-203.

To, C.W.S., Liu, M.L., 1995. Hybrid strain based three node flat triangular shell elements II: numerical investigation of nonlinear problems. Comput. Struct, 54: 1057-1076.

To, C.W.S., Wang, B., 1998-a. Transient responses of geometrically nonlinear laminated composite shell structures. Finite. Elem. Anal. Des, 31: 117-134.

To, C.W.S., Wang, B., 1998-b. Hybrid strain-based three-node flat triangular laminated composite shell elements. Finite. Elem. Anal. Des, 28(3): 177-207.

Tocher, J.L., Hartz, B.J., 1967. Higher order finite element for plane stress. J. Engng. Mech. Div, Proc. ASCE, 93: 149-172.

Touratier, M., 1991. An efficient standard plate theory. Engng. Sci, 29(8): 901-916.

Turner, J.M., Dill, E.H., Martin, H.C., Melosh, R.J., 1960. Large deflection of structures subject to heating and external load. J. Aero. Sci, 27: 97-106.

Turner, J.M., Martin, H.C., Weikel, B.C., 1964. Further developement and applications of stiffness method. In B. Fraeijs de Veubeke: editor, Matrix methods in structural analysis. pages 203-266. Pergamon Press.

Turner, M.J., Clough, R.W., Martin, H.C., Topp, L.J., 1956. Stiffness and deflection analysis of complex structures. Journal of Aeronautical Sciences, 23: 805-824.

-U-

Utku, S., 1967. Stiffness Matrices for Thin Triangular Element of Nonzero Gaussian Curvature, AIAA J, 5(9): 1659-1667.

Utku, S., Melosh, R.J., 1967. Behavior of triangular shell element stiffness matrices associated with polyhedron deflection distributions. AIAA paper No. 67-114, AIAA 5th Aerospace Sciences Meeting, New York.

-V-

Valente, R.A.F., Jorge, R.M.N., Cardoso, R.P.R., Cesar de Sa, J.M.A., Gracio, J.J.A., 2003. On the use of an enhanced transverse shear strain shell element for problems involving large rotations. Comput. Mech, 30: 286-296.

Valipour, H.R., 2011. ASCE, Nonlinear dynamic analysis of frame structures by modal superposition, Proceedings of the 8th International conference on structural dynamics, Eurodyn, 2011, ISBN 978-9-760-1931-4.

Ventsel, E., Krauthammer, T., 2001. Thin Plates and Shells: Theory, Analysis, and Applications. Marcel Dekker, Inc. New York.

Villaverde, R., Hanna, M.M., 1992. Efficient mode superposition algorithm for seismic analysis of nonlinear structures. Earthquake Engineering & Structural Dynamics, 21(10): 849-858.

Visser, W., 1969. A refined mixed type plate bending element. Technical Note. AIAA J, 7(9) 1801-1803.

Vlasov, V.Z., 1944. The basic differential equations in the general theory of elastic shells. Prikladnaja Matematika i Mekhanika, 8: 109-140.

Vu-Quoc, L., Tan, X.G., 2003-a. Optimal solid-shells for non-linear analysis of multilayer composites. Part I: statics. Comp. Meth. Appl. Mech. Eng, 192: 975-1016.

Vu-Quoc, L., Tan, X.G., 2003-b. Optimal solid-shells for non-linear analysis of multilayer composites. Part II: dynamics. Comp. Meth. Appl. Mech. Eng, 192: 1017-1059.

-W-

Wall, W.A., Bischoff, M., Ramm, E., 2000. A deformation dependent stabilization technique, exemplified by EAS elements at large strains. Comp. Meth. Appl. Mech. Eng., 188:859-871.

Wang, C., Hu, P., 2012. Quasi-conforming triangular Reissner-Mindlin shell elements by using Timoshenko's beam function. Comput. Model. Eng. Sci, 88: 325-350.

Wang, L., Thierauf, G., 2001. Finite rotations in non-linear analysis of elastic shells. Comput. Struct, 79: 2357-2367.

Wang, X.J., Belytschko, T., 1987. An efficient flexurally super convergent hexahedral element. Engineering Computation, 4: 281-288.

Wang, Z., Sun, Q., 2014. Corotational nonlinear analyses of laminated shell structures using a 4-node quadrilateral flat shell element with drilling stiffness. Acta. Mech. Sin. 30(3): 418-429.

Wanji, C., Cheung, Y.K., 2001. Refined 9-DOF triangular Mindlin plate elements. Int. J. Num. Meth. Eng. 51(11): 1259-1281.

Washizu, K., 1982. Variational Methods in Elasticity & Plasticity, (3rd Edition), Pergaraon Press.

Wempner, G.A., 1969. Finite Elements, Finite rotations and small strains of flexible shells. Int. J. Solids. Struct, 5: 117-153.

Wempner, G.A., 1971. Discrete approximations related to nonlinear theories of solids. Int. J. Solids. Struct, 7: 1581-1599.

Wempner, G.A., Oden, J.T., Kross, D.A., 1968. Finite element analysis of thin shells. J. Engng. Mech. Div, ASCE, 94(6): 1273-1294.

Whitney, J.M., 1973. Shear correction factors for orthotropic laminates under static load. J. Appl. Mech, 40: 302-304.

Wilson, E.L., 1985. A New Method of Dynamic Analysis for Linear and Nonlinear Systems. Finite. Elem. Anal. Des, 1: 21-23.

Wilson, E.L., Farhoomand, I., Bathe, K.J., 1973-b. Nonlinear dynamics analysis of complex structures. International Journal of Earthquake Engineering and Structural Dynamics, 1: 241-252.

Wilson, E.L., Ibrahimbegovic, A., 1990. Addition of incompatible displacement modes for the calculation of element stiffness and stress. Finite. Elem. Anal. Des, 7: 229-242.

Wilson, E.L., Taylor, R.L., Doherty, W.P., Ghaboussi, J., 1971. Incompatible Displacement Models, International Symposium on Numerical and Computer Methods in Structural Mechanics, University of Illinois, Urbana, September.

Wilson, E.L., Taylor, R.L., Doherty, W.P., Ghaboussi, J., 1973-a. Incompatible displacement models. In Numerical and Computer Methods in Structural Mechanics, (Eds. S.J. Fenves et al.), 43-57, Academic Press, New York.

Wisniewski, K., Turska, E., 2006. Enhanced Allman quadrilateral for finite drilling rotations. Comp. Meth. Appl. Mech. Eng, 195: 6086-6109.

Wood, R.D., 1973. The application of finite element methods to geometrically nonlinear structural analysis, Ph. D. thesis (Univ. Wales, Swansea).

Wood, R.D., 1977. Geometrically non linear finite element analysis of beam, frames, arches and axissymetric shells. Comput. Struct, 7: 725-735.

Wood, R.D., Zienkiewicz, O.C., 1977. Geometrically nonlinear finite element analysis of beams, frames, arches and axisymmetric shells. Comput. Struct, 7: 725-735.

Wood, W.L., Bozzak, M., Zienkiewicz, O.C., 1980. An alpha modification of Newmark's method. Int. J. Num. Meth. Eng, 15: 1562-1566.

Wriggers, P., Simo, J.C., 1990. A general procedure for the direct computation of turning and bifurcation points. Int. J. Num. Meth. Eng, 30(1): 155-176.

Wriggers, P., Wagner, W., Miehe, C., 1988. A quadratically convergent procedure for the calculation of stability points in finite element analysis. Comp. Meth. Appl. Mech. Eng, 70(3): 329-347.

Wright, E.W., Gaylord, E.H., 1968. Analysis of unbraced multistory steel rigid frames, American Society of Civil Engineers Proceedings. Journal of the Structural Division, 94(ST5): 1143-1163.

Wu, R.W.H., Wirmer, E.A., 1974. The dynamic responses of cylindrical shells including geometric and material nonlinearities. Int. J. Solids. Struct, 10: 243-260.

Wu, T.H., 2013. Dynamic nonlinear analysis of shell structures using a vector form intrinsic finite element. Engineering Structures, 56: 2028-2040.

Wunderlich, W., Stein, E., Bathe, K.J., 1981. eds., Nonlinear Finite Element Analysis in Structural Mechanics, Springer-Verlog.

-X-

Xiao-Ming, C., Song, C., Yu-Qiu, L., Zhen-Han, Y., 2004. Membrane elements insensi- tive to distortion using the quadrilateral area coordinate method. Comput. Struct, 82(1): 35-54.

Xiaoqin, C., Kumar, K.T., Desong, S., 1995. Virtual-pulse time integral methodology: A new approach for computational dynamics. Part: 2. Theory for nonlinear structural dynamics. Finite. Elem. Anal. Des, 20: 195-204.

Xue-zhang, W., Yu-qiu, L., Fang-long, H., 2002. The generalized conforming triangular membrance elements with rotational degree of freedom. Eng. Mech, 19: 11-15.

-Y-

Yaghmai, S., 1968. Incremental analysis of large deformations in mechanics of solids applications to axisymmetric shells of revolution. Technical Repon SESM 68-17, L-niv. California, Berkeley, Dec.

Yaghmai, S., Popov, E.P., 1971. Incremental analysis of large deflections of shells of revolution. Int. J. Solids. Struct, 7: 1375-1393.

Yamada, Y., Iwata, K., Kakimi, T., Hosomura, T., 1974. Large Deflection and Critical Loads Analysis of Framed Structures, Computational Methods in Nonlinear Mechanics, Edited by Oden, J.T., University of Texas, Texas, pp. 819-829.

Yang, C.H., Zhang, Y.X., 2002. Two simple membrane elements with vertex degrees of freedom. In Y.C. Loo, S.H. Chowdhury and S. Fragomeni (eds.) Proceeding of the 17th Australian conference on the mechanics of structures and Materials, Gold Coast, Queensland, Australia, pp. 113-118

Yang, H.T.Y., Saigal, S., Liaw, D.G., 1990. Advances Of Thin Shell Finite Elements And Some Applications-Version I. Comput. Struct, 35(4): 481-504.

Yang, H.T.Y., Saigal, S., Masud, A., Kapania, R.K., 2000. Survey of recent shell finite elements. Int. J. Num. Meth. Eng, 47: 101-127.

Yang, J.S., Xia, P.Q., 2012-a. Finite element corotational formulation for geometric nonlinear analysis of thin shells with large rotation and small strain. Science China Technological Sciences, 55(11): 3142-3152.

Yang, J.S., Xia, P.Q., 2012-b. Energy conserving and decaying algorithms for corotational finite element nonlinear dynamic responses of thin shells. Science China Technological Sciences. 2012 Vol.55 No.12: 3311-3321.

Yang, P.C., Norris, C.H., Stavsky, Y., 1966. Elastic wave propagation in heterogeneous plate. Int. J. Sol. Struct, 2: 665-684.

Yang, T.Y., 1973. High order rectangular shallow shell element. J. Engng. Mech. Div, ASCE, 99(1): 157-181.

Yang, Y., Tang, X., Zheng, H., 2014. A three-node triangular element with continuous nodal stress. Comput. Struct, 141: 46-58.

Yang, Y.B., Chang, J.T., Yau, J.D., 1999. A simple nonlinear triangular plate element and strategies of computation for nonlinear analysis. Comp. Meth. Appl. Mech. Eng, 178: 307-321.

Yang, Y.B., Chang, J.T., Yau, J.D., 1999. A simple nonlinear triangular plate element and strategies of computation for nonlinear analysis. Comp. Meth. Appl. Mech. Eng, 178: 307-321.

Yang, Y.B., Lin, S.P., Leu, L.J., 2007. Solution strategy and rigid element for nonlinear analysis of elastically structures based on updated Lagrangian formulation. Engineering Structures, 29: 1189-1200.

Yang, Y.B., McGuire, W., 1984. A procedure for analyzing space frames with partial warping restraint. Int. J. Num. Meth. Eng, 20: 1377-1398.

Yang, Y.B., McGuire, W., 1985. A work control method for geometrically nonlinear analysis. Proc. Int. Conf. Advance in Numerical Methods in Engineering, Swansea, U.K., pp.913-921.

Yang, Y.B., Shieh, M.S., 1990. Solution method for nonlinear problems with multiple critical points. AIAA J, 28: 2110-2116.

Yaqun, Z., Zhongqin, L., Weigang, Z., 2003. A quadrilateral thin shell element based on area co-ordinate for explicit dynamic analysis. Commun. Num. Meth. Eng, 19: 169-178.

Yeh, J.T., Chen, W.H., 1993. Shell elements with drilling degree of freedoms based on micropolar elasticity theory. Int. J. Num. Meth. Eng, 36: 1145-1159.

Yeo, S.T., Lee, B.C., 1997. New stress assumption for hybrid stress elements and refined four-node plane and eight-node brick elements. Int. J. Num. Meth. Eng, 40: 2933-2952.

Yunus, S.M., 1988. A study of different hybrid elements with and without rotational degrees of freedom for plane stress/plane strain problems. Comput. Struct, 30: 1127-1133.

Yunus, S.M., Saigal, S., Cook, R.D., 1989. On improved hybrid finite elements with rotational degrees of freedom. Int. J. Num. Meth. Eng, 28: 785-800.

Yuqiu, L., Yin, X., 1994-a. Generalized conforming triangular membrane element with vertex rigid rotational freedoms. Finite. Elem. Anal. Des, 17: 259-271.

Yuqiu, L., Yin, X., 1994-b. Generalized conforming quadrilateral membrane element with vertex rigid rotational freedom. Comput. Struct, 52(4): 749-55.

-Z-

Zagari, G., Madeo, A., Casciaro, R., de-Miranda, S., Ubertini, F., 2013. Koiter analysis of folded structures using a corotational approach. Int. J. Solids. Struct, 50(1): 755-65.

Zengjie, G., Wanji, C., 2003. Refined triangular discrete Mindlin flat shell elements. Comput. Mech, 33(1): 52-60.

Zhang, Q., Lu, M., Kuang, W.Q., 1998. Geometric non-linear analysis of space shell structures using generalized conforming flat shell elements-for space shell structures. Commun. Num. Mech. Eng, 14: 941-957

Zhang, Y., Zhou, H., Li, J., Feng, W., Li, D., 2011. A 3-node flat triangular shell element with corner drilling freedoms and transverse shear correction. Int. J. Num. Meth. Eng, 86: 1413-1434.

Zhang, Y.X., Kim, K.S., 2005-a. A simple displacement-based 3-node triangular element for linear and geometrically nonlinear analysis of laminated composite plates. Comp. Meth. Appl. Mech. Eng, 194: 4607-4632.

Zhang, Y.X., Kim, K.S., 2005-b. Linear and Geometrically nonlinear analysis of plates and shells by a new refined non-conforming triangular plate/shell element. Comput Mech, 36: 331-342.

Zhanxin, M., Zhongqi, F., 2002. A high precision quadrilateral element with rotational degree of freedom. Chin. J. Appl. Mech, 19: 119-123.

Zhao, Q., Tianqi, Y., 1995. On the adaptive parameter incremental method for analyzing the snapping problems. Applied Mathematics and Mechanics, 16(9): 851-858.

Zheng, H., Liu, D.F., Lee, C.F., Tham, L.G., 2005. Displacement-controlled method and its applications to material non-linearity, Int. J. Num. Analytical Methods in Geomechanics, 29(3): 209-226.

Zhong, H.G., Crisfield, M.A., 1998. An energy-conserving co-rotational procedure for the dynamics of shell structures. Engrg. Comput, 15: 552-576.

Zhong, W.X., Zeng, J., 1996. Rational finite elements. J. Comp. Struct. Mech. Appl, 13: 1-8.

Zhou, Z., Murray, D.W., 1994. An Incremental Solution Technique for Unstable Equilibrium Paths of Shell Structures. Comput. Struct, 55(5): 749-759.

Zhu, Y., Zacharia, T., 1996. A new one-point quadrature, quadrilateral shell element with drilling degrees of freedom. Comp. Meth. Appl. Mech. Eng, 136: 165-203.

Zhu, Y.Y., Cescotto, S., 1996. Unified and mixed formulation of the 8-node hexahedral elements by assumed strain method. Comp. Meth. Appl. Mech. Eng, 129: 177-209.

Zienkiewicz, O.C., 1971-a. The Finite Element Method in Engineering Science, McGraw-Hill, London.

Zienkiewicz, O.C., 1971-b. Incremental Displacement in Nonlinear Analysis. Int. J. Num. Meth. Eng, 3: 587-592.

Zienkiewicz, O.C., 1977. The finite element method, London Mc Graw Hill, U.K. Third edition.

Zienkiewicz, O.C., Cheung, Y.K., 1964. The Finite Element Method for Analysis of Elastic Isotropic and Orthotropic Slabs, Proc. Institution of Civil Engineers, August.

Zienkiewicz, O.C., Parekh, C.J., King, I.P., 1965. Arch dams analysed by a linear finite element shell solution program. In Proc. Symp. on Theory of Arch Dams, Southampton University, Pergamon Press, Oxford.

Zienkiewicz, O.C., Parikh, C.J., Kina, I.P., 1968. Arch dam analysis by a linear finite element shell solution program. In Proc. Symposium on Arch Dams, pp. 19-22. I.C.E., London.

Zienkiewicz, O.C., Taylor, R.L., 2000. The finite element method. Fifth edition, Butterworth-Heinemann, Oxford.

Zienkiewicz, O.C., Taylor, R.L., Too, J.M., 1971. Reduced integration technique in general analysis of plates and shells. Int. J. Num. Meth. Eng, 3: 275-290.

Zienkiewicz, O.C., Wood, W.L., Taylor, R.L., 1980. An alternative single step algorithm for dynamics problems. Earthquake Engineering and Structural Dynamics, 8: 31-40.

APPENDICES

Appendix A: Nonlinear dynamic analysis recurrence scheme

The various steps to be taken into account for the developed nonlinear dynamic incremental approach using the co-rotational updated Lagrangian formulation are as follows:

1-INITIAL CALCULATIONS

- Select time step *Δt* and calculate b_i constants
- Form the matrices *K*, *M* and *C*
- Initialize $u(0) = u_0$, $\dot{u}(0) = v_0$ and solve for the initial acceleration:

  $M\ddot{u}_0 = F_0 - C\dot{u}_0 - Ku_0$

2-FOR EACH TIME STEP

- calculate tangent stiffness matrix $K_t = \int_v B_t^T D B_t \, dv$
- form and triangularize the effective stiffness matrix $\bar{K} = K + b_1 M + b_4 C$
- form the effective load vector $\bar{F}_{t+\Delta t}$

3-FOR EACH ITERATION

- solve for displacements at (*t+Δt)* : $\bar{K}\,\Delta u_{t+\Delta t} = R_{t+\Delta t}$

  - update the new system of axis on the preceding position of the element nodes before evaluation of the tangential stiffness and internal forces

  - the internal strains and stresses are calculated in the new reference system of the precedent step

  - the new solution is obtained after linearization of the problem by calculating the internal strains and stresses in the new reference system of the precedent step

  - the solution is used to proceed to the next step.
- check for convergence of the iteration process (if *OK* continue, else go to **3**)
- Calculate velocities and accelerations at (*t+Δt)* :

$$\begin{cases} \ddot{u}_{t+\Delta t} = b_1(u_{t+\Delta} - u_t) + b_2\dot{u}_t + b_3\ddot{u}_t \\ \dot{u}_{t+\Delta t} = b_4(u_{t+\Delta} - u_t) + b_5\dot{u}_t + b_6\ddot{u}_t \end{cases}$$

- *t = t+Δt*
- *go to* ***2***

Appendix B. Triangular plate bending polynomial shape functions

We used the following cubic polynomial interpolation in order to formulate geometric stiffness and mass matrix for the "*DKT*" plate bending element:

$$P(\xi,\eta)=\langle 1 \quad \xi \quad \eta \quad \xi^2 \quad \eta^2 \quad \xi\eta \quad \xi^2\eta \quad \xi\eta^2 \quad \xi^3 \quad \eta^3 \rangle$$

Using static condensation, we obtained the following shape functions:

$$N_1=\alpha^2(3-2\lambda)+2a$$

$$N_2=\xi\alpha^2+\frac{1}{2}a$$

$$N_3=\eta\alpha^2+\frac{1}{2}a$$

$$N_4=\xi^2(3-2\alpha)+2a$$

$$N_5=\xi^2(\xi-1)-a$$

$$N_6=\eta\xi^2+\frac{1}{2}a$$

$$N_7=\eta^2(3-2\eta)+2a$$

$$N_8=\xi\eta^2+\frac{1}{2}a$$

$$N_9=\eta^2(\eta-1)-a$$

With: $\alpha=1-\xi-\eta$

$$a=\xi\eta\lambda$$

Appendix C. Quadrilateral plate bending polynomial shape functions

We used the following cubic polynomial interpolation in order to formulate geometric stiffness and mass matrix for the "*DKQ*" plate bending element:

$$P(\xi,\eta)=\left\langle 1 \quad \xi \quad \eta \quad \xi^2 \quad \eta^2 \quad \xi\eta \quad \xi^3 \quad \eta^3 \quad \xi^2\eta \quad \xi\eta^2 \quad \xi^3\eta \quad \xi\eta^3 \right\rangle$$

We obtained the following shape functions:

$$N_1(\xi,\eta)=\frac{a_1}{8}(\alpha-\xi-\eta)$$

$$N_2(\xi,\eta)=\frac{a_1}{8}(1-\xi^2)$$

$$N_3(\xi,\eta)=\frac{a_1}{8}(1-\eta^2)$$

$$N_4(\xi,\eta)=\frac{a_2}{8}(\alpha+\xi-\eta)$$

$$N_5(\xi,\eta)=\frac{-a_2}{8}(1-\xi^2)$$

$$N_6(\xi,\eta)=\frac{a_2}{8}(1-\eta^2)$$

$$N_7(\xi,\eta)=\frac{a_3}{8}(\alpha+\xi+\eta)$$

$$N_8(\xi,\eta)=\frac{-a_3}{8}(1-\xi^2)$$

$$N_9(\xi,\eta)=\frac{-a_3}{8}(1-\eta^2)$$

$$N_{10}(\xi,\eta)=\frac{a_4}{8}(\alpha-\xi+\eta)$$

$$N_{11}(\xi,\eta)=\frac{a_4}{8}(1-\xi^2)$$

$$N_{12}(\xi,\eta)=\frac{-a_4}{8}(1-\eta^2)$$

With: $a_i=(1+\xi_i\xi)\cdot(1+\eta_i\eta)$

$$\alpha=2-\xi^2-\eta^2$$

Appendix D. Triangular membrane element with rotational *d.o.f* shape functions

In this work, we aim to present a unified formulation that could be generalized for all triangular and quadrilateral elements that are based on the Allman-type in-plane displacement field. So, when expressing the in-plane displacement field that is used for calculating initial stress matrix and mass matrix, we limited to the original Allman-type displacement field terms even if the element uses a complimentary terms to describe the displacement field. In fact, these neglected additional terms, have no considerable effect on the initial stress and mass matrices, and make them need less time for integration.

Using natural coordinates, Allman-type displacement field is written as:

$$\begin{Bmatrix} u \\ v \end{Bmatrix} = \sum_{i=1}^{n} N_i(\xi,\eta) \begin{Bmatrix} u_i \\ v_i \end{Bmatrix} + \sum_{k=n+1}^{2n} NL_k(\xi,\eta)(\varphi_j - \varphi_i) \begin{Bmatrix} y_{ji} \\ -x_{ji} \end{Bmatrix}$$

For a triangular element, it could be written as:

$$\begin{cases} u = \sum_{i=1}^{3} N_i(\xi,\eta)\{u_i\} + \omega_1\left(NL_6 y_{13} - NL_4 y_{21}\right) + \omega_2\left(NL_4 y_{21} - NL_5 y_{32}\right) + \omega_3\left(NL_5 y_{32} - NL_6 y_{13}\right) \\ v = \sum_{i=1}^{3} N_i(\xi,\eta)\{v_i\} + \omega_1\left(-NL_6 x_{31} + NL_4 x_{21}\right) + \omega_2\left(-NL_4 x_{21} + NL_5 x_{32}\right) + \omega_3\left(-NL_5 x_{32} + NL_6 x_{13}\right) \end{cases}$$

Where: NS_k are shape functions for serendipity element.

We can express *u* and *v* using the following shape functions:

$$\left[\overline{N}_1\right] = \langle N_1 \quad 0 \quad Py_1 \quad N_2 \quad 0 \quad Py_2 \quad N_3 \quad 0 \quad Py_3 \rangle^T$$
$$\left[\overline{N}_2\right] = \langle 0 \quad N_1 \quad Px_1 \quad 0 \quad N_2 \quad Px_2 \quad 0 \quad N_3 \quad Px_3 \rangle^T$$

With:

$$\begin{array}{l|l} Py_1 = \left(NL_6 y_{13} - NL_4 y_{21}\right) & Px_1 = \left(NL_4 x_{21} - NL_6 x_{13}\right) \\ Py_2 = \left(NL_4 y_{21} - NL_5 y_{32}\right) & Px_2 = \left(NL_5 x_{32} - NL_4 x_{21}\right) \\ Py_3 = \left(NL_5 y_{32} - NL_6 y_{13}\right) & Px_3 = \left(NL_6 x_{13} - NL_5 x_{32}\right) \end{array}$$

Where: $N_1 = 1-\xi-\eta$, $N_2 = \xi$, $N_3 = \eta$

$$NL_4 = 4\xi(1-\xi-\eta)$$

$$NL_5 = 4\xi\eta$$

$$NL_6 = 4\eta(1-\xi-\eta)$$

Appendix E. Quadrilateral membrane element with rotational *d.o.f* shape functions

For a quadrilateral element with drilling rotation, in-plane displacement field is:

$$\begin{cases} u = \sum_{i=1}^{4} N_i(\xi,\eta)\{u_i\} + \omega_1\left(NS_8 y_{14} - NS_5 y_{21}\right) + \omega_2\left(NS_5 y_{21} - NS_6 y_{32}\right) + \\ + \omega_3\left(NS_6 y_{32} - NS_7 y_{43}\right) + \omega_4\left(NS_7 y_{43} - NS_8 y_{13}\right) \\ v = \sum_{i=1}^{4} N_i(\xi,\eta)\{v_i\} + \omega_1\left(-NS_8 x_{14} + NS_5 x_{21}\right) + \omega_2\left(-NS_5 x_{21} + NS_6 x_{32}\right) + \\ + \omega_3\left(-NS_6 x_{32} + NS_7 x_{43}\right) + \omega_4\left(-NS_7 x_{43} + NS_8 x_{14}\right) \end{cases}$$

Where: NS_k are shape functions for serendipity element.

We can express *u* and *v* using the following shape functions:

$$\left[\overline{N}_1\right] = \left\langle N_1 \quad 0 \quad Py_1 \quad N_2 \quad 0 \quad Py_2 \quad N_3 \quad 0 \quad Py_3 \quad N_4 \quad 0 \quad Py_4 \right\rangle^T$$
$$\left[\overline{N}_2\right] = \left\langle 0 \quad N_1 \quad Px_1 \quad 0 \quad N_2 \quad Px_2 \quad 0 \quad N_3 \quad Px_3 \quad 0 \quad N_4 \quad Px_4 \right\rangle^T$$

$$\begin{array}{l|l} Py_1 = \left(NS_8 y_{14} - NS_5 y_{21}\right) & Px_1 = \left(NS_5 x_{21} - NS_8 x_{14}\right) \\ Py_2 = \left(NS_5 y_{21} - NS_6 y_{32}\right) & Px_2 = \left(NS_6 x_{32} - NS_5 x_{21}\right) \\ Py_3 = \left(NS_6 y_{32} - NS_7 y_{43}\right) & Px_3 = \left(NS_7 x_{43} - NS_6 x_{32}\right) \\ Py_4 = \left(NS_7 y_{43} - NS_8 y_{14}\right) & Px_4 = \left(NS_8 x_{14} - NS_7 x_{43}\right) \end{array}$$

Where: $N_i = \frac{1}{4}(1-\xi_i\xi)(1-\eta_i\eta)$.

$$\begin{array}{l|l} NS_5(\xi,\eta) = \frac{1}{2}\left(1-\xi^2\right)(1-\eta) & NS_7(\xi,\eta) = \frac{1}{2}\left(1-\xi^2\right)(1+\eta) \\ NS_6(\xi,\eta) = \frac{1}{2}(1+\xi)\left(1-\eta^2\right) & NS_8(\xi,\eta) = \frac{1}{2}(1-\xi)\left(1-\eta^2\right) \end{array}$$